SOME PROBLEMS IN STELLARATOR REACTOR DESIGN

by

W.N.G. Hitchon

Merton College, Oxford.

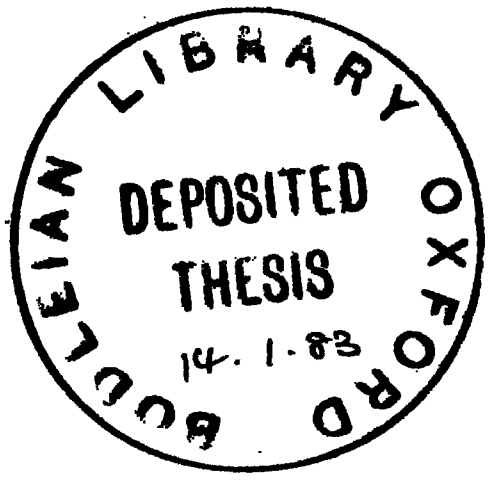

This thesis is submitted in partial fulfilment of the requirements for the Degree of Doctor of Philosophy at the University of Oxford.

July 1981.

Abstract

Title: Some Problems in Stellarator Reactor Design.
Author: W.N.C. Kitchon, Merton College, Oxford.
Degree: D.Phil.
Term of Submission: Trinity 1981.

This thesis examines theoretically the potential of the plasma confinement device known as a Stellarator as a fusion reactor.

Chapter one contains a survey of the requirements for nuclear fusion to take place in a device employing magnetic confinement. The range of reactor parameters which are appropriate is derived, both from the point of view of plasma physics and on the basis of a rather crude economic model.

Chapter two begins with a discussion of the equilibrium of plasma in Stellarators. Solutions of the equilibrium equations are obtained, employing an inverse aspect ratio expansion of the field quantities.

Chapter three indicates which macroscopic instabilities are cause for concern in Stellarators without net longitudinal current. A stability criterion appropriate to Stellarators is evaluated, using the equilibrium fields found in the preceeding chapter.

Chapter four is devoted to the study of the effects of particles which are localised in the ripple of the Stellarator magnetic field on transport. A random walk theory of their contribution to diffusion is given.

Chapter five contains a description of the coil systems capable of generating Stellarator fields, and their properties. Specialising to "twisted" coils, geometrical scaling laws are sought, which describe the properties of the fields they produce.

Chapter six is a brief indication as to how such coils may be incorporated into a reactor.

Chapter seven considers the parameters of a Stellarator reactor based on "twisted" coils, and shows how they may be written in terms of the major and minor radii of the device. An economic model of the reactor is given, which allows us to optimise the reactor, to obtain the cheapest system at fixed total power output and wall loading. The result is shown to be considerably less expensive than similar Tokamak designs.

Acknowledgement.

I should like to thank my supervisors, Drs. P.C. Johnson and C.J.H. Watson, for their help and interest whilst this work was being done, and J.C. Hitchon for being patient during the same period.

I should also like to thank the following people:

Dr. P.J. Fielding, for suggesting some of the work of chapter two, and for help and encouragement.

R.J. Hastie, for answering all manner of questions and for helpful suggestions with regard to the work of chapters three and four.

T.J. Martin, for providing the computer programs used principally in chapter five.

W.R. Spears, for information used in chapters one, six and seven on the design of fusion reactors and for discussions of their feasibility.

Introduction

It is the object of this thesis to study the Physics and Engineering problems relevant to the design of a fusion reactor of the Stellarator type, and then to attempt the conceptual design of such a reactor. With the help of a set of preliminary component cost estimates, we shall then demonstrate how it can be made as cheaply as possible, and compare the estimated cost with the expected costs of other fusion reactors.

Before proceeding with this programme, it is useful to recall the approximate values of the parameters of a fusion plasma, which may be established by means of rather simple arguments, and also to list the main components of any fusion reactor. Chapter one begins with a summary of the well-known plasma conditions necessary for fusion reactions to occur at an economically acceptable rate.

A "burning" plasma is however only one of a number of areas to be studied during fusion reactor design. It would be impossible to give a full account of them all in the present work. We shall, however, attempt to give an indication of the scope of such studies in chapter one. We then introduce a rather primitive economic analysis which identifies the parameter ranges within which we shall study in more detail the behaviour of the plasma and the performance of the field-coils of a particular system, namely a modular Stellarator. This allows us to discuss the design of a set of coils of this type, and to give a description of the essential features of the other components of the reactor.

As we shall henceforth be concerned principally with Stellarators, it is appropriate to define here what we shall use this word to mean: a Stellarator will be taken to be any device capable of containing a fusion plasma whose vacuum fields generate a unique set of topologically toroidal, nested magnetic surfaces. This definition implies the existence

of a rotational transform, which is responsible for the existence of these surfaces and which ensures plasma containment. The general properties of Stellarators are discussed in [1,2].

In practice the Stellarator field is made up of a main toroidal field modulated by "helical" fields which give a non-zero rotational transform to the field lines. The rotational transform, i, is defined to be the ratio of the number of rotations of the field lines about the minor axis (in the poloidal direction) to the number of rotations about the major axis (toroidal direction) averaged over many orbits. It can be shown on a single particle model (see e.g. [2]) that non-zero rotational transform is necessary to prevent particles drifting straight to the wall. In chapter two we shall see that finite transform is also required on the basis of M.H.D. equilibrium calculations. The plasma confinement properties of Stellarators which we shall use are derived in chapters two and three, which represent an extension to the existing M.H.D. theory of equilibrium and stability of plasma in a Stellarator. In all of this the Tokamak is included as a special case, which aids the comparison which we wish to make.

Chapter four is devoted to a discussion of particle and heat transport in Stellarators. Transport rates have previously been estimated on the basis of approximate analytic calculations (e.g. by Frieman,[3]) and have been found to be relatively high. The explanation of this result is the fact that the ripple in the Stellarator field due to the helical part of the field, combined with the radial variation in the toroidal field, should give rise to drift motions which may carry a class of particles out of the device. (In a system which is symmetric in the toroidal angle, ξ, where the toroidal component of angular momentum, RP_ξ, is conserved, particles move on closed surfaces over which RP_ξ is constant. However, the Stellarator field breaks axisymmetry, so that the corresponding component of angular momentum is not conserved.)

This would mean that, in the low collision-frequency regime in which a reactor plasma should lie, a Stellarator would be at a considerable disadvantage in comparison with a Tokamak, which in principle need have no such ripple. (In practice, Tokamak coils do give rise to a ripple in the fields due to the gaps between them, and similar diffusion processes are predicted, on the basis of the same model.)

The model employed in [3] neglects a number of factors which are likely to be important, in reality, including the effects of ambipolar fields on particle orbits, and is, in any case, not correct for the most energetic particles. This is despite the fact that the model predicts that the diffusion is primarily due to these particles. We show that when such particles are properly accounted for, the predicted diffusion rate is considerably reduced. Experimentally observed confinement times for particles and energy in Stellarators do not seem to be worse than in a Tokamak, and may well be better, so our theory is partially confirmed. (One may advance a plausible explanation why they should be better based on probable fluctuation levels in the devices, and we shall touch upon this point in that chapter.)

Analytic and numerical calculations of the behaviour of the fields, produced by the particular type of conductor which we shall claim to be the most suitable, are presented in chapter five. From the preceeding chapters it emerges that we are limited to rather small aspect ratios, and so the task becomes to study the achievable rotational transform as a function of the magnetic surface parameters, for low aspect ratio devices, subject to the constraint that the coils can be built in practice. It is then necessary to assess the prospects for inclusion of some sort of "divertor", and to estimate the forces on the coils.

The basic system which we eventually propose (in chapter six) consists of a set of twelve identical twisted coils laid out on a toroidal surface in a manner which possesses a three-fold rotational symmetry. The

main engineering problem in the coil design is to support the forces on them.

The Tokamak, on the other hand, has what is essentially a toroidal solenoid as its main coil set. The provision of a divertor causes major difficulty in this case, as considerable forces act upon bundle divertors, and poloidal divertors occupy a great deal of space within the coils. As there are in addition vertical field coils, poloidal shaping coils and the means for driving the toroidal current to be included, we believe that the overall coil design appears less attractive than the "equivalent" Stellarator which we are proposing. Some comparison with the Tokamak, together with the discussion of divertor design and of coil forces, is also given in chapter six.

Finally, in chapter seven we draw together all the threads from other chapters to produce an outline reactor design. The method of optimisation employed makes use of a detailed set of reactor component cost estimates, in contrast to the very crude cost model invoked in chapter one. Although some factors are ignored by use of such a model (e.g. practicability of support of coil forces), it is preferable to the model used in chapter one, which takes the cost to be simply proportional to the engineered volume. The result of the optimisation based on these costs turns out to lie within the parameter range identified in chapter one as broadly credible, and the coils required are the type which we attempt to demonstrate as feasible in chapters five and six, so even though the more detailed costing still has its limitations, the resulting optimised design has reasonable credentials.

The costs of a number of recent Tokamak designs are calculated on the same basis, and are compared with the cost of a Stellarator with similar total output power and similar assumptions as regards, for instance, wall-loadings. We conclude that a Stellarator reactor is potentially cheaper and easier to build than a Tokamak, even though we

have made a number of optimistic assumptions about the performance of the Tokamak. (It may be remarked that the Tokamak is not able to operate at the same wall loadings if it has to be pulsed, and so this would put it at a considerable disadvantage.)

Chapter One: The Fusion Reactor

In this chapter, the methods used to find an optimised Stellarator reactor design are described.

The plasma parameters necessary for fusion are considered. The major components of a fusion reactor are then introduced. Engineering problems associated with each of them are discussed, in order to indicate the areas to be investigated later.

Simple arguments are given which help to determine the range of reactor dimensions to be employed. This is particularly important for the coil design studies of chapter five. Although the economic model used in the present chapter is relatively crude, the parametric choices based upon it can be justified a posteriori using the more complete optimisation of chapter seven.

The only defensible approach to fusion reactor design is to seek the cheapest reactor design which is compatible with all that is currently known, both as regards plasma physics and engineering. By contrast, the temptation to identify some one desirable physics or engineering characteristic of a reactor as being most important, and to use this to optimise the design - without attempting to apply the constraints due to all the other desirable characteristics - has to be resisted. In other words, a systematic analysis has to be attempted which keeps all the options open until the whole system has been taken into account. (By the "system" we mean the plasma, the walls surrounding it, the blanket, the coils, the heat extraction and conversion system, the control systems and the electricity grid into which power is fed - in short, every component involved in this method of electrical power generation.)

We shall find several strong constraints on design which push us

toward particular shapes and sizes of reactor. No one of these, according to the above, is to be allowed to determine a precise value for any quantity. This philosophy need not prevent us from simplifying the analysis by a reasonable anticipation of the outcome, however. It may be abundantly clear at the outset that if we push too far in some direction we shall have a reactor concept which will inevitably cost vastly more than its competitors or exhibit some other property which makes it implausible that it could ever be built, (see e.g. [4]). We save considerable labour by excluding such possibilities as soon as we can demonstrate them to be unworkable.

In practice we shall find that it is possible on the basis of quite simple economic considerations to identify the parameter range within which we must work. In fact, it turns out that this is the range within which all existing Tokamak reactor designs lie - the device which we are compelled to consider is somewhat like a Tokamak reactor because similar economic factors apply to all toroidal magnetic fusion reactors.

In order to establish a basis for comparison of reactor economics it is tempting to attempt to adopt the Fast Breeder as standard. However, there are still considerable uncertainties about Fast Breeder economics which have no parallel in economic assessments of fusion reactors, so at present it is easier to make comparison with the Tokamak, which is the potential fusion reactor most widely studied at the moment. Consequently, in this thesis we limit ourselves to giving the argument for a Stellarator reactor in relation to a Tokamak.

The stance which we are about to adopt does not necessarily imply that we believe that the Tokamak designs with which we shall make the comparison are technically or economically feasible, indeed there are certain problems inherent in Tokamaks (but not Stellarators) which are a matter for concern, for instance, disruptions, the effects of pulsed

operation and the topological complexities resulting from the use of several crossed magnetic fields in order to maintain the plasma equilibrium.

We now discuss general considerations in fusion reactor design.

1.1 The Fusion Plasma

The first generation of Fusion Reactors will probably make use of the nuclear reaction

$$ {}^{2}_{1}D + {}^{3}_{1}T \longrightarrow {}^{4}_{2}He(3{\cdot}52MeV) + n(14{\cdot}06MeV) \qquad (1.1,1) $$

as the other candidate reactions, for instance

$$ {}^{2}_{1}D + {}^{3}_{2}He \longrightarrow {}^{4}_{2}He\ (3{\cdot}67MeV) + p\ (14{\cdot}67MeV) \qquad (1.1,2) $$

and

$$ {}^{2}_{1}D + {}^{2}_{1}D \longrightarrow \begin{cases} {}^{3}_{1}T(1{\cdot}01MeV) + p(3{\cdot}03Me \\ {}^{3}_{2}He(0{\cdot}92MeV) + n(2{\cdot}45MeV) \end{cases} \qquad (1.1,3) $$

are significantly more difficult to initiate. As we shall see, the conditions for even the D-T reaction to take place are extremely stringent, and so for the purposes of this discussion it is appropriate to consider only D-T.

The D-T reaction has the disadvantage that most of the energy released would be carried away by the neutron, which cannot be contained by a magnetic field. Hence in a reactor utilising magnetic confinement there

must be a blanket which surrounds the reaction chamber and is capable of slowing down the neutron and extracting its kinetic energy. The energy would then be produced as heat, which would be converted to electricity with an efficiency of the order of 30%. (If the reaction products had been charged, virtually 100% efficiency of conversion would in principle have been possible.)

The cross-section for the chosen reaction reaches its peak value at a temperature of order 100 keV and varies rapidly elsewhere: in practice it is necessary to reach temperatures of order 10 keV before the fusion rate becomes reasonably high. With the possible exception of some high-Z ions which may not be fully stripped of electrons, the gas is a fully ionised plasma at this temperature and so magnetic confinement is appropriate.

A well-known criterion which specifies the minimum condition necessary for fusion to be feasible is known as the Lawson criterion. It may be summarised as follows: if we assume that the losses from the plasma must be exceeded by the gross electrical energy generated, we obtain a condition on nt (the product of the particle density of each species and the confinement time), that it be greater than 5×10^{13} s/cc.

A more interesting condition which turns out, not surprisingly, to be more stringent is the ignition condition. This results from equating the power lost from the plasma to the power deposited in the plasma by the reaction products (i.e. the alphas) as they slow down. If we let F denote the fraction of the fusion energy which is delivered to the plasma and supposing that energy E is released per reaction and that the rate of reaction per unit volume is R, then the ignition condition is

$$FRE = \frac{3nT}{t} + P \qquad (1.1,4)$$

where P is the power lost as Bremsstrahlung per unit volume, and t is the

energy confinement time for all other processes. With fE equal to 3.52 MeV for D-T we obtain an nt value four times as big as that given by Lawson. These considerations show that a fusion plasma needs to have an nt value of order 10^{14} s/cc.

One possible operating point for a fusion reactor is at the minimum of the nt curve which occurs at about 25 keV. A slightly different optimum operating condition is obtained by considering the effect of a limit on the attainable plasma beta value. The fusion power per unit volume, RE, expressed in terms of beta and in units of MW/m^3 varies as

$$RE = 0.7\ \beta^2 B^4\ f(T) \qquad (1.1,5)$$

where f(T) is a dimensionless number, containing all of the temperature dependence of RE, whose maximum value is one. The beta to be used is the peak beta, and we have assumed a pressure profile which is slightly flatter than parabolic. (The reason why we believe this to be appropriate is that our equilibrium calculation indicates that l=2 Stellarators are suited to containing plasmas with parabolic profiles. The l=2 reactor we eventually consider has negative shear, however, so that the transform decreases with radius, and similarly the pressure gradients must be less steep at the edge than for flat transform profiles.)

The maximum of f(T) occurs at about 14 keV, although it is fairly broad, extending from 10 to 20 keV.

When impurities are allowed for radiation losses get much worse, firstly because Bremsstrahlung due to high Z impurities varies as the square of Z and secondly because many impurity atoms will not be fully ionised. As a result, line and recombination spectra will typically lead to radiation of much more power than Bremstrahlung. For this reason, any reactor design has to ensure that the level of impurities remains suitably

bounded.

1.2 The Components of a Fusion Reactor

A great deal of work has been done on the design of a Tokamak reactor, for example [5,6], and much of this is also applicable to Stellarators. These have, however, received relatively little attention in their own right, although Gibson et al. compared Stellarator and Tokamak in an early paper, [7]. More recent work largely remains unpublished, [8].

Before we embark on a Stellarator reactor design study, we consider the main components of a fusion reactor.

If we start at the heart of the reactor and work outwards then we should logically begin with the plasma itself. Plasma physics largely dictates the nature of the various conductors which generate the fields, and the spatial extent of the plasma fixes a surface outside which the first wall must lie. However, as we shall consider the plasma behaviour in detail in later chapters, we shall pass over the plasma in this chapter and begin with the first wall.

1.2.1 The First Wall

The First Wall, the first material barrier and inner surface of the blanket region is the most vulnerable part of this structure since it is subject to bombardment by neutrons of average energy about 14 MeV, carrying 1-10 MW per square metre ($1MW/m^2$ corresponding to 4×10^{13} $n/cm^2.s$), by electromagnetic radiation and by particles which diffuse out of the plasma. As a result, it must withstand high heating rates of about $10MW/m^3$ for each $1MW/m^2$ delivered to the wall by neutrons for

Stainless Steel, and $6MW/m^3$ for Aluminium, - see e.g. Mioduszewski, [9], - and the pressure associated with the coolant flow which is needed to keep the wall at a reasonable temperature. (Aluminium may well be excluded from reactor applications, however, for its strength decreases at high temperatures, so that it appears unlikely that it could be used above 200^0C.) The design of the first wall needs to take into account the temperature gradients and thermal and mechanical stresses which will be set up as a result.

Two further threats to its integrity, radiation damage and sputtering, are considered below.

Radiation Damage

As a consequence of the neutron and charged particle bombardment to which it is subjected, radiation creep, swelling and embrittlement of the wall are likely to occur. The implications of these are by no means fully understood.

One cannot hope to study in full the effects of these fluxes by simulation experiments, as the only known way to achieve the high fluxes and energies of neutrons simultaneously is a fusion reactor itself. Consequently, the life-time of the first wall, measured in MW-years/m^2, which is probably the most important unknown in the study of the fusion reactor, can only be estimated by extrapolating from measurements made in very different conditions. As the mechanisms involved in the evolution of damage in the metal under reactor conditions could well also be quite different, such estimates are of limited value. Thus the maximum economically sustainable power flux at the first wall (known as the "wall loading") remains an uncertain, though vitally important, design parameter. For this reason, in this thesis optimum reactor parameters will be presented as functions of the wall loading, which will be left as an unspecified parameter.

It is generally believed that the probable value lies in the range 2-6MW/m^2 . This is because life-times of about 10MW-years/m^2 are expected, and replacement of wall sections in less than 2-3 years is considered unacceptable. (In a two year replacement "cycle", half the modules in a reactor might be replaced during the summer months of each year, [10].)

Radiation damage is most serious in a pulsed device since cycling stresses greatly enhance the rate of growth of defects in the walls.

Sputtering

A second reactor design constraint is due to wall erosion by ion bombardment. Sputtering can be expected to remove large quantities of metal from the wall during the lifetime of the reactor, if no measures are taken to impede the process. (This material is then injected into the plasma with a consequent effect on the level of high-Z impurities.) Such measures include the use of a cool gas mantle, a divertor or a graphite screen inside the first wall.

The sputtering rate has been estimated on various occasions. For example, in [11] rates for sputtering of Nb by plasma particles are given for a Tokamak or Stellarator reactor without a divertor. The energy flux to the wall due to particles is taken to be about 70% of the alpha energy (depending on how much energy is lost as Bremsstrahlung or Synchrotron radiation). If we envisage the neutrons, each having energy of about 14MeV, giving rise to a wall loading of about 3MW/m^2 , then 70% of the alpha energy (each alpha having about 3MeV) will result in 0.5MW/m^2 . About 2cm of the first wall would be removed per year, on this basis, and as the wall is often taken to be less than a centimetre thick, this is clearly intolerable.

The very thin first wall is chosen because of thermal stresses,

which are produced by the temperature gradients set up in the wall. In a pulsed device, the stresses are cyclical, and the upper limit on the cyclical stress, being rather severe, (about 200MPa for Stainless Steel), imposes a bound on the permissible wall thickness (<4mm. in INTOR, [9]). In a steady state device such as a Stellarator, this restriction, which is very stringent, would be greatly relaxed.

In a pulsed system the problem of sputtering may be worsened by cycling for another reason: a cold gas mantle may well be unacceptable in such a device, [12], as the fusion power which is not carried away by the neutrons is transmitted to the first wall in the form of radiation by the mantle. If this radiation is pulsed it may do severe damage to the first wall.

Where the many tons of sputtered material will finally be deposited depends on the measures adopted to protect the first wall and on other factors as yet unknown, but it seems likely that the (e.g. divertor) pumps will bear the brunt of it. We shall make no attempt to solve this problem here, but note only that some Stellarators can more naturally incorporate non-axisymmetric divertors than Tokamaks, and this makes the problem potentially more tractableby removing it outside the main reactor volume.

The plasma may be prone to disruptions, a feature of Tokamak operation which has not, as yet, been totally eradicated, (and is not necessarily likely to be). If so, the lifetime of the wall can be reckoned in terms of the number of disruptions it can stand before being completely eroded, this being the most damaging single process. That number is not large, (of order a thousand for INTOR [13]), in relation to the rate of incidence of disruptions. Stellarators with zero net toroidal

current are essentially immune to this class of instability.

1.2.2 The Blanket

Electrical power can only be produced economically if the neutron deposits its kinetic energy in some region exterior to the plasma - the blanket - from which we may recover it. However, as Tritium does not occur naturally, having a half-life of 12.6 years, the blanket is called upon to play a second role, that is, it must breed the Tritium from the neutrons and Lithium. The two natural isotopes of Lithium are

^{7}Li(92.58%) and ^{6}Li(7.42%)

and the reactions employed are

$$^{6}Li + n \longrightarrow {}^{4}He + T + 4{\cdot}86\,MeV \qquad (1.2.2,1)$$

and

$$^{7}Li + n \longrightarrow {}^{4}He + T + n - 2{\cdot}87\,MeV \qquad (1.2.2,2)$$

Note that although the first is exothermic, the second requires a neutron energy in excess of 2.87 MeV.

Associated with the blanket there is the problem of choosing a coolant which is compatible with the structural materials whilst being capable of performing its principal task of removing heat effectively. The choice of structural materials needs to take account of radiation damage and problems of replacement and disposal resulting from radioactivity induced in them.

The blanket also has to shield components exterior to itself from

the neutrons and from gamma radiation. These functions require a certain minimum thickness of material, set by the stopping length for 14MeV neutrons, which in most designs is taken to lie in the range 1-1.5 metres. [10]

1.2.3 The Shield

After the blanket is a shield region which protects the next component, the superconducting coils, from the temperatures of the interior, reducing the heat flux by about four orders of magnitude and needing about a metre of material to do it [10].

In most designs it is considered appropriate to include about a metre of concrete to protect the superconducting coils from the energy flux from the plasma. Thus the combined thickness of blanket and shield lies in the range 2-3 metres.

1.2.4 Coil Systems

The design of the coils is one of the principal aims of all of this work: the impact of each area studied on the coils will thus be indicated in the appropriate section.

In chapters five and six we study in some detail the coils which generate the magnetic field. As mentioned previously, the coil shape is largely dictated by plasma physics. Conversely, however, as the practical difficulties of building elaborate coil systems are considerable, a study of the structural implications of the coils and their support system for the more exotic magnetic configurations is, we believe, sufficient to exclude them as the basis of a potential reactor. Several authors have studied Stellarators whose axis is grossly non-planar in an attempt to increase the beta value attainable. It must be recalled, however, that the reason for wishing to achieve high beta is an economic one, and we feel that increasing beta in this way will be uneconomical when the cost of the complex engineering involved is calculated. For these reasons we

have restricted our attention to configurations having an essentially circular minor axis about which the coils, which are all the same shape, are rotated with respect to each other.

The superconducting coils must be kept at an extremely low temperature. If the temperature is to be 4K then a theoretical minimum of 290W is needed to remove four Watts from the coil - in reality, the efficiency of the pump is likely to be rather low, so refrigeration is liable to require a considerable amount of power and this leads to a requirement for very efficient thermal insulation of the coils. (If superconductors which have been reported as operating at much higher temperatures become viable, this consideration would become less vital.)

As we do not wish to have to have to refrigerate the coil supports, as well as the coils, we shall attempt to arrange that all the forces which are applied to the coil are compressive, so that the contact need be less intimate than would otherwise be the case, (see chapter six).

1.2.5 Reactor Maintenance

When a component of a fusion reactor needs replacement or repair it is essential that it be possible to perform the necessary operations in a reasonably short time. The length of the down-time will necessarily be one of the most important parameters determining the economic viability of the reactor. As a result we must design for easy access to the reactor and for whole sections of the torus to be capable of being moved bodily out of the device by remote handling methods.

The need for remote handling stems from the radioactivity of the interior of the reactor, induced by neutron bombardment and slightly aggravated by absorbed Tritium. The difficulties involved in performing intricate tasks under these conditions are legion and robot servicing techniques will have to be developed and improved.

It has sometimes been suggested that having one module which is relatively free to move radially whilst the others were permanently in place would allow portions of the blanket which might be in need of replacement to be removed by moving them azimuthally inside the torus. When they were at the right azimuth they could then be taken out of the torus. However the technology to move heavy objects around inside the torus does not exist and the task is such that it does not appear likely to be developed in time, [14]. In our judgement, it is thus necessary that all the segments of the torus be removable radially, perhaps on some sort of tracks or on hover pads.

1.2.6 Waste Management

A related problem which has not been taken account of in the majority of reactor designs is that of the disposal of radioactive waste from a fusion reactor.

Depending on the materials present in the blankets, shielding etc., radioactive wastes may be produced by the neutron bombardment which require special handling and disposal. The nature of the waste, unlike that from a fission reactor, will depend very strongly on the materials employed and on the details of the reactor design. For instance, aluminium is an attractive structural material from this point of view; a few years storage should be sufficient before it may be disposed of by simply burying it. There are probably reasons for wishing to avoid using aluminium in the first wall of a fusion reactor, however, as discussed above. Molybdenum is an unattractive choice, whilst stainless steel is possible but not ideal. It would be highly active immediately after removal from the reactor, but would have become sufficiently inactive in what is considered a short period of time (about a hundred years) to be disposed of, or recycled, [15].

Whatever material is employed it is likely that facilities will

have to be available for on-site storage of the material, for about a year, before it would be possible to ship it elsewhere.

In comparison with fission reactors it is claimed in [15] that the waste from fusion reactors has a greatly reduced "biological hazard potential", B.H.P. and also that after 200 years the activity of the waste should be less (measured in BHP/kW(th)) than that of the ash from a coal-fired plant.

1.2.7 Plasma Heating

In a pulsed reactor design there is an optimum economic level of heating. Slow heating decreases the capital cost of the necessary heating equipment, but it also decreases the fraction of the cycle during which the reactor is producing power, and this increases the cost per kilowatt. In a steady-state device such as a Stellarator heating is only necessary very occasionally, to initiate the burn. Consequently the heating rate need be no higher than is necessary to ensure that the power input to the plasma is greater than the losses during the start up process.

At present, few heating methods have serious claims as burn initiation procedures. The possible ways of heating the plasma are neutral injection, lower hybrid resonance heating and electron or ion cyclotron resonance heating. (Ohmic heating, which is highly effective and economical at low temperatures, becomes ineffective as ignition is approached because the plasma resistivity falls off at high temperatures.) Neutral injection is further advanced at present than RF heating methods, but the latter are believed to have the greater potential.

In general one would expect that economic considerations would select a single heating method. It seems likely that RF heating in some form would be most effective. However, as neutral injection may be desired for profile control, it may be necessary to include this heating method also.

(Start-up using E.C.R.H. has already been demonstrated in a Stellarator, [16], so that the case for using RF is strengthened.)

1.2.8 Plasma Engineering

We encounter yet more constraints on the design by considering plasma physics requirements of a slightly different sort: in order to fuel the reactor, to heat it to ignition, to monitor the plasma state and control the burn and remove the exhaust plasma, we need access to it. This means that there must be substantial gaps in the hardware that we have been discussing to give access to various pieces of external apparatus. The coil sets of chapter six will be seen to meet these requirements.

1.3 Power Output and Reactor Economics

This section is intended to make two points:

(i). A very simple (but essentially correct) cost model is used to show that we are likely to be compelled by economic factors to work at a plasma "aspect ratio" of order five, and minor radius of order two metres.

(ii). In general, the wall loading is a rather stringent limit on the power output from the reactor. As a result, the useful value of beta is limited to the range 5-15%, for devices of arbitrary aspect ratio.

If the reactor is to be economical, it must produce as much power as possible for a given capital cost of the station. A fundamental figure of merit is thus the cost of the station divided by the total power output of which it is capable, the cost per kilowatt.

To calculate the cost per kilowatt, we first need to know what

factors limit the power output.

The power produced by the plasma may be found from (1.1,5) multiplied by the plasma volume. There are other factors which place an upper bound on the power, however: one is the wall loading, the reason for which has already been discussed, and the other is the maximum total power allowable from the power station.

As a power station must be incorporated into an electrical grid, it cannot have a power output greater than the maximum which can be accomodated in the grid. Designs usually take that value to be less than or equal to 2GW(el), corresponding to about 6GW(th), ("el" and "th" denoting electrical and thermal respectively), this figure representing a few percent of U.K. consumption, at present. The reason for this limit is the difficulty of transmitting power economically over long distances, which means that regions of a certain size must be nearly self sufficient in electricity. Then within the region there must be a sufficient surplus generating capacity to compensate for complete failure of at least one station. If the unit size is very great, this implies a large excess capacity which will, beyond a certain point, be too costly.

Using the fact that the total power output is nearly fixed, we may discover the permissible range of aspect ratios, by minimising the cost per kilowatt with respect to the reactor geometry.

To calculate the cost per kilowatt we employ throughout this section what is probably the simplest reasonable cost estimate - that is, the cost is taken to consist of a term proportional to the engineered volume plus a term proportional to the power output, to allow for conventional generator costs. In this model the cost is independent of the magnetic field strength, up to some arbitrarily specified maximum.

On the basis of this model the minimisation of the cost per

kilowatt is straightforward and gives an indication of the range of geometric parameters for the reactor to be considered.

The mean plasma minor radius, r, is defined so that if the semi-minor (major) axis is a(a') and e = a'/a then

$$r = a\,e^{2}$$

The major radius will be denoted R_m: the plasma aspect ratio is $A=R_m/r$. The volume of the torus is

$$V = 2\pi^{2} r^{2} R_m \qquad (1.3,1)$$

and its surface area is

$$A_w = 4\pi^{2} r R_m (1 + e^{2})^{1/2} (2e)^{-1/2} \qquad (1.3,2)$$

We now determine the cheapest geometry, (in terms of cost per kilowatt), for a given wall loading P_w, (which may not be the limiting wall loading).

In general, it would then be necessary to find r, R_m at the optimum, as functions of P_w, and hence, by varying P_w up to some maximum, (which may be greater than the expected maximum) map out the whole space available to us, and so complete the optimisation. This procedure is followed in chapter seven: it turns out to be unnecessary, here, for r, R_m are independent of P_w.

If the reactor is assumed circular (e = 1) and the the power density over the engineered volume is taken to be

$$\frac{P_w A_w}{\text{Eng.Vol.}} = \frac{4\pi^2 r R_m P_w}{2\pi^2 R_m (r + t + s)^2} \qquad (1.3,3)$$

where t is the blanket thickness and s the shield thickness, (i.e. including the plasma volume in the engineered volume) then as (t + s) is effectively constant, the maximum power density is obtained when $r = t + s$, which would imply $r \simeq 2m$.

More properly, the plasma volume should be subtracted from the denominator of (1.3,3), and allowing for the plasma ellipticity, we find that if b = t + s, the engineered volume is

$$2\pi^2 R_m \{(ae + b)(a + b) - (a^2 e)\} = 2\pi^2 R_m^2 \{ab(1 + e) + b^2\}$$

The effect of ellipticity on the numerator is simply to multiply it by a constant dependent on e: see (1.3,2).

The maximum power density occurs when $a/(a(1 + e) + b)$ is maximum, i.e. when r is infinite. However, as various effects which are small, O(1/A), have been neglected, we might expect that the real optimum could occur for any a such that

$$\frac{a}{(a + b/(1 + e))} > 1 - \frac{1}{A}$$

Taking the equality in the above the required value of a is $a = b(A - 1)/(1 + e)$.

Now $P(th) = P_w A_w$, and from (1.3,2), dropping factors which are very close to unity, we have

$$\frac{P(th)}{40P_w} \simeq a^2 eA = b^2 \frac{(A-1)^2}{(1+e)^2} eA$$

P(th) should lie in the range 2-6GW; $2MW/m^2 < P_w < 4MW/m^2$; thus $P(th)/40P_w$ should be between 12.5 and 75. For $e \simeq 2$, (typically) and $b \simeq 2m.$, A is then between 3.2 and 5, (implying $a \sim b$).

These estimates are rather low, principally because the errors are more like ε, the coil inverse aspect ratio, which is greater than 1/A, (and not due to any failure in principle): nevertheless, these are comparable to the values we obtain in chapter seven, where we find $A \sim 6$. ε, in turn, is $\sim 2/A$, i.e. 1/2 - 1/3.

In the light of these results, it is interesting to calculate which is likely to be most restrictive on the power output, the attainable beta, or the wall loading, for it has often been stressed (e.g. in [7]) that high beta is essential for fusion to be economical. We shall attempt to show that this is an oversimplification.

We believe that the following are reasonable assumptions about those parameters which the reactor designer is not free to specify:

(i). the plasma temperature is in the range 10-15keV, so that the power density is given, roughly, by (1.1,5), with $f(T) = 1$.

(ii). The range of sensible values for B_a is probably $4T. < B_a < 8T.$, for the maximum attainable magnetic field at the superconductor (using superconducting NbTi) is about 10T, (although going to NbTi alloyed with Ta may give a material whose structural strength allowed 12T). The field on axis is given by $B_a = (1 - \varepsilon)B_c$. This is the explanation of the upper limit, for in practice ε is not likely to be less than 1/5.

On the other hand, it is not permissible to work at very low B, for the confinement times of particles and energy scale as a positive power of B: it is usually assumed in Tokamak designs that B>4T. is tolerable. As we shall argue, in chapter four, that transport in Stellarators should be comparable with that in Tokamaks, then such a limit may be appropriate to Stellarators also.

The total power output from the plasma may then be estimated as

$$P(th) = 1.4\pi^2 r^2 R_m B_a^4 \beta^2 \qquad (1.3,4)$$

The value of e is not crucial, at this point, but for our applications we typically have e=2-3, and so the wall loading in MW/m^2 is approximately equal to

$$P_w = .27\, r^2 \beta^4 B_a \qquad (1.3,5)$$

For any given r, we may estimate the beta for which this wall loading exceeds some maximum tolerable value, P_w, which we might expect to be about $3MW/m^2$. We find beta to be limited to the range

$$\beta \lesssim 1.9 \sqrt{\frac{P_w}{r}}\, B_a^{-2} \qquad (1.3,6)$$

Typical values of P_w and r in Tokamak designs might be $3MW/m^2$ and 2m. For B_m=10T, then even if ε=1/3, beta of more than 5% would lead to an intolerably large flux of neutrons. If B_a = 4T., which is the other limit discussed above, then beta of 15% would be allowed, although the lower confinement time may make this operating point unattractive. In general, only rather low values of beta are allowed by this relation. Consequently, it does not seem appropriate to attempt to achieve very high

beta (of order 20%) by going to high aspect ratios, for the resulting device would either be uneconomical because of its relatively low minor radius, or produce an extremely large power output, which is equally unacceptable. In any case, at such a high beta and for reasonably high magnetic fields the wall loadings could not be supported.

1.4 Summary

Taking the power output to be given by $P(th) = P_W A_W$, for some $P_W < P_W(max)$, we have calculated the most economical Reactor geometry. We found that r must be made large, and as P_W and P(th) are bounded by some maximum tolerable value, this implies that we must take relatively low aspect ratio.

We have also argued that for magnetic fields which reach the technological limit and for reasonable values of the plasma beta, the wall loading which the plasma is capable of providing is greater than that which the wall can withstand, unless the minor radius is rather small. If the minor radius is small, the reactor becomes uneconomical, however.

In chapter seven this topic is revisited, using a better model, in which, for instance, the extra cost involved in using a higher magnetic field is allowed for, and the simple picture is essentially confirmed.

Chapter Two: Equilibrium of Plasma in a Stellarator

We now develop a method of describing the equilibrium of Stellarator plasmas. We begin by discussing the general mathematical properties of 3D equilibria, and then give details of the calculation and the results obtained. Their application to a reactor is described at the end of the chapter.

2.1 Equilibrium Equations

On a time-scale much greater than the mean collision times of electrons and ions we may represent the plasma pressure as a scalar quantity, provided no effect (like neutral injection) prevents the species from relaxing to a local thermodynamic equilibrium. Then, employing the ideal M.H.D. equations, the equilibrium conditions are:

$$\nabla P = \underline{J} x \underline{B} , \qquad \nabla x \underline{H} = \underline{J}, \qquad \nabla . \underline{B} = 0, \quad (2.1.1i\text{-}iii)$$

These equations describe the equilibrium of an ideal infinitely conducting fluid (somewhat like a perfectly conducting molten metal) exactly, and a plasma insofar as it is similar to such a fluid. (Kulsrud, [17].) These are also the leading terms in whatever other set of equations might be considered more appropriate.

It is worthwhile considering some immediate consequences of these equations, always assuming that solutions exist.

The scalar products of $\underline{B}$ and $\underline{J}$ with (2.1.1i) give $\underline{B}.\text{grad}P = 0$ and $\underline{J}.\text{grad}P = 0$. Hence in equilibrium lines of both $\underline{B}$ and $\underline{J}$ lie in surfaces of constant pressure. Let us now consider the former equation in more detail.

The equation $\underline{B}.\text{grad}\,\psi = 0$ may be taken to define the magnetic surface function ψ. It has been shown by Kruskal, [18], that solutions for ψ exist in the asymptotic sense, that is, if ψ is expanded in an asymptotic series, employing the inverse aspect ratio, ε, as a small parameter,

$$\psi = \psi^{(o)} + \varepsilon\psi^{(1)} + \varepsilon^2\psi^{(2)} + \ldots\ldots \qquad (2.1.2)$$

and similarly $\underline{B}$ and the operator "grad", then

$$\sum_{i=m+n+p}^{N} \varepsilon^{m+n+p}\, \underline{B}^{(m)}.\nabla^{(n)}\,\psi^{(p)} = O(\varepsilon^{N+1}) \qquad (2.1.3)$$

(For finite values of ε there may be regions where a single valued ψ does not exist.)

The surface function ψ is significant in the theory which we are about to develop, firstly because $P = P(\psi)$. A second reason follows from (2.1.1i) as we may write

$$\underline{J} = h\underline{B} + \frac{\underline{B}\times\nabla P}{\underline{B}^2} \qquad (2.1.4)$$

so defining the (as yet arbitrary) scalar function h.

Applying divJ = 0, which may be deduced from (2.1.1ii), we obtain the magnetic differential equation for h:

$$\underline{B}.\nabla\, h = -\underline{B}\times\nabla\, P.\nabla\,(1/\underline{B}^2) \qquad (2.1.5)$$

If gradP = 0 then $h = h(\psi)$, and even when gradP is non-zero this may

still be a useful approximation.

On a different level, ψ = constant is the equation for the surfaces on which field lines lie. In some circumstances, particles may describe drift-surfaces which, depending on the region in phase space in which the particles lie, are more or less close to the magnetic surfaces. As particle orbits should not intersect the walls and as we wish to have a fat plasma column the magnetic surface structure is of considerable interest. (The surfaces are bounded on the outside by a separatrix, outside which field lines cease to lie on surfaces which are nested about the magnetic axis, but orbit the coils.) We shall investigate the surfaces analytically in this chapter using the equilibrium fields to solve B.grad $\psi = 0$. In chapter five we present the results of computer field line following for the vacuum field of the type of twisted coil which we shall advocate. (Particle orbits and transport are discussed in chapter four.)

2.2 Methods of Calculation of Equilibria

In a toroidal geometry where exact solutions to the M.H.D. equations are not known it is necessary to apply approximate methods, either analytic or numerical, 3D codes having recently become feasible. We shall derive the results which we need by means of an analytic approximation.

Before beginning it is interesting to note that some controversy exists as to the status of solutions of the M.H.D. equations in a system like the Stellarator which does not possess symmetry with respect to at least one coordinate. In a symmetric system such as a straight cylinder (with two ignorable coordinates) or a straight Stellarator or a Tokamak (each having one ignorable coordinate) the equilibrium equations can be

written as a single partial differential equation for a flux-function in terms of the appropriate number of coordinates. The existence of solutions is then guaranteed. However, in general geometry no proof has yet been found that solutions will always exist, and there are even reasons to believe that they will not, as has been pointed out by Grad, [19]. (Lortz, [20], has succeeded in finding such a proof for devices of the "Bumpy Torus" type, however.) Lo Surdo and Sestero, [21], have argued that, although the theoretical case against existence is strong, the experimental evidence for there being good equilibria is also convincing. They further argue for the existence of solutions to all orders in an asymptotic expansion which they develop, although they feel that a convergence proof is probably not possible. Any imbalance in forces which could exist, for finite values of the expansion parameter, presumably gives rise to effects involving finite Larmor radius and time dependence, amongst other things. In this case, it is most important to use a more appropriate set of equations, and so we feel that it will not be fruitful to attempt to pursue this topic further, except to make two remarks:

(i). All the above methods of solution for non-symmetric fields are essentially asymptotic and it is difficult, if not impossible, to find convergence proofs for their solutions.

(ii). The possibility that equilibria may not exist in the general case is connected with the fact that in certain regions field lines do not always lie on nested surfaces but may move throughout a volume ergodically. This behaviour is due to resonances which arise in the neighbourhood of the rational surfaces, on which field lines might be expected to close on themselves, and is characterised by resonant denominators in some ordering schemes, whilst remaining hidden in others. (See chapter five.) The method we shall introduce is capable of describing magnetic islands, which are the basic resonant phenomenon, but what the error terms may be remains a problem.

(In a numerical solution the mesh size can be regarded as the small expansion parameter. Numerical solutions will also represent the resonances with varying degrees of success depending, for example, on the mesh size.)

There are two main methods of analytic approximation, differing in the way in which what is essentially the same small expansion parameter is introduced into the equations to be solved. The first we consider, which was originally used by Mercier [22] and Shafranov (see, for instance, [23]) and more recently by Lortz and Nuhrenberg [24] takes the distance from the magnetic axis, r, of points within the plasma to be small. Solutions of the equilibrium equations are then sought at the various orders in r. As powers of r constitute a complete set of functions in any interval, the method may be regarded as exact for the orders involved.

The other method is to expand certain quantities involved in the equations (2.1.1i-iii) in powers of the inverse aspect ratio of the boundary, ε , and to solve successively the equations which arise at the various orders in ε . This ordering necessarily brings in a degree of arbitrariness, but the former method is limited in only being accurate close to the magnetic axis. Having said that, the two are in a sense rather similar because when we take the inverse aspect ratio to be small we are restricting ourselves to a torus in which all points are close to the axis. Alternatively, the Mercier expansion may be regarded as an expansion in $\varepsilon\rho$, ρ being normalised to the minor radius, the results of which are similar but not identical to the ε expansion, expansion in ε in our experience usually picking up more terms before the equations become unmanageable.

The first application of the inverse aspect ratio expansion to a Stellarator was performed by Greene and Johnson [25], who introduced what

we shall refer to as the conventional Stellarator ordering. For the moment we shall only point out that this ordering gives rise to a 2D partial differential equation for the lowest order solution which can only be treated numerically. There are two reasons for this. One is that the pressure is high $\beta \sim O(\varepsilon)$, and it turns out that whatever else is assumed this case can only be solved numerically. The other is that with this ordering the vacuum field is, even in lowest order, composed of a set of Bessel functions which consist of an infinite series in ρ.

Partly in order to overcome the latter difficulty Dobrott and Frieman devised an "optimal" ordering for the vacuum fields, [26]. They were able to find the vacuum magnetic fields and surfaces of a pure l=3 Stellarator using this ordering. The details of the ordering are given in (2.3.2) below.

It is well known that analytic Tokamak equilibria can be calculated with $\beta \sim O(\varepsilon^2)$. Using the optimal ordering and taking $\beta \sim O(\varepsilon^2)$ we have solved the equilibrium equations, for the specific case of l=3, [27] and in general for a Stellarator with one l-number dominant, [28]. The result is a description of the equilibrium which, for many cases of interest, can be used without resorting to numerical methods.

2.3 Equilibrium Calculation

Our equilibrium calculation is now described in detail. We initially consider a low beta Stellarator equilibrium in which the field has one l-value dominant and which has an arbitrary net toroidal current. This permits the transition from a pure Stellarator (with no net toroidal current) to a pure Tokamak (with no non axisymmetric fields) to be followed. The Tokamak limit is specially noted in all that follows.

2.3.1 The Method of Averaging

If it is assumed that magnetic surfaces ψ exist, then solving the equation

$$\underline{B} \cdot \nabla\psi = 0 \qquad (2.3.1,1)$$

for ψ is equivalent to solving the equations for the field lines lying in the surfaces

$$\frac{dx^1}{B^1} = \frac{dx^2}{B^2} = \frac{dx^3}{B^3} \qquad (2.3.1,2)$$

to obtain ψ as a first integral. (Upper indices indicate contravariant components of vectors, and lower indices will be used to indicate covariant components.) The latter set of equations is formally equivalent to those governing a certain non-linear oscillator and so methods originally devised in that context may be applied. In particular, when a suitable small parameter exists, asymptotic methods, such as the method of averaging, are applicable.

The method of averaging [29] was developed to study the behaviour of non-linear oscillators in which departures from exact periodicity are in some sense small. We shall now outline the particular variant of the method of averaging which is used in our calculation. Although all of the variants are in fact equivalent, we believe this to be the most straightforward.

Our calculation, being a generalisation of that of Dobrott and Frieman, [26], which employed an asymptotic expansion resulting from their

"optimal ordering", naturally gives rise to a set of equations at each of the orders in $\lambda = \varepsilon^{1/3}$

Integrating the lowest order equation does not determine the lowest order solution uniquely. The extra information needed is obtained from a constraint arising from an equation associated with a higher power of λ . This situation recurs at each order at which a solution is sought.

To be precise, at the n+3 order of the expansion of (2.3.1,1) in powers of λ we obtain an equation of the form

$$\frac{\partial \psi^{(n+2)}}{\partial s} = f(\psi^{(n)}, \rho, \theta, s) \qquad (2.3.1,3)$$

where all the functions are periodic in θ ,s or independent of them, (and θ,s are angle-like variables to be introduced below).

If magnetic surfaces exist, there can be no secular term (by which we mean a term with a non periodic dependence on s) in the solution, so that there can be no term independent of s on the right hand side. (If there were such a term, there would be a term proportional to s in the solution.) Setting any such term to zero provides the extra information we need to solve the appropriate lower order equation. The indeterminacy due to the constant of integration is in turn resolved in higher order still. This elimination of the secular term is the method of averaging.

Morozov and Solovev have applied the method of averaging to the set of equations (2.3.1,2), [1], for a symmetric magnetic field perturbed by a small non-symmetric field. An expression for ψ was obtained which is seldom accurate, being a first approximation only. As a result, for most present day Stellarators it describes circular surfaces only. Its derivation is relatively complicated and will not be given here. The result is:

$$\overline{\Psi}(\overline{x}_1, \overline{x}_2) = \overline{A}_3 - \frac{1}{\sqrt{gB}} \overline{\hat{\sqrt{gB}}^{1}\,\hat{\sqrt{gB}}^{2}} \qquad (2.3.1,4)$$

with

$$\overline{a} = \frac{1}{L}\int_0^L a\, dx\,, \quad \tilde{a} = a - \overline{a}\,, \quad \hat{a} = \int \tilde{a}\, dx$$

(g is the metric determinant.) The actual coordinates are given in terms of the average coordinates by

$$x_i = \overline{x}_i - \hat{\sqrt{gB}}^{i} \qquad (2.3.1,5)$$

x_3 is the ignorable coordinate of the symmetric field, thus Ψ is the exact expression for the surface function when the field is symmetric and $\tilde{a} = 0$.

The equilibrium problem was solved with the same accuracy by Greene and Johnson, [25]. In [26], Dobrott and Frieman used the method of averaging to find vacuum magnetic surfaces to considerably better accuracy, and in [27,28] we solve the equilibrium equations, also to high accuracy, in an ordering scheme which is a modification of that of Dobrott and Frieman.

Rosenbluth et al. [30] and Hamzeh [31] have studied the destruction of magnetic surfaces by resonances. The latter is of interest in the present context, as it uses a version of the method of averaging, having written the equations to be used in a form appropriate to a set of non linear oscillators.

By analogy with the method of the phase plane it is to be expected that when two magnetic islands overlap the surface structure is lost. This is because the local axis is a centre (or elliptic singular point) but where islands meet are x-points (hyperbolic singular points or saddle-points). When two x-points meet, the system deviates from the orderly behaviour of other regions. In our case, field lines then move ergodically throughout the volume. The loss of surfaces due to this sort of effect is amply illustrated by the field line following calculations of chapter five.

2.3.2 Ordering Scheme and Vacuum Fields

In order to solve the equations (2.1.1) we order various quantities in powers of the inverse aspect ratio, ε. The particular ordering scheme which we employ combines a number of desirable formal attributes:

(i). The hierarchy of partial differential equations which arises as a result of this choice can be solved in successive orders.

(ii). The solution in each order is given in terms of an unknown function of radius which satisfies an ordinary differential equation in ρ. This is a considerable simplification and means that we can solve for as many orders as necessary, in order to incorporate all the relevant physical effects. The radial boundary condition is then applied in each order.

(iii). The ordering is also designed to incorporate physical effects in the correct orders so that they are able to "compete" with each other in the appropriate fashion. In some cases this is essential, and in others only desirable. An instance where it is essential is provided by the ordering of the rotational transform: if it were too small, there could be no equilibrium in the lowest orders of the solutions which we shall seek. Because of the property of bringing together effects which we

know balance each other, we call this an "optimal" ordering scheme.

We now consider the vacuum field of a Stellarator and at the same time introduce the ordering to be employed.

It is well known (see, e.g., [32]) that the solution of Laplace's equation which is appropriate to toroidal boundary conditions may be found using toroidal coordinates $\{\eta, \tau, \xi\}$, which are related to the cylindrical coordinates $\{r, \xi, z\}$ illustrated in Fig.2.1 by:

$$r = \frac{R_o \cdot \sinh \eta}{(\cosh \eta - \cos \tau)}$$

$$z = \frac{R_o \cdot \sin \tau}{(\cosh \eta - \cos \tau)} \qquad (2.3.2,1)$$

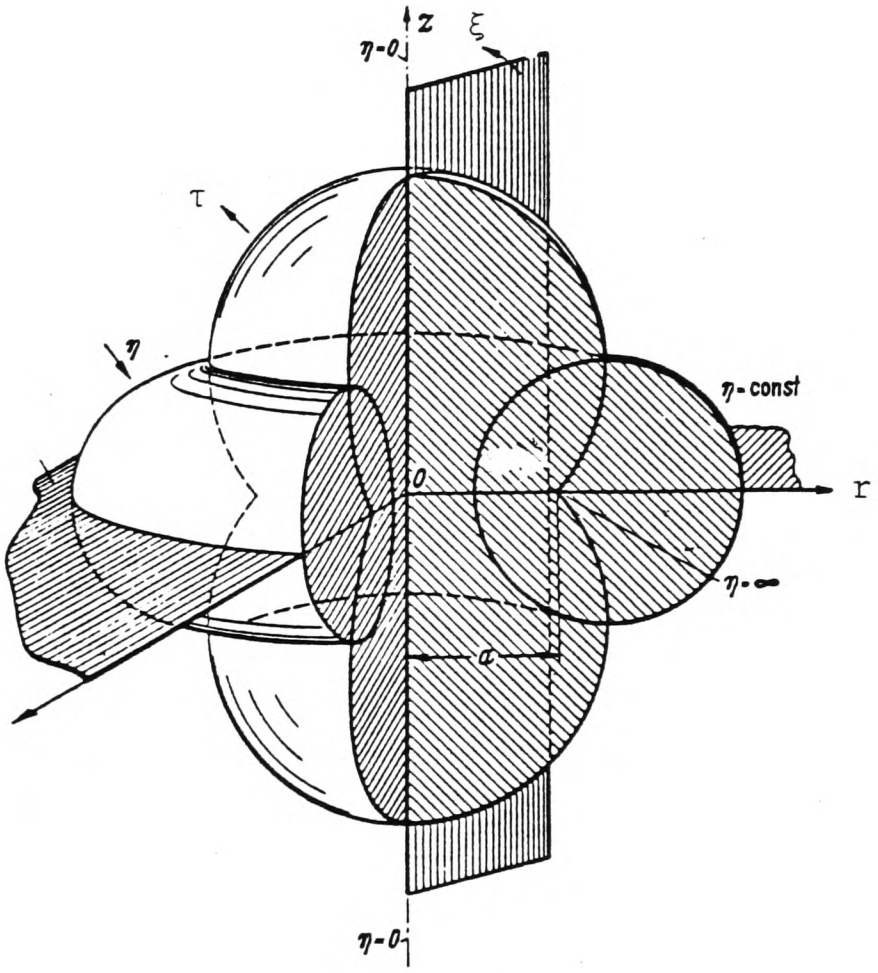

Fig. 2.1a Toroidal vs: Cylindrical coordinates

The general solution is:

$$V = B_o R_o \xi + (\cosh\eta - \cos\tau)^{1/2} \sum_{m,n} \{A_{m,n} P^m_{n-\frac{1}{2}}(\cosh\eta) \cos(n\tau + m\xi) + B_{m,n} Q^m_{n-\frac{1}{2}}(\cosh\eta) \cos(n\tau + m\xi)\} \quad (2.3.2,2)$$

(plus terms in $\sin(n\tau + m\xi)$) where $\underline{B}=\text{grad}V$.

$P^m_{n-\frac{1}{2}}(\cosh\eta)$ and $Q^m_{n-\frac{1}{2}}(\cosh\eta)$ are the associated Legendre functions of half integral order. R_o is the radius of the ring about which the coordinate system is defined.

$A_{m,n} = 0$, here, as the $P^m_{n-\frac{1}{2}}(\cosh\eta)$ are singular at the magnetic axis. For a particular value of m=p, in order to obtain a separable set of equations with particular properties discussed above, we take

-2/3

$$p = \bar{p}\varepsilon \qquad \bar{p} \sim O(1)$$

and normalise the fields to $B_o = 1$. Note that in a Stellarator with one harmonic dominant, n is the l-number.

If we now expand the expression for the potential, (2.3.2,2), in powers of ε for particular n,m=p, using ρ , the local radial coordinate defined by $\rho = r/a$, (Fig.2.1,b), where a is a convenient minor radius, we obtain a more useful approximate expression for the vacuum magnetic potential. (We also write $s=p\xi$, for the choice of p to be employed.)

The functions $Q^m_{n-\frac{1}{2}}(\cosh\eta)$ are given by

$$Q^m_{n-\frac{1}{2}}(\cosh\eta) = \tanh^m\eta \cosh\eta^{-(n+1/2)} F(m/2+n/2+1/4, m/2+n/2+3/4; n+1; \cosh\eta^{-2}) \quad (2.3.2,3)$$

where a number of multiplicative constant factors have been omitted.

The hypergeometric function F(a,b;c;z) is most conveniently

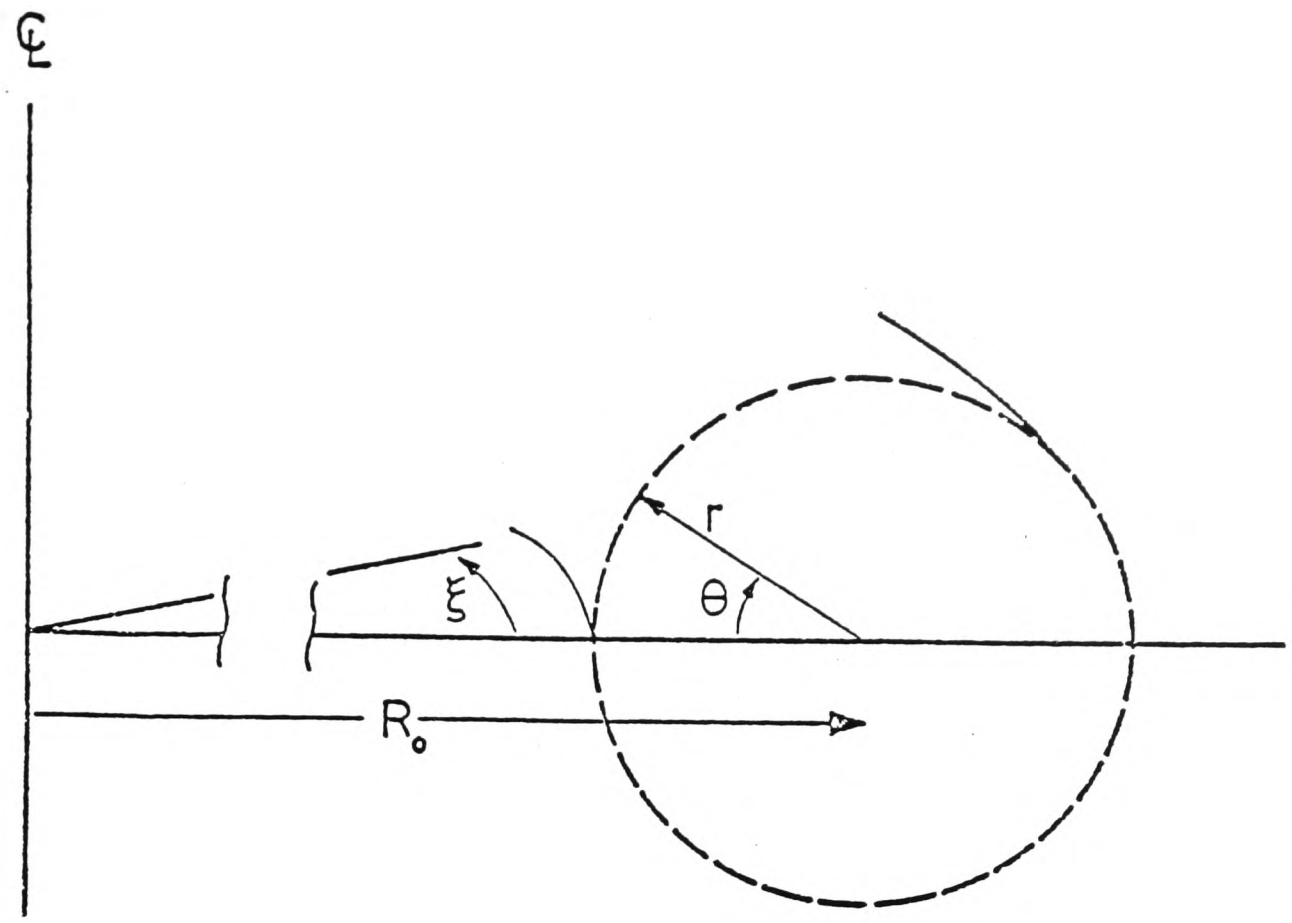

Fig. 2.1b Local Coordinates

written as

$$F(a,b;c;z) = \sum_{n=0}^{\infty} \frac{(a)_n (b)_n}{(c)_n} \frac{z^n}{n!} \qquad (2.3.2,4)$$

where e.g. $(a)_n$ is defined by

$$(a)_n = \frac{\Gamma(a+n)}{\Gamma(a)} = a(a+1)\ldots(a+n) \qquad (2.3.2,5)$$

Using the relation

$$\cosh\eta = \frac{r^2}{a^2}\frac{(1 + x/a + r^2/4a^2)}{(1 + x/a + r^2/2a^2)^2} \qquad (2.3.2,6)$$

where $x = r \cos\theta$, we may show that

(i). $\cosh\eta^{-1} = \varepsilon\rho\,(1 - 1/2\,\varepsilon\rho\cos\theta\,) + O(\varepsilon^3)$.

(ii). $\tau = \theta + \alpha$, where $\alpha = \varepsilon\rho \sin\theta/2 + O(\varepsilon^2)$.

These allow us to re-express (2.3.2,2), in the local coordinate system.

Evaluating the first terms in (2.3.2,4) we obtain

$$V_n^p = B_{p,n}(\varepsilon\rho)^n \left\{\cos(n\theta+s) + \frac{\bar{p}^2\varepsilon^{2/3}\rho^2}{4(n+1)}\cos(n\theta+s)\right.$$

$$+ \frac{\varepsilon\rho}{4}\left\{(2n+1)\cos([n+1]\theta+s) + \cos([n-1]\theta+s)\right\}$$

$$\left. + \frac{\bar{p}^4\varepsilon^{4/3}\rho^4}{32(n+1)(n+2)}\cos(n\theta+s) + \frac{\bar{p}^2\varepsilon^{5/3}\rho^3}{16(n+1)}\left\{(2n+3)\cos([n+1]\theta+s)\right.\right.$$

$$\left.\left. + 3\cos([n-1]6+s)\right\}\right\} + O(\varepsilon^{n+2}) \quad .$$

(2.3.2,6)

The terms which have been omitted are $O(\varepsilon^{8/3})$, and with $\varepsilon \simeq 1/10$ in CLEO, ($\simeq 1/20$ in WVII-A), $\varepsilon^{8/3} \simeq 1/400$ (1/4,000).

With this expression, the magnetic surface function may be found, using the method of averaging. Before proceeding, however, we specialise somewhat and take all the components of the potential except those with a particular value of n to be small. The dominant term is chosen to have:

$$B_{p,n} = \varepsilon^{(2/3 - n)}\,\alpha\, B_o a\,/\bar{p} \qquad (2.3.2,7)$$

This choice ensures that the helical ripple in the field amplitude is of similar magnitude to the toroidal variation, as well as being appropriate for use in the calculations which follow, in that, given our other

ordering assumptions, it is necessary in order to obtain a rotational transform of order unity. (The parameter α is determined for a given coil geometry by the helical winding current.)

In order to describe the fields produced by the winding of a classical Stellarator we choose the other non-zero coefficients as follows:

To simulate a winding law like

$$\frac{d\xi}{d\theta} \sim (1 + \varepsilon\Omega \cos\theta) \qquad (2.3.2,8)$$

(Ω being a dimensionless parameter of order unity) we add in small amounts of the side-band potentials which we expect such a winding to create, with $\ell = n \pm 1$, of amplitudes γ, δ respectively, γ, δ are still to be determined. The other term we shall add in, which does not involve γ, δ, converts the toroidal harmonic to a potential corresponding to a single l-number, (to $O(\varepsilon^{n+1})$).

$$V^p_{n+1} = B_{p,n}\left[\frac{\gamma}{4} - \frac{(2n+1)}{4}\right](\varepsilon\rho)^{n+1}\left\{\cos\left([n+1]\theta+s\right) + \frac{\bar{p}^2\varepsilon^{2/3}\rho^2}{4(n+2)}\cos\left([n+1]\theta+s\right)\right\} \qquad (2.3.2,9)$$

$$V^p_{n-1} = B_{p,n}\,\frac{\delta}{4}\,\varepsilon^2\,(\varepsilon\rho)^{n-1}\left\{\cos\left([n-1]\theta+s\right) + \frac{\bar{p}^2\varepsilon^{2/3}\rho^2}{4n}\cos\left([n-1]\theta+s\right)\right\}$$

We now calculate γ,δ.

If the coils are wound on the cylindrical surface $\rho = \rho_c$,

$$\left.\frac{d\xi}{d\theta}\right|_{coil} = \left.\frac{\varepsilon\rho_c j_\xi}{j_\theta}\right|_{\rho=\rho_c} = -\left.\frac{\varepsilon\rho_c b_\theta}{b_\xi}\right|_{\rho=\rho_c}, \text{ where } b_{\theta,\xi}\ (j_{\theta,\xi})$$

correspond to the helical winding fields (currents) only.

$$b_\theta \sim \sin(n\theta+s) + \frac{\varepsilon\rho_c}{4n}\left\{\gamma(n+1)\sin([n+1]\theta+s) + \frac{\delta}{\rho_c^2}(n-1)\sin([n-1]\theta+s)\right\}$$

$$b_\xi \sim \sin(n\theta+s) + \frac{\varepsilon\rho_c}{4}\left\{\gamma\sin([n+1]\theta+s) + \frac{\delta}{\rho_c^2}\sin([n-1]\theta+s)\right\}.$$

$$\therefore \frac{d\xi}{d\theta} \sim \left(1 + \frac{\varepsilon\rho_c}{4n\sin(n\theta+s)}\left\{\gamma\sin([n+1]\theta+s) - \frac{\delta}{\rho_c^2}\sin([n-1]\theta+s)\right\} + O(\varepsilon^2)\right),$$

but if $\gamma = -\frac{\delta}{\rho_c^2}$, then $\frac{d\xi}{d\theta} \sim \left(1 + \frac{\varepsilon\gamma\rho_c}{2n}\cos\theta\right)$.

Thus a winding law of the desired form is represented by choosing $\gamma = \frac{2n\Omega}{\rho_c}$ and $\delta = -2n\rho_c\Omega$. Of course, a field with the same properties could also be generated by means of appropriately shaped modular coils.

2.3.3 Vacuum Magnetic Surfaces

The equation to be solved is

$$\underline{B}.\nabla\psi = 0 \qquad (2.3.1,1)$$

We define

$$g = 1 - \varepsilon\rho\cos\theta \qquad \hat{\nabla} = ag\nabla \qquad \underset{\sim}{b} = \underset{\sim}{B}/B_o$$

where a is a convenient minor radius. The field is known from the gradient of V, and so it remains to expand the operator $\hat{\nabla}$ and the function ψ in powers of ε, so that if $\lambda = \varepsilon^{1/3}$

$$\psi = \psi^{(o)} + \lambda\psi^{(1)} + \lambda^2\psi^{(2)} \qquad (2.3.3,1)$$

and $$\hat{\nabla}f = \hat{\nabla}^{(o)}f + \lambda\hat{\nabla}^{(1)}f + \lambda^3\hat{\nabla}^{(3)}f,$$

$$\hat{\nabla}^{(o)} = \hat{\rho}\frac{\partial}{\partial\rho} + \frac{1}{\rho}\hat{\theta}\frac{\partial}{\partial\theta} \quad ; \quad \hat{\nabla}^{(1)} = \hat{\xi}\,\bar{p}\frac{\partial}{\partial\bar{s}} \qquad (2.3.3,2)$$

$$\hat{\nabla}^{(3)} = -\rho\cos\theta\,\hat{\nabla}^{(o)}.$$

We may now proceed with the calculation.

At the lowest order in λ we find

$$\frac{\partial \psi^{(o)}}{\partial s} = 0 \qquad (2.3.3,3)$$

so $\psi^{(o)}$ is a function of ρ,θ only. The next order is

$$\underset{\sim}{b}^{(2)} \cdot \hat{\nabla}^{(o)} \psi^{(o)} + \frac{}{p} \frac{\partial \psi^{(1)}}{\partial s} = 0 \qquad (2.3.3,4)$$

However, in third order we find that we cannot integrate the equation to obtain a periodic function of s unless

$$\frac{\partial \psi^{(o)}}{\partial \theta} = 0 \qquad (2.3.3,5)$$

The most general choice of $\psi^{(o)}$ allowed is thus

$$\psi^{(o)} \equiv \psi_o(\rho)$$

The fourth order equation has a similar integrability condition, with $\bar{\psi}^{(1)}$ taking the place of $\psi^{(o)}$ in (2.3.3,5). This we solve without loss of generality by taking $\bar{\psi}^{(1)} = 0$, which is equivalent to absorbing $\bar{\psi}^{(1)}$ into $\psi^{(o)}(\rho)$. A considerable simplification thus results. The fifth order, similarly, implies that $\bar{\psi}^{(2)} = 0$.

The solution to second order in λ is:

$$\psi = \psi_o(\rho) - \lambda \frac{n\alpha\rho^{n-1}}{\bar{p}^2} \sin(n\theta+s)\psi' - \lambda^2\left(\frac{n\alpha\rho^n}{2\bar{p}^2}\right)^2 \frac{1}{\rho}\frac{d}{d\rho}\left(\frac{\psi_o'}{\rho}\right) \cos 2(n\theta+s) \qquad (2.3.3,6)$$

2.3.4 Effects of Pressure and Current

A full description of one method of calculation of equilibria is given in appendix 1; here we shall describe an alternative in detail. We begin this section by outlining the first method, and then present the results of the calculation and show that they may also be obtained by iteration about the vacuum result, allowing for the effects of plasma pressure and current.

In order to treat plasma pressure and current, we introduce new variables

$$\hat{\underset{\sim}{J}} = \underset{\sim}{J}ga/B_o \qquad \hat{P} = P/B_o^2 \tag{2.3.4,1}$$

and the orderings

$$\hat{P} = \lambda^6 \hat{P}^{(6)} + \ldots ; \qquad \hat{\underset{\sim}{J}} = \lambda^3 \hat{\underset{\sim}{J}}^{(3)} + \ldots ; \tag{2.3.4,2}$$

The equilibrium equations become, in terms of these variables,

$$\hat{\nabla}\hat{P} = \hat{\underset{\sim}{J}} \times \underset{\sim}{b} \quad (i); \qquad \hat{\underset{\sim}{J}} = \hat{\nabla} \times \underset{\sim}{b} \quad (ii); \qquad \hat{\nabla} \cdot \underset{\sim}{b} = 0 \quad (iii) \tag{2.3.4,3}$$

Equations (2.1.1i-iii) may now be solved order by order in λ, with the above orderings and the lowest order field given by

$$\underset{\sim}{b} = \underset{\sim}{b}^{(o)} + \lambda^2 \underset{\sim}{b}^{(2)} \ldots \tag{2.3.4,4}$$

the second term being the lowest order term from V, the vacuum potential. (In the cases we shall study in chapter five we add to an l=2 field a small amount of l=6. Although this significantly improves the integrity of the surfaces in the vicinity of islands, especially near the

separatrix, it is not, we believe, important for the equilibrium properties of the plasma at the lower radii at which the plasma is to be found in a reactor geometry.)

We now go straight to the solution obtained in the appendix. The set of fields which is obtained, correct to $O(\varepsilon^2)$, is:

$$b_\rho = \lambda^2 \frac{n\alpha\rho^{n-1}}{\bar{p}} \cos(n\theta+s) + \lambda^4\left\{\bar{p}\alpha\rho^{n+1}\frac{(n+2)}{4(n+1)} + U(\rho)\right\}\cos(n\theta+s)$$

$$+ \lambda^5\left\{\frac{\alpha}{4\bar{p}}\left[\left(\rho^n(n+1) + \delta\rho^{n-2}(n-1)\right)\cos([n-1]\theta+s) + \gamma\rho^n(n+1)\cos([n+1]\theta+s)\right]\right.$$

$$\left. + V(\rho)\sin 2(n\theta+s)\right\}$$

$$+ \lambda^6\left\{A(\rho)\sin\theta + \left(f(\rho) + \frac{\bar{p}^3\alpha(n+4)\rho^{n+3}}{32(n+1)(n+2)}\right)\cos(n\theta+s) + W(\rho)\cos 3(n\theta+s)\right\}$$

$$b_\theta = -\lambda^2 \frac{n\alpha\rho^{n-1}}{\bar{p}} \sin(n\theta+s) + \lambda^3 b(\rho) - \lambda^4 \left\{ \bar{p}\alpha\rho^{n+1} \frac{n}{4(n+1)} + \frac{1}{n} \frac{d}{d\rho}(\rho U(\rho)) \right\} \sin(n\theta+s)$$

$$- \lambda^5 \left\{ \frac{\alpha}{4\bar{p}} \left[\left(\rho^n + \delta\rho^{n-2} \right)(n-1) \sin([n-1]\theta+s) + \gamma\rho^n (n+1) \sin([n+1]\theta+s) \right] \right.$$

$$\left. - \frac{1}{2n} \frac{d}{d\rho} (\rho V(\rho)) \cos 2(n\theta+s) \right\}$$

$$+ \lambda^6 \left\{ B(\rho) \cos\theta + \left(g_1(\rho) - \frac{\bar{p}^3 \alpha n \rho^{n+3}}{32(n+1)(n+2)} \right) \sin(n\theta+s) - \frac{1}{3n} \frac{d}{d\rho}(\rho W(\rho)) \sin 3(n\theta+s) \right\}$$

$$b_\xi = 1 + \lambda^3 (\rho\cos\theta - \alpha\rho^n \sin(n\theta+s))$$

$$- \lambda^5 \left\{ \frac{\alpha\bar{p}^2\rho^{n+2}}{4(n+1)} + \frac{\bar{p}\rho}{n^2} \frac{d}{d\rho}(\rho U(\rho)) - \frac{\alpha\rho^n \sigma(\rho)}{\bar{p}} \right\} \sin(n\theta+s)$$

$$+ \lambda^6 \left\{ \rho^2 \cos^2\theta + \left[\frac{\bar{p}}{n} \frac{d}{d\rho}(\rho V(\rho)) + \left(\frac{n\alpha\rho^{n-1}}{\bar{p}} \right)^2 \frac{\sigma'(\rho)}{2\bar{p}} \right] \frac{\rho}{2n} \cos 2(n\theta+s) + b_\beta(\rho) \right.$$

$$\left. - \frac{\alpha}{4} \left((2+\gamma)\rho^{n+1} \sin([n+1]\theta+s) + (3\rho^{n+1} + 2\delta\rho^{n-1}) \sin([n-1]\theta+s) \right) \right\}$$

(2.3.4,5)

where the functions which are as yet undefined are to be determined from the following ordinary differential equations in ρ :

$$\frac{1}{\rho}\frac{d}{d\rho}(\rho b) = \sigma(\rho) \tag{i}$$

$$-\frac{1}{n\rho}\frac{d}{d\rho}\left(\rho\frac{d}{d\rho}(\rho U)\right) + \frac{nU}{\rho} = -\frac{n\alpha\rho^{n-1}}{\bar{p}^2}\sigma' \tag{ii}$$

$$\frac{1}{2n}\frac{d}{d\rho}\left(\rho\frac{d}{d\rho}(\rho V)\right) - 2nV = -\left(\frac{n\alpha\rho^{n}}{2\bar{p}^2}\right)^2\frac{d}{d\rho}\left(\frac{\sigma'}{\rho}\right) \tag{iii}$$

$$\frac{db_\beta}{d\rho} = -\left(\frac{dP}{d\rho} + b(\rho)\sigma(\rho) + \left\{\left(\frac{n\alpha\rho^{n-1}}{\bar{p}^2}\right)^2\frac{\bar{p}\sigma'}{2}\right\}\right) \tag{iv}$$

$$\sigma_1(\rho) = \left\{-\frac{\alpha\rho^{n+1}}{4}\frac{(n+2)}{(n+1)} + \frac{n\alpha\rho^{n-2}}{\bar{p}^3}b(\rho) - \frac{U(\rho)}{\bar{p}}\right\}\sigma' - \alpha\rho^n\sigma$$
$$+\left(\frac{n\alpha\rho^{n-1}}{2\bar{p}^2}\right)^3\left[4n\frac{d}{d\rho}\left(\frac{\sigma'}{\rho}\right) + \rho^2\frac{d}{d\rho}\left(\frac{1}{\rho}\frac{d}{d\rho}\left(\frac{\sigma'}{\rho}\right)\right)\right] \tag{v}$$

$$\sigma_2(\rho) = \frac{1}{3}\left(\frac{n\alpha\rho^{n}}{2\bar{p}^2}\right)^3\frac{1}{\rho}\frac{d}{d\rho}\left(\frac{1}{\rho}\frac{d}{d\rho}\left(\frac{\sigma'}{\rho}\right)\right) \tag{vi}$$

$$\frac{1}{\rho}\frac{d}{d\rho}(\rho g) + \frac{nf}{\rho} = \sigma_1(\rho) \tag{vii}$$

$$\frac{1}{\rho}\frac{d}{d\rho}(\rho f) + \frac{ng}{\rho} = -\left\{\alpha\rho^n\sigma(\rho) - \frac{\bar{p}^2}{n^2}\rho\frac{d}{d\rho}(\rho U)\right\} \tag{viii}$$

$$- \frac{1}{3n\rho} \frac{d}{d\rho} \left(\rho \frac{d}{d\rho} (\rho W) \right) + \frac{3n}{\rho} W = \sigma_2 (\rho) \qquad \text{(ix)}$$

$$\frac{1}{\rho} \frac{d}{d\rho} (\rho A) - \frac{B(\rho)}{\rho} = - b(\rho) \qquad \text{(x)}$$

$$- b^*(\rho A'' + 3A') + \rho A\sigma' + 2\rho P' - b^*b$$

$$+ \frac{n\bar{\alpha}^2 \rho^{2n-1}}{4\bar{p}^3} \sigma' \left[5n + (n+1)\nu + \frac{(n-1)\delta}{\rho^2} \right] = 0 \qquad \text{(xi)}$$

where b^* is defined after eqn. (2.3.4,9).

(2.3.4,6i-xi)

In the absence of an Ohmic heating current, $\sigma = 0$ and so we are able to set $b_\beta = -P$, whereupon the only non-trivial relations remaining are those governing A and B, all the other quantities being zero. We may solve these relations analytically for some special choices of the pressure profile, and we return to this point presently.

We now show how these results may be derived in a more intuitive fashion.

The solution obtained for (2.1.1ii) is

$$\hat{\underset{\sim}{J}} = \frac{ga\,\underset{\sim}{J}}{B_o} = g\,h\,\underset{\sim}{b} + \frac{\underset{\sim}{b} \times \hat{\nabla}\hat{P}}{\underset{\sim}{b}^2}$$

$$g\,\underset{\sim}{b} \cdot \hat{\nabla} h = - \left(\underset{\sim}{b} \times \hat{\nabla}\hat{P}\right) \cdot \hat{\nabla}\left(\frac{1}{\underset{\sim}{b}^2}\right) \qquad (2.3.4,7)$$

Using (2.1.1ii,iii) and the above orderings we may write

$$h = \lambda^3 h_c^{(3)} + \lambda^4 h_c^{(4)} + \lambda^5 h_c^{(5)} + \lambda^6 h_c^{(6)} + \lambda^6 h_p^{(6)} + \ldots.$$

where h_c, h_p are defined by

$$g\,\underset{\sim}{b} \cdot \hat{\nabla} h_p = - \left(\underset{\sim}{b} \times \hat{\nabla}\hat{P}\right) \cdot \hat{\nabla}\left(\frac{1}{\underset{\sim}{b}^2}\right)$$

$$g\,\underset{\sim}{b} \cdot \hat{\nabla} h_c = 0 \qquad (2.3.4,8)$$

In order to indicate the significance of the various terms in (2.3.4,6), the equation (2.3.1,1) must be solved for ψ. Once we know ψ, we also have h_c as a function of the lowest order force free current, $\sigma(\rho)$. (2.1.5) gives an expression for the only other current apart from the diamagnetic current, and combining these three the total plasma current may be found. The non-vacuum contributions to the field may be derived from a knowledge of these currents, and combined with the known vacuum field to find the total magnetic field. It is then possible to compute ψ, which was originally presumed known. The solution may thus be shown to be self-consistent. We now consider how a similar program permits an iterative solution of the problem.

As the effects of plasma pressure and current on ψ are small ($O(\varepsilon)$) in this ordering scheme, a knowledge of the vacuum fields allows ψ to be calculated to $O(\lambda^2)$. This is sufficient accuracy for the pressure profile to be determined to the required order, and almost sufficient for h_c to be similarly fixed, both as functions of some

arbitrarily specified lowest order profile, which in each case is a function of ρ only. If we take the expressions for the currents which we thus obtain and find their fields, we may determine ψ to sufficient accuracy to complete the solution of the problem.

We now show that the solution we have obtained satisfies the criteria for the above method of solution to be consistent and to have been carried far enough. We compute ψ for the fields (2.3.4,5) and hence the plasma currents. From these currents, we are able to show that these fields are indeed the right ones.

The solution proceeds exactly as indicated above for the vacuum field. The main difference is that the force-free current, h_c, gives rise to a poloidal field in $O(\varepsilon)$, $\varepsilon b(\rho)$. The integrability condition which arises in each order now has the form

$$\frac{b^*(\rho)}{\rho}\frac{\partial\bar{\psi}^{(n)}}{\partial\theta} = g(\rho,\theta) \qquad (2.3.4,9)$$

where $b^*=b(\rho)+bo$,

$$b_o = -\frac{n^2(n-1)\alpha^2}{\bar{p}^3}\rho^{2n-3}$$

$b(\rho)$ is the actual poloidal field due to the lowest order plasma current, suggesting that the second term, which is due to the Stellarator part of the field, represents an effective poloidal field due to the Stellarator transform. This indicates that the total effective poloidal field is b^*. It may thus be anticipated that the rotational transform is

$$i = \frac{b^*}{\rho} = \frac{b(\rho)}{\rho} + i_{vac} \qquad (2.3.4,10)$$

$$i_{vac} = -\frac{n^2(n-1)\alpha^2}{\bar{p}^3}\rho^{2n-4}.$$

The solution for ψ to third order is given by (2.3.3,6) plus the third order term:

$$\lambda^3\Big\{ \rho\frac{\psi_o'}{b^*}\cos\theta\Big[A(\rho) + \alpha^2\rho^2(n-1)\,\frac{n}{4\bar{p}^3}\left(5n + (n+1)\gamma + \frac{(n-1)\delta}{\rho^2}\right)\Big]$$

$$+ \pi_1(\rho)\sin(n\theta+s) + \pi_2(\rho)\sin 3(n\theta+s)\Big\} + O(\lambda^4) \qquad (2.3.4,11)$$

where

$$\pi_1(\rho) = \left\{ -\frac{\alpha\rho^{n+1}}{4}\,\frac{(n+2)}{(n+1)} + \frac{n\alpha\rho^{n-2}}{\bar{p}^3}\,b(\rho) - \frac{u(\rho)}{\bar{p}}\right\}\psi_o'$$

$$+ \left(\frac{n\alpha\rho^{n-1}}{2\bar{p}^2}\right)^3\left[4n\,\frac{d}{d\rho}\left(\frac{\psi_o'}{\rho}\right) + \rho^2\,\frac{d}{d\rho}\left(\frac{1}{\rho}\,\frac{d}{d\rho}\left(\frac{\psi_o'}{\rho}\right)\right)\right]\Big\}$$

$$\pi_2(\rho) = \frac{1}{3}\left(\frac{n\alpha\rho^n}{2\bar{p}^2}\right)^3\,\frac{1}{\rho}\,\frac{d}{d\rho}\left(\frac{1}{\rho}\,\frac{d}{d\rho}\left(\frac{\psi_o'}{\rho}\right)\right)$$

Note that ψ_o' must vary with ρ at least as fast as b^*, if this third order term is to regular at the origin. As the pressure profile is expressible in the form $P=P(\psi)$, one may expect that the 1-number will influence the pressure profiles which may be supported in the various systems appropriately.

(Specialising to 1=3, and retaining only vacuum field terms, taking $\gamma = \delta = 0$, this is the expression obtained in [26].)

Setting $h_c^{(3)} = \sigma$, the force-free current is given by (2.3.3,6) and (2.3.4,11) with $\psi^{(o)}(\rho) = \sigma(\rho)$.

The method of averaging applied to (2.3.4,8) yields an integrability condition in ninth order,

$$h_p^{(6)} \equiv h_p^{(6)}(\rho, \theta) \quad \text{and} \quad \frac{b^*(\rho)}{\rho} \frac{\partial h_p^{(6)}}{\partial \theta} = -2P'(\rho) \sin\theta \qquad (2.3.4,12)$$

thus

$$h_p^{(6)} = 2\rho \frac{dP}{d\rho} \cos\theta / b^* \qquad (2.3.4,13)$$

which is commonly referred to as the Pfirsch-Schluter current, being the return flow necessary for divJ=0 to be satisfied, in the presence of the diamagnetic current.

The relations (2.3.4,6) are obtained by equating curl B to these currents, whilst ensuring that divB=0. The remaining terms are from the vacuum field, as may be seen by comparison with (2.3.2,6).

2.3.5 Boundary Conditions and Vertical Field

In order to complete the solution to the appropriate order, and, in particular, to relate the quantities (2.3.4,6) to the applied vertical field, one may apply the exterior boundary condition on the fields, making use of the "virtual casing principle", [34].

The calculation which is summarised here was performed, for l=3, by P.J.Fielding, and is described in some detail in appendix One. In this section we describe the technique employed, and present the important results, (having generalised that calculation to arbitrary l-number).

Suppose that the plasma column is enclosed by a perfectly conducting casing, the casing being coincident with a flux surface. The vacuum fields within the enclosed volume are produced by currents flowing in this casing, outside which there are no fields. The currents in the surface, which also include image currents, are given by

$$\underset{\sim}{I} = \frac{\underset{\sim}{B} \times \hat{n}}{\mu_o} \qquad (2.3.5,1)$$

where $\hat{n}$ is outward normal to the casing, given by

$$\hat{n} = \nabla\psi / |\nabla\psi| \qquad (2.3.5,2)$$

Note that these currents alone, calculated assuming the presence of a plasma would, if the plasma were removed, give rise to fields exterior to the casing.

In the absence of such a casing, the vacuum fields must be produced by discrete conductors outside the column. However, within any given surface the equilibrium would be unchanged if the discrete conductors were replaced by a casing of the above type, coincident with the chosen surface. This is the "virtual casing principle", which we shall now employ.

Transforming to coordinates $\{\rho', \theta', \xi\}$ centred on the new magnetic axis, (and dropping the ' on ρ', θ') we obtain $\rho(\psi)$ in the form:

$$\rho(\psi,\theta,\bar{s}) = \rho_o(\psi) + \lambda \frac{n\alpha\rho_o^{n-1}}{\bar{p}^2} \sin(n\theta+s) + \lambda^2 \left(\frac{n\alpha\rho_o^{n-1}}{\bar{p}^2}\right)^2 \frac{(2n-1)}{2\rho_o} \sin^2(n\theta+s)$$

$$+ \lambda^3 \left[- \left[\Delta(\rho_o) + \frac{\alpha^2 \rho_o^{2(n-1)} n}{b^*(\rho_o) 4\bar{p}^3} \left(5n + (n+1)\gamma + \frac{(n-1)\delta}{\rho_o^2}\right)\right] \cos\theta \right.$$

$$\left. + \left(\frac{U(\rho_o)}{\bar{p}} - \frac{n^2 \alpha \rho_o^{n-2}}{\bar{p}^3} b(\rho_o)\right) \sin(n\theta+s) + \cdots \right] \qquad (2.3.5,3)$$

where terms of order εi_{vac} have been omitted.

The main part of the current in (2.3.5,1) gives rise to the vacuum field, b_{vac}. We wish to find the field produced by the remainder of the surface current,

$$\underset{\sim}{i}_r = \{(\underset{\sim}{b} - \underset{\sim}{b}_{vac}) \times \hat{n}\}_{\rho(\psi,\theta,\bar{s})} = \{b_{eq} \times \hat{n}\}_{\rho(\psi,\theta,\bar{s})} \qquad (2.3.5,4)$$

(which field may be non zero outside the shell).

We must solve the magnetostatic equations, (2.1.1.i,ii), order by order, for the fields b_i, b_e, in the interior and exterior domains respectively.

The matching conditions at the "shell" are:

$$[\underset{\sim}{b}_I \cdot \hat{n}] = 0 \qquad (2.3.5,5)$$

and

$$[\underset{\sim}{b}_I \times \hat{n}] = - \underset{\sim}{i} \qquad (2.3.5,6)$$

with

$$\underset{\sim}{i} = \underset{\sim}{b} \times \hat{n} \qquad (2.3.5,7)$$

The behaviour of the field at large distances from the shell provides restrictions on the solutions. In the interior regularity at the magnetic axis is implied. To find the correct behaviour in the exterior domain, we again make use of Toroidal coordinates $\{\eta, \tau, \xi\}$ described by (2.3.2,1). For large η these are related to our quasi-cylindrical coordinates by

$$\begin{aligned} a\rho = r &= 2R_o e^{-\eta} \{1 + \cos\tau\ e^{-\eta} + O(e^{-2\eta})\} \\ \sin\theta &= \sin\tau \{1 + \cos\tau\ e^{-\eta}\} \\ \cos\theta &= -\cos\tau \{1 - e^{-\eta} \tan^2\tau \cos\tau \ldots\} \end{aligned} \qquad (2.3.5,8)$$

We now consider the form of the fields, in the exterior region. Expanding the $P^m_{n-\frac{1}{2}}(\cosh\eta)$ (which is the solution form appropriate to the exterior) in these coordinates we find that to lowest order the

(j,n)th. Fourier component of the potential is:

$$\varphi_n^{(j)} = \epsilon^{(j/3+1)} (A_{no}^{(j)}/\rho^n)\ e^{i(j\bar{s}+n\theta)} \qquad (2.3.5,9)$$

The axisymmetric part of the casing current produces a field which can be represented by a stream function χ such that

$$\frac{\partial}{\partial\eta}\left(\frac{1}{R}\frac{\partial\chi}{\partial\eta}\right) + \frac{\partial}{\partial\tau}\left(\frac{1}{R}\frac{\partial\chi}{\partial\tau}\right) = 0 \qquad (2.3.5,10)$$

where

$$\underset{\sim}{B} = B_o(\hat{\nabla}\chi \times \hat{\xi})/g^2 \qquad (2.3.5,11)$$

By making the substitution [35]

$$\chi = F(\eta,\tau) \Big/ \sqrt{\cosh\eta - \cos\tau} \qquad (2.3.5,12)$$

we find

$$F(\eta,\tau) = \sum_{n=0}^{\infty}\left\{A_n \frac{d}{d\eta} P_{n-\frac{1}{2}}(\cosh\eta) + B_n \frac{d}{d\eta} Q_{n-\frac{1}{2}}(\cosh\eta)\right\} \times \sinh\eta\ e^{in\tau} \qquad (2.3.5,13)$$

By applying the boundary condition at infinity, we see that only the first of these contributes to $F(\eta,\tau)$, the other being divergent as η tends to zero.

Reverting to the quasi-cylindrical coordinates and expanding in powers of ε, we find

$$\chi = \varepsilon K_o\left\{\left(2 + \ell n\frac{\rho\varepsilon}{2}\right) - \varepsilon\cos\theta\left[\frac{1}{2}\rho\left(1 + \ell n\frac{\rho\varepsilon}{8}\right) + \frac{K_1}{\rho}\right]\right\} + O(\varepsilon^3) \qquad (2.3.5,14)$$

We may make comparison between these forms and those of the

solutions obtained in the interior region, and so obtain the correct boundary conditions on the latter. Details of the calculation at each order are given in appendix one. We illustrate the method by considering the order in which we are primarily interested, the sixth, which governs the axisymmetric part of the field.

The jump conditions (2.3.5,5) and (2.3.5,6) show that

$$\left[\left\langle b_{I\rho}^{(6)}\right\rangle\right] = - A(\rho_b) \sin\theta \qquad (2.3.5,15)$$

and

$$\left[\left\langle b_{I\theta}^{(6)}\right\rangle\right] = \cos\theta\left\{- B(\rho_b) + \rho_b\sigma_b(\rho_b)\left[A(\rho_b) + \frac{\mu\ \alpha^2}{4\bar{p}^3}\ \rho_b^{2n-2}\right]\Big/ b^*(\rho_b)\right\} \qquad (2.3.5,16)$$

where $\langle x\rangle$ indicates the s-average of x . $\mu = (5n+(n+1)\gamma+(n-1)\delta/\rho_b{}^2)n$.

Now the axisymmetric part of the field may be shown from the magnetostatic equations to be, in the interior,

$$b_{I\rho}^{(6)} = A_i^{(6)} \sin\theta$$

$$b_{I\theta}^{(6)} = A_i^{(6)} \cos\theta \qquad (2.3.5,17)$$

and in the exterior

$$b_{I\rho}^{(6)} = \left\{A_e^{(6)} - B_e^{(6)}/\rho^2 + \frac{1}{2}\rho_b b(\rho_b)(1+\ell n\rho)\right\}\sin\theta$$

$$b_{I\theta}^{(6)} = \left\{A_e^{(6)} + B_e^{(6)}/\rho^2 + \frac{1}{2}\rho_b b(\rho_b)\ \ell n\rho\right\}\cos\theta\ . \qquad (2.3.5,18)$$

In order to obtain A_i, however, we need a third relation, there being three unknowns in these equations, (the jump conditions only giving the difference, $A_e - A_i$).

The exterior solution (2.3.5,14) provides the required information. Using the above form for χ we are able to make the

identifications

$$A_e^{(6)} = \frac{1}{2}\,\rho_b b(\rho_b)\,\ell n\,\frac{\varepsilon}{8}$$

$$K_o = -\,\rho_b b(\rho_b) \qquad (2.3.5,19)$$

and so finally obtain

$$B_{-v} = \frac{\varepsilon^2 B_o}{2}\left\{A(\rho) + \frac{d}{d\rho}\,(\rho A(\rho)) + \rho\, b(\rho)\left(\frac{3}{2} + \ell n\,\left(\frac{\varepsilon\rho}{8}\right)\right)\right.$$

$$\left. - \frac{\rho\sigma(\rho)}{b^*}\left[A(\rho) + \frac{\alpha^2\rho^{2(n-1)}n}{4\bar{p}^3}\left(5n+(n+1)\gamma + \frac{(n-1)\delta}{\rho^2}\right)\right]\right\}_{\rho=\rho_b} \qquad (2.3.5,20)$$

where ρ_b is the lowest order radius of a (closed) flux surface, outside the plasma.

With this result, the determination of the equilibrium up to sixth order in λ is complete. When $\alpha = 0$, this also reduces to the Tokamak result given in [33].

When $\sigma = 0$, (2.3.4,6) gives

$$-\frac{2\bar{p}^3\rho^{2(3-n)}}{n^2(n-1)\alpha^2}\,\frac{dP}{d\rho} = \frac{d}{d\rho}\left(\rho^3\,\frac{dA}{d\rho}\right)$$

and using $P=P(f)$, where f is given by

$$f = \int_0^\rho b^*(\rho)\,d\rho$$

to ensure that P is regular at the origin (see above), we choose

$$P = P_o \left(1 - (\rho/\rho_a)^{2(n-1)}\right)$$

and find

$$A(\rho) = A_o - \frac{P_o}{i_a} \frac{(n-1)}{2} \left(\frac{\rho}{\rho_a}\right)^2$$

where ρ_a is the plasma boundary radius and i_a is the rotational transform at ρ_a.

Finally, the vertical field becomes

$$B_v = \frac{\varepsilon^2 B_o}{2} \left\{A(\rho) + \frac{d}{d\rho} (\rho A(\rho))\right\}_{\rho=\rho_b}$$

so

$$\frac{B_v}{\varepsilon^2 B_o} = A_o - \frac{P_o(n-1)}{i_a}$$

2.3.6 Equilibrium Quantities

A number of important characteristics of these equilibria may now be computed.

The rotational transform may be found, either from

$$i = \frac{1}{2\pi} \frac{d\chi}{d\phi}$$

where χ (ϕ) is the poloidal (toroidal) flux, or from the method of averaging, [1]. In either case, (2.3.4,10) is confirmed.

The position of the axis is found using the fact that

$$\nabla\psi = 0$$

at the axis. We rewrite ψ as

$$\psi = \psi_o \left(f + \lambda^3 \rho \cos\theta \left\{ A(\rho) + \alpha^2 \rho^{2(n-1)} \frac{n}{4\bar{p}^3} \left(5n + (n+1)\gamma + \frac{(n-1)\delta}{\rho^2} \right) \right\} \right) \qquad (2.3.6,1)$$

where

$$f = \int_o^\rho b^*(\rho)\, d\rho \qquad (2.3.6,2)$$

and where we have omitted helical terms, (valid near the axis for $n > 1$).

To the required accuracy, the axis has coordinates $\{ \rho_x, \pi \}$, where

$$b^*(\rho_x) = \lambda^3 \frac{d}{d\rho} (\rho A(\rho)) \Big|_{\rho=\rho_x} + \lambda^3 \frac{(2n-3)}{4n} \delta i_{vac} \qquad (2.3.6,3)$$

The last term is only necessary for 1=2, where it contributes a small, uniform shift to all the surfaces. We neglect it henceforth.

If we also define $\Delta(\rho) = \rho A(\rho)/b^*$, then provided $\Delta(o) \sim 0(1)$ e.g. when $A_o = 0$, (2.3.6,3) becomes

$$b^*(\rho_x - \lambda^3 \Delta(\rho)) = 0 \qquad (2.3.6,4)$$

The solution is then $\rho_x = \lambda^3 \Delta(o)$, to lowest order. In terms of $\Delta(\rho)$, (2.3.4,6xi) becomes

$$b^{*2}\Delta'' + b^*(2b^{*\prime} + \frac{b^*}{\rho})\Delta' + b^*\Delta \frac{d}{d\rho}\left(\frac{1}{\rho}\frac{d}{d\rho}(\rho b_o)\right)$$

$$= 2\rho P' - b^* b + \alpha^2 \rho^{2(n-1)} \frac{n}{4\bar{p}^3} \sigma' \left(5n + (n+1)\gamma + \frac{(n-1)\delta}{\rho^2} \right) \qquad (2.3.6,5)$$

which is the toroidal shift equation [33], when $\alpha = 0$, $\lambda^3 \Delta(o)$ being the axis shift.

Using $q'/q = (1/\rho - b^{*\prime}/b^*)$ we have

$$\Delta'' + \frac{3\Delta'}{\rho_o} - \frac{2\rho_o P'}{b^{*2}} = -\frac{b}{b^*} + \frac{\sigma'}{\rho_o^2 b^*}\,\Omega(\rho_o) + 2\Delta'\,\frac{q'}{q} - \frac{\Delta}{b^*}\,\frac{d}{d\rho_o}\,\frac{1}{\rho_o}\,\frac{d}{d\rho_o}\,(\rho_o b_o) \qquad (2.3.6,6)$$

with

$$\Omega(\rho_o) = \frac{n\alpha^2 \rho_o^{2n}}{4\bar{p}^2}\, q\left[5n + (n+1)\,\gamma + \frac{(n-1)\,\delta}{\rho_o^2}\right] \qquad q = \frac{\rho_o}{b^*(\rho_o)} \qquad (2.3.6,7)$$

For l=2 the term in Δ is zero, and in this case a first integral may be obtained:

$$\Delta' = \frac{1}{\rho_o b^{*2}} \int_0^{\rho_o} \left[2\rho P' - b^* b + \frac{\sigma'}{\rho^2}\, b^* \Omega(\rho)\right] \rho d\rho \qquad (2.3.6,8)$$

If A_o is not equal to zero, and the lowest order current, σ , is zero,

$$\rho_x = \varepsilon^{1/(2n-3)} \left| \frac{A_o \bar{p}^3}{n^2(n-1)\alpha^2} \right|^{1/(2n-3)} \qquad (2.3.6,9)$$

2.4 Discussion

These theoretical results have been applied to the calculation of equilibria for two recent experiments, WVII and CLEO. We now describe the equilibria we obtain and discuss the relative merits of various l-numbers. Finally, we consider how these results might be extrapolated to reactor conditions.

Figures 2.2 and 2.3 depict theoretical WVII flux surfaces for peak beta of 1% and 2% respectively, without an externally applied field. The flux surfaces are distorted only slightly, at these beta values. In this case, i= 0.4 and A=20.

The equilibrium beta scales as i^2/A, a commonly quoted result

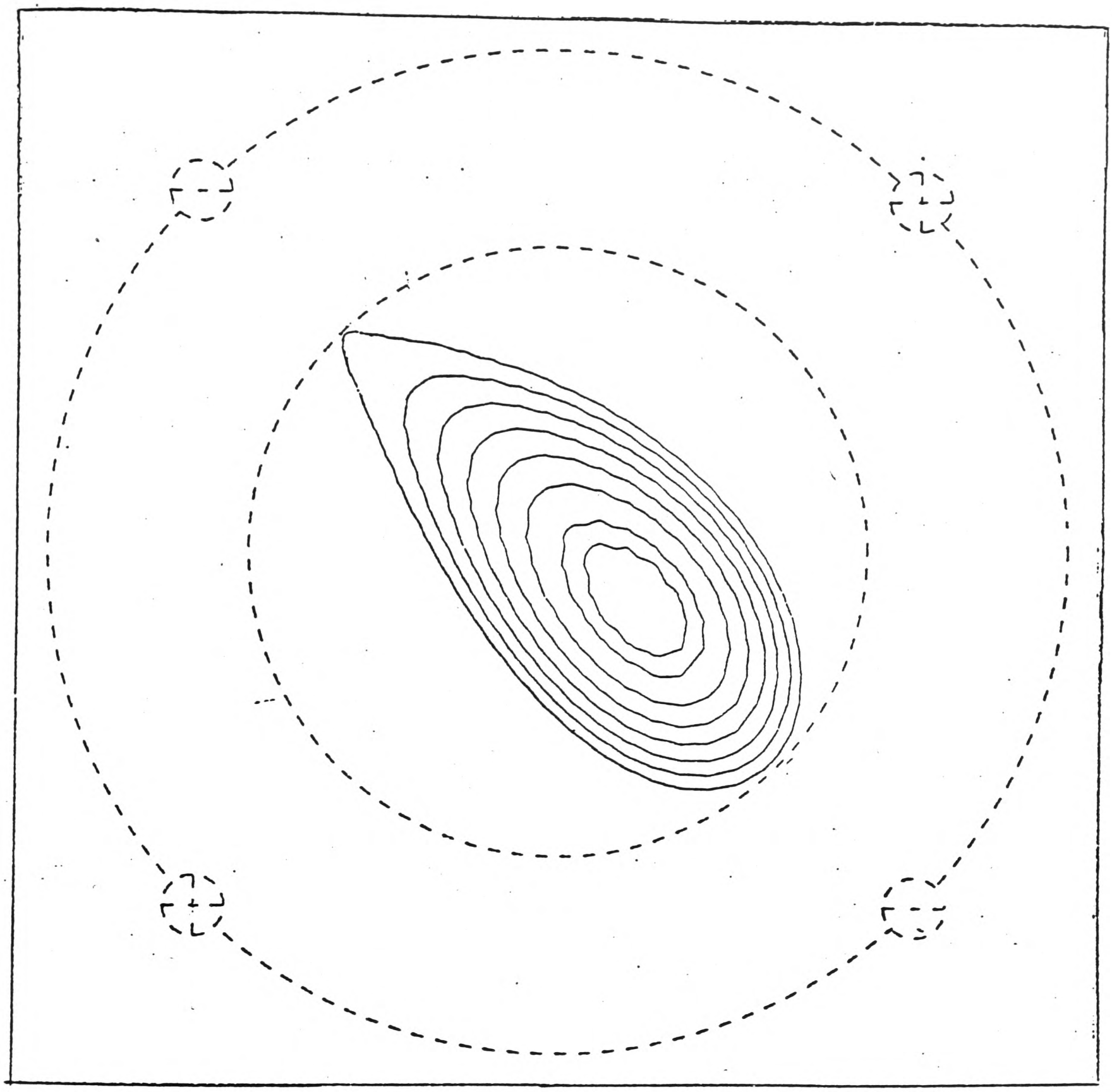

Fig 2.2 WVII flux surfaces for $i = 0{\cdot}5$, $\beta \sim 1\%$, $B_v = 0$. The torus axis is to the left of the figure, the location of the stellarator windings in this cross-section and their polarity (+into the paper) being indicated on the outer circle (dashed). The limiter radius is given by the inner dashed circle.

which may derived in a semi-quantitative fashion from the expressions for the flux surfaces (2.3.3,6) and(2.3.4,11) given above.

We may obtain the beta limit, from this form, either by finding

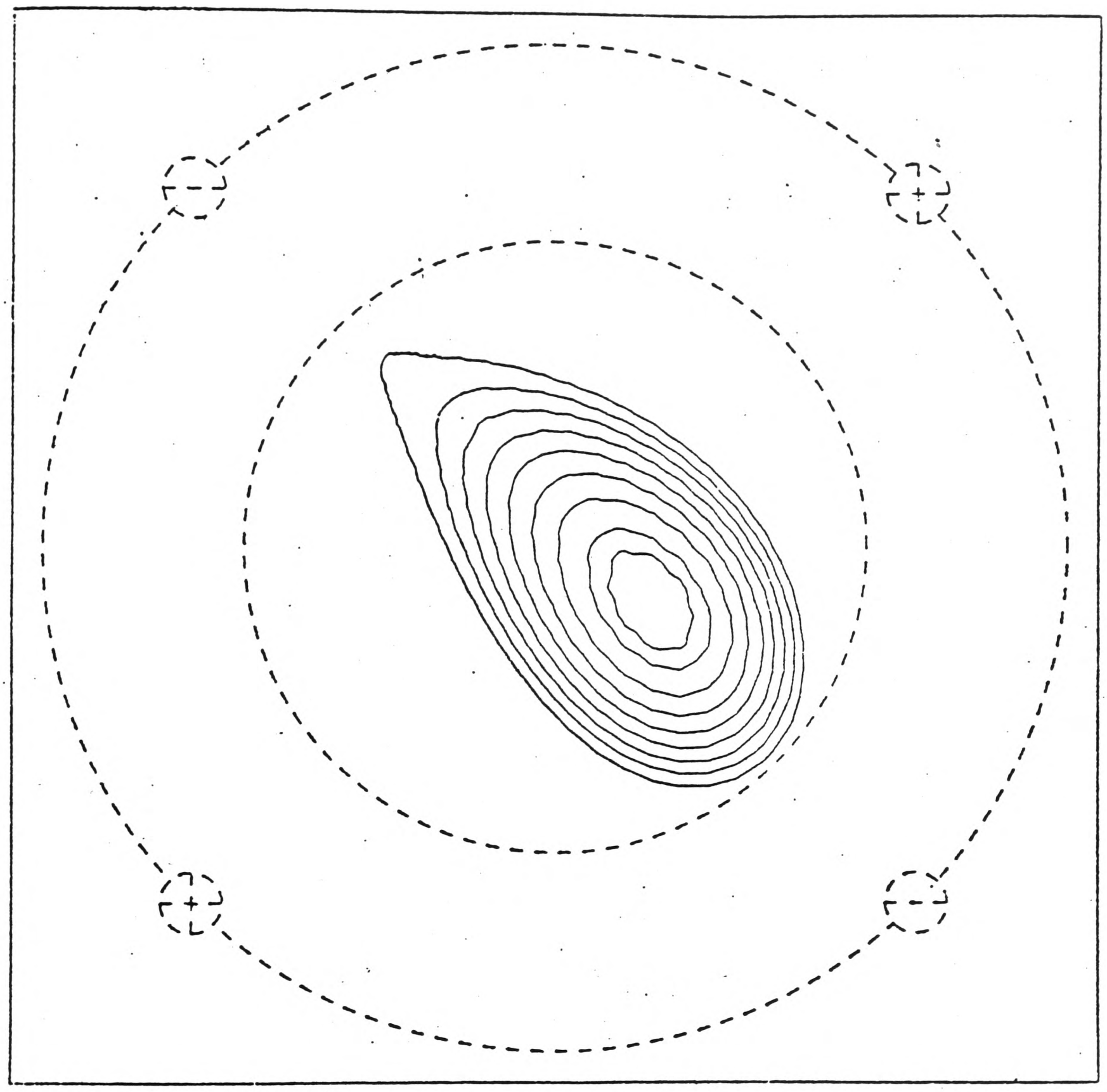

Fig 2.3 WVII flux surfaces for $i = 0{\cdot}5$, $\beta \sim 2\%$, $B_v = 0$. Although β is twice as large as in the case of fig.2.2, the flux surface displacements are only slightly greater.

the axis shift, which we have already done, and demanding that it be less than the minor radius, or by searching for stagnation points in the magnetic surfaces and finding the conditions for which they encroach upon the plasma. The results are similar, in either case. We shall adopt the latter course, to facilitate comparison with other work.

The stagnation point occurs at $\nabla\psi = 0$. To find the point at which increasing plasma pressure permits this condition to be satisfied at the boundary, we allow the term in $A(\rho)$ to balance the lowest order term, for finite values of ρ. For this to occur, we must have that $\varepsilon\, qA(\rho) \sim O(1)$, which implies that $P_o \sim i^2 A$, or $\beta = i^2/A$, (A being the aspect ratio).

As we shall demonstrate in chapter five that $i \sim 0.5$ is possible in a device with $A = 7$, then we may expect, extrapolating using the above scaling, that beta values of 6-8% should be possible in such a device without a significant loss of plasma volume.

An important ingredient in the calculation of the stagnation points, which has been omitted from this argument, is the role of the vacuum field in locating the separatrix.

From Figs. 2.2 and 2.3, we see that as beta goes from 1% to 2%, the tip of the elliptical separatrix surface which is on the inside of the torus (and which is very close to its vacuum position in the former case) begins to encroach upon the plasma. The position of the stagnation point is clearly, even at this rather high beta value, determined largely by the vacuum fields.

The vacuum separatrix position depends crucially on the terms of higher order in ε and ρ, - indeed, in the case of CLEO, where the separatrix position is known from field line following, we had to include terms up to fourth order in λ, (which involved very high powers of ρ) to obtain agreement. (The necessity to include such terms depends on the choice of $\psi^{(o)}$ employed, for with a suitable admixture of small terms in $\psi^{(o)}$,

the vacuum result may be written as the square of an expression containing terms up to $O(\varepsilon)$. The square then contains terms which are formally smaller than we should retain, but which are important to obtain the correct separatrix position. See appendix One.)

It is of interest to note that the magnetic axis appears, when other values of s are considered, to spiral in the case where beta is non zero. This behaviour is predicted, if we include higher order terms in (2.3.6,3)for $\rho_x \simeq \lambda^3\Delta(0)(1+\frac{4\alpha\lambda}{\bar{p}^2}\sin s)$. As $\lambda \sim 0.5$ in WVII, this is a substantial effect, being of the order of half the axis shift.

In a simple 1=2 Stellarator, with $\sigma = 0$, the only way that ρx can be made to remain constant is to set $\Delta(o) = 0$, i.e. $A_o = 0$. This implies a substantial externally applied vertical field, in general, and so the calculation of Lortz and Nuhrenberg, [36], which assumed a circular magnetic axis, is less general than they had supposed. This last work has had a considerable impact upon attitudes to certain Stellarator configurations, and so we shall discuss it in more detail.

Lortz and Nuhrenberg employed a Mercier expansion of the equilibrium quantities about an assumed circular magnetic axis, in [36], to study the equilibrium and stability of plasma in an 1=2 Stellarator, (this being a special case of the equilibria they considered in [24]). They found optimised profiles for the case of no net toroidal current and for the parameters of WVII, by allowing for an equilibrium beta limit set by the presence of stagnation points in the flux function and a stability limit due to instabilities of the Mercier type.

Apart from their having artificially limited their discussion to cases with circular axes, which form a rather special, small, subset of the possible equilibria, there must also be doubts about their calculation

of the stagnation point positions, for they carry their Mercier expansion up to third order only. In defence of their calculation they point out that, in their experience of Tokamak calculations, the fourth order term was not capable of shifting the stagnation points found in third order by much. We have seen, however, that in the Stellarator calculation presented above, it was crucial to include terms of much higher order still, to obtain correct results.

For these reasons, we believe that the stagnation points are not described correctly by such a treatment, and that, in any case, the space within which their optimisation was performed was unduly restricted. Their results (which they summarised by predicting that the maximum stable beta in WVII was between 1/3 and 2/3%) are probably unduly pessimistic, therefore.

We shall not examine the stability criteria which these authors employ in detail. It is tempting to speculate, however, that the neglect of the spiralling of the axis from their calculation for WVII may have adversely affected their predicted lower bounds on stable beta, even neglecting the effect on the equilibrium properties of the configuration. For they have argued in more recent (unpublished) work for the use of systems with spiralling axes, although they assume that external fields supply such an effect, in their calculations, and, as we shall see, this spiralling does give rise to additional magnetic well.

Fig. 2.4 shows CLEO flux surfaces, for beta of 1% and the same peak transform. Despite CLEO having an aspect ratio which is half that of WVII, the loss of surfaces is much more marked in CLEO. This is attributable to the low transform in the middle of the l=3 system. An applied vertical field (which is undesirable in a reactor because of the difficulty of construction) is capable of recentring the plasma, but only

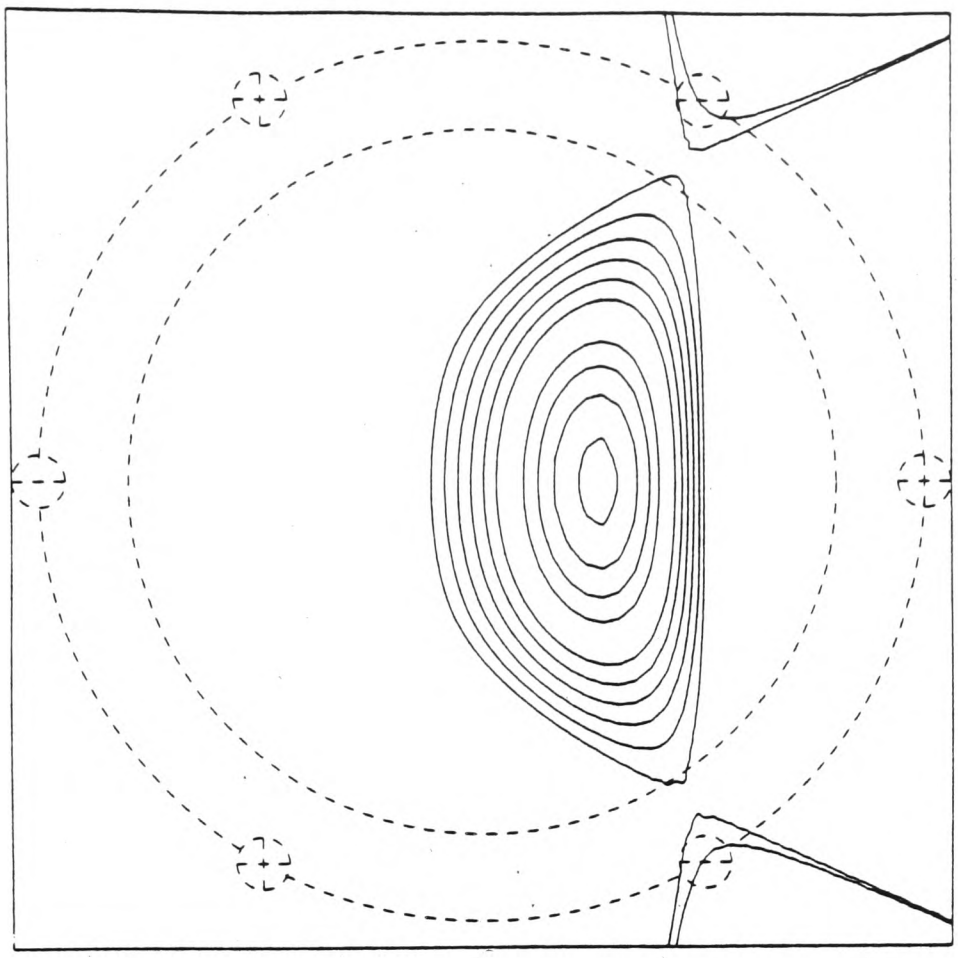

Fig. 2.4 CLEO surfaces for β = 1%

at the cost of destroying most of the surfaces. A compromise between restoring the axis position and retaining the surface structure is shown in Fig. 2.5, where a reduced vertical field has been applied. This probably represents the optimum operating configuration for an 1=3 Stellarator with finite beta. The substantial shifts of the inner surfaces mean that most of the plasma lies on one side of the device. Very little increase in beta could be sustained, in this configuration.

The equilibrium properties of the Stellarator which we have investigated seem to be reasonably well confirmed experimentally in the very few places where checks are possible: see for instance appendix one, Fig. 7 . Thus the theoretical comparison of 1=2 and 1=3 equilibria is quite significant.

As we have seen that 1=2 is capable of providing satisfactory equilibria, probably even at high aspect ratio without the use of an applied vertical field (which, as noted above, is undesirable for a Reactor) then it has a definite advantage over 1=3, which does not provide

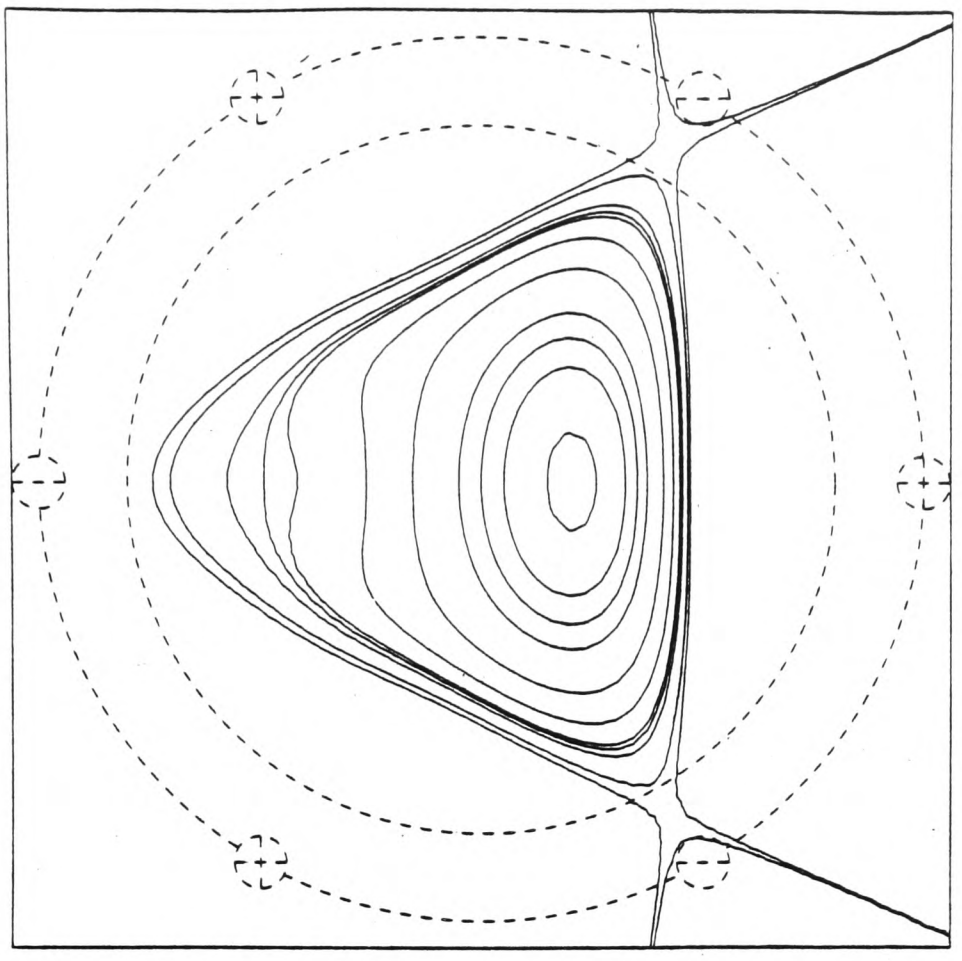

Fig 2.5 As Fig 2.4, with applied B_V

satisfactory equilibria without a vertical field, as beta is increased. What is more, even in the presence of such a field the surface distortions and destruction are substantial in l=3.

(The advantage which is normally claimed for l=3 is the shear of the system which theoretically stabilises interchanges on the time scale on which ideal instabilities alone are in evidence, and possibly prevents islands from having a very great width. The advantage claimed for an l=2/3 mixture is that it should combine the good features of both l=2 and 3, and provide additional magnetic well. Unfortunately, a device incorporating both harmonics in its field is less easy to build and will be argued against, in chapter five)

On the basis of our equilibrium calculations, then, we may conclude that an l=2 Stellarator is considerably better able to sustain high values of beta than an l=3 Stellarator of similar (peak) transform and aspect ratio. Further comparison will be made in chapter five, when more information on other aspects of the performance of the two devices is

available.

Chapter Three: Stability of Plasma in a Stellarator

When considering the suitability of a toroidal magnetic confinement system for containment of a thermonuclear plasma (say), and having determined an equilibrium configuration of the plasma in that system, it is necessary first to investigate the plasma stability on an "ideal" magnetohydrodynamic model. If stability is indicated, it is then appropriate to go on to consider non-ideal effects. In this chapter we shall be particularly concerned with the effects of resistivity on stability.

"Ideal" instabilities must be considered first, since they are the fastest growing instabilities which are likely to occur. Analytic stability criteria are known, for certain special types of ideal instability, and numerical techniques are able to bridge the gaps between these. Thus the required ideal M.H.D. stability analysis can be performed.

Having discussed ideal instabilities we shall consider, in particular, the effects of resistivity, as Stellarator configurations tend to have strong shear in the magnetic field, which is effective in stabilising ideal modes. Shear is not so effective on the time scale on which resistivity is important, and so it might be expected that the inclusion of resistivity in the theoretical model of the plasma could have a profound effect on predictions of plasma stability in Stellarators.

This chapter begins with a brief discussion of the types of instabilities which may occur in a plasma. Considering macroscopic instabilities, the energy principle is introduced and its role in describing "ideal M.H.D." modes is indicated. A form of the energy principle is quoted which shows the role of net toroidal current, and the combined role of plasma pressure gradients and field line curvature in driving such instabilities.

Restricting the discussion to "pressure driven" modes, which are the modes most likely to occur in a "pure" (i.e. current free) Stellarator, we consider the nature of two types of instability which have been studied analytically: "ballooning" modes, and modes of the Mercier type. The appropriate stability criteria are discussed.

Numerical results on Stellarator stability, which complement these analytic results, are mentioned. Although such work indicates that the most dangerous modes in a Stellarator may well be similar to those for which the Mercier criterion was derived, the criterion is itself usually satified in Stellarators. We limit our discussion to a qualitative one, therefore, indicating (for instance) the type of perturbation which is probably the most dangerous.

The effect of resistivity on these modes is considered. Using a result of Mikhailovskii, [37], (which may be shown to be the appropriate generalisation of the Mercier criterion to allow for finite resistivity, in the cases we wish to study) and the Stellarator equilibria of chapter two, a criterion for stability against resistive interchanges is evaluated for a Stellarator.

Finally, the status of stability theory is surveyed, and the role these results will play in the reactor design to be undertaken is discussed.

3.1 Plasma Instabilities

Plasma instabilities may be divided into two main classes: hydrodynamic or macroscopic and kinetic or microscopic. Macroscopic instabilities involve bulk motions of the plasma, all the charged particles acting collectively. Microscopic instabilities arise due to differences in the motions of particles in the same volume. They are

characterised by high frequencies and short wavelengths, as opposed to the larger scale, slower macroscopic instabilities.

We shall principally be concerned with treating the former class, as the macroscopic instabilities are likely to be the more catastrophic for plasma containment. The effect of the microinstabilities will probably be to give rise to enhanced diffusion and so they will be considered only briefly, under transport theory, in what follows.

A simplifying assumption which is frequently made in M.H.D. stability theory is the neglect of various non-ideal effects. This involves taking infinite conductivity, negligibly small Larmor radii for particles, isotropic pressure and so on. We shall begin by discussing so-called ideal M.H.D., where all of these assumptions are made: the ideal M.H.D. approximation, as defined by Kulsrud, [17], consists of representing the plasma as a single ideal fluid with infinite conductivity and an adiabatic equation of state. We follow this with a section on the effects of resistivity. The other non-ideal effects are in general less easy to treat than resistivity, and we shall indicate only briefly what their likely consequences will be.

Mathematically, the problem of M.H.D. stability may be reduced in a linear approximation to the investigation of small oscillations about the equilibrium state. There are two means of approaching this: one is the normal mode technique and the other involves the use of an energy principle. The latter is applicable when the operator $\underline{\underline{K}}$ appearing in the eigenvalue equation for the plasma displacement, $\underline{\xi}$,

$$\rho \ddot{\underline{\xi}} = \underline{\underline{K}} . \underline{\xi} \qquad (3.1,1)$$

is self adjoint. That is

$$\int \underline{\eta}.\underline{\underline{K}}.\underline{\xi}\, dV \quad = \quad \int \underline{\xi}.\underline{\underline{K}}.\underline{\eta}\, dV \qquad (3.1,2)$$

for any $\underline{\eta},\underline{\xi},\underline{Q},\underline{A}$ satisfying the boundary conditions. $\underline{\eta},\underline{\xi}$ are perturbations and $\underline{Q},\underline{A}$ are the corresponding vector potentials. This may be shown to be the case in ideal M.H.D., [38].

In a simple geometry the eigenvalue problem can be solved, but in general this is not easy to do, and so in order to study ideal M.H.D. stability we shall turn to the other approach.

3.2 The Energy Principle

The ideal M.H.D. equations describing linear perturbations about an equilibrium can be reduced to the form

$$\rho\, \ddot{\underline{\xi}} = \underline{\underline{K}}.\underline{\xi} \qquad (3.2,1)$$

The latter equation, multiplied by $\dot{\underline{\xi}}$ and integrated over the volume subject to the boundary condition $\xi_{\perp} = 0$, yields

$$\int \rho\, \dot{\underline{\xi}}.\ddot{\underline{\xi}}\, dV = \frac{\partial}{\partial t}\int \frac{1}{2}\rho\dot{\xi}^2\, dV = \int \dot{\underline{\xi}}.\underline{\underline{K}}.\underline{\xi}\, dV \qquad (3.2,2)$$

As the equations are self adjoint we see that

$$\frac{\partial}{\partial t}\int \left[\left(\frac{1}{2}\rho\dot{\xi}^2 - \frac{1}{2}\,\underline{\xi}.\underline{\underline{K}}.\underline{\xi}\right)dV\right] = 0 \qquad (3.2,3)$$

The quantity which has been shown to be constant can be shown to be the

total energy associated with the perturbation. The first term is the kinetic energy, and the second term, which we shall call δW, is the potential energy. Consequently any $\underline{\xi}$ which gives negative δW increases the kinetic energy and so the velocity perturbation grows - linear instability is indicated. Conversely, if no $\underline{\xi}$ exists for which $\delta W < 0$, the system is linearly stable.

Various forms for δW have been derived, the most widely used being that due to Bernstein et al. [39]. They write

$$\delta W = \delta W_f + \delta W_s + \delta W_v \tag{3.2,4}$$

where

$$\delta W_f = \frac{1}{2}\int dV\Big(\frac{1}{\mu}|B^1 + \mu\hat{\underline{n}}.\underline{\xi}\,\underline{J}^{\circ}\hat{\underline{x}}\hat{\underline{n}}|^2$$
$$+ \Gamma\, p^{\circ}|\nabla\cdot\underline{\xi}|^2 - 2\underline{J}^{\circ}\hat{\underline{x}}\hat{\underline{n}}.(\underline{B}^{\circ}\cdot\nabla\hat{\underline{n}})(\hat{\underline{n}}.\underline{\xi})^2\Big)$$

$$\delta W_s = \frac{1}{2}\int d\underline{S}.[\nabla\,(p^{\circ} + \frac{1}{2\mu}(\underline{B}^{\circ})^2)]\,(\underline{n}.\underline{\xi})^2 \tag{3.2,5}$$

$$\delta W_v = \frac{1}{2}\int dV\,\frac{1}{\mu}|\underline{B}^1|^2$$

(where Q° is an equilibrium quantity, Q^1 a perturbed one)

In these expressions, [x] describes the jump in x, $x_e - x_i$, across the plasma vacuum boundary. δW_f is the change in potential energy of the fluid due to the perturbation. δW_s is a surface integral which vanishes in the absence of surface currents. δW_v is an integral over a vacuum region which may exist outside the plasma. Only δW_f contributes in the cases we wish to study.

One interesting form for δW_f, [40], is

$$\delta W_f = \frac{1}{2}\int \left(\frac{1}{\mu}|\underline{B}_\perp^1|^2 + \mu\left|\frac{1}{\mu}\underline{B}_\parallel^1 - \frac{\underline{B}^0\underline{\xi}\cdot\nabla p^0}{|\underline{B}^0|^2}\right|^2 \right. \tag{3.2,6}$$

$$\left. + \Gamma p^0|\nabla\cdot\underline{\xi}|^2 + \frac{\underline{J}^0\underline{B}^0\underline{B}\times\underline{\xi}\cdot\underline{B}^1}{|\underline{B}^0|^2} - 2\underline{\xi}\cdot\nabla p^0\underline{\xi}\cdot\underline{\kappa} \right)$$

where $\underline{\kappa}$ is the normal curvature of the equilibrium field.

Each of the terms has an obvious interpretation: the first three all correspond to the energy of waves in the fluid plasma, (Alfven, fast magnetosonic and sound waves, respectively), and are incapable of going negative and so contributing a destabilising effect. The fourth is associated with kink instability, describing the potentially destabilising effect of an equilibrium current parallel to the equilibrium field. The class of instabilities for which the last term is responsible will be referred to as "pressure driven" instabilities in this thesis. This form indicates the combined role of pressure and field line curvature in driving such instabilities.

The current-driven modes (kinks or, in the presence of resistivity, tearing modes) are driven by the magnetic potential energy of the whole system, whereas pressure driven instabilities are driven by the local pressure gradient and field line curvature. The effects of a pressure driven instability are also local, therefore. Kinks, on the other hand, may carry the entire plasma to the wall.

In a Stellarator with no externally driven current, and ignoring the problematic "bootstrap current", the only the equilibrium current parallel to the field is the Pfirsch-Schluter current, which averages to zero over a flux surface. Representing a kink mode by a perturbation which varies with ξ but not across the minor cross section, then δW, when

the integration in (3.2,6) is performed, may be seen, in this case, to be zero. (The bootstrap current is considered in the next Chapter.) Thus current driven instabilities are not believed to pose a problem in Stellarators, the expected instabilities being pressure driven instabilities.

3.3 Pressure Driven Instabilities

It is not possible, in general, to determine the displacement $\underline{\xi}$ which will minimise δW: to make progress in the analysis of pressure driven instabilities it has therefore been necessary to impose somewhat artificial restrictions on the form of $\underline{\xi}$, i.e. to divide the instabilities into further categories in order that they may be studied mathematically. Stability criteria for each of the various sub-categories envisaged have then been derived, by minimising δW with respect to that class of displacement. Two such classes of instability will now be introduced, whose properties we may discuss in a semi-quantitative fashion: ballooning modes, and modes of the Mercier type. We shall then consider the conclusions which may be drawn from the numerical studies which are available, as to the effects of other types of perturbation.

3.4 Ballooning Modes

It was noted above that the field line curvature had a bearing on pressure driven instabilities. It is well known that for (in)stability the field lines should be (concave) convex to the plasma. However, in a toroidal system this situation cannot be everywhere realised. The connection length, L, between regions of good curvature is an important parameter with regard to stability against ballooning modes, [39],[41]. Ballooning modes are pressure driven instabilities which are localised in regions of bad curvature, the perturbation being capable of being represented as a superposition of components which vary slowly along a field line and rapidly perpendicular to it, and having a high toroidal wave number. (They are like aneurisms in a plastic bottle full of gas at high pressure, which grow at the weakest point, and in so doing weaken it still further.) This property could allow them to go unstable before modes which do not show this behaviour. As a result they are often described as the most dangerous instabilities, in that they may limit the achievable beta most of all in a tokamak.

In those papers, the parameter

$$\frac{r_p \, R_c}{L^2}$$

is introduced: r_p is the length scale on which the pressure varies and R_c is the mean radius of curvature. For stability, this parameter should be not very much less than one.

Taking $r_p = r/\beta$, $L = qR_m$, $R_c = R_m$ for a Tokamak, we obtain the usual result for the ballooning stability limit in a Tokamak. In Stellarators, the connection length can be shorter than this, so the ballooning limit may be less stringent.

We have seen that there is an equilibrium beta limit on the class of equilibria which we have considered, $\beta \sim O(i^2\varepsilon)$. We now have a ballooning stability limit, which is probably rather less stringent than the equilibrium limit, although similar in form. (Note that if we assume that ballooning modes arise when $\beta \sim O(i^2\varepsilon)$, the low-beta equilibria calculated above are formally ballooning stable.)

The connection between the two limits may be that when beta reaches this value the plasma is able to cause substantial changes in the equilibrium magnetic fields, and so a ballooning type instability would then appear likely. (The exact value of the maximum beta depends on the details of the fields, etc, [41], and so a certain amount of optimisation of profiles should be possible.)

It seems unprofitable to attempt to treat ballooning modes fully. One reason is that the equilibria which we could calculate would not be sufficiently accurate to give meaningful results. Another is that the analytic theory which has been applied to Tokamaks has not produced results which agree with experiment to better than a factor of two, in that observed values of beta exceed the maximum predicted value by such a factor.

3.5 The Mercier Criterion

The Mercier criterion is a necessary criterion for stability against ideal interchanges, and is derived by restricting attention to perturbations which are localised radially (in the vicinity of a rational surface) but not in angle.

The calculation is performed by employing a set of Hamada

coordinates $\{V,\theta,\xi\}$ to describe the effect of a perturbation, $\underline{\xi}$, which is localised in the vicinity of a rational field line with $qo=B_o^{\xi}/B_o^{\theta}=m/n$, using the energy principle described above. The most important feature of the perturbation is expressed as $|\underline{\xi}|\rightarrow 0$ as $|x|\rightarrow 1$, where $x = (V-V_o)/\varepsilon$, and ε is formally small. The energy integral is minimised in successive orders, employing an expansion in powers of the small parameter, ε, characterising the radial length-scale over which the perturbation varies and the new variable x, to find the most unstable perturbation. The leading non-vanishing order of the radial perturbation is constant along field lines in the rational surface on which the mode is centred, although in other directions it may vary. As the same is true for the radial electric field, field lines in this surface may be treated as being independent of each other. A criterion for stability against localised interchanges is eventually arrived at in the third order, which is the ε order, the lowest order being $1/\varepsilon$. The form of the Mercier criterion which is most commonly used to describe large aspect ratio Tokamaks is introduced in the next section. The criterion is to be evaluated at a rational surface within the plasma. The presence of either shear or of a "magnetic well", which corresponds to there being favourable average curvature, may lead to the criterion being satisfied, as is well known.

The experimental evidence for the existence of Mercier-type instabilities is unconvincing. For instance, experiments conducted on both WVII and on CLEO failed to find any evidence for the deleterious effects of such modes. (CLEO had sufficient shear that they might have been stabilised on the time scale appropriate to the experiment, but this seems unlikely in the case of WVII.)

The computer calculations of Garabedian, [42], indicate

that, even on the basis of ideal M.H.D., ballooning modes may not in practice be the most dangerous instabilities in a high beta Stellarator ($\beta \sim O(\varepsilon)$). (Shafranov and Shohet, [43],[44], have claimed that the high shear and short connection lengths to be found in Stellarators could impede ballooning modes, so the prediction is plausible.) Instead, Garabedian found that low m and n modes were the most troublesome. These modes were found to grow, given certain assumptions, in the neighbourhood of the corresponding rational surface.

A similar result was obtained by Strauss and Monticello, [45], who linearised the ideal M.H.D. equations, in the vicinity of equilibria found using the "conventional" Stellarator ordering. Integrating in time, to find the fastest growing modes, they too find modes of low m,n localised near a surface with a particular q-value.

A full stability analysis for a Stellarator would involve a study of the conditions for marginal stability, and such a study does not yet appear to have been undertaken. However, it is possible to argue that, provided whatever dangerous rational surfaces which are present are restricted to the centre of the plasma, the effect of the instability may even be beneficial, flattening the profiles near the axis. Alternatively, it may be possible to devise a field profile for which the more important surfaces lie outside the plasma.

The lack of agreement between theory and experiment may be due to shear stabilisation or to the instability developing non-linearly and saturating, or to various non-ideal effects such as finite Larmor radius, for example. Further, on the time scale of these discharges, resistivity, which would remove shear stabilisation, (this latter being effective in most Stellarators) may not be important. We now turn, however, to a discussion of the effects of resistivity on interchanges, which we believe may be important in a reactor plasma, if the theory is applicable.

3.6 Resistive Interchanges

Supposing that it has been determined that the plasma is stable to ideal modes, it is necessary to investigate the effects of the inclusion of resistivity. Resistivity will lead to dissipation, but its importance in stability theory stems from the fact that it allows field lines to break.

The magnetic topology can be altered by the cutting of field lines, making a profound difference to the nature of the instability. Singular layers may occur, which arise, formally, because of the high spatial derivative in the small terms associated with resistivity in the governing equations. Then, rather than the unstable eigenfunction having the same functional form throughout the plasma as in ideal M.H.D., the perturbation need only satisfy matching conditions across the singular layer and so it can change its nature. Consequently it has greater freedom to satisfy the boundary condition at the edge and thus to grow.

The perturbation which is involved in a localised interchange, being localised, does not "see" the exterior boundary. Singular parturbation theory must still be employed, for it turns out that the terms involving resistivity can only become comparable with the leading order terms if the length scale over which the instability varies is of the order of the cube root of the resistivity, (assumed small). The field line breaking is only important locally, therefore, at the mode rational surface.

Glasser, Greene, and Johnson, [46], have derived a criterion for stability against Mercier modes, in the presence of finite resistivity. (Their treatment is in fact rather general, including tearing and modified tearing modes as well.) They show how the Mercier criterion arises naturally out of their treatment, from which they obtain a criterion which is always more stringent than the Mercier criterion. (This criterion

reduces, in the cases we shall study, to that of Mikhailovskii, [37], which we evaluate below.) They comment that the difference may be attributed to the loss of the stabilising effect of the shear, (as represented by the first term in the Mercier criterion given below). The growth rate, however, does depend strongly on the shear, which acts to impede the progress of the instability rather than to prevent it.

Mathematically, dissipation means that the operator $\underline{\underline{K}}$ in the equation for the perturbation, (3.1.1), is no longer Hermitian and the reasoning which led to the use of δW as a test of stability no longer applies. It is thus necessary to solve the appropriate eigenvalue problem in order to study resistive instabilities.

Resistive ballooning modes will probably always be "boiling away", hopefully giving rise to enhanced diffusion rather than a catastrophic loss of plasma. We thus wish to study localised resistive interchanges, to see the effect of resistivity on the Mercier criterion, for stability against localised modes is more in doubt.

3.7 Localised Resistive Interchanges

Criteria for stability against flute-like modes which are only localised radially, in the presence of finite resistivity were given in [37,46]. In the latter it is shown that the resistive criterion is always more stringent than the Mercier criterion, which was to be expected, as resistivity can "untie" crossed field-lines. The criteria may be shown to be equivalent in the large aspect ratio, ($A>>1$), large toroidal field case, and so we are free to take that of Mikhailovskii, [37], which is more convenient to work with:

$$W^{(o)} - A_2 > 0 \qquad (3.7,1)$$

for stability against resistive interchanges.

$$W^{(o)} = \frac{1}{\phi'^2}\,(P'V'' + I'\chi'' - J'\phi'') - \frac{1}{\phi'^2}\,(\phi'\chi'' - \chi'\phi'')\langle\omega\rangle$$

$$- \left(\frac{2\pi P'}{\phi'}\right)^2 \left\langle \frac{\sqrt{g}}{\underset{\sim}{B}^2} \right\rangle$$

$$A_2 = \left(\frac{2\pi}{\phi'}\right)^2 \left\langle \tilde{\omega}^2 \sqrt{g}\, \frac{\underset{\sim}{B}^2}{g^{11}} \right\rangle \qquad (3.7,2)$$

$\phi(\chi)$ and I(J) are the longitudinal (transverse) magnetic and current fluxes, $\omega = \frac{\underset{\sim}{J}\cdot\underset{\sim}{B}}{\underset{\sim}{B}^2}$, $\langle x\rangle$ is the average of x over a flux surface, and $\tilde{x} = x - \langle x\rangle$. The g^{ik} are the metric coefficients of the flux-coordinate system employed, in which current and field lines are straight: $x = a$, the radial coordinate, and $' \equiv \frac{d}{da}$

The criterion was derived for perturbations which are

(i). almost flute-like in the direction of the equilibrium field, i.e.

$$|\underline{B}_o \cdot \nabla X_1| << |\underline{B}_o \times \nabla X_1|$$

where Q_1 indicates the perturbation in the quantity Q, whose equilibrium value is Q_o.

(ii). localised in the vicinity of a field line,

$$|\underline{B}_o \times \nabla \ln X_1| >> |\underline{B}_o \times \nabla \ln X_o|$$

(iii). more localised radially than in minor azimuth, ie terms of order $(\partial/\partial\theta)/(\partial/\partial a)$ are neglected.

The set of equations

$$\rho \frac{d\underline{v}}{dt} = -\nabla P + \underline{J} \times \underline{B},$$

$$\frac{d\rho}{dt} + \rho \nabla . \underline{v} = 0, \qquad (3.7,3)$$

$$\frac{d}{dt}(P \rho^{-\gamma}) = 0$$

the Maxwell equations

$$\frac{\partial \underline{B}}{\partial t} = -\nabla \times \underline{E} \qquad \nabla \times \underline{H} = \underline{J} \qquad \nabla . \underline{B} = 0 \qquad (3.7,4)$$

and the assumed form for Ohm's law,

$$\underline{E} + \underline{v} \times \underline{B} = \underline{J}/\sigma \qquad (3.7,5)$$

(the symbols having their usual meanings), are linearised in the perturbed quantities. An oscillator equation for the displacement, $\underline{\xi}$, is obtained which does not have solutions which are bounded in space unless a certain condition is satisfied. This condition reduces, in the appropriate limit, to (3.7.1) above.

We shall now evaluate this criterion, for the class of equilibria obtained in chapter two.

In [47], replacing averages over closed field lines by surface averages, we have an expression for V** which is a quantity which is important for stability against resistive interchanges:

$$V^{**} = V'' + \frac{I'\chi'' - J'\phi''}{P'} - \frac{(\phi'\chi'' - \chi'\phi'')}{P'} \frac{\langle \omega \underset{\sim}{B}^2 \rangle}{\langle \underset{\sim}{B}^2 \rangle} - P' \left\langle (\underset{\sim}{B}^2)^{-1} \right\rangle \tag{3.7,6}$$

where ' now denotes the derivative with respect to some flux surface coordinate. For convenience we shall take this to be the toroidal flux, ϕ.

When the main toroidal field is large,

$$\frac{\langle \omega \underset{\sim}{B}^2 \rangle}{\langle \underset{\sim}{B}^2 \rangle} \simeq \langle \omega \rangle$$

and allowing for the fact that

$$\sqrt{g} \approx aR(1 + O(a/R))$$

in [46], we see that

$$W^{(o)} = \frac{dP}{da} \cdot V^{**} = P' 2\pi a B_\xi V^{**} \tag{3.7,8}$$

Thus we obtain from Mikhailovskii's result $W(o) - A_2 > 0$ a modified form of the V** criterion:

$$V^{**} - \frac{1}{P' 2\pi a B_\xi} A_2 < 0$$

We may write this last expression in terms of our dimensionless variables by introducing the following dimensionless equivalents of the above quantities:

$$\text{If } [x] = \int_o^{2\pi} d\theta \int_o^{2\pi} ds \int_o^{\rho(\psi, \theta, s)} x\rho(1 - \varepsilon\rho \cos\theta) d\rho \tag{3.7,9}$$

then $V = [1]$, $U = [\underset{\sim}{b}^2]$, $L = [(\underset{\sim}{b}^2)^{-1}]$ and $\hat{\phi} = \frac{1}{2\pi}[b_\xi / (1 - \varepsilon\rho\cos\theta)]$, Henceforth we work in terms of these quantities, (and drop the $\hat{}$ on $\hat{\phi}$).

If we put

$$V^{**} = V'' - \frac{V'}{U'} U'' - P'V'\left(\frac{V'}{U'} + \frac{L'}{V'}\right) \qquad (3.7,10)$$

then taking the leading order forms of $\sqrt{g}$, g^{ll} , in A_2 we find the criterion

$$V^{**} - 4\pi \hat{P}'q^2 < 0 \qquad (3.7,11)$$

where $q = \rho / b^*$.

With the present ordering, V',U' and L' are all $2\pi + O(\lambda^4)$, so $V^{**} = V''-U''- 4\pi P'$ to the required accuracy. This proves to be a convenient form, as $V - U = 2[1-b] - [(b-1)^2]$, where $b = |b|$.

The first part of this expression contains the destabilising "magnetic hill" associated with the Stellarator field plus some stabilising terms due to favourable average curvature, whilst the second is purely stabilising. The destabilising term is formally larger than the stabilising terms, that is, the ordering is non-optimal with respect to the stability criterion.

Higher order terms in general represent only corrections to those already described. In the case of a current-free l=2 Stellarator we shall see that the pressure dependent terms cancel exactly in $O(\lambda^6)$, and the next such term is in $O(\lambda^8)$. In this case we may choose not to call this term a "correction", but in any case we assume that it is sufficiently small to be neglected.

For "Tokamak-like" configurations, (2.3.3,3), is used, being written in terms of new coordinates (ρ', θ', ξ), centred on the magnetic axis by replacing $\Delta(\rho)$ by $\Delta'(\rho') = \Delta(\rho) - \Delta(o)$, and writing ρ' for ρ and θ'

for θ . We shall work in terms of these coordinates throughout the rest of this section, although dropping the primes on ρ', θ' and Δ'.

We now evaluate the terms in the stability criterion. The second term in V - U , $[(b-1)^2]$, is easily evaluated, and to lowest order is

$$\left[\varepsilon^2 \left(\rho \cos\theta - \alpha\rho^n \sin(n\theta+s)\right)^2\right] + O\left(\varepsilon^{7/3}\right)$$

$$= \pi^2\varepsilon^2 \left(\frac{\rho_o^4}{2} + \frac{\alpha^2 \rho_o^{2(n+1)}}{(n+1)}\right) + O(\varepsilon^{7/3}) \qquad (3.7,12)$$

[1-b] is less useful than [1-b]', which is also easier to evaluate, being given by

$$\int_0^{2\pi} d\theta \int_0^{2\pi} ds \, \frac{1}{2} \frac{d\rho^2}{d\phi} (1-\varepsilon\rho\cos\theta)(1-b) \qquad (3.7,13)$$

where $\rho = \rho(\psi, \theta, s)$.

To evaluate this we need b and $\frac{d\rho^2}{d\phi}$.

$$b = \left(b_\xi^2 + b_\rho^2 + b_\theta^2\right)^{1/2} = b_\xi + \frac{1}{2}\left(b_\rho^2 + b_\theta^2\right) + O\left(\varepsilon^{7/3}\right) \qquad (3.7,14)$$

and so

$$-\left(1-\varepsilon\rho\cos\theta\right)(1-b) = \frac{1}{2}\left(b_\rho^2 + b_\theta^2\right)$$

$$+ \varepsilon\left(\rho\cos\theta - \alpha\rho^n \sin(n\theta+s)\right) + \varepsilon^{5/3} b_\xi^{(5)} \sin(n\theta+s)$$

$$+ \varepsilon^2 \left\{b_\beta + - - - -\right\} \qquad (3.7,15)$$

with

$$b_\rho^2 + b_\theta^2 = \varepsilon^{4/3} \frac{n^2\alpha^2\rho_o^{2(n-1)}}{\bar{p}^2}\left[1 + \varepsilon^{1/3} \frac{2n\alpha\rho_o^{2(n-2)}}{\bar{p}^2} \sin(n\theta+s) + O(\varepsilon^{2/3}\alpha^2)\right] \qquad (3.7,16)$$

where we have omitted periodic terms which will disappear from this order

when the averaging operator is applied.

From its definition, ϕ is given by

$$\phi = \pi \left(\rho_o^2 + \varepsilon^{\frac{2}{3}} \frac{n^3 \alpha^2}{\bar{p}^4} \rho_o^{2(n-1)} \right) + O\left(\varepsilon^{\frac{4}{3}}\right) \tag{3.7,17}$$

and so

$$\frac{d\rho^2}{d\phi} = \frac{1}{\pi} \left(1 + \varepsilon^{\frac{1}{3}} n^2 \frac{\alpha}{\bar{p}^2} \rho_o^{n-2} \sin(n\theta + s) - \varepsilon^{\frac{2}{3}} n^3 \frac{(n-1)}{\bar{p}^4} \alpha^2 \rho_o^{2(n-2)} \cos 2(n\theta + s) \right.$$

$$\left. - \frac{\varepsilon \cos\theta}{\rho_o} \frac{\partial}{\partial \rho_o} \left[\frac{\rho_o^2}{b^*(\rho_o)} \left(A(\rho_o) + \frac{n\alpha^2 \rho_o^{2(n-1)}}{4\bar{p}^3} \left[5n + (n+1)\gamma + \frac{(n-1)\delta}{\rho_o^2} \right] \right) \right] \right) \tag{3.7,18}$$

Thus, integrating the product in [1-b]', we have the criterion in the form

$$\nabla^{**} - 4\pi \hat{P}' q^2 = \varepsilon^{\frac{4}{3}} 2n^2 (n-1) \frac{\alpha^2}{\bar{p}^2} \rho_o^{2(n-2)}$$

$$+ \varepsilon^2 \left(-1 + 2\left(\frac{b(\rho_o)}{\rho_o} \right) + \left[\Delta'' + \frac{3\Delta'}{\rho_o} - \frac{2\rho_o P'}{b^{*2}} \right] + \frac{1}{\rho_o} \frac{d}{d\rho_o} \frac{1}{\rho_o} \frac{d}{d\rho_o} \Omega(\rho_o) \right) \tag{3.7,19}$$

We have omitted from this expression the contribution in $O(\varepsilon)$ of terms proportional to i_{vac}, as they are expected to be small.

From (2.3.6,5) we are able to find $\left(\Delta'' + \frac{3\Delta'}{\rho_o} - \frac{2\rho_o P'}{b^{*2}} \right)$, and using $q'/q = (1/\rho - b^{*\prime}/b^*)$ we have

$$\Delta'' + \frac{3\Delta'}{\rho_o} - \frac{2\rho_o P'}{b^{*2}} = -\frac{b}{b^*} + \frac{\sigma'}{\rho_o^2 b^*} \Omega(\rho_o) + 2\Delta' \frac{q'}{q} - \frac{\Delta}{b^*} \frac{d}{d\rho_o} \frac{1}{\rho_o} \frac{d}{d\rho_o} (\rho_o b_o) \tag{3.7,20}$$

For 1=2 this may be integrated, as in chapter two to obtain

$$\Delta' = \frac{1}{\rho_o b^{*2}} \int_o^{\rho_o} \left[2\rho P' - b^* b + \frac{\sigma'}{\rho^2} b^* \Omega(\rho) \right] \rho d\rho \qquad (2.3.5,10)$$

as the term in Δ vanishes.

We thus see that for the general l=2 Stellarator, negative shear ($q'/q>0$) is stabilising.

We now consider two limits: (i). When the Stellarator field is removed, ($\alpha = 0$), we recover the Tokamak result which was given in [37], where the same point was made for Tokamaks:

$$q^2 > 1 + q\, q' \Delta' \qquad (3.7,21)$$

It is interesting to compare this with the ideal M.H.D. Mercier criterion for a large aspect-ratio Tokamak given by Shafranov and Yurchenko [48]:

$$\frac{1}{4}\left(\frac{q'}{q}\right)^2 + \frac{2\mu P'(r)}{rB_o^2}\,(1 - q^2) > 0. \qquad (3.7,22)$$

We see that the nature of the shear stabilisation has been changed, as we might have expected, making the plasma appear less stable in the presence of resistivity.

(ii). In the absence of an Ohmic heating current, the shear vanishes for l=2 (at least formally, to the order to which we are working,) and the pressure dependent terms in our criterion also vanish to $O(\lambda^6)$. We then obtain:

$$\frac{8\alpha^2}{\bar{p}^2}\,\varepsilon^{4/3} - (11 + 3\gamma)\,\varepsilon^2 = \varepsilon^2\left(2p\,|i_{vac}| - (11 + 3\gamma)\right) < 0 \qquad (3.7,23)$$

Allowing for differences in notation, this result coincides with an ideal M.H.D. criterion obtained by Shafranov [49] by means of an expansion in radius. The pressure dependent term which was omitted (being in $O(\lambda^8)$) is found by him to be

$$\varepsilon^2 p'(\rho)\ \frac{i_{vac}\beta_p}{2\pi p}$$

and so provided $\beta_\rho \lesssim 1$, this is indeed negligible. We note that there exists a substantial margin of stability to resistive interchanges of a flute-like character in an l=2 Stellarator without toroidal current, which may be enhanced by an appropriately phased modulation ($\gamma > 0$) of the l-winding pitch, provided that the rotational transform is not too large.

A point which should be made here is that, formally, given the ordering we employ, instability is predicted, as the destabilising term is of lower order in ε than the stabilising one. We take the view that this is merely a deficiency in what is otherwise a most convenient ordering, however, for in reality the relative size of the terms can be reversed, as we have seen. (Clearly, the small expansion parameter is rather large, but that is a different problem to do with the ordering.)

In other words, although the ordering is "optimal" with respect to the equilibrium calculation, in that competing terms are brought together in the same orders, it is not optimal with respect to the stability problem. (Had the ordering been non-optimal for equilibrium, we could not have performed a calculation at all.)

To support this view, we may point out that it is clear that the calculation could be repeated using different orderings, (using a Mercier expansion, as in [49], for instance) and this fault rectified. (Such a treatment would be less convenient for other purposes, however.) Even within the framework of our main ordering, we could let the coefficient describing the amplitude of the l=3 field be two orders in λ larger without changing from an l=2 Stellarator, in which case we also obtain a

stabilising term comparable with the leading order destabilising one.

For l>2 it is not always possible to use the above analysis, as the axis shift is large. However, when A(o) = 0 , which corresponds to a particular (rather unlikely) choice of the vertical field, the assumption that $\rho_x \sim 0(\varepsilon)$ is valid and for l=3 Stellarators (with $\gamma = \delta = 0$) we find the criterion

$$2pi_{vac}(\rho) - 6 - \frac{2}{\rho}\frac{P'(\rho)}{i^2_{vac}(\rho)} < 0 \qquad (3.7,24)$$

When P = 0, the criterion reduces to V**<0 , which criterion was evaluated in [26], although we find the stabilising term to be slightly larger.

Finally in this section, we may remark that the spiralling of the axis which was predicted for l=2 Stellarators in the presence of a plasma should increase the depth of the magnetic well. For considering the value of $\int dl/B$, we see that as the axis is longer than the mean circumference of the outer surfaces, this integral will decrease as we go to higher minor radii, giving a "minimum average B".

Whether this leads to greater stability, through increasing the magnetic well, or whether the effect will be cancelled out by another small correction in the stability criterion, we cannot say, however.

3.8 Discussion

We have argued that for relatively low values of beta, Stellarators can be made immune to ideal instabilities, (because of the absence of a net longitudinal current, and because of high shear and short connection lengths).

We then proceeded to consider the effects of resistivity on what we believe to be the most dangerous of the ideal modes, which, it was

felt, might cause a considerable change to predictions of stability, by removing shear stabilisation. By considering resistive interchange modes we have obtained a form of the relevant stability criterion which is appropriate to a class of Stellarators, including the type which we shall wish to study in later sections.

For sufficiently low rotational transform, i, and number of toroidal periods of the helical field, p, that is, $\iota p < 1$, current-free $l=2$ Stellarators are predicted to be stable. This requirement corresponds to the need for a magnetic well in the vacuum configuration. As the criterion employed is more stringent than the Mercier criterion, then the Mercier criterion will also be satisfied if the above holds.

The plasma is thus predicted to be stable, on the theory which we have just described. Other authors have come to the opposite conclusion, (Lortz and Nuhrenberg, [36],) but, as mentioned in chapter two we have reason to doubt their results. What is more, their prediction for WVII is clearly refuted by the experimental observation that beta of 1% has been attained in WVII.

We may now summarise the conclusions from our consideration of M.H.D. equilibrium and stability theory, which will be used to guide us in the design of a Stellarator reactor in the last two chapters.

We assume that, if Stellarator plasma pressure profiles $P(\psi)$ exist (analogous to the so-called "flux-conserving" Tokamak equilibria) for which the equilibrium beta can be much greater than those we have found, then they probably have steep pressure gradients, which make them unstable. (When the Grad-Shafranov equation is solved, there are two free profiles to be specified. One is the pressure profile, and the other governs the current in the plasma. When we specialise to a current free Stellarator, in the sense that the flux surface average of the

longitudinal current is set to zero, then the number of free parameters is reduced by one. A flux conserving scheme applied to a current free Stellarator will in general lead to equilibria with net longitudinal current, therefore. The fact that $q(\psi)$ is not allowed to vary, whilst the pressure is raised, may be used to show that that this must be the case. For the vacuum q profile, being fixed in space, cannot convect with the plasma, and so a net longitudinal current must be set up in the plasma to maintain $q(\psi)$. Thus even if the above assumption were false, we should have less freedom to optimise profiles in the pure Stellarator than in the Tokamak.)

Thus the study of the equilibrium properties of the plasma shows that there is a beta limit which coincides roughly with a lower bound on the ballooning limit, as explained above. The resistive interchange criterion may also be important, (if the theory turns out to be applicable), and so this will be used as a second measure of the suitability of a Stellarator reactor.

In the light of these considerations, the Reactor optimisation will make use of a beta limit like fi^2/A, where f is a number of order unity, dependent on various non geometric factors (like, for instance, the l-number). We shall also ensure that the resistive interchange criterion indicates stability, but this condition turns out to be rather less stringent than the equilibrium limit, in so far as it is satisfied automatically in the optimised reactor geometries which we find.

Chapter Four: Transport in Stellarators

A discussion of the contribution to Stellarator particle (and, to some extent, heat) transport of particles which are "localised" or trapped in the helical ripple of the Stellarator field is given. This class of particles is singled out because:

(i). they have been identified in previous work as being responsible for the dominant component of Stellarator "transport", and

(ii). a complete discussion would be prohibitively difficult to undertake.

First, those concepts from neoclassical theory which are necessary to describe the above mentioned transport processes in a Stellarator are introduced. Various different predictions for the transport rates are explained and reconciled. In particular, the point at which the expansion in gyrofrequency breaks down is discussed, as well as how this must be allowed for when using neoclassical theory. Estimates are then given for the diffusion due to classes of particles which were not properly accounted for in the earlier neoclassical theory.

Before any of this, however, we shall outline the likely impact of the electron diffusion on the ion transport to which this chapter is principally devoted.

Ambipolar Diffusion

It has not, to date, been possible to adequately represent the effects of an ambipolar electric field on the diffusion in a Stellarator, although the presence of such a field can have a profound effect on transport processes, as we now attempt to indicate.

An ambipolar field is set up when one of the charged species, ions or electrons, diffuses faster than the other, and tends to prevent the

continuing charge separation.

The effect of the field may be understood in terms of the change in the energy required for a particle to escape, but the explanation in terms of the forces on particles is not trivial. (It could also cause particles which would otherwise lie on loss orbits to drift poloidally and remain in the device, "annealing" the drift surfaces.)

The ion diffusion is usually taken to be described by neoclassical theory, albeit with some reservations. Electrons, on the other hand, behave "anomalously", possibly because, being much less massive than the ions, they are much more sensitive to the effects of imperfections in the fields. The ion diffusion processes are relatively well understood, and may be taken to depend linearly on the radial field and the density gradient. We may thus distinguish two possible situations, one of which may divided further:

(i). The electron diffusion is relatively insensitive to the ambipolar potential, in which case the ion rate must be adjusted to equal the electron rate by the ambipolar potential.

(ii). The electron diffusion depends quite strongly on the potential, and in the absence of the potential would be

(a). much bigger than the ion rate. In this case, one has to equate two expressions for the fluxes, each containing a sum of terms involving density gradients and the electric field, one formally larger than the other. Without making the ambipolar potential formally large, the only way to do this is to arrange near cancellation between the terms in the larger of the two, by choosing the correct potential. In other words, the electrons will be slowed to the ion rate.

(b). The ion flux may appear the larger. Exactly the same arguments apply, - the rate will be determined by the electron diffusion rate.

In fact we shall argue that the ion diffusion rate (neglecting ambipolar effects) is likely to be slightly higher than in a Tokamak,

whilst the electron diffusion could be a good deal lower, for Stellarator fields are likely to be less turbulent than Tokamak fields, in the absence of a net toroidal current.

If this were the case, then the diffusion would be at the electron rate, which we suppose to be low, but which is not sufficiently well understood for us to predict a value for it. The work of this chapter may thus be considered to set an upper bound on the diffusion, unless the electron diffusion is large and independent of the potential, and it is not clear what mechanism could allow this to be the case in a well designed Stellarator.

4.1 Particle Motions

The motion of a charged particle in a magnetic field consists, to a first approximation, of translation along a field line and rapid gyration about a "guiding centre", which coincides with the field line, to this approximation. In the next approximation, a number of slower drift motions (of the guiding centre) appear due, for instance, to electric fields or gradients in the magnetic field. The drift velocity of a particle of charge q in static electric and magnetic fields, $\underline{E}$ and $\underline{B}$ respectively, is given by

$$\underline{V}_d = \frac{\underline{E}\times\underline{B}}{\underline{B}^2} + \frac{\mu}{q}\frac{\underline{B}\times\nabla B}{\underline{B}^2}\left(1 + \frac{2v_{\parallel}^2}{v_{\perp}^2}\right) \qquad (4.1,1)$$

where μ is the magnetic moment of the particle, and $v_{\parallel}, v_{\perp}$ are the parallel and perpendicular velocities.

The need for rotational transform may be explained on a "particle"

basis, using this result. In a torus the main toroidal field has a "radial" gradient directed towards the major axis of the torus. This gives rise to a charge-dependent vertical drift of particles and the resulting charge separation creates an electric field. The electric field causes a charge-independent drift along the major radius which will carry the plasma to the wall.

To overcome the effects of the vertical drift it is necessary to provide a rotational transform of the field. The rotational transform ensures that field lines and, hence, particles, are rotated around the minor cross-section as they move in the toroidal direction. Particles which have, for instance, drifted upwards onto an outer surface whilst at the top of the minor cross section will, whilst at the bottom, drift upwards onto an inner surface. As a result the average value of the minor radius at which a particle is to be found remains constant.

Alternatively, and from a macroscopic point of view the rotation of field lines allows an electric current to flow from the top of the minor cross-section to the bottom, preventing the build-up of charge.

The details of particle behaviour are extremely complex, there being many possible motions depending on the particle's position in phase space. As a result, fluid treatments of the plasma are not capable of describing a number of important effects, and the very complicated kinetic theory of plasmas must be used. The usual approach to the subject, as exemplified by the work of Frieman, [3], is to consider the Fokker-Planck equation for the evolution of the ion distribution function, along with Poisson's equation for the electrostatic field. The standard procedure would be to expand in the ratio of the Larmor radius to a typical macroscopic length (equivalent to the ratio of some typical frequency to the Larmor frequency), and to seek solutions in the successive orders. In

a general geometry it would be necessary to use the method of averaging or some equivalent technique to find such solutions.

The expansion in the Larmor radius has been used to demonstrate the existence of a number of adiabatic invariants, one in each successive order. The invariants are E, μ,J, the energy (trivially), the magnetic moment and the longitudinal invariant respectively. The validity of the expansion in each order in which it is applied would guarantee the conservation of the invariant which is thrown up in the same order, (Haas, Hastie and Taylor, [50],).

The ordering in gyrofrequency employed, (which may be described more properly as an expansion in m/e) may be put into perspective by considering the timescales of interest for particle motions. These are set by the Larmor frequency, the frequency of travelling a typical macroscopic length scale L along a field line, which is, roughly speaking, the same as the bounce frequency, $\omega_b = v_{||}/L$, and the frequency of drifting around a minor cross section, $\omega_d = V_d/L$. As these frequencies are in the ratio

$$1 : \frac{a}{L} : \left(\frac{a}{L}\right)^2 \qquad (4.1,2)$$

("a" being a Larmor radius), we see that the ordering demands that $v_{||} >> V_d$. We know, however, that this cannot always be true, for when particles "mirror", $v_{||} = 0$.

Provided the particle spends very little time near a bounce point (with $v_{||}=0$) this may not be significant. In some circumstances, (when a particle has just sufficient energy to pass over a local maximum in the magnetic field strength, for instance) $v_{||}=0$ for a considerable time, and the particle is able to move some distance simply due to its drift motion. The ordering is not appropriate to such a particle.

It has been shown that the longitudinal invariant is not always conserved even for single particles in a Stellarator, [51]. This discovery is a consequence of the breakdown in the gyrofrequency ordering, and has been claimed to explain why Monte-Carlo calculations of diffusion rates in Stellarators do not give the neoclassical result, at least as estimated naively, but show a rather more optimistic picture. We shall return to this point, presently.

In order to be able to discuss these and other aspects of transport theory in detail we shall now give a brief survey of neoclassical theory as applied to the motion of localised particles in Stellarators.

4.2 Neoclassical Transport Theory

Single Particle Orbits

Neoclassical transport theory differs from classical transport theory principally in that it is a non-local theory. It predicts that transport at any point depends strongly on the global structure of the fields, the knowledge of conditions at distant points being carried rapidly around the device by particles moving along field-lines.

As a result of the influence of geometry, particles may move radially (i.e. out of the device) even in the absence of collisions, in which case the loss process is no longer diffusive. Indeed, it has been shown on certain models that collisions could impede transport by creating diffusion where otherwise unidirectional drifts would take place.

The basic ideas of neoclassical theory are now introduced.

It has usually been considered convenient to classify particle motions by the region in phase space in which the particle lies. As virtually all of the literature makes use of this classification it is a prerequisite for a discussion of transport theory that the various possible motions be described.

It is well known that a particle, travelling along a field line, may be reflected as the field strength increases if its direction of motion makes a sufficiently large angle with the field. (As B increases, $\mu = mv_\perp^2/2B$ is constant, so $1/2mv_{||}^2 = E - \mu B$ decreases - to zero, at a bounce point.)

In a Stellarator there are several different effects which give rise to a variation in the field strength along a field line. The variation with major radius of the main toroidal field and the ripple due to the discreteness of the coils are common to the Stellarator and the Tokamak. In addition the Stellarator field has a ripple due to its helical component.

Each of these ripples will reflect some particles. As the field strength varies periodically, it may be expected that unless a reflected particle is removed (e.g. by a collision or by the detrapping mechanism which we shall discuss below) to a different region in phase space it will be reflected again after travelling a fraction of the ripple period. Such a particle is said to be trapped in the ripple.

As mentioned previously, gradients in the magnetic field have another consequence for particle motions, namely, they give rise to particle drifts. If a particle is trapped in a ripple, and there is no other gradient in the field apart from that which traps the particle, then its drifts due to that ripple will cancel out over a complete orbit (around the ripple). However, if more than one inhomogeneity is present

in the field, a particle may be trapped in one ripple and drifting unidirectionally due to another. During many bounces it would then escape from the device.

The simplest trapped-particle motion is known as a Banana orbit, which occurs when a particle is bouncing due to the radial gradient of the toroidal field, that being the sole variation in the field: this situation may be realised in an idealised Tokamak. The finite width of the orbit is due to the vertical drift, induced by the same gradient in which it is trapped. Consequently, this drift does not produce a net displacement over the complete orbit, (Fig.4.1).

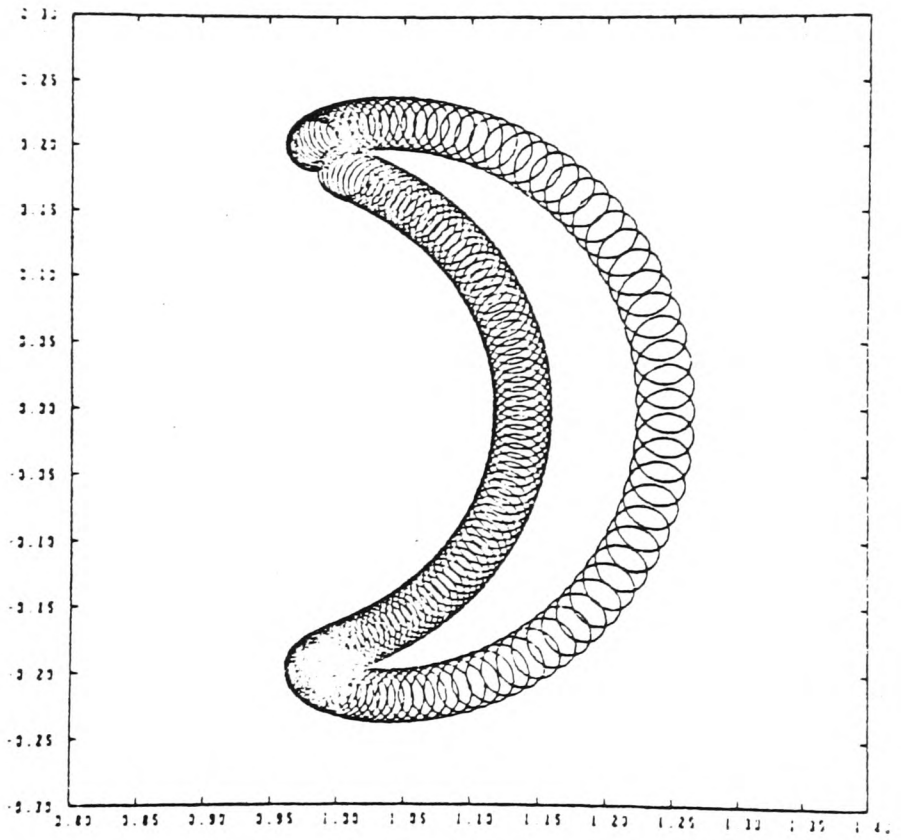

Fig. 4.1. Banana Orbit.

In a Tokamak the effect of the discreteness of the coils is to remove the symmetry of the system, so the bananas have a drift which is not compensated. Similarly, some particles will be trapped in the coil-ripple and drift out of the device due to the radial gradient of the field.

In a Stellarator there is an extra gradient, due to the helical ripple of the field, so there will be six drifts in all which will not average out. Perhaps the most worrying motion is that which was first

dubbed a Superbanana. A variety of Superbanana was observed computationally by Gibson and Taylor, [52] and was identified as being the motion of a particle trapped in the helical ripple of the Stellarator field (known as a "localised" particle) and drifting primarily because of the inward (radial) gradient of the toroidal field. The characteristic shape of the orbit in a classical Stellarator is depicted in Fig.4.2.

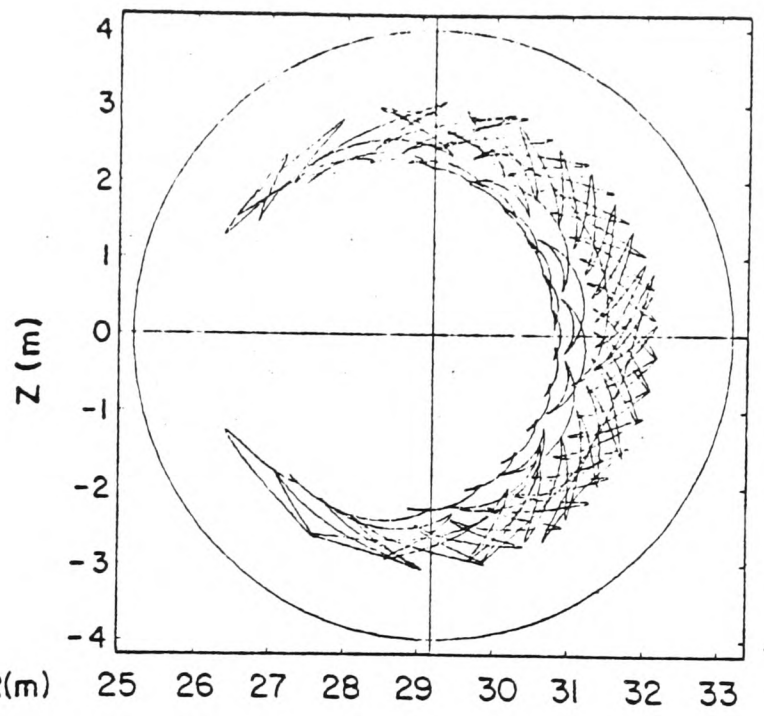

Fig. 4.2. "Exterior" Superbanana Orbit.

Let us consider the orbits of localised particles in detail, employing the model field with field strength

$$B = B_o \ (1 + \delta_h .\cos(n\theta + p\xi) + \varepsilon_t .\cos\theta) \qquad (4.2,1)$$

An illuminating starting point is provided by the work of Dobrott and Frieman, [26]. Employing the Stellarator expansion introduced in Chapter Two and the m/e expansion, they describe particle orbits in terms of constant-P and constant-J surfaces, where P is an average (in the Stellarator ordering sense) toroidal component of the canonical momentum, (the effects of the helical ripples having been averaged out). J has already been defined.

Four classes of particles are distinguished, as a result of this work:

(a). permanently localised particles,

(b). blocked particles,

(c). quasilocalised particles, and

(d). passing particles.

Permanently localised particles cannot emerge from the helical magnetic well at any point in their orbit, as their parallel velocity is too low.

Blocked particles are the class of particles which, in a Tokamak, execute banana orbits, having too low a parallel velocity to pass all the way around the minor cross section because of the toroidal variation in the field.

Some localised particles are able to escape from the helical ripple at some point in their motion, and turn into blocked particles, which execute something akin to a banana orbit, except that rather than bounce in the toroidal gradient of the field, they may retrap in the helical ripple, becoming localised again. Such particles are described as quasilocalised.

Passing particles travel around the device without mirroring in any of the field ripples. These will not be studied in detail, here.

Figure 4.3, which is taken from [26], shows constant P and J surfaces (full lines), for a particular l=3 magnetic field configuration. The broken line is a transition curve between the two domains, along which particles are predicted by the model to escape from the helical ripple, going from class (b) to class (c) and vice versa. (The major axis is to the right, in this figure.)

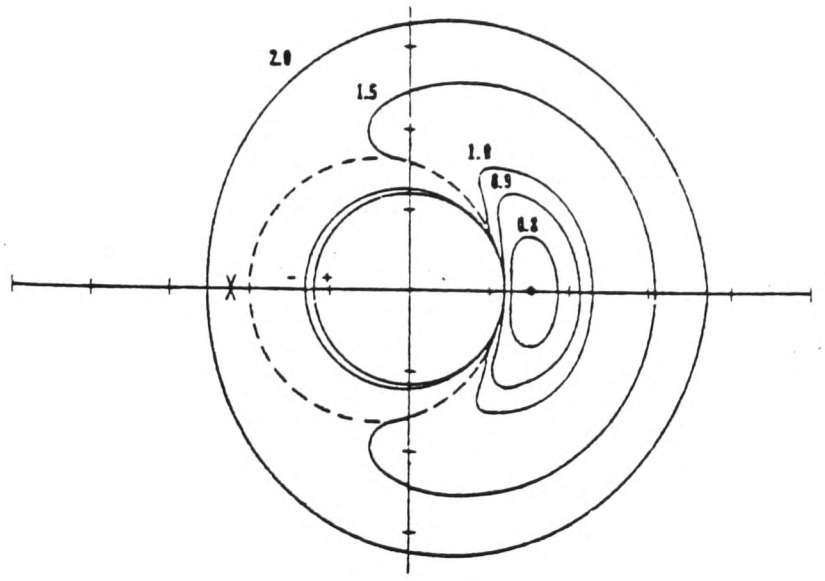

Fig.4.3. Drift Surfaces and Transition Curve.

Referring to this diagram, we see that some particles lie on constant J surfaces which never intersect the transition curve. Of these, some are confined to the inside of the torus whereas some have orbits which encircle the whole of the minor cross section. The former are known as "interior" superbananas, in the literature, and were first described by Galeev et al., [53].

Consider a particle in the latter class, (of localised particles which pass all the way around the minor cross section), which at some instant is at the outside of the torus. If its parallel velocity is large enough, it can pass all the way around in θ , the poloidal angle, as implied in the figure. However, if its parallel velocity is very low, it might be expected that an effect which has not been accounted for so far, namely the variation of the field due to the discrete nature of the coils, could prevent its passage around the minor cross section. Such a particle, which remains on the outside of the minor cross section, is the "exterior" superbanana of Fig.4.2.

Thus, the majority of localised particles should, if J were conserved, remain trapped in the helical ripple, and execute a motion

which carries them some or all of the way around the minor cross section without leaving a constant J surface.

Because of the fact that the ordering breaks down at the transition curve, this analysis is also flawed. We now examine the consequences of this breakdown.

Recently, Derr and Shohet have shown, using a computer to "follow" particle guiding centres, that if a particle does detrap, it then moves into a new region in phase space, where the action, J, takes a different value, [51]. J is thus not always conserved, and previous work which assumed conservation of J must be treated with caution. (What is more, they claim to have found no localised particles at all for which J was conserved, and consequently no particles which stayed on constant J surfaces, even for the classes for which detrapping is absent. This observation is less easy to understand in terms of the asymptotic theory of particle motions, although it could arise because of terms which are unexpandable in the small parameter m/e, which go to zero very rapidly in the limit, but which are considerable elsewhere.)

The non conservation of J seems to have contributed to the detrapping, in that all the particles whose constant J surfaces were confined to the inside of the device and which did not intersect the transition curve, were found to detrap when they approached the transition curve, although they otherwise could not have done. Interior Superbananas, it was thus concluded, do not exist.

Finally, we note that, as Derr and Shohet point out, the exterior superbanana is trapped in "spatially localised absolute magnetic wells", which occur beneath alternate l-windings in a classical Stellarator, where the l-windings pass close to the toroidal field coils. Such wells, they assert, do not exist in a Torsatron, nor (so far as we are able to discover) in a suitably designed modular Stellarator. (We may add that,

in a reactor they would probably lie outside the plasma volume, in any case.)

In the absence of these wells, the exterior superbananas are not observed computationally, either, (for e.g. in Torsatrons particles are able to drift helically, in the well between the helical windings, without ever being blocked by the ripple due to a toroidal field coil.)

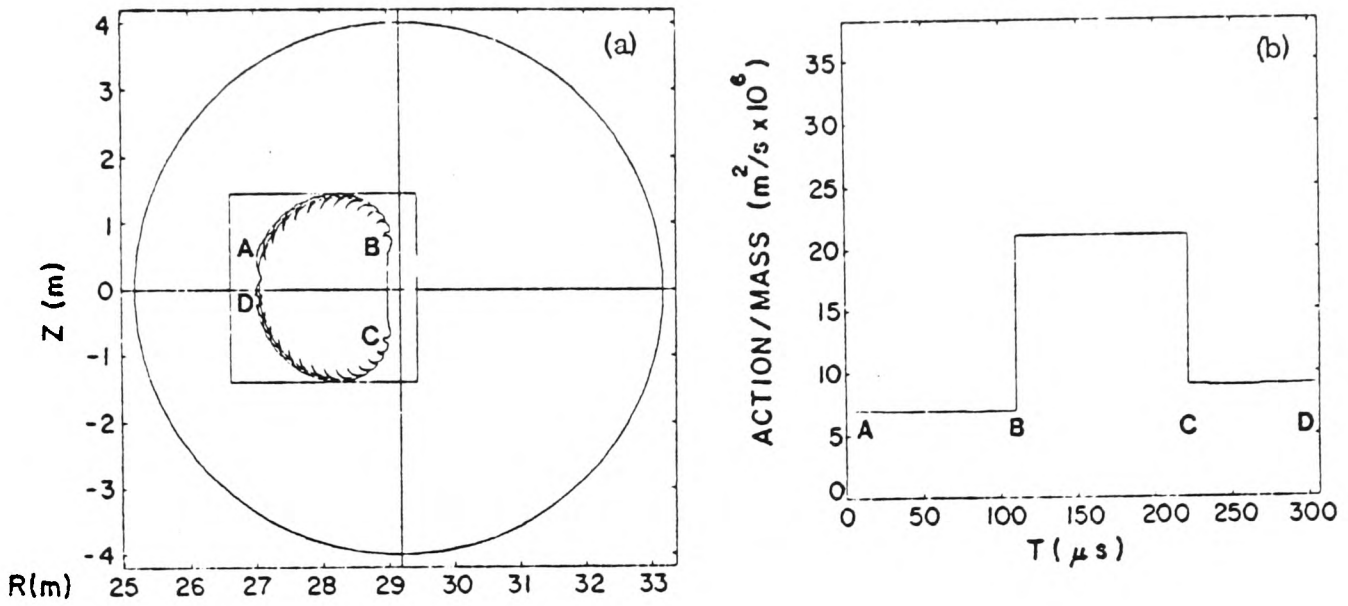

Fig. 4.4. Detrapping of Interior Superbanana.

As Derr and Shohet define a superbanana to be a particle orbit which is localised in θ, ξ (poloidally and toroidally) they conclude that superbananas do not exist in Torsatrons, (and we infer that the same is true for certain modular Stellarators).

In what follows, we shall use the phrase superbanana orbit to describe one of the class of particle orbits in which the particle is trapped in a ripple, at least some of the time, and which, as a result of the drift surface being some distance from the flux surface with which the particle is associated, may give rise to enhanced diffusion.

Effects of Collisions

Suppose the collision regime considered is such that many collisions can take place before the particle is able to drift around a flux surface. The superbanana orbit allows particles, drifting as a result of the radial gradient of the field, to move away from the flux surface with which they are associated. When they eventually undergo a collision they are then transferred onto an appropriately distant flux surface and into what is, in general, a different type of orbit. The process thus gives rise to a radial random walk with a large step-length. As collisions impede the unidirectional drift which gives rise to the excursion from the flux surface (being the only mechanism which was considered, originally, which does so) then they also hinder transport by this process. The above collisionless detrapping mechanism should not be important, in such conditions, for nearly all the particles concerned scatter to another orbit in a collision before they can drift around the minor cross-section and detrap. (Stated slightly differently, the ordering discussed above and in the next section is appropriate to most, but not all, of the particle distribution in velocity space.) The old theory is probably correct for most particles, therefore, but it must be applied with caution, and we shall return to this point after further preliminaries.

4.3 Random Walks and Collisionality

The dominant diffusion processes which are believed to take place may now be described physically in terms of these concepts.

Provided we have a rigorous theory (which may be based on analytic, or, as in this Chapter, computational, methods) which tells us what to look for, we may use random-walk theory to derive diffusion

coefficients in a transparent fashion, [54]. Apart from numerical constants of order unity, the diffusion coefficient is estimated from

$$D \sim \delta n \frac{\langle \Delta x \rangle^2}{t} \qquad (4.3,1)$$

where $\langle \Delta x \rangle$ is the step-length of the random walk, t is the characteristic time between steps, and δn is the fraction of the particles undergoing the particular motion. The one other piece of information we need is the fact that the effective collision frequency, ν_e, for small angle scattering (out of the region in velocity space appropriate to localised particles, such that $q^2/v^2 < \delta_h$), varies as $\nu v^2/q^2$, where q is now the velocity along the field line of the particle concerned, v is the total velocity of the particle, and ν is its mean collision frequency.

We immediately specialise to the "collisionless" regime, which is the case most relevant to a reactor. We shall first describe the conventional view, which is that the dominant diffusion process in this region is due to Superbananas, that is, a random walk with a step length determined by the excursion of a localised particle from a flux surface. This class of orbit is due to the drift of localised particles in the radial gradient of the field.

$$\underline{V}_d = \frac{v_\perp^2}{2\omega_c R_m} \qquad (4.3,2)$$

where ω_c is the ion cyclotron frequency and R_m the major radius. Whilst the particle remains localised, this drift is assumed unidirectional (i.e. vertical), although from Fig.4.3. this is not the case if the particle has the opportunity to drift far. Our treatment is, consequently, only

appropriate for $\omega_d << \nu_e << \omega_b$, where ν_e is the effective collision frequency and the other symbols were defined above.

For a particle to be localised, its velocity must obey

$$\frac{q^2}{v^2} < \delta_h \qquad (4.3,3)$$

Then the time for which it is localised , $t(loc) = 1/\nu_e = (\delta_h / \nu)$. The motion is a random walk with step-length $\langle \Delta x \rangle = Vd.t(loc)$, provided t(loc) is shorter than the time to drift around the minor radius or to detrap by any other means.

Using $\delta n \sim q/v \sim \delta_h^{1/2}$, then the diffusion coefficient due to these particles is seen to be

$$D \sim \frac{v^4}{(\omega_c R_m)^2} \frac{\delta_h^{3/2}}{\nu} \qquad (4.3,4)$$

This expression contains a $1/\nu$ dependence which has led to doubts as to the suitability of the Stellarator as a reactor. This dependence is only predicted over a limited range of ν, however: from the above we recall that the result is not applicable when ν is too small, as the localised particle performs a motion which carries it around the minor cross section, rather than a simple vertical drift.

Further, any mechanism which is capable of causing detrapping, one of which we shall describe in a later section, may have the same effect of reducing the diffusion. It would then seem appropriate to replace ν in the above by whichever is greater of ν_e and ν_d (= detrapping frequency).

Thus when $\nu_e \sim \nu/\delta_h \lesssim \nu_d$ we expect

$$D = \frac{\nu}{(\omega_c R_m)^2}^4 \frac{\delta_h}{\nu_d}^{1/2} \qquad (4.3,5)$$

(For ν very small, and provided no other mechanism apart from collisions is present to take particles into and out of these orbits, then there would be a loss cone from which the particles escape and which is not refilled, so ultimately we would have $D \to 0$ as $\nu \to 0$.)

4.4 "Patching-Up" Neoclassical Theory

So far, we have presented a contradictory picture of Superbanana diffusion: in the first instance, we said that, computationally, it appears that non-conservation of J is associated with a decrease in Superbanana transport. We had already commented that non-conservation of J meant that the small gyro-radius expansion broke down at some order, for some classes of particles. However, we then argued that the presence of "collisionless detrapping" did not mean that neoclassical theory was completely inapplicable, but only that it should be treated with caution.

The discussion of the last section gives a clue to the resolution of the conflict: The treatment was only appropriate for a certain ordering of frequencies, $\omega_d < \nu_e < \omega_b$. Provided this ordering holds, non conservation of J does not have a significant effect on transport processes.

Note that this is essentially the ordering described in (4.1) above as having been employed to solve the Fokker-Planck equation. Indeed, Frieman [3] specialises to precisely this case, to treat localised

particles. The two treatments apply to exactly the same classes of particles, embodying the same physics and essentially the same defects.

It is not sufficient, however, for the ordering to hold for the majority of particles: it must hold for those responsible for Superbanana diffusion, if the above result is to be useful.

When estimating diffusion coefficients from the full kinetic theory of neoclassical transport, it is necessary to evaluate an integral like

$$\int_{x_1}^{x_2} x^n e^{-x} dx \qquad (4.4,1)$$

If v_T is the thermal speed of particles, then we may write $x = v^2/v_T^2$. Then n = 4 and 5 for particle and heat transport, respectively. For consider the result just derived using a random walk argument: $D \sim v^4/\nu$. Using the Spitzer form for the resistivity, $\nu \sim T^{-3/2}$, i.e. $D \sim v^7$. Integrating over the entire distribution, using $P(v)dv \sim v^2 \exp(-v^2/v_T^2)dv$, we obtain the above form for the total flux of particles, with n=4. (For energy we multiply the integrand by $1/2mv^2$, so that n=5.)

The lower limit may be set to zero. The upper limit must be treated with caution, however; because of the exponential dependence on x, it has often been assumed that the upper limit can be taken to be at infinity. This leads to serious errors, because of the high power of x which is also in the integrand. The maximum value of $x \exp(-x)$ is at $x = n$, so if we let the upper limit be at infinity we are principally finding supposed diffusion due to particles with $(v^2/v_T^2) = n$ (4 or 5). We now put the question again: is $\omega_d < \nu_e$ for these particles? $\omega_d \sim v^2/\omega_c R_m r, \nu_e \sim 1/v^3$, and so the inequality is $n^{5/2}$ times harder to satisfy

than for thermal particles, that is, 32 times for particle transport and over 50 times for energy transport.

We must take the upper limit so as to exclude that fraction of the distribution which violates the ordering, and as the condition becomes very stringent in just the region where the integrand is biggest, we find a much smaller diffusion rate.

The problem then arises: how do we account for the effects of the particles which do not satisfy the above ordering, when estimating diffusion coefficients? They are not described by the neoclassical theory which has been developed to date, and it is not clear to us how to develop a satisfactory analytic approximation to treat them. The only theoretical technique which is available at present and which describes ripple diffusion satisfactorily involves the use of Monte-Carlo simulations. However, we can use random walk theory to derive qualitatively correct expressions which should be useful when used in conjunction with such computations, and this we now attempt to do. The results can then be added on, in an ad hoc fashion, to that found from an expression like (4.4,1), with x_2 set equal to the value of $x=x_c$ such that the ordering is just satisfied.

We have already seen that there are at least two distinct types of behaviour, for the very collisionless particles excluded by the ordering. In the absence of detailed information as to the distribution of localised particles between these, we assume that for any given v which is high enough to be in the range considered, a fraction of the particles $\delta n \sim \delta_h^{\frac{1}{2}}$ is involved in each motion.

We shall then be able to find approximate values for the diffusion coefficient, as a function of the distribution of localised particles between the two classes, and hence assess the likely effects of non

conservation of J on diffusion.

For the purposes of estimating diffusion rates we shall assume that, for those orbits for which transitions between trapping states do not occur, the excursion away from a flux surface is $\lesssim r$, a typical minor radius.

(Note that $\langle \Delta x \rangle = Vd.t(loc) \sim \delta_h^{\frac{1}{2}}/\nu$, which was assumed above, is clearly unphysical in the small ν limit, giving a step length greater than the dimensions of the device, and this is the source of the overestimate pointed out above.)

With this assumption, we may find the diffusion coefficient due to these particles.

The motion is a random walk of step length $\langle \Delta x \rangle \sim r$, this distance being typical of the displacement of a drift surface away from a flux surface. We shall take t, as before, to be the inverse of the effective collision frequency. This is probably the most appropriate choice, for the time to drift out of the device on an exterior superbanana orbit will be large compared to $1/\nu_e$ evaluated at $x=x_c$, which is also equal to $1/\omega_d$ given above, where we assumed a simple vertical drift. The number of particles which do drift straight out of the device without undergoing collisions will thus be small, even assuming that such loss orbits exist, (see above). The assumption is not crucial, since the times are the same at $x=x_c$, which is where the dominant contribution to the diffusion arises, as we shall see.

The diffusion coefficient is thus:

$$D \sim \frac{r\nu^2}{\delta_h^{1/2}} \qquad (4.4,2)$$

The particle following computations reported in [51] show that particles which detrap as their orbits carry them round to the outside of the torus travel around the outside in something akin to a banana orbit, and then, so it is claimed, they retrap when they reach the inside of the torus. This is important, because had they been reflected at this point they could have spent a substantial amount of time as a banana, and it would have been more difficult to allow for their contribution to the diffusion. However, if they do retrap immediately, (or even fairly quickly) they spend virtually all of their time as localised particles.

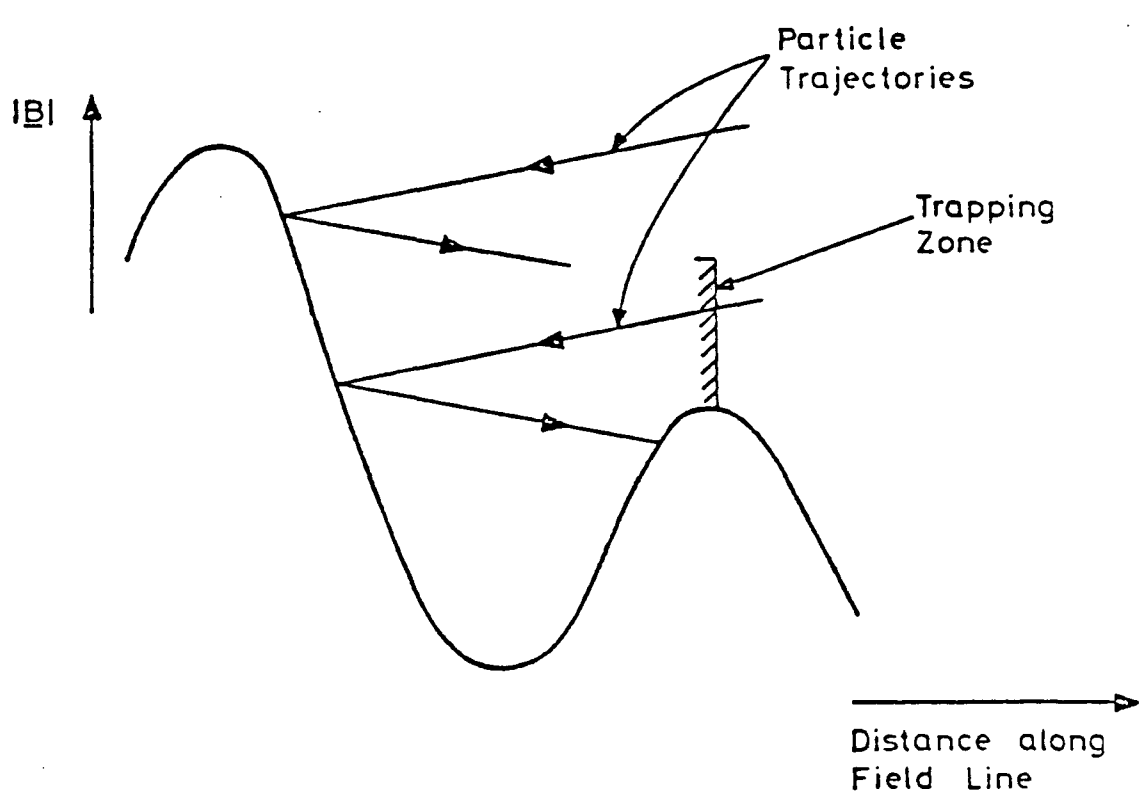

Fig.4.5. Mod B along a Field Line.

The difference between Stellarators and Tokamaks (where the retrapping probability $<<1$) may be understood in terms of the difference in the variation of the modulus of B along a field line in the two cases.

Consider Fig. 4.5, which depicts the modulus of B in such a

system. As the particle travels along the field line, its drift motion carries it into a region where the "hills" of |B| appear to be rising around it, so that it gets closer to being marginally trapped. In an attempt to indicate the result of this drift, the particle has been shown travelling downwards, towards the tops of the hills.

If the particle passes low enough over the hill immediately before the one which finally reflects it, then it will have drifted far enough by the time it returns to the penultimate hill that it cannot pass over it: it is then said to be trapped.

The region within which it must fall for this to happen is indicated on the diagram. The ratio of this region to the non-trapping region determines the probability of trapping. This in turn depends on three things: the drift velocity, the difference in height of successive hills, and the distance between successive hills. The drift velocity induced by the toroidal gradient of the field and the difference in height of the two hills effective in the trapping both scale as the inverse of the major radius, R_m, (although when drifts due to the helical Stellarator field are allowed for, a drift which is independent of R_m appears which could take part in the trapping.) The third factor depends on the number of toroidal periods in the Stellarator (typically $p \sim 5$) and the number of coils in the Tokamak case (about $N \sim 20$).

If the trapping zone is of width $\delta W/R_m N$ in the Tokamak, then in the Stellarator it is $\delta W/pR_m$, for the particle has time to drift further. Let the total "target area" above a hill be T/R_m: the trapping probability is $\delta W/pT$ for the Stellarator, and $\delta W/T$ for the Tokamak, even neglecting the effects of drifts in the helical field, (which may be relatively large at large aspect ratio). As δ/δ_T could be about four, this alone could make the difference between a rather low trapping probability, of about 1/4 for a Tokamak, say, and virtual certainty of trapping in a Stellarator.

Consider the class of particles which are capable of passing

several times around the orbit of Fig. 4.1, without being scattered into another orbit by a collision. We may characterise their radial position in terms of the minor radius of the banana like part of the orbit.

As the relatively collisionless particles drift, whilst localised in the helical ripple, the effect of collisions is principally to cause a series of small changes in the magnetic moment of the particle, which will do a random walk. This is important for diffusion, because the value of the magnetic moment will determine the point at which the particle untraps by the collisionless mechanism described above. It may, as a consequence, emerge onto a banana like orbit which is at larger or smaller radius than before. Its mean radius also does a random walk, therefore, dependant upon the change in μ during each pass through the localised region.

In each collision, the magnetic moment changes by an amount

$$\Delta\mu = \frac{\Delta(mv_\perp)}{2B} = \frac{mv_\perp \Delta v_\perp}{B} \qquad (4.4,3)$$

These are small angle scatters, with an effective collision frequency

$$\nu_e \sim \nu\,(v^2/\Delta v_\perp^2) \qquad (4.4,4)$$

and so in the time it takes to drift around the minor cross section, t, (which we may calculate, but which will cancel out of the final answer exactly, so we prefer not to) there are $N=t\nu_e$ collisions of this type.

The distance "walked" in μ -space is thus

$$\Delta_{tot}\,\mu = N^{1/2}\,\Delta\mu \qquad (4.4,5)$$

Following Derr and Shohet, we assume that $\delta_h >> \varepsilon_t$, so that the helical variation is primarily responsible for the detrapping observed. (This is certainly reasonable as we are discussing what would have been interior superbananas, which eventually pass close to the magnetic axis where they must detrap as $\delta_h \to 0$.)

To a first approximation, we find the maximum value of the field on a field line, given by (4.2,1) as a function of the starting point of that field line on a given minor cross section to be simply

$$B_{max} = B_o (1 + \varepsilon\alpha\rho^n), \varepsilon\alpha\rho^n = \delta_h \qquad (4.4,6)$$

When the particle detraps, it has just enough energy to pass over the helical ripple and escape: its parallel velocity goes to zero, (the source of the difficulty with the neoclassical theory which we have discussed). We assume that its total energy is virtually constant during the small angle scatters. At the detrapping point the total energy is μB, and so we may say that the change in μB at the detrapping point, produced by the small angle scatters, is also zero.

Then $\Delta(\mu B) = \mu.\Delta B + \Delta\mu.B = 0$, and

$$\Delta\mu/\mu = - \Delta B/B = \frac{-n\delta_h}{\rho} . \Delta\rho; \ \rho \lesssim 1. \qquad (4.4,7)$$

This result allows us to determine the step length, $\langle\Delta x\rangle \sim r\Delta\rho$.

The diffusion coefficient may be found from (4.3,1); the only other piece of information needed is the fraction of particles involved, which, as we pointed out above, is

$$\delta n \sim (\delta_h)^{1/2}$$

The diffusion coefficient is thus:

$$D \sim \frac{4r_2^2 \nu}{n^{2/3} \delta_h} \qquad (4.4,8)$$

which is the same as the above result, but multiplied by a constant factor of order unity.

The total diffusion coefficient, representing the effects of localised particles, may now be estimated in terms of the fractions of the high energy tail of the distribution which participate in each of the single particle orbits described above, for localised particles. The fraction which detrap will be denoted f_1, the fraction which do not f_2. Then $f_1+f_2=1$.

We note that the distribution function can be written in terms of x (defined above) using

$P(x)dx = 2\pi^{-1/2} x^{1/2} e^{-x} dx$, for a Maxwellian distribution,

and as the collision frequency may be written

$$\nu = \nu_t \frac{3\pi}{4}^{1/2} x^{-3/2} A(x) \qquad (4.4,9)$$

where $A(x) = (\eta + \eta' - \eta/2x)$, with

$$\eta = 2\pi^{-1/2} \int_o^x t^{1/2} e^{-t} dt, \qquad (4.4,10)$$

so that $A(x) = 1$ for $x>1$, and

$$\nu_t = \frac{4}{3}(2\pi)^{1/2} \frac{ne^4 \ln\Lambda}{m^{1/2} T^{3/2}} \qquad (4.4,11)$$

then we find a diffusion coefficient given by

$$D \sim \frac{8\pi}{3} \frac{\delta_h^{3/2}}{\nu_t} \left(\frac{2T}{eBRm}\right)^2 \int_o^{xc} \frac{x^4 e^{-x}}{A(x)} dx + \frac{\nu_t r^2}{\delta_h^{1/2}} \left(\frac{4f_1}{n\delta_h^2} + f_2\right) \int_{xc}^{\infty} \frac{A(x)e^{-x}}{6x} dx \qquad (4.4,12)$$

We see that, somewhat surprisingly, the detrapping particles give rise to a diffusion which is $1/\delta_h$ faster than that due to the permanently localised particles. This is a consequence of their taking steps more often.

It is of interest, now, to make comparison between this estimate and the "equivalent" result for transport in an axisymmetric system in which a "collisionless" plasma is contained. In this case, the particles executing banana orbits are most significant.

The banana orbit depicted in Fig.4.1 has a finite width Δ_b, which is the distance the particle is carried away from a flux surface by the banana orbit. As a result of scattering, particles in such orbits do a random walk of step length Δ_b.

The banana particles are trapped by the toroidal variation of the magnetic field, so their parallel velocity obeys $q^2/v^2 < r/R_m$. The frequency of scattering out of banana orbits is thus $\nu_e \sim\sim \nu R_m/r$, and the number of such particles is $\delta n \sim (r/R_m)^{\frac{1}{2}}$

The banana width is roughly

$$\Delta_b \sim a \frac{B_o}{B_p} \left(\frac{r}{R_m}\right)^{1/2} = aq\left(\frac{r}{R_m}\right)^{-1/2} \quad (q=1/i, \text{ the "safety factor".}) \quad (4.4,13)$$

which may be deduced from the expression for the drift surface, (see Hinton and Hazeltine, [55],) and so the diffusion coefficient is found to be

$$D \sim a^2 q^2 \left(\frac{R_m}{r}\right)^{3/2} \quad (4.4,14)$$

The total diffusion rate for these particles is then

$$D \sim \frac{3}{2}\nu_t \bar{a}^2 q^2 \left(\frac{R_m}{r}\right)^{3/2} \int_o^\infty A(x) e^{-x} dx \quad (4.4,15)$$

where $\bar{a}$ is the Larmor radius of a thermal particle.

To proceed, we need to know x_c. For a number density of $2 \times 10^{14}/cm^3$, at 10keV, we find

$$\nu_e \sim 200x^{-3/2}$$

The drift frequency, for a Stellarator with B=7T., Rm=15m., r=2m., is roughly 40x. At $x=x_c$, these are equal, which implies $x_c=2$.

If we compare the second term in (4.4,12) to the banana result, with $x_c=2$, we obtain a ratio

$$\frac{1}{180} : \frac{(\bar{a}q)^2}{(r)}$$

The first integral in the localised particle diffusion coefficient and the banana result are in the ratio

$$8v^2 : (\nu_t q R_m)^2 (\varepsilon\delta_h)^{-3/2}$$

If q=3 and r=1m, then for 10keV deuterons/tritons, the first ratio is roughly 20:1. The diffusion rate due to these particles is obtained from this result by multiplying it by f_1, the fraction of the localised particles which are involved in the motion. Naively, one might expect that the fraction of the total number of particles involved would be the root of ε_t, assuming that the particles are those which would perform banana orbits in a Tokamak. However, the orbits are sufficiently complex that it cannot be assumed that toroidicity is responsible for the detrapping, as we have seen above.

The detrapping particles occur in the region close to the magnetic axis, where the helical field strength is relatively small, so there are probably fewer of them than permanently localised particles, partly because of the smaller ripple well and partly because of the smaller volume in which they can exist. For this latter reason we shall take f_1 to be about 1/4. The rate due to these particles is then predicted to be about 5 times the banana rate. The other localised particle term is probably comparable with the banana term, however.

4.5 Comments and Conclusions

We have considered the contribution of localised particles to the diffusion in a Stellarator. As the neoclassical theory does not appear to be adequate to deal with all the classes of particles which are important for diffusion, a simple random walk model has been developed. On the basis of this model, a diffusion rate up to an order of magnitude greater than the banana rate is predicted. (We note also that it is not the usual Superbanana term which gives rise to the dominant contribution.)

This result, if it were correct, (and the most appropriate theoretical test would be a Monte-Carlo code) would imply that the diffusion in a Stellarator need not be worse than in a Tokamak. For in practice the confinement of ions in Tokamaks is in the range 3-10 times neoclassical: the above result is not sufficiently different, given that various factors (such as the electron diffusion rate) are unknown, to suggest that it should be any higher in a Stellarator.

The result may be put another way: we have established that the transport does not scale as the inverse of the collision frequency, but rather as the collision frequency, (neglecting the effects of x_c varying with temperature) and so if we were to extrapolate from current experiments to a reactor using these results we would obtain rather low transport rates.

We have already seen that, on the basis of the M.H.D. theory which has been developed in the previous chapters, it should be possible to obtain plasmas with beta values comparable with those obtained in Tokamaks, in Stellarators of similar aspect ratios and shapes. It is thus reasonable to expect that the two could be operated with similar plasma parameters, for the ion transport rates are similar, (although the electron transport may be slower in a Stellarator, which would decrease the ion rate). Thus we shall assume that if a Tokamak can meet the

ignition condition, for given plasma beta, magnetic field, etc., then a Stellarator can also.

Before leaving this section, we consider two topics related to transport theory, having a significance for the present work which we wish to indicate very briefly.

Bootstrap Current

The bootstrap current is supposed to arise due to the motion of electrons in banana orbits, which, viewed from above the torus appear as in Fig. 4.6:

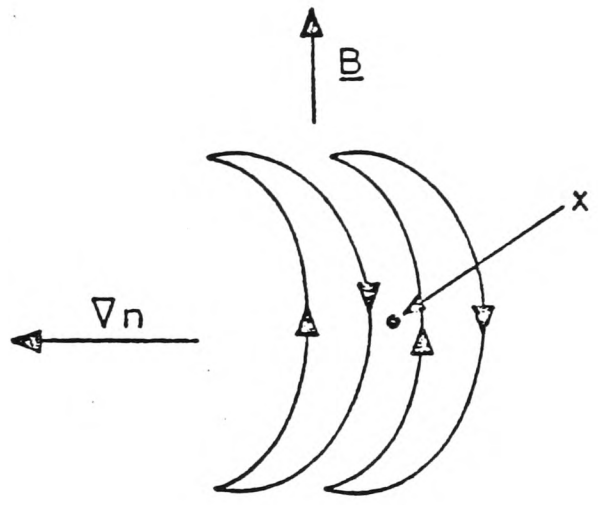

(From above plane of torus)

Fig. 4.6. Mechanism of Bootstrap Current.

In the presence of a density gradient, then at point x in this diagram, more electrons are moving to the bottom than to the top. This current is amplified by the interaction of these particles with the passing electrons, giving rise to the bootstrap current.

This effect, which is due to the "neoclassical" behaviour of the electrons, has not been adequately confirmed experimentally. One possible reason is that although the ions behave neoclassically, the electrons do not. This is chiefly a consequence of the mass ratio of the two, [56], in

that electrons, being lighter, are better able to "see" imperfections in the field, (produced by microinstabilities or otherwise) giving rise to their "anomalous" (non neoclassical) behaviour.

For the moment we shall assume that the bootstrap current will not be significant in our Stellarator reactor.

Flutter Transport

As a current free Stellarator might be expected to predominantly support electrostatic waves rather than electromagnetic, which are likely to occur in a Tokamak in addition, there may be considerable differences in the wave driven transport in the two cases, [56]. In particular, if there is less "flutter" in the fields in Stellarators, electron transport may be slower than in Tokamaks.

Chapter Five: Coil Systems

In this Chapter we discuss the properties of the fields due to specific coil sets. We begin by considering the different ways of producing a Stellarator field.

The discussion of the field structure which follows is in several stages and degrees of complexity, similar material being discussed in more and more detail. Interspersed at appropriate intervals are details of the computational (and other) methods employed.

The stages are:

(i). The nature of the field in a straight Stellarator is described using the method of averaging, in order to explain the basic features which are revealed during field line following computations.

(ii). The results for the toroidal case are described in qualitative terms, and computational studies of the fields due to a type of modular coil are introduced. We distinguish two types of separatrix:

(a). A helical separatrix may be formed by the Stellarator part of the field.

(b). A Tokamak like separatrix arises in some circumstances due to the gaps between the coils.

We outline how the coil parameters are varied until a broad optimum region is reached.

(iii). An attempt is made to infer the mechanisms governing separatrix formation and transform production so that the field may be modelled analytically, for the optimisation of a Stellarator reactor. Finally, ways of providing a divertor are examined.

5.1 Types of Stellarator coils

The Stellarator field is composed of a main toroidal field and a smaller helical field, whose function it is to provide the necessary rotational transform. The precise nature of these fields and the role of rotational transform in maintaining the plasma equilibrium and in certain stability criteria have already been discussed. We shall now describe the various ways of generating the fields.

In the original work of Spitzer [57] two conductor configurations capable of generating rotational transform were put forward. (i). A topologically toroidal solenoid with a non-planar axis: in this case a transform arises naturally due to the geometry. (ii). A circular toroidal solenoid plus 21 helical windings carrying current in alternate directions, as shown in Fig.5.1. In this case a Stellarator field with 1 periods in the poloidal direction is set up. The former concept has received little attention in recent years because of practical difficulties in its implementation. The latter concept, which will be referred to as the "classical" Stellarator, has been widely investigated, but it is increasingly recognised that this concept cannot form the basis of a credible fusion reactor design, because of the large forces which act on the 1 windings, and the consequent massive retaining structure which is required, as well as the difficulty of making such a system modular.

More recently, it has been pointed out that a set of 1 helical windings all carrying current in the same direction will create a toroidal field plus a helical field of the Stellarator type, having the same, 1-fold, periodicity, [58]. In such a system, which is known as a Torsatron, it is usually necessary to apply an external vertical field to compensate that due to the windings, although a suitable modulation of the helical conductor winding law can achieve the same end.

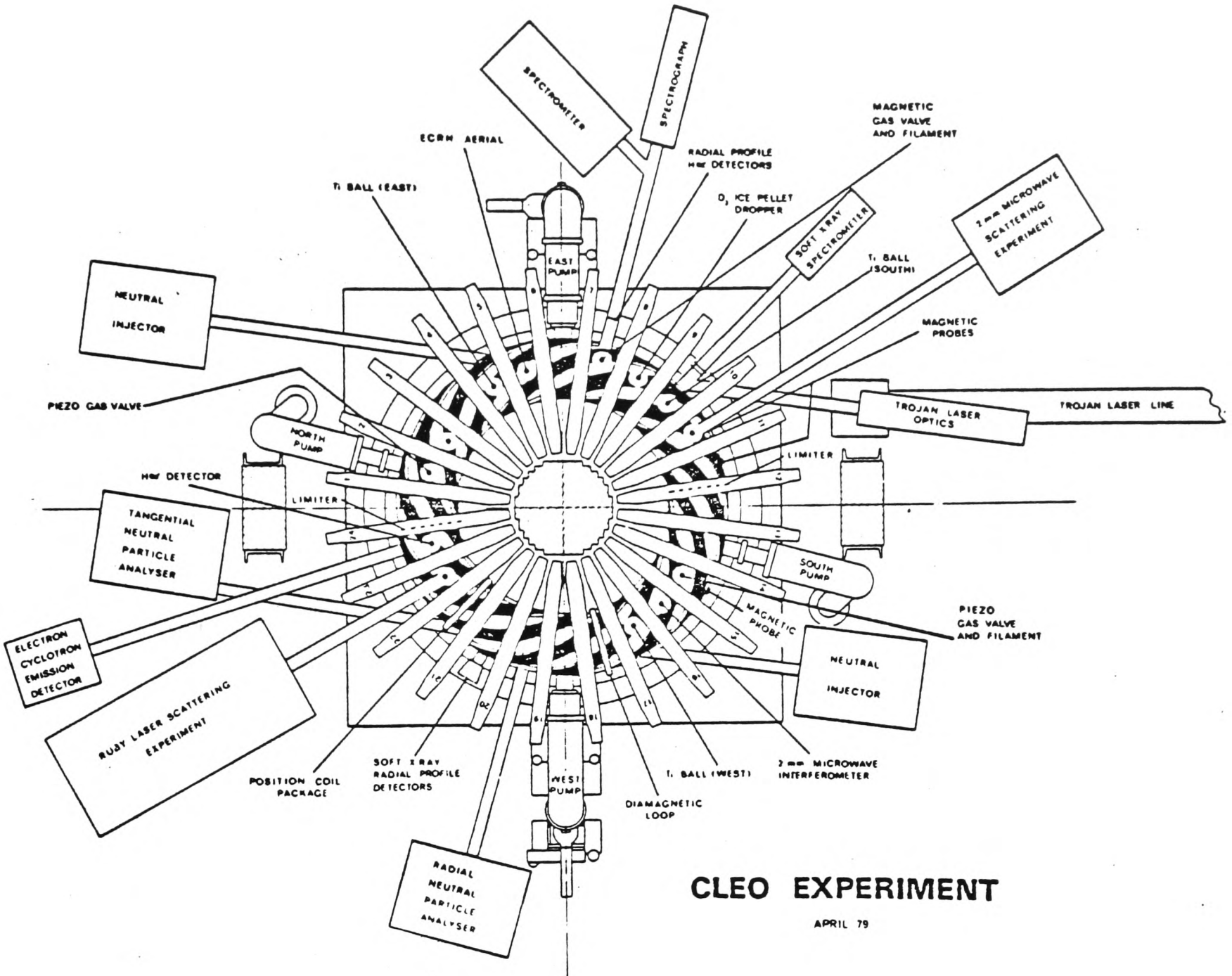

Fig. 5.1 A "classical" stellarator

Both the conventional Stellarator and the Torsatron suffer from the fact that they are difficult to construct in modular form.

Another possible configuration which we shall argue to be optimal is the Wobig-Rekker coil system. This configuration can be regarded as the natural way of producing a Stellarator field in that it reproduces, at least qualitatively, the currents which would flow on a virtual casing enclosing the desired magnetic fields. The configuration consists of a set of twisted coils, as depicted in Fig 5.3, capable of producing all the fields necessary for reactor operation. Such coils were first discussed by Wobig and Rekker [59] and more recently by Derr [60] and Chu [61].

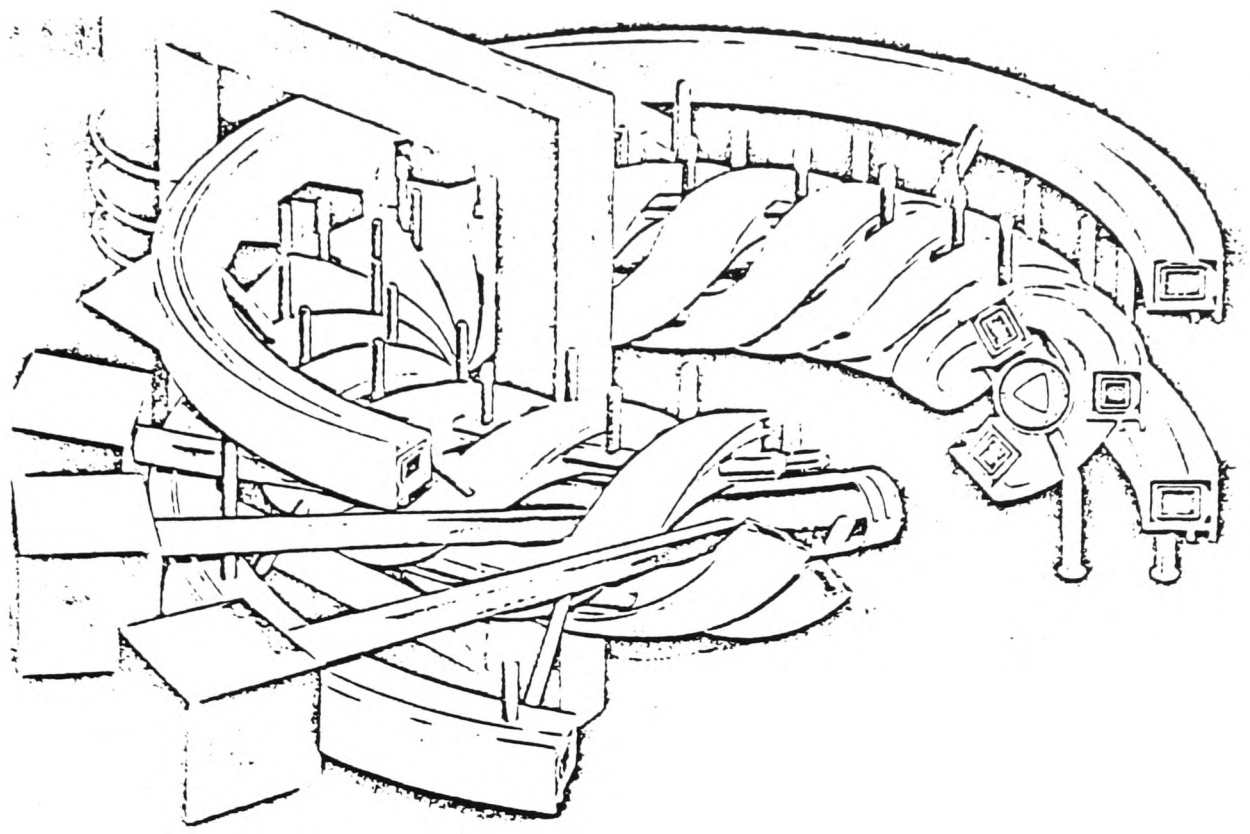

Fig. 5.2 A "Torsatron"

5.2 Basic Ideas

The topics to be discussed, namely the structure of the magnetic field and the choice of the coils, are introduced.

5.2.1 Field Line Behaviour

Before going into details of the choices made, a description will be given of the main features of the field line behaviour in the type of Stellarator which we are considering.

As the set of equations (2.3.1,2) govern the field lines rather

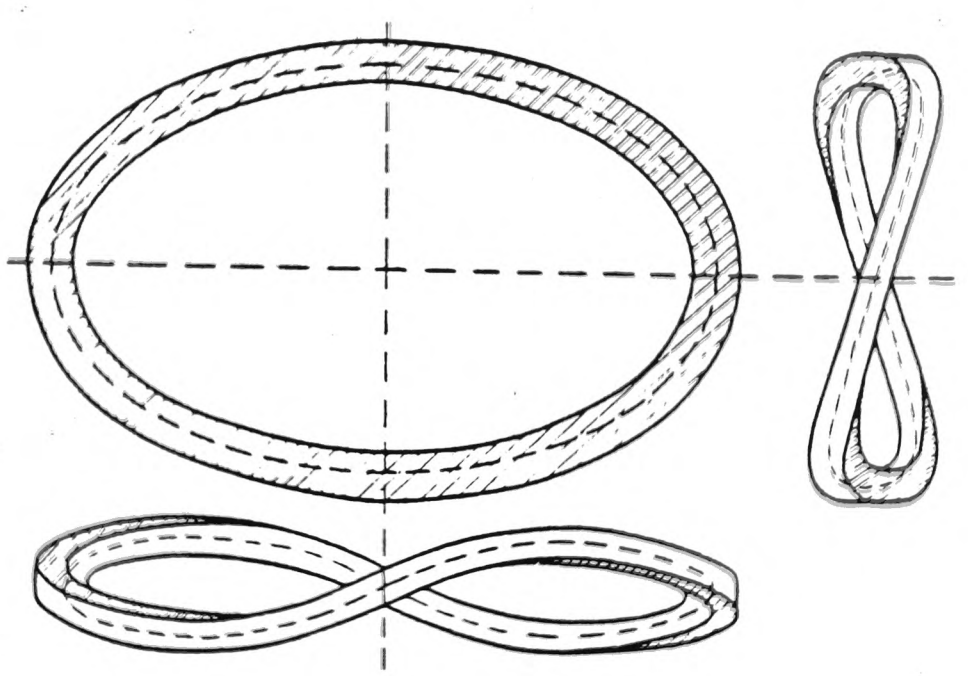

Fig. 5.3 A "twisted" $\ell = 2$ coil

than just the surface in which they lie, the solution they yield contains information as to the position of the field line within the surface, as well as the equation for the surface. Morozov and Solov'ev [1] found the solution of (2.3.1,2) in the form given by (2.3.1,4), by writing the original equations in the form:

$$\frac{dx_1}{dx_3} = \frac{1}{\sqrt{g}B^3} \frac{\partial \psi}{\partial x_2}, \text{ etc.} \qquad (5.2.1,1)$$

Applying this general result to a straight Stellarator they found ψ to a first approximation to be a function of radius only.

Integrating (5.2.1,1) and writing deviation magnitudes $x=r-r_o$, $y=r_o(\theta - \alpha z)$, with

$$\alpha = \frac{d\theta}{dz}$$

they are able to relate x and y :

$$\frac{x^2}{a^2} + \frac{y^2}{b^2} = 1 \qquad (5.2.1,1)$$

where a and b vary as the helical field strength.

The surface is to the first approximation a cylinder and the field lines' lowest order motion is a spiral on its surface. The deviations are due to a second spiralling motion on an elliptical tube, whose axis is the first spiral, wound around the larger cylinder.

It is to be expected that in a toroidal Stellarator, the field lines' gross behaviour would be rather similar, and indeed very similar qualitative features are observed, in the field line following calculations we have performed. Fig.5.4 shows the intersections of a field line with a minor cross section, and Fig.5.5 shows the same field lines' position plotted in the cylindrical coordinates Z,R (in other words, projected onto a running minor cross section).

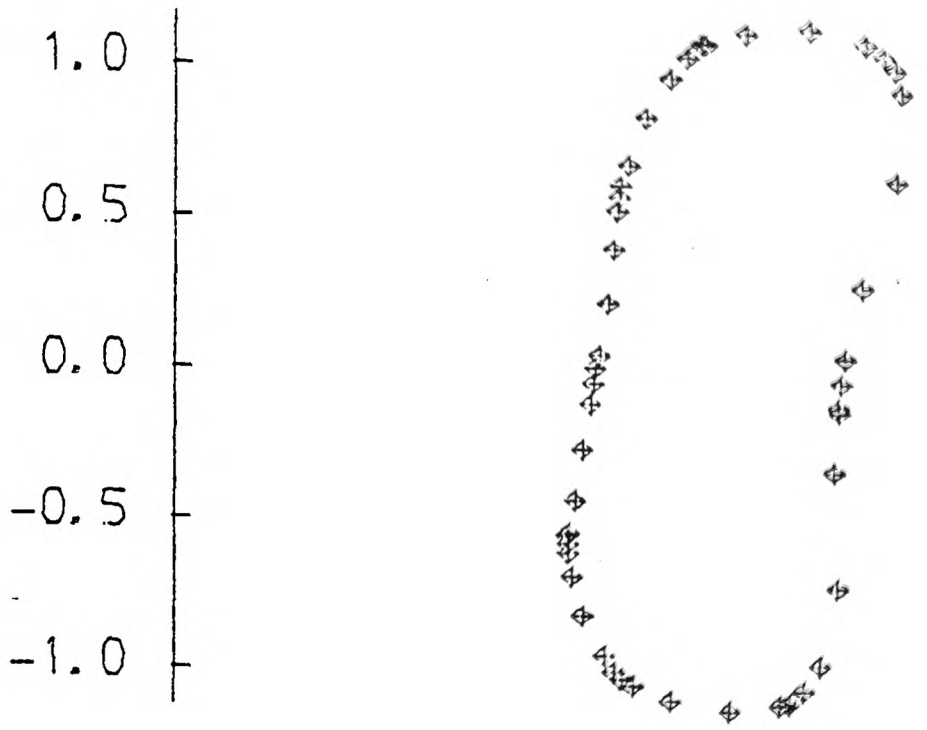

Fig. 5.4. Field Line Intersections with a Minor Cross-Section.

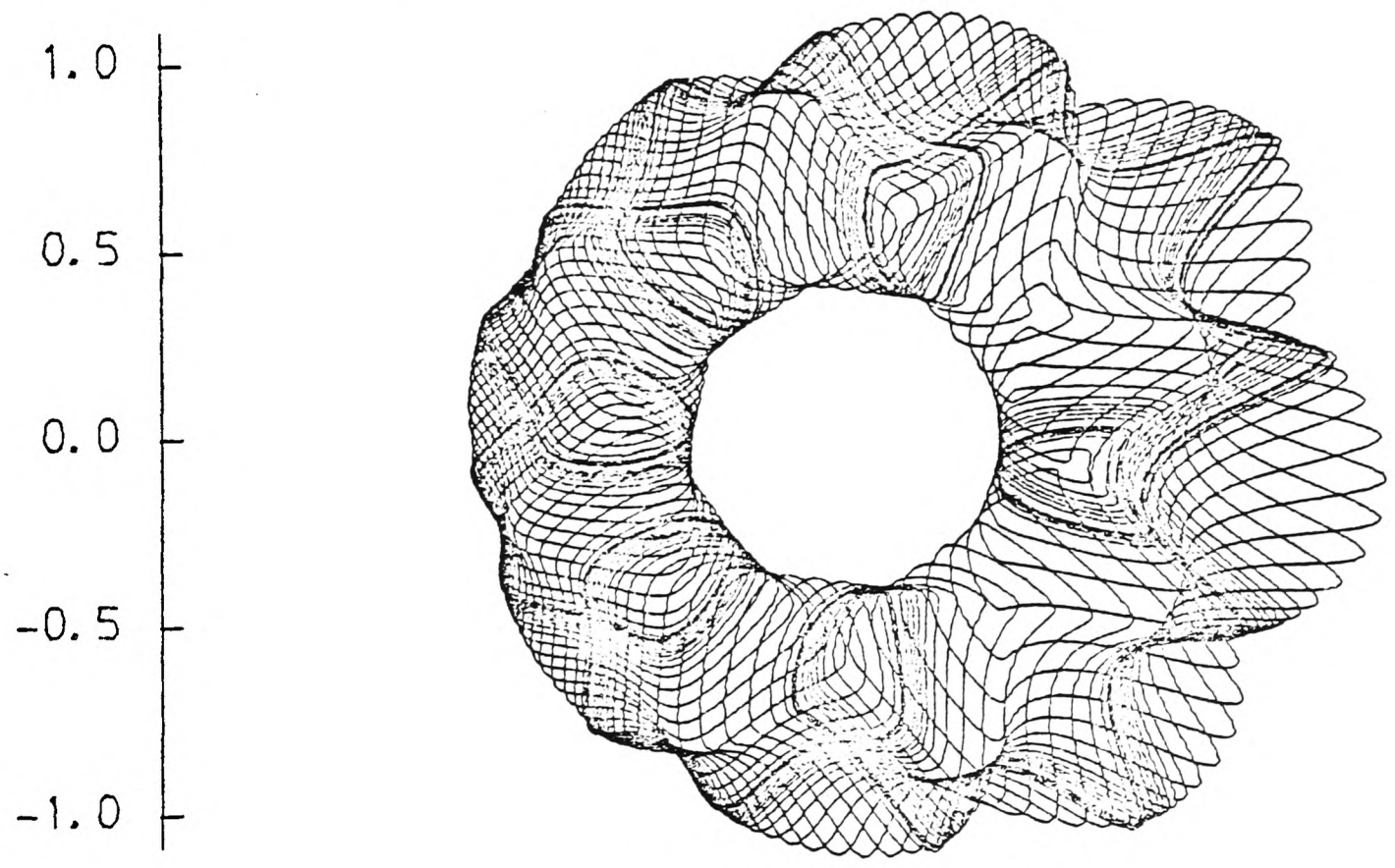

Fig. 5.5. Projected Field Line Trajectory.

5.2.2 Coil Parameters

In theory it might appear to be a simple matter to decide on the optimum set of Stellarator windings, once the plasma physics has been understood. First one should specify a field corresponding to a plasma column of suitable aspect ratio which allows a sufficiently high beta and, if required, divertor action. Given that field the magnetic surfaces can

be found. Then the "virtual casing principle" described in Chapter Two, applied to an outer surface, could be used to determine the currents flowing on it which would create the given field. One can imagine a process of aggregation of these continuous current sheets into a finite number of discrete current loops lying in this outer surface, and in turn these may be approximated by a set of twisted coils. Unfortunately this program does not lead to a realistic Stellarator design: although the currents on the virtual casing can indeed be simulated by filaments, it turns out that the result is a large number of filaments which are of very different shapes. In other words, it fails to satisfy the requirement which we have imposed above, for practical reasons, that is, that the configuration should consist of a small number of identical, filamentary coils each with a relatively small deformation away from a planar circle, so that they can constitute the modules of the configuration. It does not follow that such a modular configuration is impossible - only that its design cannot be evolved in precisely this way. Instead it is necessary to turn to computation.

Once a coil configuration has been found, there still remains the problem of the mechanical structure of the coils, and of the forces on them and how to support them. This we shall attempt to deal with in the next Chapter.

5.3 Twisted Coil Systems

The properties of the magnetic fields due to twisted coils, as found from field-line-following calculations, are described in more detail. The procedure for searching the parameter space is described.

5.3.1 Analytic Models

If one attempts to use analytic theory alone as a guide to the design of the coils one is likely to be misled. The behaviour of field lines is extremely complex and it is very difficult to identify valid approximations before making computer calculations to indicate which effects are important. In particular, the separatrix position is not described even approximately by the expression which is usually appropriate to a classical Stellarator and may also differ widely from that in an equivalent (i.e. modular) straight system. Nevertheless, the parameter space in which the designer of a Stellarator reactor has to work is so large that it is virtually essential to discover some workable analytic model. In what follows, we shall derive some analytic estimates of the dependence of separatrix radius and rotational transform on the coil shape and layout, and discuss the accuracy with which they represent the computer results. The comparison can fortunately be made rather brief, for our predictions for separatrix radius and transform are extremely simple, once the relevant mechanisms are established.

In the case of transform, we find a surprisingly high level of agreement. As regards the separatrix radius, the position is less straightforward, since this can in unfavourable cases be severely reduced by island formation in the vicinity of rational surfaces, so that the predicted separatrix radius is merely an upper bound, for such effects are not accounted for in the model. However, it represents this upper bound rather well.

We begin our discussion of these quantities by considering the analytic theory of separatrix formation in an ideal straight Stellarator. The discussion serves principally as a warning, for we shall discover shortly that the theory is virtually irrelevant to to the separatrix in the Stellarator we shall study. However, it serves to introduce some of the relevant ideas.

By an "ideal" Stellarator, we mean a Stellarator in which the field is derived from the scalar potential:

$$V = B.z + b_n.I_n(n\alpha r).\cos(n\theta - \alpha z),\ \alpha = p/\ell R_m \qquad (5.3.1,1)$$

(i.e. only one periodic term). Clearly such an expression would not be expected to hold in the immediate neighbourhood of the coils, but it might be hoped that it would represent the field with sufficient accuracy out to the separatrix, if this lay well inside the coils. The exact expression for the magnetic surface in this case is given in [1], and is:

$$\psi = B.r^2 + \frac{2r.b_n}{\alpha}.I'_n(n\alpha r).\sin(n\theta - \alpha z) \qquad (5.3.1,2)$$

If it is tentatively assumed that the separatrix is at a sufficiently low radius that we may expand the Bessel function in powers of r and obtain a good approximation by retaining only the first term, then the expression for the surface function becomes

$$\psi = r^2(1 + 2\delta\, r^{n-2}\sin(n\theta - \alpha z)).\ \delta = \frac{b_n}{2B}\left(\frac{n}{2}\right)^{n-1}\frac{1}{(n-1)!} \qquad (5.3.1,3)$$

This suggests that if $\delta < 1/2$, then for $l=2$ a separatrix will not be formed, whereas for $l=3$ a helical separatrix is always predicted, as r increases.

To see whether this approximation is likely to be valid, and to verify the prediction, we may find the exact condition for a separatrix to occur, using the fact that $\nabla\psi = 0$ at the separatrix, and the relation

$$I_n'' + \frac{I_n'}{n\alpha r} - (1 + (\alpha r)^{-2})I_n = 0 \qquad (5.3.1,4)$$

The condition is found to be

$$\frac{b_n}{B} = \{n(1 + (\alpha r)^{-2})I_n(n\alpha r)\}^{-1} \qquad (5.3.1,5)$$

Now $I_2(2\alpha r) = (\alpha r)^2/2$ provided $r \ll 1$, therefore $\delta = 1/2$ is no longer the condition for separatrix formation, but

$$\delta(1 + (\alpha r)^2) = 1/2.$$

As $r \leq R/3$ then $\alpha r < 1/2$ for $p=3, l=2$, and for such a separatrix to form within the coils we must have $\delta \gtrsim 2/5$, which is only a slight relaxation of the above condition, in the cases we shall study - such a separatrix could perhaps be formed, but we have not been able to observe it.

We may note that this "ideal" straight Stellarator theory predicts that when a separatrix does arise, it has 1-fold helical symmetry. It occurs when the term in grad ψ due to the helical deformation of the surface balances that from the square of the radius. In a "real" straight classical Stellarator, such a helical separatrix does indeed occur, even if its radius is not correctly predicted by the "ideal" theory. This is because the separatrix is formed when field lines cease to lie on surfaces and orbit poloidally about the 1-winding, which follows a helical path, so locally it runs roughly toroidally. This separatrix is consequently "tied" to the 1-winding, and has the same symmetry.

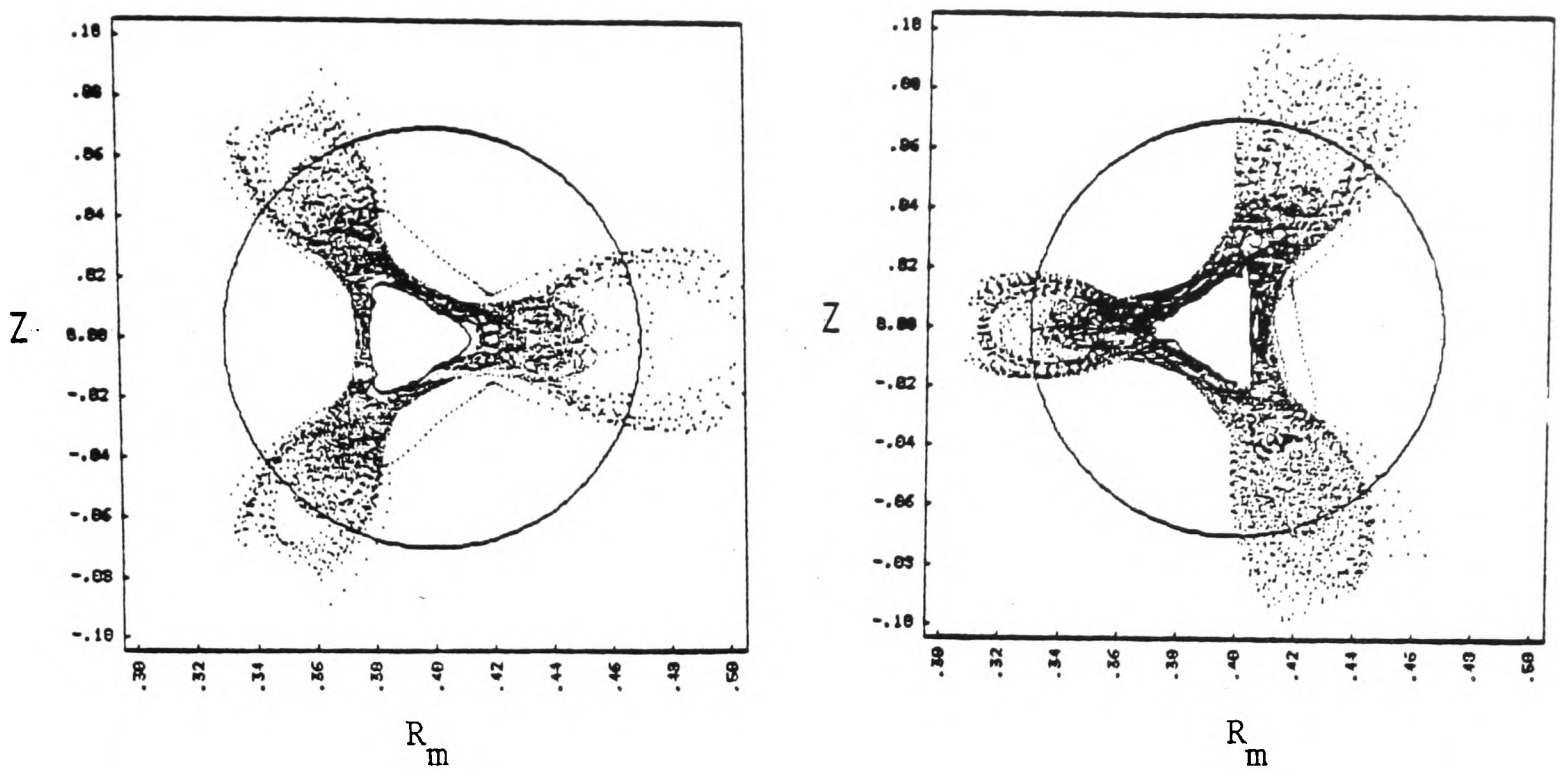

Fig.5.6. Helical Separatrix.

By contrast with this discussion of a classical stellarator, in a modular l=2 system the separatrix is likely to be quite different. It still occurs when surfaces break open and the field lines orbit the coils, but as the coils run poloidally the field lines orbit toroidally about them. The finite toroidal spacing of the coils is responsible for this separatrix, exactly as in a Tokamak. The analytic theory discussed above is evidently irrelevant to the calculation of the separatrix radius in this case, unless the predicted radius of the "ideal" helical separatrix is well inside the coils. Since we have seen that this not true for the l=2 Stellarators which are of interest to us, we shall presently have to consider what factors determine the Tokamak-like separatrix radius in this case. We should recall at this point that the nature and position of the separatrix depend crucially on various error fields, as pointed out by Gibson, [62]. If a rational surface lies near the outside of the useful volume, the surfaces can break open on the outside, as the errors in the field create islands of finite width centred on the local magnetic axis. The separatrix is then in the neighbourhood of the rational surface in question.

The rotational transform may also be shown to exhibit different behaviour in the two cases.

An ideal straight Stellarator (with only one field harmonic present) has helical symmetry, all quantities being functions of $(r, \theta - \alpha z)$ only. A field line which lies on the separatrix can be shown to approach a ridge of the (analytically calculable) helical separatrix asymptotically, [1]. (A ridge is an apex of the separatrix, one of which is located beneath alternate l-windings.) As a result, the rotational transform at the separatrix should be that of the ridge. Further, as the ridge position depends only on the winding position in this symmetric situation, the transform should be given by the rate of rotation of the winding.

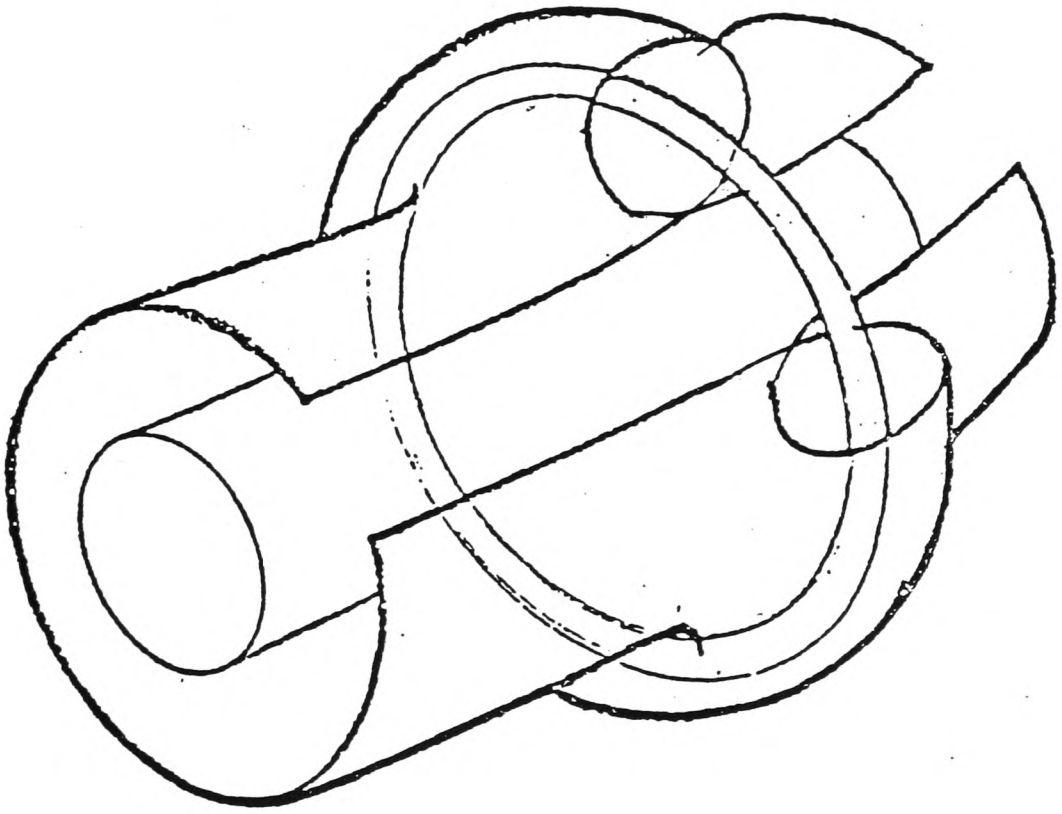

Fig.5.7. "Tokamak-like" Separatrix.

Computation proves that this is not true in a modular or a toroidal system - there is no reason in the former case why the separatrix should have a ridge which field lines approach, asymptotically, at all: see above.

5.3.2 Procedure for Optimisation of Parameters

Without the guidance of analytic estimates we are faced with the task of determining the point corresponding to the optimum coil set in a huge parameter space. Fortunately, a major simplification of the task results from the fact that an economic reactor with an acceptable total power output has a low aspect ratio: we shall show below that it follows from this that the fields must be based on l=2. (It may, however, prove advantageous to include a small amount of l=6.)

Optimising l=2 coils, subject to certain structural constraints, to produce as large a rotational transform as possible without losing too much plasma volume is a formidable task, however, even with this restriction. The number of variables is still too large for a methodical search of parameter space. For each set of coil parameters it proves to be essential to study flux surfaces at many different radii and not just at the centre and the separatrix, for instance, because of the possibility that at some intermediate radii, the field lines do not lie on closed surfaces.

Such ergodic regions occur in the neighbourhood of each rational surface. (Formally, there is a rational surface arbitrarily close to any point in the volume; fortunately the region of ergodicity around each such surface is normally correspondingly narrow, and it is only the rational surfaces corresponding to the ratio of a pair of small integers which prove to be troublesome).

In order to minimise the loss of closed surfaces we endeavour to avoid the most dangerous rational surfaces. This we do by attempting so far as possible to ensure that the rotational transform does not take on the corresponding values within the plasma volume. Examples of such values would be i = 1, 1/2, 1/3, 2/3, whilst 2/5, 3/5, 4/5 may or may not be dangerous - it is precisely because we cannot be sure about the extent to which field errors affect these latter that we need to do computer

checks on them. (In some cases it may be possible to take steps to minimise the effects of any rational surfaces which cannot be excluded, and so to live with them. For instance, we attempt to avoid resonant errors in the field, so that islands are less likely to form at rational surfaces.) All this is extremely costly in terms of computer time and makes it impossible to explore the parameter space exhaustively.

The method by which we have represented the Stellarator coils in our computational field line following is not ideal, in that we have had to use straight-line filaments to approximate the curved winding, [63], (which itself is represented by a Fourier series similar to that used in [59], and is adequate given the restrictions outlined above). The field errors that this representation gives rise to are responsible for the formation of magnetic islands of finite width, (Fig. 6 .7).

By doubling the number of filaments allowed by the program (from 1500 to 3000) we have been able to significantly reduce the effects of island formation on the surfaces, confirming that the filamentary representation is indeed the culprit. Even with 3000 filaments, however, there are still significant errors in the field, particularly near the conductors. These errors create islands which, we believe, would be of negligible width in the real system.

At the same time, we should report that this doubling the number of filaments decreased the rotational transform by about 20%, to the value we have quoted, without our making any other changes in the coil parameters. (Calculation with varying numbers of filaments per coil suggested that there would be little or no further change in i if the number were increased still further.) We can offer no satisfactory explanation of this observation.

A second source of difficulty inherent in the computations is connected with the choice of the step-length: for accuracy it is desirable to take the step-length as small as possible, (although rounding

errors would eventually prevent further increases in accuracy), but the fact that the computations run for several hours means that the step-length must be as large as possible, if we wish to follow the line for an appreciable distance around the device. In the centre of the plasma region a step-length of six degrees was found to give results which are also reproducible with smaller step-lengths, which was not the case for very much larger step-lengths. Near the coils, however, steps of less than or equal to one degree were found to be necessary, which meant that the technique was very cumbersome indeed.

In the light of the restriction of what it is practical to do with existing computing facilities, we have been forced to find a method of proceeding which does not rely on computational "brute force". Given the initial failure of analytic approximations to provide detailed information we began to use a "variational" method to find good coils. What this means is that we guessed a starting point and varied the coil parameters, moving small amounts in all directions in parameter space. If one direction appeared preferable we moved that way and repeated the procedure.

The parameters varied, and the range through which they were varied, (some justification for which is given in the next chapter), were:

(a). The radial deformation of the coils, (0 to 60% of the minor radius).

(b). The degree of distortion of the coils away from the plane (0 to 100% of the gap between adjacent coils).

(c). l-number (2 and 3, with smaller amounts of l=3,4,5,6 added to l=2).

(d). p, the number of toroidal periods of the field, (2 to 4).

(e). N, the number of coils, (8 to 16).

(f). ε , the inverse aspect ratio, (0.2 to 0.4).

(The first requirement was to reproduce the results of Wobig and Rekker, [59], so their work helped to provide a starting point.)

After some time, an optimum region was reached, within which it

was possible to increase the transform (for instance), but only at the cost of a deterioration in the value of some other figure of merit: no clear gains were to be had. Simultaneously, it became evident that extremely simple analytic results could be written down which described all of the data obtained, given certain assumptions, and which indicated that what might otherwise have been a local optimum was in all probability the only optimum region. These results are described in the next section.

5.3.3 Choice of l-number

From Chapter Two we have that (eq.(2.3 4,10))

$$i = \frac{n\,(n-l)}{3}\,\alpha^{2}\,\rho^{2n-4}$$

(We recall the normalised radius is unity, at the coil.) Thus for n=l, i(vac)=0. As l=n increases above two the coil system produces less and less transform at lower radii. In a reactor, where the plasma radius is of the order of half the coil radius, the higher l-values are likely to be at a disadvantage.

Field-line following calculations demonstrate that for low aspect-ratio systems even l=3 is extremely inefficient at producing transform at all radii low enough to be within the separatrix. To be more precise, for a coil inverse aspect ratio of 1/3 and for coils meeting the criteria discussed elsewhere, of modularity, we have been unable to achieve transform significantly greater than 0.1 at any radius, so that over most of the plasma volume the transform was less than 1/20. Fig.5.8 shows the trajectory of a field line in an l=3 "best case", near the separatrix, where the transform is greatest, during approximately twelve passes around the major circumference. Note that the transform is second

order in the amplitude of the field, δ , whilst the amplitude of the field line gyration is of first order - compare with Fig.5.5.

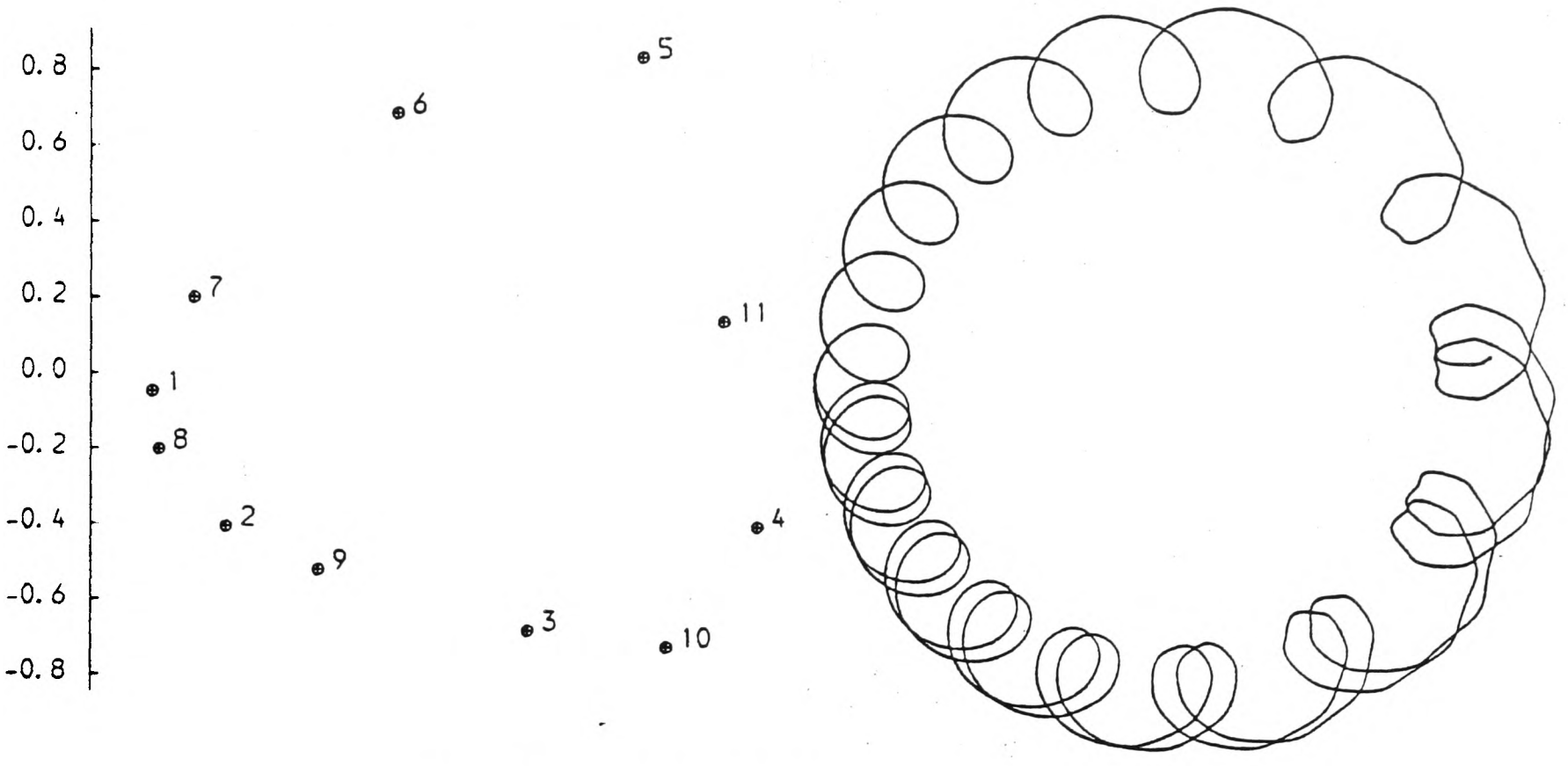

Fig.5.8. l=3 field line trajectory.

We may demonstrate that it is possible to achieve an arbitrarily large rotational transform, if we are prepared to employ arbitrarily high aspect ratio, by the following argument: suppose we have a section of Stellarator coil, corresponding to one field period, which provides a certain amount of transform along its length, di. If we arrange N such sections, one after another, we must obtain a total transform of Ndi from the resulting coil set. Thus, as N can be made arbitrarily large (resulting in a high aspect ratio, of order N), then so can the transform. Given the economic arguments presented above, which rest on the fact that it is necessary to have a considerable thickness of blanket, etc., between the coils and the plasma, a small value of A is essential: $\varepsilon = 1/3$, with a minor radius of 2m, corresponds to a plasma aspect ratio $A = 7$, which is already rather large, in terms of the equilibrium beta limit. We are compelled to work at these low aspect ratios, consequently, and an l=3 Stellarator would, on this basis, be unable to provide the necessary fields. On the other hand, l=2 coils with similar deformation and aspect

ratio are capable of producing i = 0.5 at all radii. Such a value for the transform is adequate, being comparable to the value in a Tokamak for instance.

The analytic theory predicts that the l=2 transform profile is flat. For modular coils it turns out that it actually decreases towards the outside, [64], so that the maximum is in the centre of the plasma. Hence, although it is still difficult to achieve sufficiently high transform at low aspect ratio, it is much easier with l=2 than with any other value. In the case for which we present the coil system in the next chapter, i runs from just below 0.5 in the centre, to about 1/3 at the edge - the plasma is consequently bounded by a q=3 island, which forms the separatrix. The more dangerous q values are excluded from the plasma volume by this arrangement, which is important, from the points of view of equilibrium and of stability.

With a modular coil system of the type envisaged in this work it is difficult to obtain satisfactory fields containing large amplitudes of more than one harmonic. For consider the effect on an l=2 field (which we believe to be necessary to provide sufficient rotational transform) of the inclusion of an l=3 modulation of the coils: provided that the coil shape is completely free from structural constraints then such a modulation can be accomodated. However, as the coils are to be designed so that they do not overlap (in order to facilitate removal of damaged coils) then the extra width given to the coil by the l=3 ripple has to be compensated by a corresponding decrease in the l=2 ripple. If the ripples are of equal amplitude, for example, the l=2 field must decrease by a factor of about two. The rotational transform is a second order effect - it is proportional to this amplitude squared, and so it goes down by a factor of about four as a result. Such a decrease is catastrophic in terms of its effect on the equilibrium beta, which scales as the transform squared. For this reason we choose not to consider e.g. an l=2/3 mixture, which

might otherwise be a desirable combination, but restrict ourselves to l=2 only.

5.4 Discussion of Results for l=2 and Conclusions

Details of the magnetic field computations are given, and compared with analytic expressions. These in turn have been deemed appropriate on the basis of the qualitative conclusions of the field line following.

5.4.1 General

It is difficult to perceive the underlying trends of field line behaviour, for rational surfaces intervene to obscure the systematic behaviour which is present (by destroying the outer surfaces and bringing the separatrix in towards the plasma, for instance). Thus the set of "best cases" is to be considered most significant in what follows, as they are the least disrupted by such effects.

The problem is made worse by the fact that there is some reason to believe that the computational method is inherently not very accurate. For although it is possible to increase the accuracy obtained per step by decreasing the step length, it is not always possible to improve global accuracy in this way, for the decrease in the error per step can be more than compensated by the increase in the number of steps, [65].

We have remarked elsewhere that we need to take very short steps to obtain reproducible results in the vicinity of magnetic islands. We cannot be sure that we are necessarily improving our accuracy as a result, however. Such a failing is particularly important as many of the cases we have studied have (for instance) a q=3 (i=1/3) surface at the separatrix, and the nature of the separatrix is crucial if a magnetic divertor is to be employed.

The relationship between the coil shape and the field parameters may be derived very simply and rather crudely by using the ideas of the virtual casing principle, but by imposing a circular casing, instead of allowing the fields to dictate the shape of the casing.

One then obtains the currents on the casing, from the relation

$$\frac{R_m}{r}\frac{d\xi}{d\theta} = \frac{J_\xi}{J_\theta} = \frac{-B_\theta}{B_\xi}$$

as in chapter two, (except that in chapter two only the helical parts of the currents and fields were to be included, whereas here the total current and field is to be used).

This representation of the fields is accurate enough to yield information as to the overall nature of the field, but of course not about the structure of the fields in detail.

In terms of the quantities defined in chapter one, we find that the amplitude of the coil modulation is given by

$$\Delta\xi = \frac{4\alpha\varepsilon}{p} \qquad (5.4.1,1)$$

but $\alpha = p\varepsilon\delta^2/2$, so

$$\Delta\xi = 2\varepsilon\,\delta^2 p \qquad (5.4.1,2)$$

If we write the equation for a surface in the form (5.3.1,3), thus defining δ, then from the expression for δ in terms of α, above, it is straightforward to show by substitution into (2.3.4,10) that $i = p\,\delta^2$.

Fig. 5.9 shows a small typical sample of the computational

results (using different aspect ratios, coil shapes, etc.,) for the transform per field period (as computed) vs: the surface deformation squared, compared with the line given by this result. (The major source of error here comes from the estimation of the surface ellipticity.)

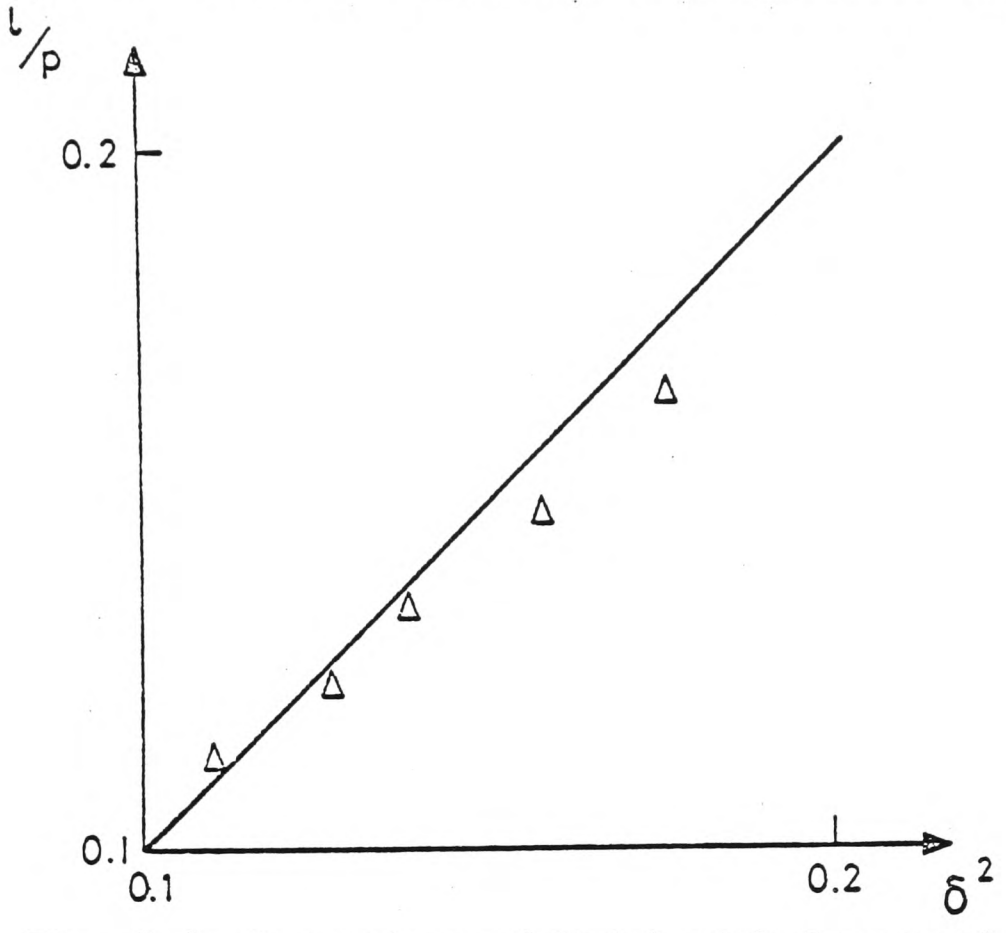

Fig. 5.9. Comparison of Model with Computation.

That this simple result holds rather well is perhaps the most important result of this Chapter, for in Chapter Seven we are able to write down expressions which determine p, given certain assumptions, in terms of geometrical factors. The transform is then seen to be closely linked to the shape of the device, through p and δ, which shows what the consequences of maximising the transform must be.

The separatrix seems to lie at a distance no less than half the maximum coil separation, inside the coils. This is a rather obvious restriction, but in these modular systems succeeds in accounting for the separatrix position, in the absence of resonant surfaces.

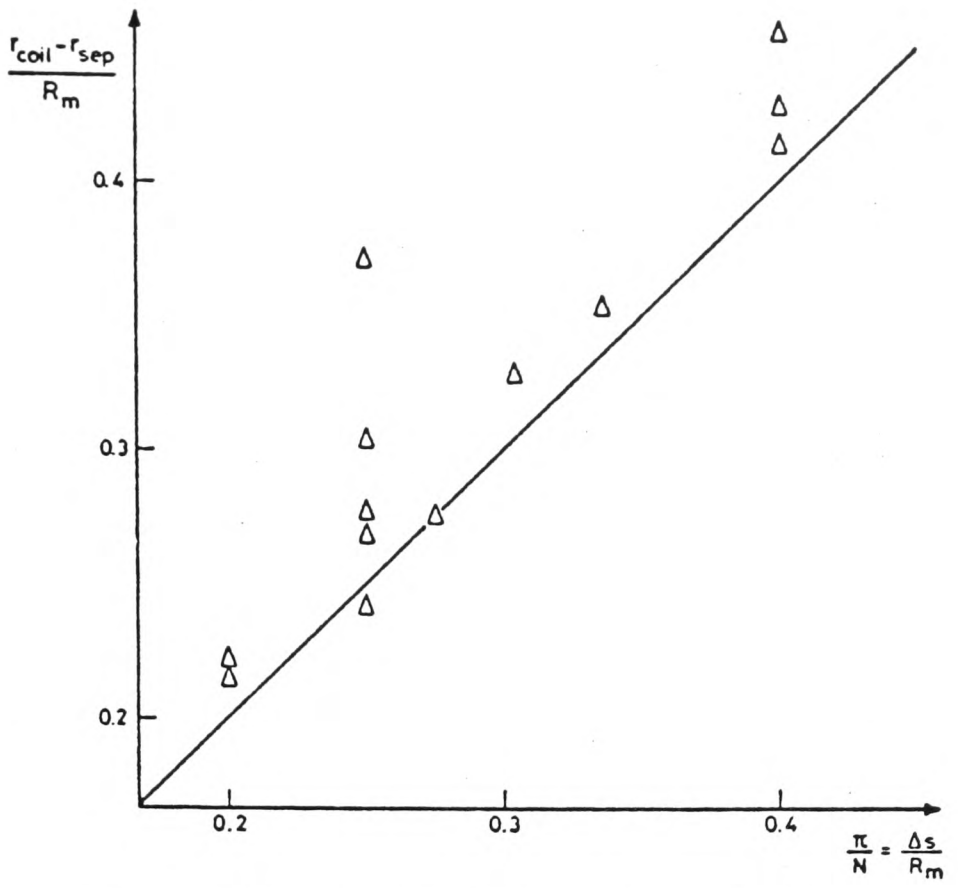

Distance of Separatrix from Coil vs: Δs = Coil Separation ÷ 2

Fig.5.10. Separatrix Position.

An observation which holds consistently, and which leads to predictions in agreement with what is observed, is that there is an upper limit on the amount of deformation which the surfaces can stand, before they break open to such an extent that they are no longer suitable for plasma containment. Using δ, above, to describe the surface shape, then in the parameter range we have been considering, the acceptable range of δ is somewhat arbitrarily taken to be $0 < \delta \lesssim 0.4$. (It may be emphasised that for different types of coils or for widely different aspect ratios this may not be the appropriate limit and it may thus be possible, although probably not desirable, to exceed it.) Fig.5.11 shows the results of attempting to increase δ, in the presence of an admixture of $l=6$.

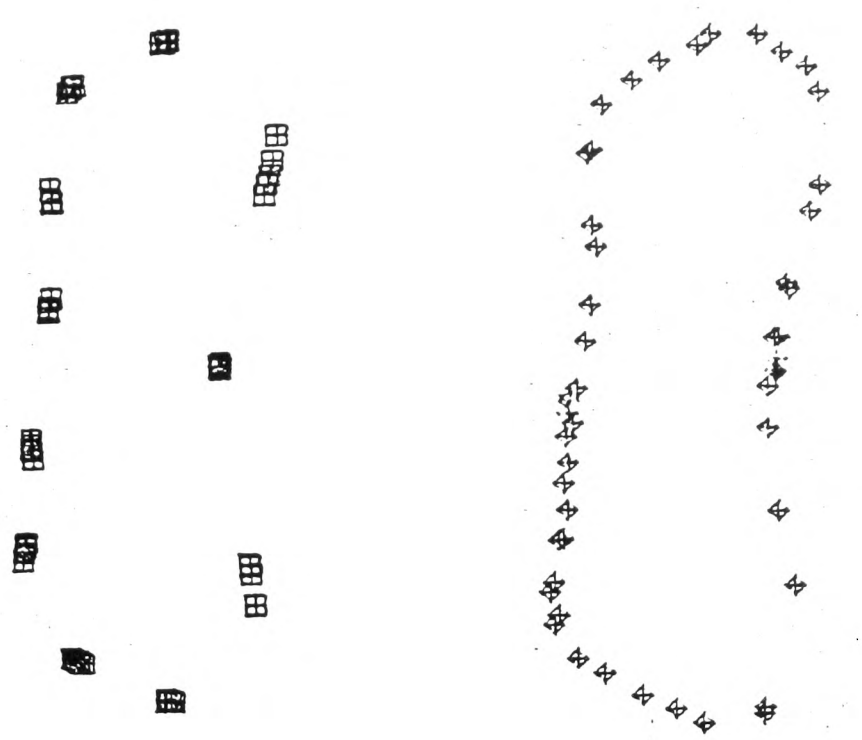

Fig.5.11. Effect of Surface Deformation.
Extra surface deformation causes degradation of the surface, (to be compared with Fig.5.4).

The use of a small amount of l=6 in the field, suggested by Chu, [61], was found to improve the quality of the surfaces considerably. This is probably the major difference between these coils and those proposed by Wobig and Rekker, apart from the difference in the number of periods chosen. It also produces the major change in the fields, for, using the filamentary representation of the coils discussed above and the parameters which were given by Wobig and Rekker, the surfaces were found to be severely disrupted by islands. At least within the limitations of the computational method employed, then, we have found a 10% increase in rotational transform over this earlier work but, more importantly, a much better set of surfaces have been obtained. If it turned out that the surfaces were in fact less prone to island formation than these calculations indicate, then significant increases in rotational transform might be possible, as δ could be larger. As pointed out above, however, this may not be desirable.

Chapter Six: Module Construction

Means of supporting the coils which allow the requirements detailed in previous chapters to be met are discussed. (These include the possibility of divertor action, removability of modules and separate refrigeration of each coil.) Comparison with Tokamak coils is made.

6.1 Coil Forces

The forces on a coil due to the main toroidal field are all in the R,Z plane, for any given ξ . The forces between neighbouring coils are attractive and in the toroidal direction, however.

The means by which we propose to support the former is relatively independent of the choice of modular coil configuration. The forces between coils are more strongly geometry-dependent, and so it is necessary to go into details of the coil shape.

A set of four coils, which forms a unit, from three of which a twelve coil, $l=2$, $m=3$ device could be made, is illustrated in Fig. 6.1.

In general, it would not be possible to divide the coil set up into such units: it is because N/p is equal to an integer that it is possible in this case. There are a number of possible reasons why it may be desirable to make the reactor out of such units - for instance, the forces between coils sum to zero over a unit, and may thus be contained within that unit. More obviously, there is an advantage in that the number of different types of module is reduced by a factor of N/p. For these reasons, as the optimisation of the next chapter results in $p=3$, with N approximately equal to 12, it is natural to take $N=12$. A unit similar to the one considered would, of course, be obtained with $p=4$,

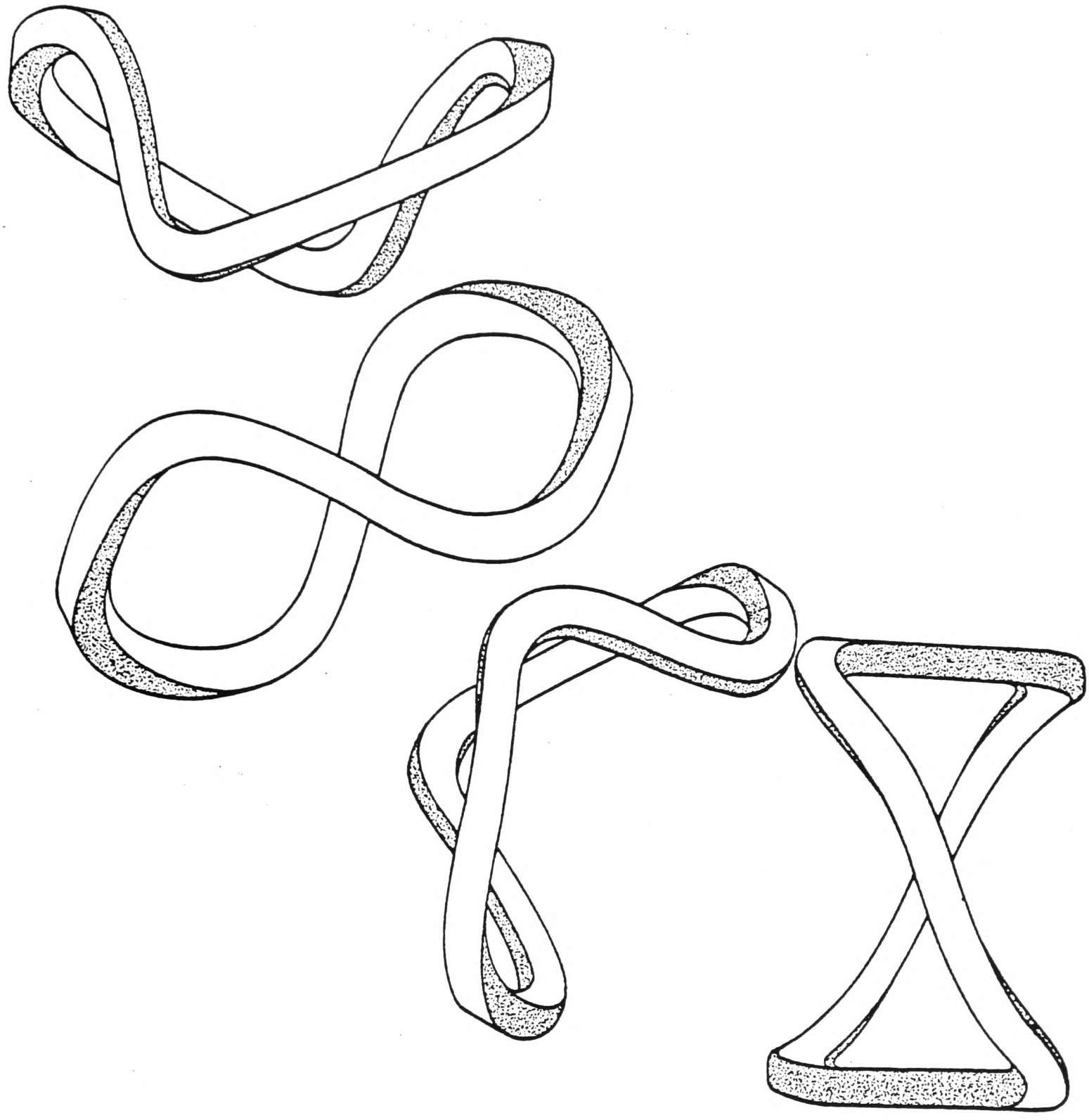

Fig. 6.1 One "unit" of a twisted coil set

N=16, etc.

Fig. 6.2 is a sketch of one of these coils, showing its position in a casing having a projection onto a minor cross-section of the same shape as itself.

Note that the ratio of the sideways (i.e. toroidal) deformation of

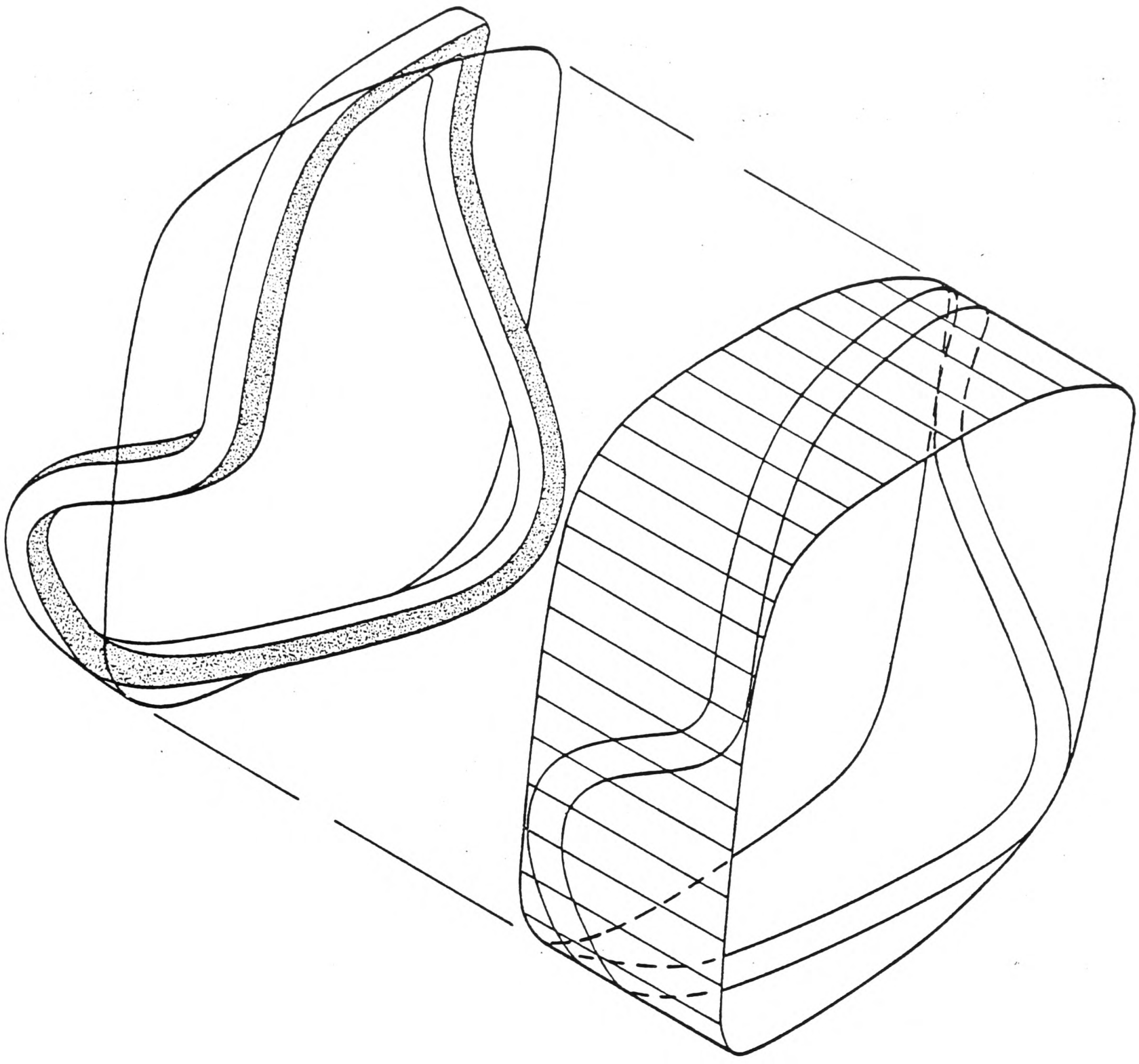

Fig. 6.2 A twisted coil and its casing

the coil to the projected length (either vertically or horizontally) is less than 0.5 . We may thus estimate the increase in coil length due to the fact that it is non-planar, using Pythagorus' theorem - the length is multiplied by a fraction which is less than one half of root five. This is negligible, from the point of view of costing the copper involved. (It is

also much less than the effect of making a Tokamak coil D-shaped, for instance.)

Let us estimate the magnitude of the forces on these coils. The mean field is probably about 5T. according to the results of the optimisation which is described in Chapter Seven. The current in each coil, with about ten coils, will be roughly $2.5R_mMA$, and so the force per unit length, with R=10m, is about 7.5×10^7 N/m. As this is applied to the whole coil, the total force will be about 10^9N. This figure is very similar to estimates of the force, per coil, on the central pillar in a Tokamak design. We shall need such a support in the Stellarator also, therefore.

The casing described above is to be contained in a circular band around its mid-plane, to which the radial forces from the coil are transmitted, (Fig. 6.3).

Similarly, if we try to find the force between coils, as they approach each other to a distance of the order of tens of centimetres, we find $F=\mu_o I^2/2\pi d \simeq 1.2 \times 10^9$ N/m. and this force is applied over lengths of order ten cm. so the total force resulting will be less than or of order 10^9N.

The difference between these forces and those on the coils in a Tokamak is that there are extra attractive forces, between coils, which are important in the Stellarator. (A difference between the coils, from the point of view of the forces, is that in the Tokamak the minor radial forces are allowed to dictate the shape of the coil.)

The above attractive force will only be applied over short distances, where the coils are close, and its local nature may even help to prevent the coil from trying to stretch to a "relaxed" position (where it would have a shape similar to a Tokamak coil), but maintain its twisted nature.

As mentioned below, the forces in this Stellarator are all applied

to the coil support in such a way as to be compressive, which makes them much easier to deal with than they would be were they tensile.

6.2 Coil Refrigeration

The coil support system has been selected so far as possible to allow the coils to be refrigerated separately, each within its own cryostat, without having to also take the coil supports down to liquid helium temperatures. A first step in this direction is to ensure that all the forces applied to the coil are pushing, rather than pulling, on it, which means that the join between coil and support need be much less intimate than otherwise. This is important for it means that when a coil has to be replaced, it is not necessary to bring more than the one coil up to normal temperatures, because each coil can be kept in its own cryostat.

6.3 Blanket

The position of the blanket relative to the coil and plasma is illustrated in Fig. 6.3.

6.4 Vacuum Vessel

The vacuum vessel could be put in any one of a number of places, rang ing from immediately outside the first wall to somewhere beyond the coils, or even covering the whole reactor like a lid on a cheese plate, without passing through the hole in the middle at all.

For the present, we shall consider a "grommet-like" vacuum vessel,

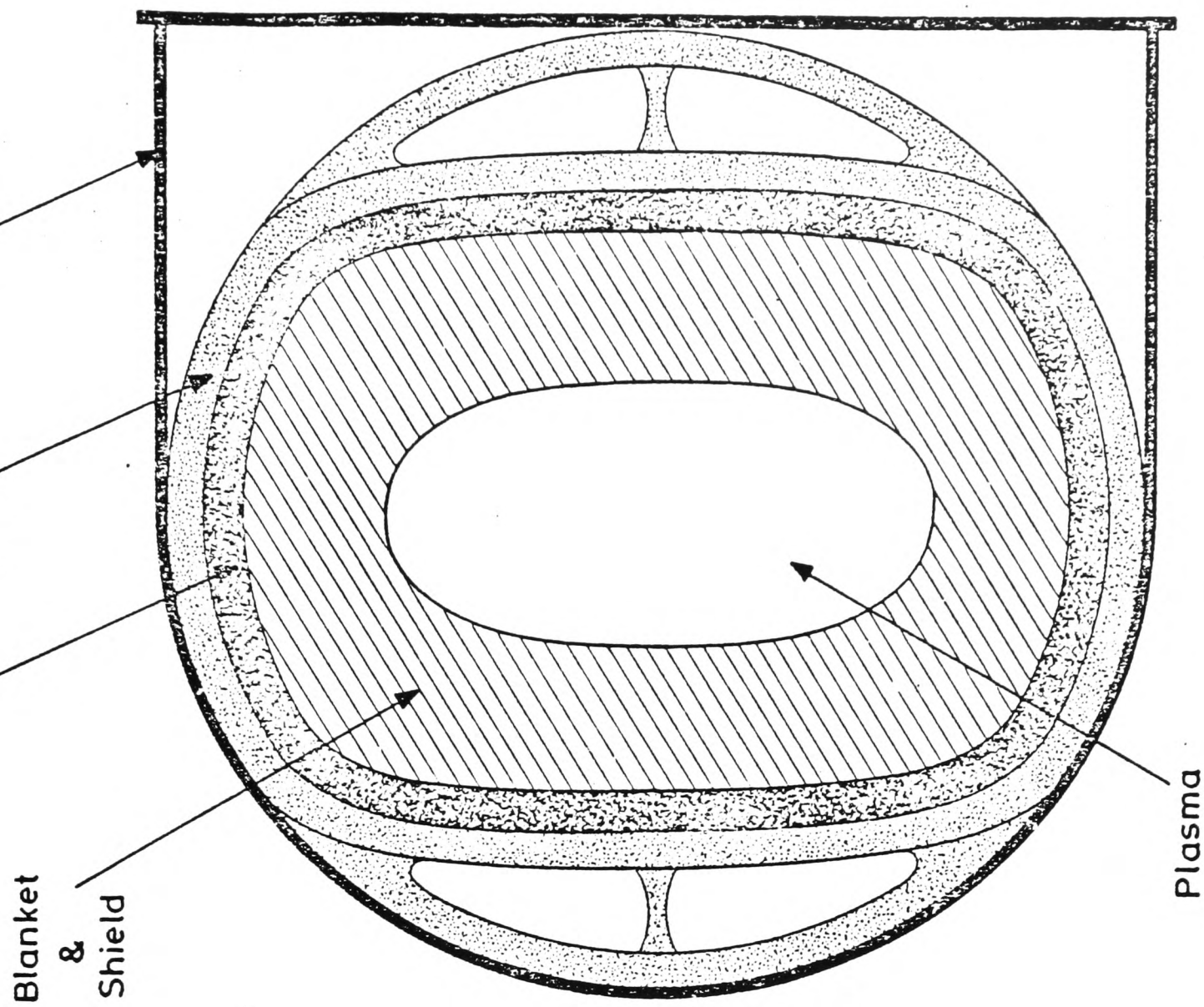

Fig. 6.3 Blanket, coil and coil support

which is made up of two parts: the "grommet", which encloses all the other components of the reactor itself, as shown in Fig. 6.3, and through which all detachable piping and electrical connections must pass, and an outer cylindrical casing, also as shown, which can be moved away vertically for the removal of modules. The advantage of such a scheme is

its simplicity - the vacuum vessel causes no additional difficulties beyond those discussed above, [14].

6.5 Coil Removal

In this design it is necessary to remove a coil from its position in the torus whenever it is required to replace either the coil or the structure inside the coil. With the coil must be taken all the blanket and shield; the module is thus likely to be very heavy indeed, though possibly somewhat lighter than a Tokamak, because fewer components are required. The weight of such a module is of the order of a thousand tons, which is virtually at the limit of what it is technically feasible to handle.

In some Tokamak designs it has been possible to allow for removal of blanket segments between the toroidal field coils, thus easing the problem. However, it is not entirely satisfactory to have to leave the coil in place throughout the lifetime of the reactor, which is the situation envisaged in this case.

6.6 Divertor

If field lines are to be taken out of the device near the tip of the ellipse or at a small number of points above a magnetic island then apertures must available at the appropriate places in the coil support.

There are two widely-studied types of Tokamak divertor: the poloidal (or axisymmetric) divertor, and the bundle divertor. (A hybrid divertor has also been proposed.) The bundle divertor takes a "bundle" of field lines from the outside of the plasma, (Fig. 6.4), creating an

x-point as shown.

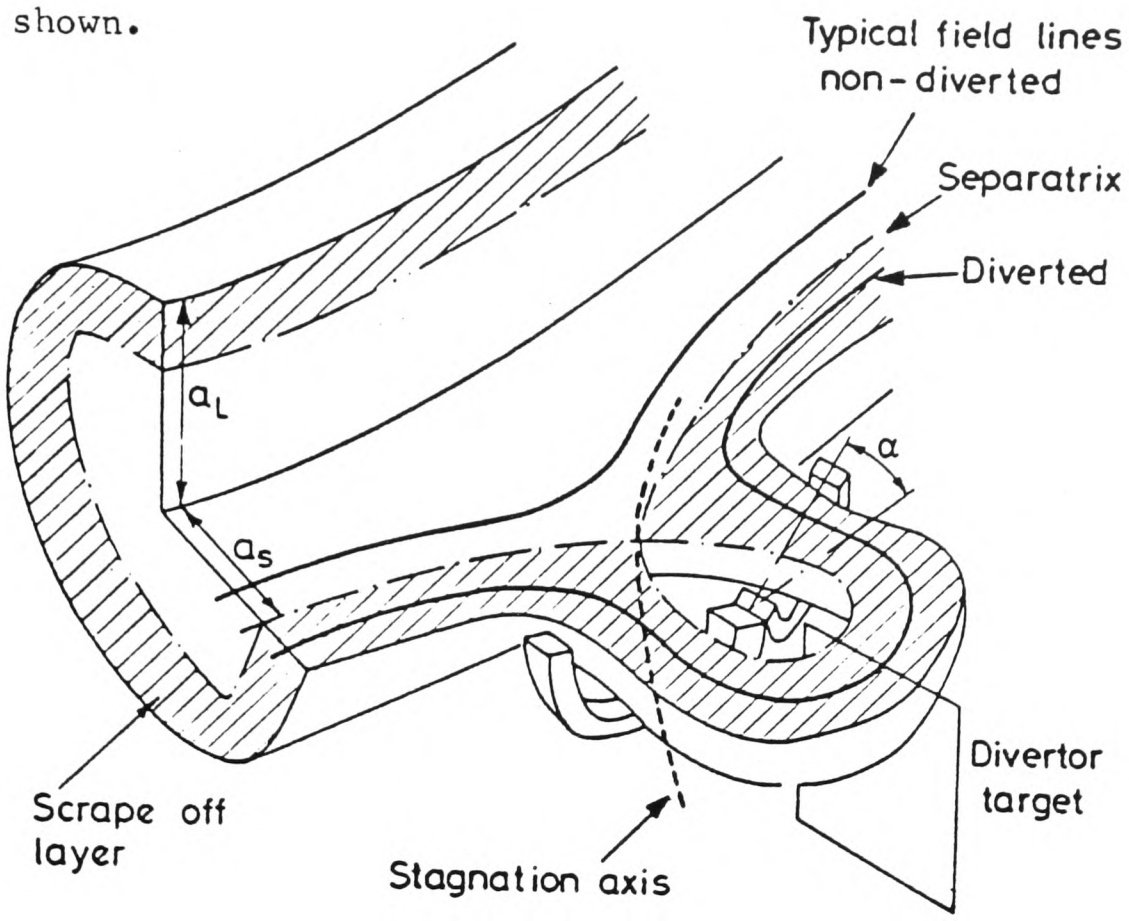

Fig. 6.4. Bundle Divertor Action.

The poloidal divertor creates one or two x-points, (Fig. 6.5), but now the "point" runs around the device, axisymmetrically, and field lines from the separatrix leave the plasma first at these points.

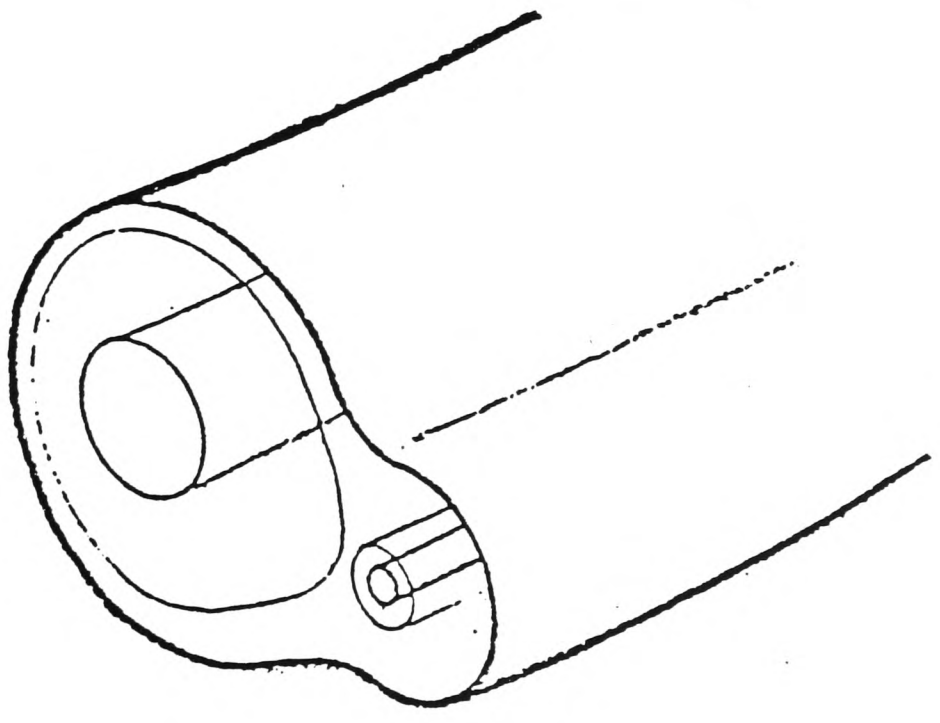

Fig. 6.5. Poloidal Divertor.

In either case, the effect is to carry particles from the plasma edge to divertor plates, from whence they may be pumped off.

It is often said that the Stellarator possesses a "natural" divertor. Such statements usually refer to the ridge with helical symmetry which occurs at the separatrix in certain classes of Stellarator, (in "classical" Stellarators, and straight Stellarators with helical symmetry.) Referring to (5.4.1) and the accompanying discussion, we see that the helical ridge of the separatrix is an x-point, and except for its following a helical path around the torus it is very similar to an x-point of the poloidal divertor. The divertor which they form has been discussed by Derr, [66], for his "Ultimate Stellarator" configuration, (which is a modular, l=3 system) - he concluded that there were a large number of bundles of field lines which emerge at points around each modular coil. The divertor plates could thus be outside the coils, so that some of the features of a bundle divertor are also in evidence.

As has already been pointed out, however, the modular system we have been studying, being l=2 and of low aspect ratio, does not have a separatrix with "ridges", so it does not have a poloidal divertor, either. On the other hand, as the flux surfaces are slightly more elliptical than the coils the field lines might be expected to emerge at the tips of the ellipse first. Something akin to a bundle divertor could exist, therefore, and some evidence for this was found computationally, but not enough to prove its existence conclusively, because of the doubts (expressed above) as to the accuracy of the field line calculations near the separatrix. Very substantial computations would be required to prove its existence, even assuming that the method does not fail due to rounding errors at very short step lengths.

If this divertor did exist, two bundles would emerge per coil, one at each of the tips of the coil, so that the collector plates would be outside the coil, at the appropriate positions. It would probably be

possible to include an extra coil to make field lines come out preferentially at one position, and cut down the number of bundles, however.

Another interesting possibility exists in this configuration: a "resonant helical divertor" has been described by Karger and Lackner, [67], which employs helical windings on a Tokamak to create a q=3 island (this being a typical value of q at the outside of envisaged Tokamak reactors) near the plasma edge. This configuration is illustrated in Fig. 6.6.

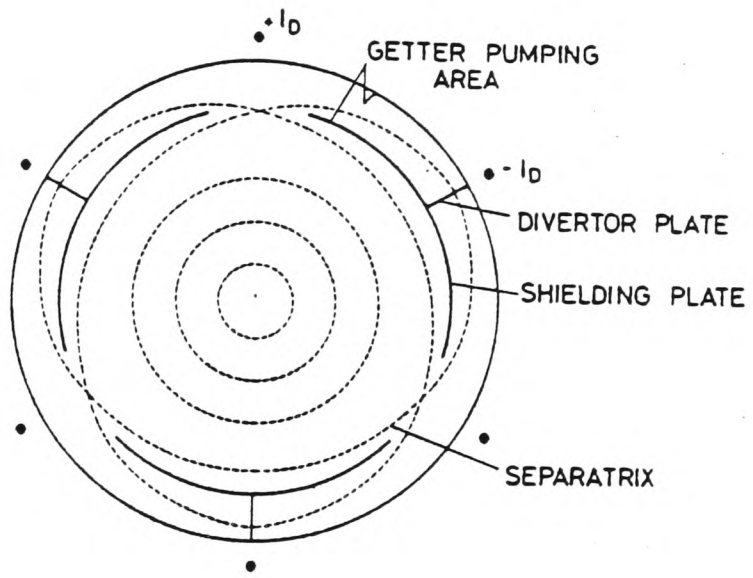

Fig. 6.6. Resonant Helical Divertor.

As discussed above, a number of magnetic islands are in evidence during our field line following. These are to some extent a computational artifact, as it is true, especially near the coils, that errors in the fields due to the method of representation will be significant. However, at the plasma edge various other fields, due, for instance, to the gaps between the coils, may interact with the main field to produce islands. It would be of interest, then, to discover the origin of the q=3 island which falls at the outside of the plasma region in our standard case

described above. (Fig. 6.7)

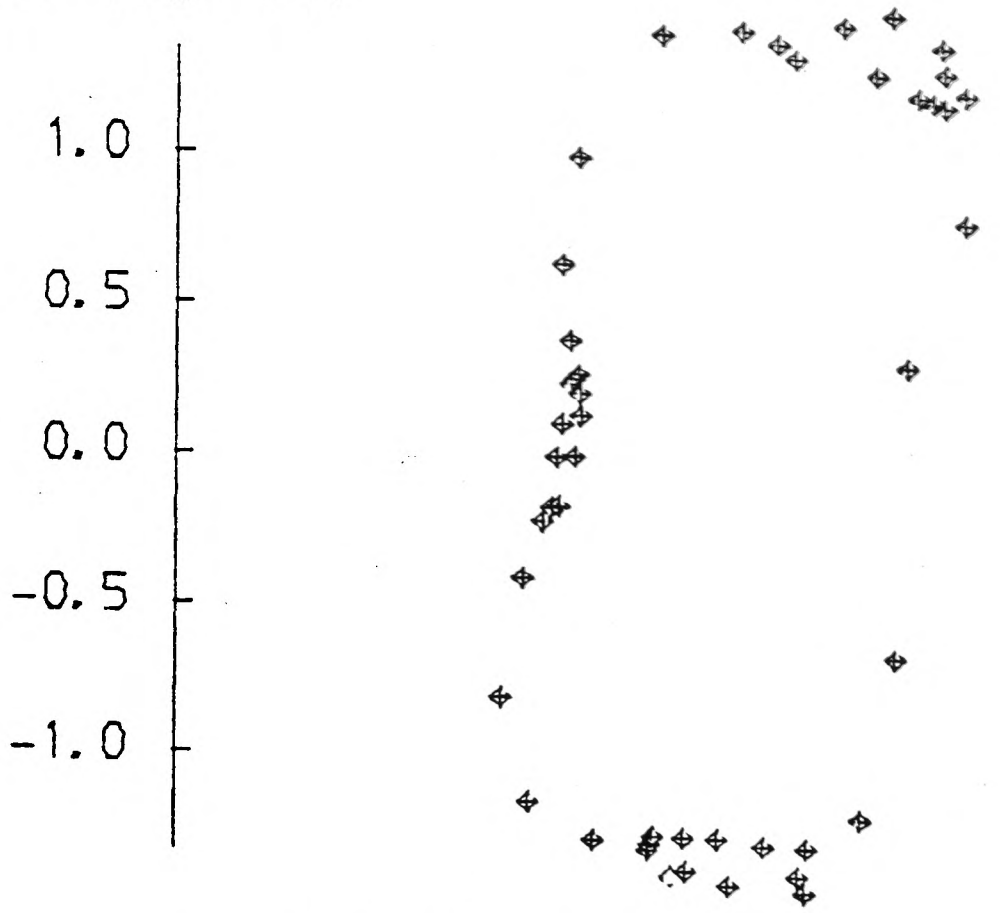

Fig. 6.7. q=3 Magnetic Island.

Should this island exist, in fact, we could make use of it as a helical divertor, including an interior divertor plate and shielding plates as shown, (Fig.6.6). The distance to the divertor plate from the point at which particles leave the separatrix can be made large, so as to reduce back-streaming. A possible disadvantage is the fact that the pumping channel needs to be surrounded by upwards of half a metre of high density shielding, to protect the coils from radiation damage, if the divertor plate is inside the coils, as here or in a poloidal divertor in a Tokamak. (One other method of providing a divertor which we attempted to demonstrate was to include a current carrying filament above and parallel to the local q=3 axis at the separatrix, in an attempt to induce the island to grow in width and encircle the filament. To date we have only succeeded in moving the whole island slightly inwards, however.)

6.7 Comparison with the Tokamak

Let us enumerate the coils required for each system: the Stellarator described above employs a small number (typically around twelve) of identical twisted coils, (and possibly divertor coils). The Tokamak, in general, requires a set of toroidal field coils, a "primary" winding, (which often implies that there must be a transformer core through the hole in the centre of the torus) poloidal shaping coils, vertical field coils and possibly divertor coils.

Consider the set of tokamak reactor coils depicted in Fig. 6.8. Note that the poloidal field coils prevent removal of modules. This is inevitable unless they are outside the toroidal field coils and are removable vertically. (The presence of superconducting coils interior to other sets of coils partially shields the plasma from the fields due to the outer coils, so that such an arrangement has difficulty in producing the required fields at all.)

Without going into detail, it is the case that Tokamak reactor designers have found it difficult to avoid these coils becoming to some extent interlocked, and have faced additional problems because their fields are crossed, giving rise to forces in awkward directions. For these reasons, we feel that the overall Stellarator coil set we have described is probably easier to construct than that of a Tokamak. If this is indeed the case, then a major objection to the Stellarator as an alternative to the Tokamak as a reactor is not valid.

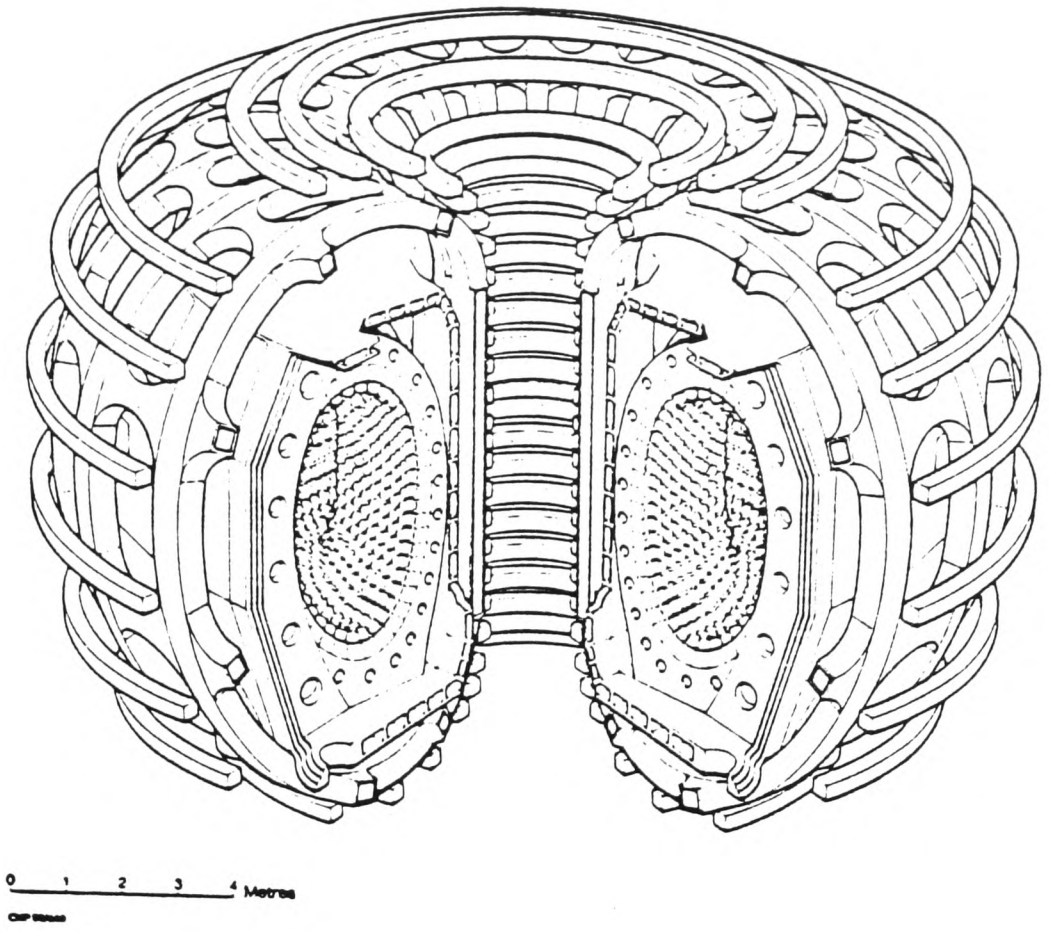

Fig. 6.8. Tokamak Coils.

Chapter Seven: A Stellarator Reactor

It is the purpose of this Chapter to show how the optimum parameters for a Stellarator reactor may be determined for given total power output, wall loading, etc. The result must, if it is to be of any interest, represent a considerable improvement over an equivalent Tokamak. Further comparison between the two devices is made.

7.1 Optimisation

Relations between the many parameters describing the reactor must be obtained, in order that an optimisation may be performed. Such relations are now given.

Plasma Elongation

The magnetic surface shape may be written as

$$\rho = \rho_o(1 + \delta .\cos(2\theta + p\xi)) \qquad (7.1,1)$$

with

$$\delta = \frac{2\alpha}{\varepsilon p^2} \qquad (7.1,2)$$

From Chapter Five, $\delta \leq 0.4$. The elongation, e , (the ratio of semi-major and semi-minor axes of the ellipse), is given by

$$e = \frac{(1 + \delta)}{(1 - \delta)} \qquad (7.1,3)$$

Number of Toroidal Periods of the Field

From chapter five, the mean angle subtended by each coil is roughly

$$\Delta\xi = \frac{4\alpha\varepsilon}{p} \qquad (7.1,4)$$

but $\alpha = p\varepsilon^2 \delta/2$, so

$$\Delta\xi = 2\varepsilon^2 \delta p \qquad (7.1,5)$$

The width of the coil is $R_m \Delta\xi$. If we let $b = (t + s)$, then on the inside of the torus this must fit into

$$\frac{2\pi (R_m - (b + r))}{N} \qquad (7.1,6)$$

where N is the number of coils and t,s were defined in Chapter One to be the blanket and shield thicknesses, respectively. We then have that

$$p \leq \frac{\pi}{N\varepsilon^2 \delta} (1 - \varepsilon) \qquad (7.1,7)$$

Number of coils

The gap between the coils is $2\Delta S = 2\pi R_m/N$. Provided the magnetic surfaces are not destroyed by field errors, the separatrix should lie at a distance ΔS inside the coil. This follows from assuming that when flux surfaces break open, the field lines orbit the coils in circular paths. The results of field line following indeed confirm this - see Figs. 7.1. and 5.10.

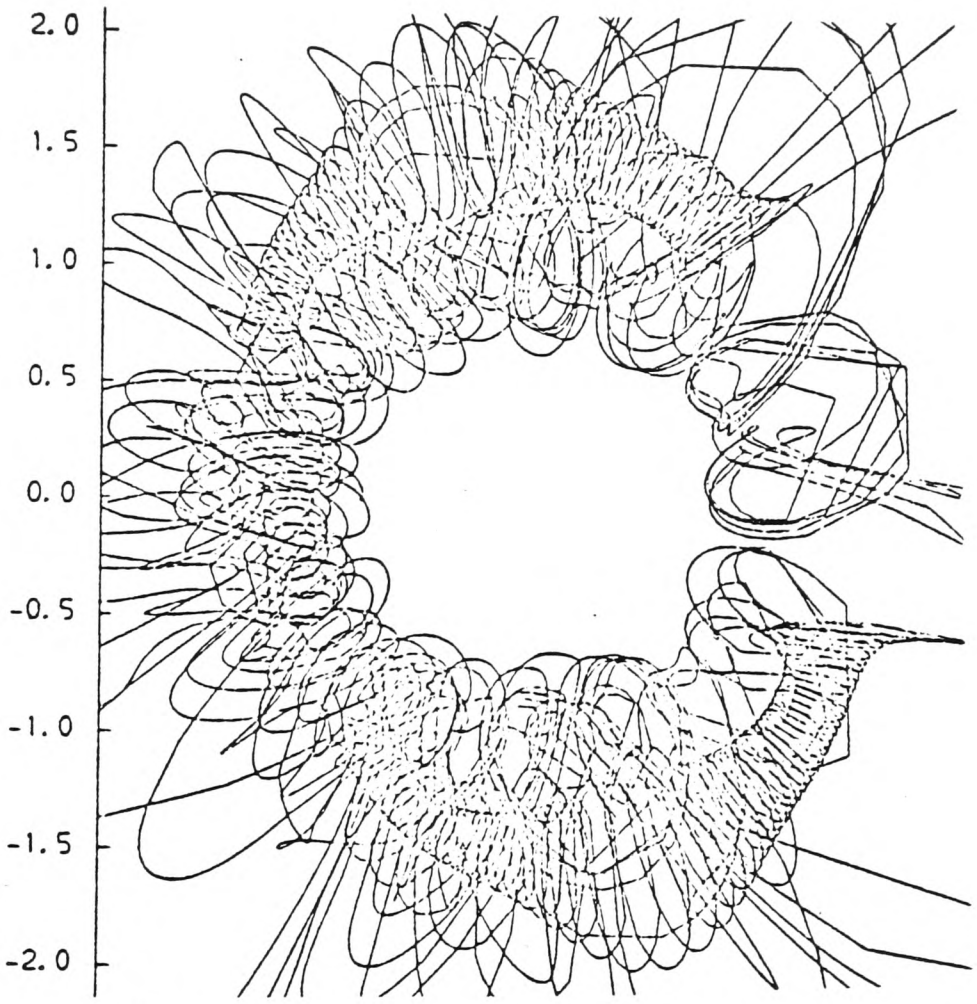

Fig. 7.1 Separatrix formation

We assume that the separatrix should be not much more than b inside the coil, or the available plasma volume will be wasted. We wish the gaps between the coils to be as large as possible, for access to the plasma and to allow a large amplitude modulation of the coil shape in the toroidal direction, without the coils being allowed to overlap. Thus N is chosen to be as large as possible whilst still having a value which is consistent with the above requirement. This ensures that the separatrix is inside the first wall, which is important if a divertor is to be included.

Then $b = \pi R_m/N$. If we define the plasma aspect ratio $A = R_m/r$,

whilst ϵ , the inverse aspect ratio of the coils, is (b + r)/Rm, then

$$N = \frac{\pi R_m}{b} = \frac{\pi \Delta r}{b} = \frac{\pi (b + r)}{\epsilon b} . \qquad (7.1,8)$$

Rotational Transform

Combining the above and using

$$i = p\delta^2$$

we have that

$$i = \frac{\delta b}{\epsilon(b + r)} (1 - \epsilon) \qquad (7.1,9)$$

When designing an actual reactor, we would wish to avoid the values of i which were mentioned in chapter five: in fact the coil system of chapter six meets this requirement, as pointed out in that chapter.

Beta

A beta limit like $\beta \lesssim i^2\epsilon$ is set by considerations of equilibrium and of ballooning stability. The g-mode criterion is $2pi < 11$, and we shall scarcely be able to approach this limit, in an optimised reactor.

The first of these limits has often been used in the past as part of an argument which claimed to show that a Stellarator reactor would

necessarily have very high rotational transform and aspect ratio. As this school of thought has held sway for many years, we shall examine the argument in some detail.

Gibson et al., [7], assert that, in a Stellarator design, little is to be gained by using anything other than a 45^0 l-winding. Specialising to Stellarators with such a winding, it follows that $i \sim p \sim 1/\varepsilon$, and substituting this into the above beta limit they conclude that $\beta \propto 1/\varepsilon$. As they also claim that the cost of a fusion reactor is principally determined by the maximum beta attainable, this leads them to wish to take ε as small as possible. This in turn leads them to a system with a very high power output, and so they conclude that the Stellarator is at a disadvantage with respect to the Tokamak, because it necessarily produces too much power.

To show that this is an incorrect argument, three points may be made:

(a). The beta limit which they assume to hold is not adequate, and by increasing the beta allowed by the equilibrium/ballooning limit, they violate the criterion for Mercier-type modes. To show this, we apply the same set of assumptions as they did, but this time to the second criterion. We find that $\lambda(i/\varepsilon) < 11$, so we cannot go to very high aspect ratio at all. We recall that our resistive criterion is identical to the ideal M.H.D. criterion found by Shafranov, who has argued similarly on many occasions, (see e.g. [68],).

(b). A 45^0 l-winding does not produce an optimal Stellarator field. This has been shown for l-windings by Sharp et al., [69], and the advantages of other forms of coils have been discussed above.

(c). As we saw in chapter one, the reactor power output may be regarded as being primarily limited by the permissible wall-loading, and not by the beta-limit. The beta-limit is, consequently, not a sufficiently important economic factor that all other considerations may

be neglected by comparison.

To anticipate the detailed optimisation which we shall perform, on the basis of the model introduced in the next section, we shall see that if, as in chapter two, we write $\beta = fi^2\varepsilon$, then the cost depends strongly on f, but the optimisation does not give rise to large $i^2\varepsilon$, as was assumed in [7]. If we consider beta as having two parts, a geometrical part, $i^2\varepsilon$, and the constant f, then our result shows that it is most helpful if f is large, but increasing the "geometrical" part of beta beyond a rather low value is not cost advantageous.

7.2 Reactor Costing

We are now in a position to estimate the cost of a Stellarator or Tokamak reactor. The component cost estimates were made by Spears, [70], for use in Tokamak design. All the items, several of which are inapplicable in a Stellarator Reactor design, have been listed for the sake of comparison with Tokamaks. Items c,d and e have been written in a form appropriate to Tokamaks, where the aspect ratio is always low. In this case the approximation used gives rise to errors of the order of ten percent, which is considered acceptable.

This is not a good enough approximation for use in Stellarator design, where it is not obvious at the outset that A may be taken to be small. These terms will be corrected to make them more accurate at large A, therefore.

The following are required as input data:

I(TF)	-	Total toroidal field coil current (A)
l(TF)	-	Length of one toroidal field coil (m)
B(TF)	-	Peak flux density at coil (T)

I(PR)	-	Peak primary current (A)
R(PR)	-	Mean major radius of primary winding (m)
I(VF)	-	Total vertical field current (A)
R(VF)	-	Mean vertical field coil radius (m)
B(TC)	-	Peak flux density in transformer core (T)
A_w	-	First wall area (m^2)
N_r	-	Number of replacement walls/blankets
P(th)	-	Thermal power output (MWth)
R_m	-	Major radius of reactor (m)
H	-	Height of reactor (m)
E(PR)	-	Primary field energy storage (J)
E(VF)	-	Vertical field energy storage (J)
E(H)	-	Product of P(H) and operating time (J)
n(H)	-	Heating efficiency
P(REF)	-	Coil heat deposition rate at 4K (kW)
P(H)	-	N.I. or E/ICRH power to plasma (MW)
P(el)	-	Gross electrical power (MW)

The costs were given, evaluated at 1976 prices, in pounds, to be:

(a). Toroidal Field Coils

The costs of the components of the superconducting magnets are:

Superconductor - $C_a = 8.33 \times 10^{-5} I(TF).1(TF).B(TF)$

Copper - $C_a = 1.68 \times 10^{-2} I(TF).1(TF)$

The copper cost was subsequently decided to be a factor of two too large, on the basis of experience on JET.

(b). Poloidal Field Coils

$$\text{Superconductor} - C_b = 1.7 \times 10^{-3} \{I(PR).R(PR) + I(VF).R(VF)\}.B(TC)$$

$$\text{Copper} - C_b = 1.1 \times 10^{-1} \{I(PR).R + I(VF).R(VF)\}$$

(c). First Wall/Blanket

$$C_c = 1.6 \times 10^{4} A_w$$

(d). Replacement Walls/Blankets

$$C_d = (N_r - 1) \times 0.363 \times 1.6 \times 10^{4} A_w$$

(The factor 0.363 allows for the fact that less interest is paid on later expenditure.)

(e). Neutron Shield

$$C_e = 5.54 \times 10^{4} A_w$$

(f). Thermal Circuits

$$C_f = 9 \times 10^3 \; P(th)$$

(This assumes that the blanket is cooled by high pressure Helium.)

(g). Auxiliaries

$$C_g = 6.5 \times 10^3 \; P(th)$$

(Includes vacuum pumping, in house power, etc.)

(h). Contingency

$$C_h = 0.05 \; (C_c + C_e + C_f + C_g)$$

(i). Building

$$C_i = 450\pi \; (R_m(1 + \varepsilon) + 4)^2 \; (H + 4)$$

(n.b. this is not based on the exact size of the reactor hall - in particular, it does not imply that there is only 4m. around the reactor.)

(j). Energy Storage

$$C_j = 7 \times 10^{-3} \left(E(PR) + E(VF) + E(H)/n(H)\right)$$

(Assumes homopolar generators.)

(k). Refrigeration

$$C_k = 5 \times 10^{6} \left(P(REF)/25\right)^{2/3}$$

(l). Neutral Injection or E/ICRH

$$C_l = 2.5 \times 10^{6} \; P(H)$$

(Assumes Neutral Injection, - E/ICRH costs are about half.)

(m). Conventional Plant

$$C_m = 0.2 \times 10^{6} \; P(el)$$

(n). Miscellaneous

$$C_n = 100 \text{ to } 200 \times 10^6$$

(Attributable to site structures, tritium handling facilities, and instruments and control systems.)

In a Stellarator, there is no need for items (b). and (j)., and (l). is reduced to a small fraction of the value in a Tokamak.* (The Tokamak would require facilities to deliver substantial heating power for pulsed operation - and if a steady-state current were to be driven in the plasma, the same sort of equipment would be necessary to drive the current.) In addition, if the Tokamak reactor is pulsed, (d). will be larger, as N_r will be increased.

A significant difficulty with pulsed systems in general becomes evident when the cost per kilowatt is calculated, however, for the acceptable wall-loading is reduced by a factor of two or three, the fraction of the time when power is produced is significantly reduced and the fraction of the time when the reactor must be supplied power rises from zero to a finite value. Thus a pulsed station with the same geometry produces something like a quarter of the power that it would were it steady-state.

*This is an oversimplified argument which is not strictly correct. See Appendix three for a more complete discussion.

The total cost of a Stellarator reactor is thus

$$C = C_a + \sum_{\alpha=c}^{i} C_\alpha + \sum_{\alpha=k}^{n} C_\alpha$$

A number of these (e.g. $C_{k,1}$) are relatively small and may be neglected.

Using $B = \mu_o I(TF)/2\pi R_m$, then $I(TF) = 2\pi BR_m/\mu_o$, and as

$l(TF) = 2\pi (b + a)k$, with

$$k = ((1 + e'^{2})/2)^{1/2}, \quad e' = \frac{(ae + b)}{(a + b)}, \text{ the coil ellipticity,}$$

$$I(TF)l(TF) = \frac{BA_w(b + a)k}{hr}. \tag{7.2,1}$$

where

$$h = (1 + e^{2})^{1/2} \quad (2e)^{-1/2}$$

Thus

$$C_a = 0.85 \times 10^{-2} \frac{BA_w(b + a)k}{\mu_o\, hr} \tag{7.2,2}$$

$$= 0.7 \times 10^{4} \frac{BA_w(b + a)k}{hr}. \tag{7.2,3}$$

Consider items c-e: in a typical Tokamak design r=3m. t=s=1m., and e=5/3. The volume of the first wall/blanket, which is given by

$$2\pi R_m^2((t + a)(t + ea) - ea^2) = 2\pi R_m^2((1 + e)ta + t^2) \simeq tA_w g$$

where we have defined g to be

$$g = (1 + e)/(2(1 + e^{2})^{1/2})$$

as 2r>>t.

This "paper-thin" approximation is not appropriate to more general geometries than very tight aspect ratio devices with large minor radius,

so instead of A_w, a factor like $A_w(g + t/2hr)$ should be used in C_c and C_d. Similarly, in C_e we should have $A_w(g + (b + t)/2hr)$.

Note that as we use this formula for the Stellarator, we increase the cost of the first wall considerably - on the other hand, we use the paper thin approximation for the Tokamaks we assess, which leads to a relative underestimate of about 20% in their wall costs.

Taking $N_r = 2$, we obtain

$$C_c + C_d + C_e = 10^4 A_w (6g + (3b + 2t)/hr).$$

$$C_f + C_g + C_m = 8.5 \times 10^4 P(th).$$

The total power output is limited by the maximum tolerable wall loading and the maximum power which the plasma is capable of producing. If the wall loading to be employed is taken to be P_w, (which may be other than the maximum), then we have two expressions for P(th), which must be equal; and which allow us to relate P(th) to A_w:

$$P(th) = P_w A_w \tag{7.2,4}$$

and

$$P(th) = 0.7 \beta^2 B^4 V \tag{7.2,5}$$

As

$$A_w = 4\pi^2 rR_m (1 + e^2)^{1/2} (2e)^{-1/2} \tag{7.2,6}$$

then from (7.2,5) the major and minor radii are related by

$$rR_m = \frac{P(th)\ (2e)^{1/2}}{4\pi^2 (1 + e^2)^{1/2}\ P_w} \simeq \frac{P(th)}{50 P_w} \tag{7.2,7}$$

$$C_i = 3 \times 10^3 (ae + b + 3)(R_m(1 + \varepsilon) + 4)^2$$

$$C_n = 1.5 \times 10^8$$

The total cost per kilowatt is thus approximately

$$\frac{C}{P_w A_w} = 8.5 \times 10^4 + \frac{10^4}{P_w}\left(6g + \frac{(3b + 2t)}{hr} + 0.7B\frac{(b + a)k}{hr}\right) \qquad (7.2,8)$$

$$+ \frac{3 \times 10^3}{P_w A_w}(ae + b + 3)(R_m(1 + \varepsilon) + 4)^2$$

$$+ \frac{1.5 \times 10^8}{P_w A_w}$$

We assume that the peak equilibrium beta is given by $\beta \gtrsim f i^2/A$. Our equilibrium calculation is not intended to be applied to cases with low aspect ratio, but extrapolating from the calculation which employed WVII parameters, $f \gtrsim 2$ seems appropriate. (Note that (i). the usual ballooning stability limit for Tokamaks is $\beta \sim i^2 e/A$, which in this case gives a higher value than the above, and (ii). the g-mode criterion $pi<11$ reduces to $p<8$, given the assumptions about i described above.)

The minimisation is made possible by use of (7,2,5) and (7.2,7). by minimising at fixed P_w, and then by varying P_w, to find an overall minimum. Details of the method used to find the minimum are as follows:

For fixed P(th) and f, and an initial choice of P_w, a very small value of the minor radius, r, is chosen and the major radius found, from (7.2,7). The aspect ratio, the number of coils, (7.1,8), the number of field periods, (7.1,7), and the rotational transform, (7.1,9), to be

employed follow immediately.

Using the above value for beta in (7.2,5), we find the field which is required to produce the total power stipulated. The cost per kilowatt is then computed.

The calculation is then repeated for slightly larger r, and the new cost per kilowatt found. This is repeated until the cost goes up, or the magnetic field exceeds the assumed technological limit, (which occasionally happens, at high wall loading), and the configuration is deemed to be the optimum for that wall loading. The calculation is then repeated at slightly higher wall loading, and so on.

The results of the minimisation are shown in Fig.7.2. The cases we have illustrated are:

P(th) (GW)	f	B_m (T)
2	2	10
3	2.5	12
4		

In all these cases, b=3 and δ =0.4. The coil set of chapter six corresponds roughly to the choice P(th)=3GW, f=2, at Pw=2.5MW/m^2.

We may summarise one set of possible Reactor parameters as follows:

P(th)=3GW, and with a conversion efficiency of 1/3, P(el)=1GW.

Pw=2.5MW/m^2

Major radius=13m.

Minor radius=2m.

Plasma Elongation=3

Number of coils=12

l=2

p=3

i=0.48

Beta=8%(peak):6%(rms):4%(average).

Cost per kilowatt=£650

Total Station Cost=£650M

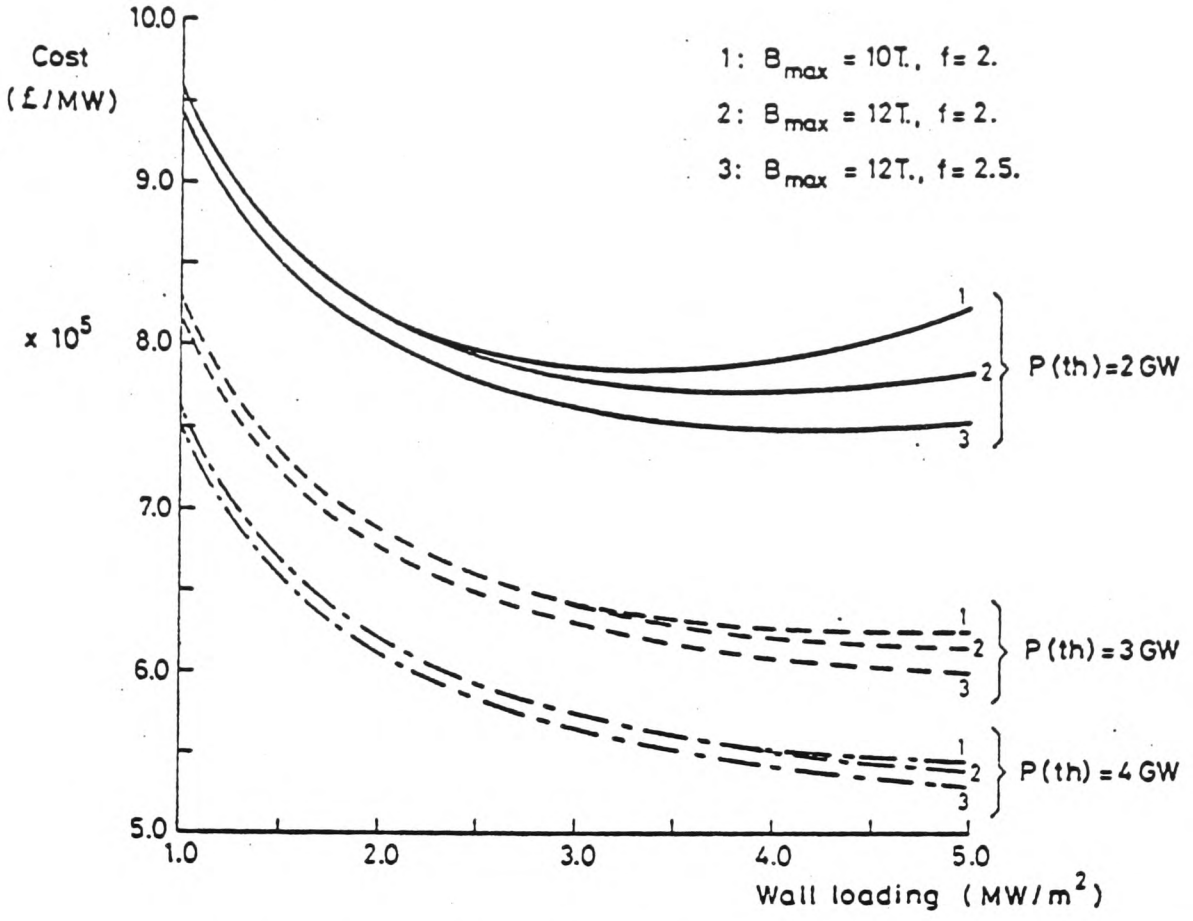

Cost per megawatt for optimised reactor

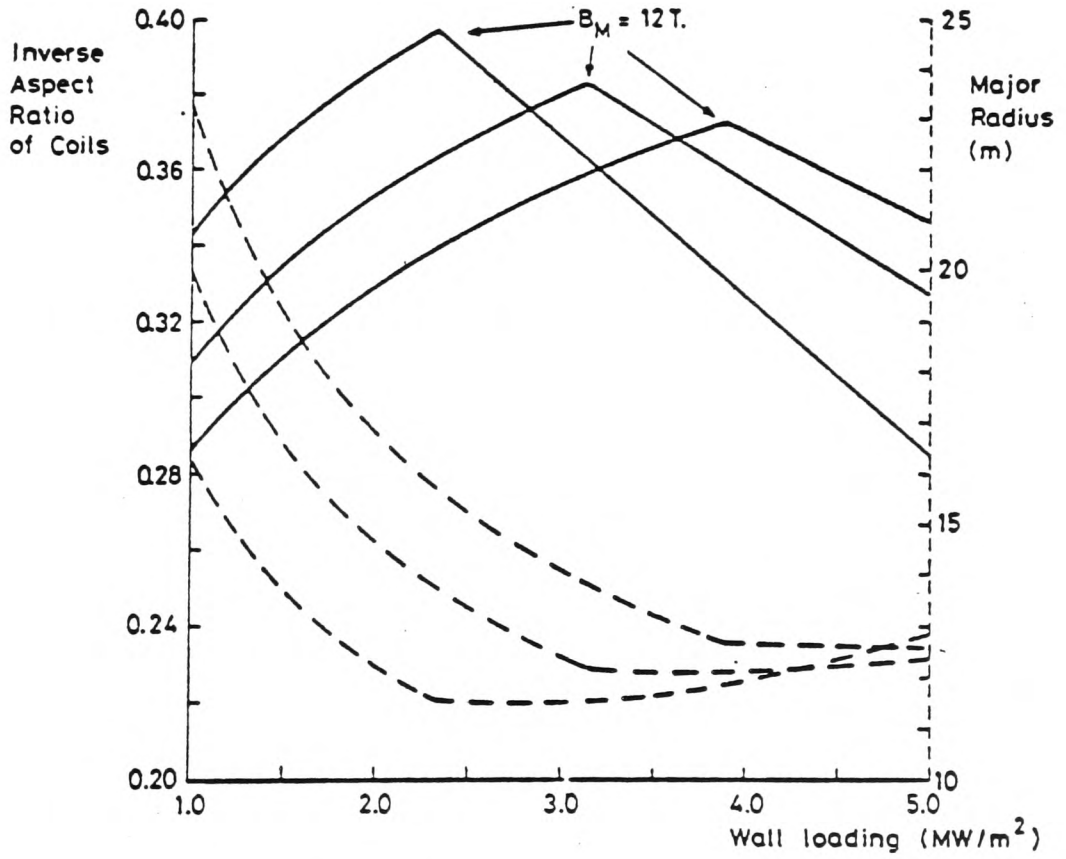

P(th) = 2,3,4 GW, f = 2, B_M = 12

Fig.7.2. Minimum Cost Curves.

Our two reference Tokamak designs are "Starfire", [6], and the Culham Mk.IIC, [71]. Their parameters are, in the same units as above:

	Starfire	MKIIC
P(th)	3.5	1.825
R_m	7.0	7.8
a	1.94	2.0
P_w	3.7	2.1
B	5.8	3.9
B_m	11.1	11
Beta	6.7%	7.7%

The MKIIC. reactor is pulsed, but the wall loading has been taken to be rather high, and so it is not inappropriate to make comparison with it.

152.7MW of R.F. power are envisaged, on Starfire, in order to maintain the steady state current. This is the item costed under heating, below.

It is clear that Starfire has been designed making rather more optimistic assumptions about wall-loading and total power output than the Stellarator outlined above. For the sake of comparison, we thus give a second set of Stellarator costs, for a Stellarator with the same wall loading and total power output as Starfire.

We have estimated the costs of the major components to be, on the basis of the above, (in £M, and at 1976 prices):

Item	Starfire	MKIIC	Stellarator(s)	
TF coils	90	60	103	102
PF coils	40	32	-	-
First Wall	18	20	123	123
Shield	45	47	(inc. above.)	
Buildings	13	14	19	19
Energy Storage	-	58	-	-
Heating	171	215	-	-
Conv. Plant	300	146	255	300

Miscellaneous	150	150	150	150
Total	827	742	650	692
Cost/kW (£)	709	1,220	650	593

When these costs are corrected to allow for inflation, up to 1981, and interest charges, an increase by a factor of up to four is likely.

The major part of these costs is not the "nuclear island", but conventional generation costs, etc. When these items are subtracted, we find substantial differences between the costs of the reactors.

Naturally, the MKIIC, having the lowest wall loading and lowest total power output is likely to have the highest cost per kilowatt. The reason for the low wall loading is that it is pulsed - in fact, the wall loading is still rather high, for a pulsed reactor.

Starfire has what we consider to be rather too high a wall loading, and the total power output is a little large. The Stellarator we propose (the costs of which are given in the first Stellarator column) makes use of what we believe to be more reasonable assumptions. As a result, it is at a disadvantage with respect to Starfire: nevertheless, it is less expensive, both in terms of total cost and of cost per kilowatt.

The reasons for this are the decreased costs of coils (PF coils being absent) and heating. Note that we have taken a rather low copper cost, in calculating the coil costs - if this were higher, the difference would be accentuated.

On the other hand, the wall area is larger, (which is a result of our wall loading assumption, and not a defect inherent in Stellarators) and the major radius and elongation are larger, so the volume of blanket and shield is increased. This pushes up the cost somewhat. (The optimisation has found rather larger R_m so as to increase the transform in the Stellarator field, and so smaller r resulted which, as we saw in chapter one, increased the engineered volume.)

The second Stellarator column has almost identical costs for all the components of the "nuclear island", which is a result of the optimisation trading coil costs against wall costs - and coming to virtually the same minimum as before. The generating cost has gone up in proportion with P(th), as it must. The cost per kilowatt has come down still further, as a result of these changes.

Conclusion

A type of Stellarator reactor has been discussed which is comparable to Tokamak designs of similar total output power and assumed wall loading.

The essential plasma physics has been introduced. The equilibrium theory seems to be supported by the experimental evidence wherever comparisons are possible, despite theoretical doubts about the existence of equilibria in finite aspect ratio machines. Stability theory, however, does not seem to be confirmed experimentally. Certain of the predicted current driven modes are very much in evidence in present day Tokamaks, and interchange instabilities have been demonstrated in mirror machines which do not have a "minimum average-B", but in toroidal systems the theoretically predicted pressure driven modes are not observed. Thus although two criteria against such modes have been given in the above work, and the reactor plasma should be stable according to both of them, they could well both be wrong. One important point is that they are not likely to be over optimistic.

The subject of superbanana diffusion has been investigated. A number of theoretical reasons have been advanced to explain why observed confinement seems to be better than had been predicted on the basis of the old neoclassical theory of superbanana diffusion, (confinement times being

comparable with those obtained in Tokamaks of similar size).

Extensive field line following calculations have allowed the identification of trends in the behaviour of Stellarator fields as the coil parameters are varied. These in turn may be fed into reactor models, and a reactor study has been done using this input and allowing for mechanical requirements upon the various components of the reactor.

The cost of the reactor has been calculated and minimised, at fixed power output for various wall loadings.

The Stellarator we propose appears to be cheaper than two recently designed Tokamaks, despite our having chosen a lower value of the wall loading than is customary for steady state devices, chiefly because of the absence of PF coils, and the decreased cost of plasma heating and energy storage.

We have argued elsewhere that the factors which are not quantified in this model should not prove more troublesome in Stellarators than Tokamaks. We thus come to the simple conclusion that a Stellarator reactor of the type considered is more economical than a Tokamak, and it may also pose fewer technological problems.

In the light of these results, it would be extremely interesting if a medium sized ($R_m \geq 1m$) low aspect-ratio stellarator experiment were built, employing $\ell = 2$ modular coils. Such an experiment would allow a relatively inexpensive test of the theories we have discussed to be made, and, if they were seen to be confirmed, would provide a powerful argument for an expanded program of stellarator research.

References

[1]. Morozov, A.I., and Solov'ev, L.S., Reviews of Plasma Physics 2, Consultants Bureau, New York, (1966), 1.

[2]. Hitchon, W.N.G., M.Sc. Thesis, Oxford, 1979.

[3]. Frieman, E.A., MATT-710, 1969.

[4]. Kulcinski, G.L., Energy Policy, 2 (1974) 104.

[5]. Grieger, G., "Controlled Fusion and Plasma Physics", 1979, Invited Papers, 525.

[6]. Baker, C.C., 11th. Symposium on Fusion Technology, Oxford, 1981, Contributed Paper 1.161.

[7]. Gibson, A., Hancox, R., Bickerton, R.J., IAEA-CN-28/K-4,375.

[8]. Miller, R., 1980, Private Communication.

[9]. Mioduszewski, P., K.F.A. Julich Report Jul 1691, 1980.

[10]. Spiers, W.R., 1981, Private Communication.

[11]. Behrisch,H., Nuclear Fusion 12, (1972), 695.

[12]. Grieger, G., 1980, Private Communication.

[13]. Grieger, G., 11th. Symposium on Fusion Technology, Oxford, 1981, Invited Papers, 141.

[14]. Sviatoslavski, I., 1980, Private Communication.

[15]. Botts, T.E. and Powell, J.R., Brookhaven National laboratory, BNL50697(1977).

[16]. CLEO Team, Proc. 8th. Int. Conf. on Plasma Physics and Controlled Nuclear Fusion Research, Brussels, 1980, H1-1 and H1-2.

[17]. Kulsrud, R.M., Princeton Plasma Physics laboratory Report PPPL-1705, 1980.

[18]. Kruskal,M.D., 1952, NYO-998(PM-S-5).

[19]. Grad, H., Phys Fluids 10, (1967) 137.

[20]. Lortz, D., Z. Angew. Math. Phys. 21, (1970) 196.

[21]. Lo Surdo, C. and Sestero, A., Phys. Fluids 18, (1975) 255.

[22]. Mercier, C., and Luc, H., in Lectures on Plasma Physics, EUR5127e, (1974).

[23]. Shafranov, V.D., and Mikhailovskii, A.B., JETP 66 (1974) 190.

[24]. Lortz, D., and Nuhrenberg, J., Z. Naturforschung, 31(1976) 1277

[25]. Greene, J.M. and Johnson, J.L., Phys. Fluids, 4 (1961) 875.

[26]. Dobrott, D., and Frieman, E.A., Phys. Fluids, 14(1971) 349.

[27]. Fielding, P.J., and Hitchon, W.N.G., J. Plasma Physics, 24, (1980),453.

[28]. Hitchon, W.N.G., and Fielding, P.J., Culham Laboratory Preprint CLM-P627, (1981).(To be published in Nuclear Fusion.)

[29]. Bogoliubov and Mitropolski, "Asymptotic Methods in the Theory of Non-Linear Oscillations", Gordon and Breach (New York) 1961.

[30]. Rosenbluth, M.N., Sagdeev, R.Z., Taylor, J.B. and Zaslavski, G.M., Nucl. Fus. 6, (1966) 297.

[31]. Hamzeh, F.M., Nuclear Fusion, 14 (1974) 523.

[32]. Morse and Feshbach, "Methods of Theoretical Physics", vol. 2, McGraw-Hill.

[33]. Greene, J.M., Johnson, J.L. and Weimer, K.E., Phys. Fluids 14(1971) 671.

[34]. Shafranov, V.D. and Zakharov, L.E., Nucl. Fus. 12(1972) 599.

[35]. Shafranov, V.D., Sov. Phys. JETP. 37(1960) 775.

[36]. Lortz, D. and Nuhrenberg, J., Nucl. Fus. 17(1977) 125.

[37]. Mikhailovski, A.B., Nuclear Fusion, 15 (1975), 95.

[38]. Kadomtsev, B.B., Reviews of Plasma Physics 2, Consultants Bureau, New York, (1966), 153.

[39]. Bernstein, I.B., Frieman, E.A., Kruskal, M.D. and Kulsrud, R.M., Proc. Roy. Soc., A244, (1958) 17.

[40]. Bateman, G., "M.H.D. Intabilities", M.I.T. Press, (1978), 97.

[41]. Furth, H.P., Killeen, J., Rosenbluth, M.N. and Coppi, B., CN-21/106, Culham (1965) 103.

[42]. Bauer, F., Betancourt, O. and Garabedian, P., J. Comp. Phys. 35(1980), 341.

[43]. Shafranov, V.D., 1979, Private Communication.

[44]. Shohet, J.L., Bull. Am. Phys. Soc. 25 (1980) 869.

[45]. Strauss, H.R. and Monticello, D.A., Phys. Fluids. 24 (1981) 1148.

[46]. Glasser, A.H., Greene, J.M. and Johnson, J.L., Phys. Fluids, 18 (1975) 875.

[47]. Greene, J.M., and Johnson, J.L., Plasma Physics, 9 (1967) 611.

[48]. Shafranov, V.D., and Yurchenko, E.I., Sov. Phys. JETP, 26 (1968), 682

[49]. Shafranov, V.D., Nucl. Fusion, 8(1968), 329.

[50]. Haas, F.A., Hastie, R.J., and Taylor, J.B., Annals of Physics, 41 (1967) 302.

[51]. Derr, J.A., and Shohet, J.L., Phys. Rev. Lett., 43(1979) 1730.

[52]. Gibson, A., and Taylor, J.B., Phys. Fluids, 10 (1967) 2653.

[53]. Galeev, A.A., Sagdeev, R.Z., Furth, H.P., and Rosenbluth, M.N., Phys. Rev. Lett., 22, (1969), 511.

[54]. Connor, J.W., Hastie, R.J., 1971, Private Communication.

[55]. Hinton, F.L. and Hazeltine, R.D., Rev. Mod. Phys. 48 (1976) 239.

[56]. Thyagaraja, A., Haas, F.A., and Cook, I., Nucl. Fusion, 20(1980), 611.

[57]. Spitzer, L., Phys. Fluids, 1(1958), 253.

[58]. Gourdon, C., Hubert, R. and Marty, D., C.R. Acad. Sci. Paris 271(1971) 843.

[59]. Wobig, H., and Rekker, S., IPP 2/215 (1973).

[60]. Derr, J.A., University of Wisconsin report ECE-80-25 (1980).

[61]. Chu, T.K., Furth, H.P. and Ludescher, C., Bull. Am. Phys. Soc. 24(1979) 956.

[62]. Gibson, A., Phys. Fluids 10 (1967) 1553.

[63]. Martin, T.J., 1979, Private Communication.

[64]. Petrenko, Yu. N. and Popryadhukhin, A.P., Proc. 3rd. Int. Symp. on Toroidal Plasma Confinement, Garching, (1973) Paper D8.

[65]. Ellis, J.J., Private Communication (1981).

[66]. Derr, J.A., University of Wisconsin report ECE-80-36 (1980).

[67]. Karger, F., Lackner, K., Phys. Lett., 61A (1977), 385.

[68]. Shafranov, V.D., 9th. European Conference on Controlled Fusion and Plasma Physics, Oxford 1979, Invited Papers, 503.

[69]. Hamberger, S.M., Sharp, L. and Petersen, L.F., Ibid, paper BP20.

[70]. Spears, W.R., private Communication, (1981).

[71]. Hancox, R., CLM-P623, 1980.

Appendix One

"Plasma Equilibrium in Toroidal l = 3 Stellarators"

by

P.J. Fielding

and

W.N.G. Hitchon

Published in J. Plasma Physics

24 (1980) 453

J. Plasma Physics (1980), *vol.* 24, *part* 3, *pp.* 453–478
Printed in Great Britain

Plasma equilibrium in toroidal $l = 3$ stellarators

By P. J. FIELDING

Culham Laboratory, Abingdon, Oxon, OX14 3DB, U.K.
(Euratom/UKAEA Fusion Association)

AND W. N. G. HITCHON

Merton College and The Department of Engineering Science,
Oxford University, Oxford, England

(Received 21 April 1980)

The equations of MHD equilibrium are solved by including plasma pressure and current in a large aspect-ratio ordering scheme for the calculation of toroidal, $l = 3$ stellarator vacuum fields. The extended ordering unifies the low-beta equilibrium theory for tokamaks and $l = 3$ stellarators, and allows solutions to be obtained simply for arbitrarily prescribed pressure and current density profiles. Expressions are given for the equilibrium magnetic field and the equation for the flux surfaces is calculated, including the effects of $l = 3$ shaping and toroidal displacement. These results are used to calculate equilibria for the parameters of CLEO stellarator, and we examine the role of an externally applied vertical field in reducing pressure-induced flux surface distortion and destruction.

1. Introduction

Many equilibrium calculations have been performed for stellarators (e.g. Solovev & Shafranov 1970). In these, two main approaches are employed, given the difficulty of exact solution in toroidal geometry. Either we can expand quantities in Taylor series about a known magnetic axis (Mercier & Luc 1974; Lortz & Nührenberg 1976), or we can adopt an ordering scheme in which the helical fields, pressure, etc., will be small in some parameter. The former approach is of greatest value in dealing with systems in which the magnetic axis is a three-dimensional curve, as in Spitzer's original figure-8 stellarator. With an ordering scheme, however, we often have greater flexibility, validity no longer being restricted to the region close to the axis.

In the 'conventional' stellarator ordering, the helical field amplitude is the basic expansion parameter, the axial current, plasma pressure and toroidicity all being treated as second order. The equilibrium configuration in a toroidal $l = 3$ stellarator was calculated by Greene & Johnson (1961) using this method; however, the triangularity of the flux surfaces was suppressed at the chosen level of approximation by the averaging technique used for their determination, and two-dimensional numerical solution of the equilibrium equation was necessary because of the equal relative orderings of pressure and toroidicity.

In many low-pressure stellarator experiments, the helical flux surface distortions are substantial, and typically these devices operate in a tokamak-like

0022-3778/80/2828-1340 $02.50

mode with regard to the size of the total rotational transform and the plasma pressure. Thus, it is of interest to derive an approximate solution to the equilibrium equations by means of an ordering scheme which better reflects the conditions in these experiments. In this way we can also unify the theory of equilibria at low pressure in tokamaks and in stellarators.

Considering only $l = 3$ stellarators, we investigate the toroidal, large aspect-ratio case using the ordering introduced by Dobrott & Frieman (1971) to define the vacuum field. Since the number of helical field periods round the torus is large and the pressure is low, the rotational transform is composed of independent additive contributions from the vacuum field and from the plasma current separately (Ohasa *et al.* 1977). Like the vacuum transform, that due to the current is of order unity in general, and we incorporate the effects of pressure at second order in the inverse aspect ratio, as in the low-pressure tokamak theory. With these orderings, a satisfactory level of approximation can be attained in solution of the general low-beta problem for arbitrary pressure and current density profiles.

In § 2, we introduce the co-ordinates and basic characteristics of the model and describe the ordering scheme. § 3 is devoted to the calculation of the equilibrium magnetic fields and in § 4 we derive the equation for the flux surfaces. The boundary value relation between the external vertical field and the plasma surface displacement is calculated in § 5, and in § 6 several interesting special cases are examined. Finally the use of these results is illustrated by application to the case of CLEO stellarator (Atkinson *et al.* 1976).

2. Co-ordinates and ordering scheme

It proves convenient to use quasi-cylindrical polar co-ordinates (r, θ, ξ) as shown in figure 1, where r is measured from the minor axis of the torus. The inverse aspect ratio ϵ is assumed small and, in order to recover the basic tokamak-like features of the system, it is supposed that the plasma current generates a poloidal field of order ϵ relative to the main field $\mathbf{B}_0$ which is directed in the ξ direction, and that the plasma pressure $P \propto \epsilon^2$. We assume that the number of $l = 3$ helical field periods round the torus, p, is large and that the helical wavelength $2\pi/h$ is large compared with a typical minor radius a, so that $ha \ll 1$: for example, the plasma radius, or the stellarator winding radius can be used for the normalizing length a. Note that $p = hR_0$, where R_0, is the major radius of the torus, so $p = \epsilon^{-1}ha$. Thus, if $ha \propto \epsilon^{\alpha}$, then $0 < \alpha < 1$. By requiring that the toroidal and helical modulations of B_ξ be of the same order and that the rotational transform be of order unity, we determine $\alpha = \frac{1}{3}$, so that $p = \bar{p}\epsilon^{-\frac{2}{3}}$, where $\bar{p} = O(1)$. This is the ordering proposed originally by Dobrott & Frieman (1971).

We introduce the scaled variables $\rho = r/a$ and $\bar{s} = hR_0\xi = \bar{p}\epsilon^{-\frac{2}{3}}\xi$. The magnetic field and plasma pressure are normalized with respect to B_0, so we have $\mathbf{b} = \mathbf{B}/B_0$ and $\hat{P} = P/B_0^2$. Further defining $\hat{\mathbf{J}} = \mathbf{J}ga/B_0$, where $g = 1 - \epsilon\rho\cos\theta$, and $\mathbf{J}$ is the plasma current density, and $\hat{\nabla} = ag\nabla$, we write the MHD equilibrium equations

$$\hat{\nabla}\hat{P} = \hat{\mathbf{J}} \times \mathbf{b}; \quad \hat{\mathbf{J}} = \hat{\nabla} \times \mathbf{b}; \quad \hat{\nabla}.\mathbf{b} = 0. \qquad (1a, b, c)$$

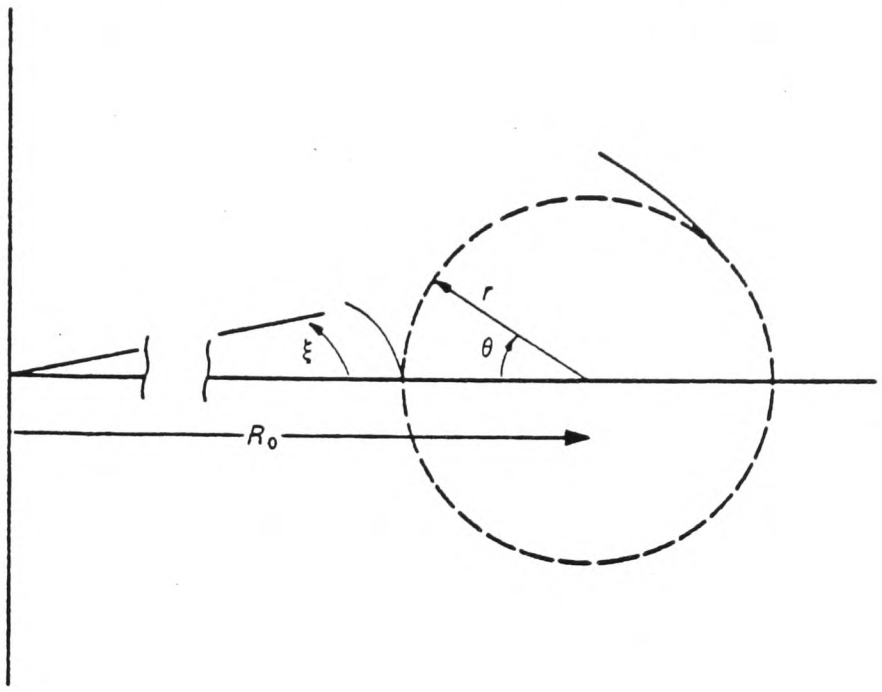

FIGURE 1. Co-ordinate geometry.

The field, current and pressure are now expanded with the orderings indicated, in powers of $\lambda = \epsilon^{\frac{1}{3}}$, so that

$$\hat{P} = \lambda^6 \hat{P}^{(6)} + \ldots; \quad \hat{\mathbf{J}} = \lambda^3 \hat{\mathbf{J}}^{(3)} + \ldots; \quad \mathbf{b} = \mathbf{b}^{(0)} + \lambda^2 \mathbf{b}^{(2)} \ldots .$$

In addition, we must expand the differential operators, so that, for example,

$$\hat{\nabla} f = \hat{\nabla}^{(0)} f + \lambda \hat{\nabla}^{(1)} f + \lambda^3 \hat{\nabla}^{(3)} f,$$

where
$$\hat{\nabla}^{(0)} = \hat{\rho} \frac{\partial}{\partial \rho} + \frac{1}{\rho} \hat{\theta} \frac{\partial}{\partial \theta}, \quad \hat{\nabla}^{(1)} = \xi \overline{p} \frac{\partial}{\partial \overline{s}},$$

and
$$\hat{\nabla}^{(3)} = -\rho \cos\theta \hat{\nabla}^{(0)}.$$

The plasma current can be represented in the form

$$\hat{\mathbf{J}} = \frac{ga\mathbf{J}}{B_0} = gh\mathbf{b} + \frac{\mathbf{b} \times \hat{\nabla} \hat{P}}{\mathbf{b}^2}, \tag{2}$$

where the force-free current h is determined by

$$g\mathbf{b} . \hat{\nabla} h = -(\mathbf{b} \times \hat{\nabla} \hat{P}) . \hat{\nabla} (1/\mathbf{b}^2). \tag{3}$$

As the right-hand side of (3) is small, it will be convenient to write

$$h = \lambda^3 h_c^{(3)} + \lambda^4 h_c^{(4)} + \lambda^5 h_c^{(5)} + \lambda^6 h_c^{(6)} + \lambda^6 h_P^{(6)} + \ldots,$$

where
$$g\mathbf{b} . \hat{\nabla} h_c = 0 \tag{4}$$

and
$$g\mathbf{b} . \hat{\nabla} h_p = -(\mathbf{b} \times \hat{\nabla} \hat{P}) . \hat{\nabla} (1/\mathbf{b}^2). \tag{5}$$

We can now proceed to the solution, order by order.

3. Equilibrium calculation

Our objective is the determination of the magnetic fields to sufficiently high order (in fact, to sixth order) that effects associated with the toroidal displacement of magnetic surfaces are recovered. To this end we use the equilibrium equations up to tenth order. We will discuss the order-by-order solution of these equations presently, but it seems appropriate to make some preliminary observations which will allow us to anticipate the form of the lower orders of this solution.

Without a plasma we have the known vacuum field (Dobrott & Frieman 1971). In Appendix A, we apply the present ordering to the exact solution in toroidal co-ordinates for the magnetic potential, and so obtain a very simple derivation of this result. Toroidal stellarator flux surfaces exist in the asymptotic sense (Kruskal 1952) so that a function ψ exists which satisfies

$$\mathbf{b}.\nabla\psi = 0, \tag{6}$$

at any order of expansion. For the vacuum field the surface functions can be put in the form (Dobrott & Frieman 1971)

$$\psi(\rho,\theta,\bar{s}) = \psi_0(\rho) - \lambda\frac{3\alpha\rho^2}{\bar{p}^2}\psi_0'(\rho)\sin(3\theta+\bar{s}) - \lambda^2\left(\frac{3\alpha\rho^2}{2\bar{p}^2}\right)^2\rho^3\frac{d}{d\rho}\left(\frac{1}{\rho}\frac{d\psi_0}{d\rho}\right)\cos(6\theta+2\bar{s}) + O(\lambda^3), \tag{7}$$

where $\psi_0(\rho)$ is some function of radius. As the main effect of the plasma pressure and current on the flux surfaces is to displace them toroidally by small amounts of order ϵ, the above form is expected to hold true for the flux surfaces in the presence of plasma, although, in fact, the third-order term would then differ significantly from the vacuum-field term (see § 4). Any small, externally applied field (for the purpose of recentring the plasma, say) will also leave the form of ψ unchanged below third order. Now we have noted already in (4) that h_c satisfies the equation of a surface function, so from (7) we can infer the structure of this part of the force-free current, up to fifth order. Likewise, the plasma pressure must satisfy (6) so that its form can be anticipated up to eighth order from (7).

The zeroth-order field is of course constant and axial: $b^{(0)} = \xi$. Following Dobrott & Frieman, there is no first-order field and in second order we introduce the helical field

$$\mathbf{b}^{(2)} = \frac{3\alpha\rho^2}{\bar{p}}(\hat{\rho}\cos(3\theta+\bar{s}) - \hat{\theta}\sin(3\theta+\bar{s})) \tag{8}$$

given by the vacuum potential (see Appendix A). The strength of the external winding current determines the quantity α.

The plasma current first appears in next order, and to satisfy (1) the third-order current σ must be axial and independent of toroidal co-ordinate $\bar{s}$. In the absence of externally applied shaping fields the lowest-order flux surfaces are circular so that $\sigma \equiv \sigma(\rho)$, and so the third-order field of the current is poloidal and given by

$$b_\theta^{(3)} = b(\rho), \tag{9}$$

where

$$\frac{1}{\rho}\frac{d}{d\rho}(\rho b) = \sigma(\rho), \quad \text{and} \quad b_\rho^{(3)} = 0,$$

as in cylindrical geometry. Since $\mathbf{b} = \xi + O(\lambda^2)$, the lowest-order part of the force-free current h_c is just $h_c^{(3)} = \sigma(\rho)$. There is a third-order correction to the vacuum field axial component

$$b_\xi^{(3)} = \rho\cos\theta - \alpha\rho^3\sin(3\theta + \bar{s}) \tag{10}$$

which contains the leading-order toroidal and helical modulations.

Proceeding now to fourth order, force balance (equation (1*a*)) requires that $\hat{\mathbf{J}}^{(4)}$ must have only an axial component, $\sigma^{(4)}$, which in order to satisfy the condition $\operatorname{div}\mathbf{J} = 0$ must take the form

$$\sigma^{(4)} = -\frac{3\alpha\rho^2}{\bar{p}^2}\sigma'(\rho)\sin(3\theta + \bar{s}) + \bar{\sigma}^{(4)}(\rho, \theta). \tag{11}$$

(From a constraint equation obtained in higher order it will be seen that the axisymmetric term $\bar{\sigma}^{(4)}$ can be set equal to zero without loss of generality, and then, since $h_c^{(4)} = \sigma^{(4)}$, we observe that (7) gives the above result directly.) We calculate the corresponding magnetic field from the fourth-order parts of (1*b*) and (1*c*)

$$\left.\begin{aligned} \hat{\nabla}^{(0)}.\,\mathbf{b}^{(4)} &= \alpha\bar{p}\rho^3\cos(3\theta + \bar{s}), \\ \hat{\nabla}^{(0)} \times \mathbf{b}^{(4)} &= \xi\sigma^{(4)}. \end{aligned}\right\} \tag{12}$$

The result may be written as

$$\left.\begin{aligned} b_\rho^{(4)} &= f^{(4)}(\rho)\cos(3\theta + \bar{s}) + \bar{b}_\rho^{(4)}(\rho, \theta), \\ b_\theta^{(4)} &= g^{(4)}(\rho)\sin(3\theta + \bar{s}) + \bar{b}_\theta^{(4)}(\rho, \theta), \\ b_\xi^{(4)} &= 0. \end{aligned}\right\} \tag{13}$$

Functions $f^{(4)}(\rho)$ and $g^{(4)}(\rho)$ are given in Appendix 2 where the final expressions for the magnetic field are written in full, and $\bar{\mathbf{b}}^{(4)}$ is the field due to $\bar{\sigma}^{(4)}$ alone.

In fifth order, force balance gives

$$\left.\begin{aligned} \hat{J}_\rho^{(5)} &= \sigma(\rho)\, b_\rho^{(2)} = \frac{3\alpha\rho^2}{\bar{p}}\sigma(\rho)\cos(3\theta + \bar{s}), \\ \hat{J}_\theta^{(5)} &= \sigma(\rho)\, b_\theta^{(2)} = -\frac{3\alpha\rho^2}{\bar{p}}\sigma(\rho)\sin(3\theta + \bar{s}). \end{aligned}\right\} \tag{14}$$

These are just the force-free currents $h_c^{(3)}\mathbf{b}^{(2)}$ due to the helical field. Using these currents in the transverse components of (1*b*) we find

$$b_\xi^{(5)} = \left\{\frac{\bar{p}\rho g^{(4)}(\rho)}{3} + \frac{\alpha\rho^3\sigma(\rho)}{\bar{p}}\right\}\sin(3\theta + \bar{s}). \tag{15}$$

The fifth-order axial current $\hat{J}_\xi^{(5)}$, which we denote by $\sigma^{(5)}$, is obtained in similar fashion to $\sigma^{(4)}$, using $\operatorname{div}\mathbf{J} = 0$:

$$\begin{aligned} \sigma^{(5)} = \bar{\sigma}^{(5)}(\rho, \theta) &- \left(\frac{3\alpha\rho^2}{2\bar{p}^2}\right)^2 \rho\frac{d}{d\rho}\left(\frac{1}{\rho}\frac{d\sigma}{d\rho}\right)\cos(6\theta + 2\bar{s}) \\ &- \left(\frac{3\alpha\rho^2}{\bar{p}^2}\right)\left\{\frac{\partial\bar{\sigma}^{(4)}}{\partial\rho}\sin(3\theta + \bar{s}) + \frac{1}{\rho}\frac{\partial\bar{\sigma}^{(4)}}{\partial\theta}\cos(3\theta + \bar{s})\right\}. \end{aligned} \tag{16}$$

At this stage we can derive a constraint on $\overline{\sigma}^{(4)}$ and its associated fourth-order field by obtaining the seventh order of $\nabla . \mathbf{J} = 0$ and of $\nabla \times (\mathbf{J} \times \mathbf{b}) = 0$. Averaging over $\bar{s}$, we find

$$b^*(\rho)\frac{\partial \overline{\sigma}^{(4)}}{\partial \theta} + \rho\sigma'(\rho)\,\bar{b}_\rho^{(4)} = 0, \tag{17}$$

where $b^*(\rho)$ is the effective mean poloidal field, given by

$$b^*(\rho) = b(\rho) - 18\alpha^2\rho^3/\overline{p}^3.$$

Thus, as indicated earlier, it is consistent to set $\overline{\sigma}^{(4)} \equiv 0$ so that $\bar{b}^{(4)} \equiv 0$. This corresponds to the absence of axisymmetric shaping fields. Using the expression just obtained for $\sigma^{(5)}$, we obtain the fifth-order poloidal fields in the usual way, the result being given in Appendix 2, where $\overline{\sigma}^{(2)}$ and associated fields are set to zero. The consistency of this will be shown later.

It is in the sixth order of expansion that the effects of pressure first appear. From the ξ-component of force balance in seventh order we see that

$$\hat{P}^{(6)} \equiv \hat{P}^{(6)}(\rho, \theta)$$

and, as we insist that there are no surface-shaping fields present, $\hat{P}^{(6)} \equiv P(\rho)$. Thus the sixth-order force balance gives

$$\left.\begin{aligned} \hat{j}_\rho^{(6)} &= -\frac{1}{2}\left(\frac{3\alpha\rho^2}{\overline{p}^2}\right)^2 \overline{p}\sigma'(\rho)\sin(6\theta + 2\bar{s}), \\ \hat{j}_\theta^{(6)} &= -\frac{db_\beta(\rho)}{d\rho} - \frac{1}{2}\left(\frac{3\alpha\rho^2}{\overline{p}^2}\right)^2 \overline{p}\sigma'(\rho)\cos(6\theta + 2\bar{s}), \end{aligned}\right\} \tag{18}$$

where we define

$$b_\beta(\rho) = -\int_0^\rho \left\{\frac{dP}{d\rho} + \sigma(\rho)\,b(\rho) + \frac{1}{2}\left(\frac{3\alpha\rho^2}{\overline{p}^2}\right)^2 \overline{p}\sigma'(\rho)\right\} d\rho.$$

These correspond to the force-free currents $h_c\mathbf{b}$ and the usual diamagnetic current. Using (18) in (1*b*) we obtain $b_\xi^{(6)}$, given in Appendix B. It remains to find $J_\xi^{(6)} = \sigma^{(6)}$, for which purpose we must obtain first the pressure and poloidal currents in seventh order.

From the ξ-component of force balance in eighth order, we find

$$P^{(7)} = -\left(\frac{3\alpha\rho^2}{\overline{p}^2}\right)\frac{dP}{d\rho}\sin(3\theta + \bar{s}) + \bar{P}^{(7)}(\rho, \theta), \tag{19}$$

where the first term is clearly just the helical modulation indicated by (7) with $\psi_0(\rho) = P(\rho)$, and the second term is to be determined. Returning now to seventh order, the poloidal components of $\hat{\mathbf{J}}^{(7)}$ can be found, and, using $\operatorname{div}\mathbf{J} = 0$, we can set

$$\begin{aligned} \sigma^{(6)} = \overline{\sigma}^{(6)}(\rho, \theta) &+ \sigma_0^{(6)}(\rho)\cos\theta + \sigma_1^{(6)}(\rho)\sin(3\theta + \bar{s}) \\ &+ \sigma_2^{(6)}(\rho)\sin(9\theta + 3\bar{s}) \\ &- \frac{3\alpha\rho^2}{\overline{p}^2}\left\{\sin(3\theta + \bar{s})\frac{\partial \overline{\sigma}^{(5)}}{\partial \rho} + \cos(3\theta + \bar{s})\frac{1}{\rho}\frac{\partial \overline{\sigma}^{(5)}}{\partial \theta}\right\}, \end{aligned} \tag{20}$$

where $\sigma_1^{(6)}(\rho)$ and $\sigma_2^{(6)}(\rho)$ are defined in Appendix B. For convenience, the $\cos\theta$ component of the as yet undetermined axisymmetric part is written separately. By using (20) in the poloidal eighth-order force balance and making use of $\operatorname{div}\mathbf{J} = 0$, we obtain the constraint equation

$$b^*(\rho)\frac{\partial\overline{\sigma}^{(5)}}{\partial\theta} + \rho\bar{b}_\rho^{(5)}\sigma'(\rho) = 0,$$

after averaging over $\bar{s}$. This is the same condition as was found for $\overline{\sigma}^{(4)}$ and by the same argument we set $\overline{\sigma}^{(5)} \equiv 0$ without loss of generality.

Solving for the sixth-order fields using the form given by (20) for $\sigma^{(6)}$, we find

$$\left.\begin{aligned} b_\rho^{(6)} &= A(\rho)\sin\theta + f_1^{(6)}(\rho)\cos(3\theta+\bar{s}) + f_2^{(6)}(\rho)\cos(9\theta+3\bar{s}) + \bar{b}_\rho^{(6)}(\rho,\theta), \\ b_\theta^{(6)} &= B(\rho)\cos\theta + g_1^{(6)}(\rho)\sin(3\theta+\bar{s}) + g_2^{(6)}(\rho)\sin(9\theta+3\bar{s}) + \bar{b}_\theta^{(6)}(\rho,\theta), \end{aligned}\right\} \tag{21}$$

where the functions $f_{1,2}^{(6)}$ and $g_{1,2}^{(6)}$ are given in Appendix B, and where

$$\left.\begin{aligned} \frac{1}{\rho}\frac{d}{d\rho}(\rho B) - \frac{A(\rho)}{\rho} &= \sigma_0^{(6)}(\rho) + \rho\sigma(\rho), \\ \frac{1}{\rho}\frac{d}{d\rho}(\rho A) - \frac{B(\rho)}{\rho} &= -b(\rho). \end{aligned}\right\} \tag{22}$$

As $\bar{\mathbf{b}}^{(6)}(\rho,\theta)$ is the field due to $\overline{\sigma}^{(6)}(\rho,\theta)$, $\bar{b}_\rho^{(6)}$ has no $\sin\theta$ component and $\bar{b}_\theta^{(6)}$ has no $\cos\theta$ component.

To complete the solution for $\mathbf{b}$ to sixth order we need to find $\sigma_0^{(6)}(\rho)$ and $\overline{\sigma}^{(6)}(\rho,\theta)$. The first step towards this end is to obtain the form of $P^{(8)}$, by considering the ξ component of ninth-order pressure balance. In this way we find

$$P^{(8)} = \bar{P}^{(8)}(\rho,\theta) - \left(\frac{3\alpha\rho^2}{2\overline{p}^2}\right)^2 \rho\frac{d}{d\rho}\left(\frac{1}{\rho}\frac{dP}{d\rho}\right)\cos(6\theta+2\bar{s}) - \frac{3\alpha\rho^2}{\overline{p}^2}\left[\frac{\partial\bar{P}^{(7)}}{\partial\rho}\sin(3\theta+\bar{s}) + \frac{1}{\rho}\frac{\partial\bar{P}^{(7)}}{\partial\theta}\cos(3\theta+\bar{s})\right]. \tag{23}$$

Next we obtain the poloidal components of $\hat{\mathbf{J}}^{(8)}$ from the force balance equation, and so after $\bar{s}$-averaging the ξ component of the same equation in tenth order, we find that

$$\frac{b^*(\rho)}{\rho}\frac{\partial\bar{P}^{(7)}}{\partial\theta} = 0. \tag{24}$$

Clearly we can set $\bar{P}^{(7)} \equiv 0$ without loss of generality as anticipated from (7). After obtaining $\hat{\mathbf{J}}_\xi^{(7)}$ from the eighth order of $\operatorname{div}\mathbf{J} = 0$ (apart from an undetermined axisymmetric part), we form the poloidal components of force balance in ninth order. Applying to these the condition $\boldsymbol{\xi}.\nabla\times\nabla p = 0$ and averaging the result over $\bar{s}$, we obtain, after some algebraic reduction, the final form

$$V(\rho)\sin\theta + W(\rho,\theta) = 0, \tag{25}$$

where

$$W(\rho,\theta) = -\left[b^*(\rho)\frac{\partial\overline{\sigma}^{(6)}}{\partial\theta} + \rho\sigma'(\rho)\bar{b}_\rho^{(6)}\right],$$

which, by virtue of the definitions earlier, has no $\sin\theta$ Fourier component. Thus the terms of (25) vanish separately, so that firstly we may set $\overline{\sigma}^{(6)} \equiv 0$ without loss of generality. From the calculated form of $V(\rho)$ we get the condition which determines $\sigma_0^{(6)}(\rho)$:

$$-b^*(\rho)\,\sigma_0^{(6)}(\rho) + \frac{d}{d\rho}(\rho\sigma A) + \rho(2P' + b\sigma) - \sigma B + \frac{45\alpha^2}{4\overline{p}^3}\rho^5\sigma'(\rho) = 0. \tag{26}$$

Combining (22) and (26), we find

$$\frac{b^*(\rho)}{\rho^2}\frac{d}{d\rho}\left(\rho^3\frac{dA}{d\rho}\right) - \rho\sigma'(\rho)\,A(\rho) = 2\rho P'(\rho) - b(\rho)\,b^*(\rho) + \frac{45\alpha^2}{4\overline{p}^3}\rho^5\sigma'(\rho). \tag{27}$$

With this last equation, given suitable boundary conditions, the determination of $\mathbf{b}$ to sixth order in λ is complete and the result is summarized in Appendix B. If we set $A(\rho) = b^*(\rho)\,\Delta(\rho)/\rho$ then (27) may be rewritten in the form

$$b^{*2}\Delta'' + b^*\left(2b^{*\prime} + \frac{1}{\rho}b^*\right)\Delta' + b^*\Delta\frac{d}{d\rho}\left(\frac{1}{\rho}\frac{d}{d\rho}(\rho b_0(\rho))\right) = 2\rho P' - b^*b + \frac{45\alpha^2}{4\overline{p}^3}\rho^5\sigma'(\rho), \tag{28}$$

where $b_0 = b^* - b = -18\alpha^2\rho^3/\overline{p}^3$. In the special case of a tokamak, $\alpha = 0$ so $b^* = b$ and (28) is just the well-known toroidal shift equation (Greene, Johnson & Weimer 1971), Δ being the major radius displacement of the flux surface with mean radius ρ. In the following section we shall see that in a slightly modified form $\Delta(\rho)$ retains its interpretation as a flux surface displacement. Furthermore, we shall find it possible to give a simple explanation for the form of (26).

4. Calculation of flux surfaces

In order to obtain the equation describing the magnetic surfaces, we solve (6) for ψ up to third order, using the fields calculated in the last section, and following the method employed by Dobrott & Frieman (1971). In leading order (first), equation (6) yields the condition $\partial\psi^{(0)}/\partial\bar{s} = 0$, and in second order gives

$$\mathbf{b}^{(2)}.\hat{\nabla}^{(0)}\psi^{(0)} + \overline{p}\,\partial\psi^{(1)}/\partial\bar{s} = 0,$$

which determines $\psi^{(1)}$ in terms of $\psi^{(0)}$, apart from an axisymmetric term $\overline{\psi}^{(1)}$. Going to third order and first of all integrating over one complete period in $\bar{s}$, we obtain a constraint on $\psi^{(0)}$ to ensure the absence of any secular term:

$$\frac{b^*(\rho)}{\rho}\frac{\partial\psi^{(0)}}{\partial\theta} = 0.$$

Thus, $\psi^{(0)} \equiv \psi_0(\rho)$, and although we could choose a particular functional form for ψ_0 at this stage we prefer to retain the general form. Apart from an axisymmetric term, $\psi^{(2)}$ is determined at this order. To ensure the absence of secular terms in fourth order, it is found that $\psi^{(1)}$ must satisfy the above constraint as well, so that without loss of generality we can set $\overline{\psi}^{(1)} \equiv 0$. An axisymmetric term in $\psi^{(3)}$ as well as that in $\psi^{(2)}$ remains undetermined at this stage. Proceeding

in the same fashion, however, we find that $\overline{\psi}^{(2)} \equiv 0$, and in sixth order the secular equation reduces to

$$\frac{b^*(\rho)}{\rho}\frac{\partial \overline{\psi}^{(3)}}{\partial \theta} = -\psi_0'(\rho)\left\{A(\rho) + \left(\frac{45\alpha^2\rho^4}{4\overline{p}^3}\right)\right\}\sin\theta. \tag{29}$$

Thus, the flux surfaces up to third order are given by

$$\psi = \psi_0(\rho) - \lambda\frac{3\alpha\rho^2}{\overline{p}^2}\psi_0'(\rho)\sin(3\theta+\bar{s}) - \lambda^2\left(\frac{3\alpha\rho^2}{2\overline{p}^2}\right)^2\rho\frac{d}{d\rho}\left(\frac{1}{\rho}\frac{d\psi_0}{d\rho}\right)\cos(6\theta+2\bar{s})$$
$$+\lambda^3\left\{\frac{\rho\psi_0'(\rho)}{b^*(\rho)}\left(A(\rho)+\frac{45\alpha^2}{4\overline{p}^3}\rho^4\right)\cos\theta + \pi_1(\rho)\sin(3\theta+\bar{s}) + \pi_2(\rho)\sin(9\theta+3\bar{s})\right\}, \tag{30}$$

where $\pi_1(\rho)$ and $\pi_2(\rho)$ are defined in Appendix B.

As anticipated in § 3, the plasma current and pressure leave ψ unaltered from its vacuum field form below third order.

Using the known expression for $\psi^{(3)}$ now we can see how the terms of (26) arise for the sixth-order current $\sigma_0^{(6)}(\rho)$. Firstly, by (5), $h_p^{(6)} \equiv h_p^{(6)}(\rho,\theta)$ and

$$\frac{b^*(\rho)}{\rho}\frac{\partial h_p^{(6)}}{\partial\theta} = -2P'(\rho)\sin\theta, \tag{31}$$

where (31) results from the elimination of terms secular in $\bar{s}$ at ninth order. Thus,

$$h_p^{(6)} = 2\rho P'(\rho)\cos\theta/b^*(\rho), \tag{32}$$

which is the so called Pfirsch–Schlüter current. The remaining force-free part of $\hat{\mathbf{J}}_\xi^{(6)}$ is $(h_c^{(6)} + (gb_\xi)^{(3)}h_c^{(3)})$, and the axisymmetric component of this is just $\bar{h}_c^{(6)}$. By virtue of (4) and the fact that $h_c^{(3)} = \sigma(\rho)$, we see from (30) that

$$\bar{h}_c^{(6)} = \frac{\rho\sigma'(\rho)}{b^*(\rho)}\left(A(\rho)+\frac{45\alpha^2\rho^4}{4\overline{p}^3}\right)\cos\theta; \tag{33}$$

and so, combining (32) and (33), we have

$$\sigma_0^{(6)}(\rho) = \rho\left\{2P'(\rho)+\sigma'(\rho)\left[A(\rho)+\frac{45\alpha^2\rho^4}{4\overline{p}^3}\right]\right\}\Big/ b^*(\rho),$$

which is equivalent to (26).

The form of the magnetic surfaces is now clear: the vacuum surfaces are subjected to an additional third-order toroidal shift due to the plasma pressure and current, and also to additional helical distortions at third order and higher which are associated with the plasma currents. Toroidicity, in fact, also produces $(2\theta+\bar{s})$ and $(4\theta+\bar{s})$ 'side-bands' of the stellarator field which are recovered at fourth order in ψ.

To calculate the magnetic axis position, we note first of all that $\psi_0(\rho)$ must tend to zero at least as rapidly as $b^*(\rho)$, otherwise $\overline{\psi}^{(3)}$ cannot be defined at $\rho = 0$. Then, defining

$$f = \int_0^\rho b^*(\rho)\,d\rho,$$

we see that $\psi_0'(f) = \psi_0'(\rho)/b^*(\rho)$ remains finite as $\rho \to 0$, and, neglecting the helical terms in (30), we have

$$\psi = \psi_0\left[f + \lambda^3\rho\left(A(\rho) + \frac{45\alpha^2}{4\bar{p}^3}\rho^4\right)\cos\theta\right] + O(\lambda^4).$$

Since $\nabla\psi$ vanishes at the magnetic axis, the co-ordinates of this point are given to sufficient accuracy by $\theta = \pi$, and $\rho = \rho_x$, where

$$b^*(\rho_x) = \lambda^3\frac{d}{d\rho}(\rho A(\rho))\Big|_{\rho=\rho_x}. \tag{34}$$

The consistency of the approximations used in obtaining (34) is verified by substitution of the result in the full expression for $\nabla\psi$. In terms of the quantity $\Delta(\rho)$ which satisfies (28), we can rewrite (34) in the form

$$b^*(\rho_x - \lambda^3\Delta(\rho_x)) = 0,$$

provided $\Delta(0) = O(1)$, and the solution in leading order is then $\rho_x = \lambda^3\Delta(0)$. Although this result covers a wide range of conditions, including the tokamak special case ($\alpha = 0$), it is less general than (34) since $\Delta(0)$ is assumed to be of order unity, which, for example, is not appropriate to currentless stellarators if $A(0)$ is non-zero: in fact, the axis shift in the latter case is $\lambda|A_0\bar{p}^3/18\alpha^2|^{\frac{1}{3}}$ to leading order in λ. Thus, in general, the magnetic axis can take up widely different positions, depending on the relative strengths of the rotational transform due to the current and that due to the vacuum field.

Sufficiently far from the co-ordinate axis, we can express the radius of a given flux surface $\rho(\psi, \theta, \bar{s})$ as a single-valued function which at leading order in λ depends on ψ alone. Then a straightforward inversion of (30) yields

$$\begin{aligned}\rho = \rho_0(\psi) &+ \lambda\frac{3\alpha\rho_0^2}{\bar{p}^2}\sin(3\theta+\bar{s}) + \lambda^2\frac{45}{2}\frac{\alpha^2\rho_0^2}{\bar{p}^4}\sin^2(3\theta+\bar{s}) \\ &+ \lambda^3\left[\frac{24\alpha}{\bar{p}^2}\left(\frac{3\alpha\rho_0^2}{2\bar{p}^2}\right)^2\sin^3(3\theta+\bar{s}) + \left(\frac{f^{(4)}(\rho_0)}{\bar{p}} - \frac{9\alpha\rho_0 b(\rho_0)}{\bar{p}^3}\right)\sin(3\theta+\bar{s})\right. \\ &\left. - \frac{\rho_0\cos\theta}{b^*(\rho_0)}\left\{A(\rho_0) + \frac{45\alpha^2\rho_0^4}{4\bar{p}^3}\right\}\right] + O(\lambda^4). \end{aligned} \tag{35}$$

Thus, when use of the variable $\Delta(\rho)$ is appropriate, the outward axis shift of a surface with lowest-order radius ρ_0 may be written as $\lambda^3\{\Delta(\rho_0) + 45\alpha^2\rho_0^5/4\bar{p}^3 b^*(\rho_0)\}$, so that $\Delta(\rho_0)$ is indeed the displacement function for tokamaks and, modified by a small extra term, remains so for stellarators, which in this case can be referred to as 'tokamak-like'. Although (35) does not apply close to the co-ordinate axis in general, a simple change of variables is possible for tokamak-like configurations which relocates the co-ordinate axis on the magnetic axis at $\rho_x = \lambda^3\Delta(0)$. In terms of the new co-ordinates, (35) now correctly describes all the flux surfaces provided $\Delta(\rho)$ is replaced by $(\Delta(\rho) - \Delta(0))$.

Finally in this section we note that the rotational transform on a given surface can be calculated, using (35), in the same way as for the vacuum field (Dobrott & Frieman 1971)

$$\iota = \frac{1}{2\pi}\frac{d\chi}{d\phi},$$

where χ and ϕ respectively measure the poloidal and toroidal magnetic fluxes. We obtain

$$i(\rho_0) = \frac{b(\rho_0)}{\rho_0} - \left(\frac{18\alpha^2\rho_0^2}{\bar{p}^3}\right) = \frac{b^*(\rho_0)}{\rho_0},$$

a result which may also be derived from the fields up to third order using the method of averaging (Morozov & Solovev 1966). Contributions from the current and from the vacuum field are additive, as usual in stellarators with many helical periods.

5. Vertical field calculation

In order to maintain a given equilibrium configuration (say one in which the magnetic axis position is specified) an externally applied vertical magnetic field is necessary in general. Of course, in contrast to tokamaks, stellarator equilibria may exist without a vertical field as we shall see, but in this case the axis displacement may be considerable under the influence of plasma current and pressure, and in addition the cross-sectional form of the surfaces is sensitive to the effects of finite pressure (Greene & Johnson 1961).

Thus, in determining the boundary condition for (27), we shall not make any particular assumption about the size of the vertical field, but rather we shall obtain the relationship between this quantity and the function $A(\rho)$.

To this end we make use of the fact that within any given flux surface the equilibrium is unchanged if that surface is replaced by a coincident, perfectly conducting shell carrying a surface current I given by

$$\mathbf{I} = (\mathbf{B} \times \hat{n})/\mu_0, \tag{36}$$

where B is the equilibrium magnetic field at the chosen surface, and $\hat{n}$ is a unit normal directed outwards. This is sometimes referred to as the 'virtual casing principle' (Shafranov & Zakharov 1972) and it allows us to calculate all the external fields necessary for maintaining a given equilibrium within the chosen surface. Thus, regarding $A(\rho)$ as known, we can select any (closed) flux surface outside the plasma as the virtual casing, and calculate the casing current I from (36) using the known field B. For the purpose of determining the external vertical field it is sufficient to have B up to sixth order and ψ up to third.

We can use (35) to describe the virtual casing, so that the unit normal $\hat{n}$ may be calculated from $\hat{n} = \nabla\psi/|\nabla\psi|$. To the order in λ required, we obtain

$$\left.\begin{aligned} n_\rho &= 1 - \lambda^2\frac{81\alpha^2}{2\bar{p}^4}\rho_b^2\cos^2(3\theta+\bar{s}) - \lambda^3\frac{24\alpha^3\rho_b^3}{\bar{p}^6}\sin(3\theta+\bar{s}) \\ &\qquad\qquad \times\{1+\tfrac{7}{2}\sin^2(3\theta+\bar{s})\} + O(\lambda^4), \\ n_\theta &= -\lambda\frac{9\alpha\rho_b}{\bar{p}^2}\cos(3\theta+\bar{s}) - \lambda^2\frac{54\alpha^2\rho_b^2}{\bar{p}^4}\sin(6\theta+2\bar{s}) + O(\lambda^3), \\ n_\xi &= -\lambda^2\frac{3\alpha\rho_b^2}{\bar{p}}\cos(3\theta+\bar{s}) + O(\lambda^3), \end{aligned}\right\} \tag{37}$$

ρ_b being the lowest-order radius of the boundary.

The vacuum field $\mathbf{b}_I B_0$ will be determined by solving the magnetostatic equations order by order in both interior (i) and exterior (e) domains. At the virtual casing surface $\mathbf{b}_I$ must satisfy the matching conditions

$$[\mathbf{b}_I . \hat{n}] = 0 \tag{38a}$$

and

$$[\mathbf{b}_I \times \hat{n}] = -\mathbf{i}, \tag{38b}$$

where $\mathbf{i}$ denotes the normalized casing current given, from (36), by

$$\mathbf{i} = \mathbf{b} \times \hat{n}, \tag{39}$$

and where $[x] = x_e - x_i$ denotes the discontinuity of a quantity at the casing. The condition of regularity in the interior provides a further restriction on the solutions. Likewise, the vanishing of exterior fields at large distance from the shell restricts the solution form for b_{Ic}; however to apply this condition to the expanded form of b_{Ie} we need to obtain first the appropriate form of exact solution in toroidal co-ordinates, and then to transform co-ordinates in these solutions to the quasi-cylindrical $(\rho, \theta, \bar{s})$ system in the limit $\rho \ll 1/\epsilon$, a procedure which was used for axisymmetric fields by Greene *et al.* (1971).

Up to second order, the fields $\mathbf{b}_I$ and $\mathbf{b}$ must coincide in the interior since the effects of currents in the plasma do not show below third order. In the exterior region, $\mathbf{b}_I$ vanishes identically up to second order, since the casing is a perfect conductor. Similarly, $b^{(3)}_{I\xi} \equiv b^{(3)}_{\xi}$ in the interior, and is zero outside, since $b^{(3)}_{\xi}$ is a vacuum field term. The third-order exterior poloidal field of the casing current does not vanish however, since it must exactly cancel the field generated by the plasma current. Thus, we have

$$\mathbf{j}^{(3)} = -\hat{\xi} b(\rho_b)$$

and

$$\left.\begin{aligned} b^{(3)}_{I\theta} &= 0 && \text{in the interior,} \\ &= -b(\rho_b)\rho_b/\rho && \text{in the exterior.} \end{aligned}\right\} \tag{40}$$

In fourth order, the matching conditions (38) may be reduced to

$$[b^{(4)}_{I\rho}] = -f^{(4)}(\rho_b)\cos(3\theta + \bar{s}),$$

$$[b^{(4)}_{I\theta}] = -\left[g^{(4)}(\rho_b) + \frac{3\alpha\rho_b^2\sigma(\rho_b)}{\bar{p}^2}\right]\sin(3\theta + \bar{s}).$$

Solving the magnetostatic equations at this order we find that $b^{(4)}_I$ can be written in the form

$$\mathbf{b}^{(4)}_I = (A^{(4)}_I \rho^2 + \tfrac{5}{16}\alpha\bar{p}\rho^4)\,\hat{\rho}\cos(3\theta + \bar{s}) - (A^{(4)}_i \rho^2 + \tfrac{3}{16}\alpha\bar{p}\rho^4)\,\hat{\theta}\sin(3\theta + \bar{s}) \tag{41}$$

in the interior, $A^{(4)}_i$ being a constant determined by the matching conditions.

The fifth-order poloidal fields are found to be expressible in the form

$$\mathbf{b}^{(5)}_I = \hat{\rho}\left\{\frac{\alpha\rho^3}{\bar{p}}\cos(2\theta + \bar{s}) + A^{(5)}_i \rho^5 \sin(6\theta + 2\bar{s})\right\}$$

$$+ \hat{\theta}\left\{-\frac{\alpha\rho^3}{2\bar{p}}\sin(2\theta + \bar{s}) + A^{(5)}_i \rho^5 \cos(6\theta + 2\bar{s})\right\} \tag{42}$$

in the interior, where $A^{(5)}_i$ satisfies the appropriate matching conditions.

The expression for the vertical field is obtained from the sixth-order casing current. After averaging the second matching condition, (38b), over $\bar{s}$ we find

$$[\langle b_{I\theta}^{(6)}\rangle] = \cos\theta\left\{-B(\rho_b)+\rho_b\sigma_b(\rho_b)\left[A(\rho_b)+\frac{45\alpha^2}{4\bar{p}^3}\rho_b^4\right]\Big/ b^*(\rho_b)\right\}, \tag{43}$$

where use is made of (40)–(42) and the known lower-order vacuum field form of $\mathbf{b}_I$, and $B(\rho)$, $A(\rho)$ are the functions appearing in (21). The $\bar{s}$-average of a quantity x is denoted by $\langle x\rangle$.

Similarly, (38a) after averaging yields

$$[\langle b_{I\rho}^{(6)}\rangle] = -A(\rho_b)\sin\theta. \tag{44}$$

At this order, the magnetostatic equations for the average poloidal field are just

$$\hat{\boldsymbol{\xi}}.\hat{\nabla}^{(0)}\times\langle\mathbf{b}_I^{(6)}\rangle = 0$$

and

$$\hat{\nabla}^{(0)}.\langle\mathbf{b}_I^{(6)}\rangle = -b_{I\theta}^{(3)}\sin\theta.$$

Dropping the average symbol, these may be solved to give, in the interior,

$$\left.\begin{aligned} b_{I\rho}^{(6)} &= A_i^{(6)}\sin\theta,\\ b_{I\theta}^{(6)} &= A_i^{(6)}\cos\theta,\end{aligned}\right\} \tag{45}$$

and, in the exterior domain,

$$\left.\begin{aligned} b_{I\rho}^{(6)} &= \{A_e^{(6)} - B_e^{(6)}/\rho^2 + \tfrac{1}{2}\rho_b b(\rho_b)\,(1+\ln\rho)\}\sin\theta,\\ b_{I\theta}^{(e)} &= \{A_e^{(6)} + B_e^{(6)}/\rho^2 + \tfrac{1}{2}\rho_b b(\rho_b)\ln\rho\}\cos\theta.\end{aligned}\right\} \tag{46}$$

Thus, the applied vertical field which we seek is given by $b_I^{(6)}$ in the interior, its strength being $A_i^{(6)}$. The jump conditions (43) and (44) determine only the difference $A_e^{(6)} - A_i^{(6)}$, there being three unknown quantities in (45) and (46). To obtain a third relation, we must recall that the quasi-cylindrical co-ordinates $(\rho,\theta,\bar{s})$ do not form a true co-ordinate system, as they apply only within the domain $\rho < 1/\epsilon$. Thus, the boundary condition at infinity cannot be applied to (46) directly, as is obvious from the presence of logarithmic terms, and must instead be deduced in the manner described earlier from the exact solution form in toroidal co-ordinates. As discussed in Appendix B, the axisymmetric part of the casing current produces a field which can be represented by a stream function χ such that $\mathbf{b}_I = \hat{\nabla}\chi\times\hat{\boldsymbol{\xi}}/g^2$. From the exact form of general solution for χ in the exterior domain, with the correct behaviour at infinity, we find that the expansion of χ for $\rho\epsilon \ll 1$ must take the corresponding form

$$\chi = \epsilon K_0\left\{\left(2+\ln\frac{\rho\epsilon}{8}\right)-\epsilon\cos\theta\left[\tfrac{1}{2}\rho\left(1+\ln\frac{\rho\epsilon}{8}\right)+\frac{K_1}{\rho}\right]\right\}+O(\epsilon^3), \tag{47}$$

where K_0 and K_1 are constants.

Identifying the $O(\epsilon)$ part of the field given by (47) with $b_I^{(3)}$, we see that

$$K_0 = -\rho_b b(\rho_b).$$

A similar comparison at $O(\epsilon^2)$ then shows that

$$A_e^{(6)} = \tfrac{1}{2}\rho_b b(\rho_b)\ln\frac{\epsilon}{8},$$

and so from (43) and (44) we find $A_i^{(6)}$ and $B_e^{(6)}$. The externally applied vertical field is thus given by

$$B_v = \frac{\epsilon^2 B_0}{2}\left\{A(\rho)+\frac{d}{d\rho}(\rho A(\rho))+\rho b(\rho)\left(\tfrac{3}{2}+\ln\frac{\epsilon\rho}{8}\right)-\frac{\rho\sigma(\rho)}{b^*(\rho)}\left[A(\rho)+\frac{45\alpha^2\rho^4}{4\bar{p}^3}\right]\right\}_{\rho=\rho_b}. \tag{48}$$

This completes our determination of the plasma equilibrium to sixth order of λ in the magnetic field, by establishing the boundary condition which, together with regularity at $\rho = 0$, fixes the solution of (27) for $A(\rho)$.

6. Specific equilibria

In a few, particularly simple cases, $A(\rho)$ may be found by analytical solution of (27). Firstly we note that, in the absence of a stellarator field, (48) may be written in the form

$$B_v = \frac{\epsilon^2 B_0}{2} b(\rho_a)\left\{\Delta'(\rho_a)+\rho_a\left(\tfrac{3}{2}+\ln\frac{a}{8R_0}\right)\right\},$$

where ρ_a is the radius of the plasma boundary. Allowing for differences in the sign convention for Δ, this agrees with the result of Greene *et al.* (1971) for tokamaks, and it is to be noted that only Δ' is determined: clearly any $O(1)$ constant term added to $\Delta(\rho)$ corresponds to a mere change of co-ordinate origin. Equation (28) possesses a well-known integral in this case

$$\rho b^2\Delta'(\rho) = \int_0^\rho \rho\{2\rho P' - b^2\}\,d\rho$$

showing that, for equilibrium, B_v must take on a specific non-zero value, determined at a given value of aspect-ratio by the plasma beta and rotational transform profiles: a given fractional change in B_v will in general induce a shift of the plasma column by a similar amount in major radius.

In stellarators, however, the helical field can provide the necessary force to maintain positional stability so that equilibria with given pressure and rotational transform profiles exist for a range of different vertical field values, including zero field, at essentially the same value of plasma column aspect-ratio. The main effect of changing the vertical field in this case is to alter the internal disposition of the flux surfaces. As a specific example, consider a current-free stellarator. Equation (27) is easily integrated, yielding

$$\rho^3\frac{dA(\rho)}{d\rho} = -\frac{\bar{p}^3}{9\alpha^2}(P(\rho)-P_0),$$

where $P_0 = P(0)$. Regularity of A at the origin constrains the form of P so that $P' \propto \rho^3$ for small ρ. This is a consequence of the fact that $P \equiv P(f)$ where, as in §4, $f = \int b^*\,d\rho$ and $dP/df = O(1)$ for the most general profile consistent with equilibrium. Then, choosing

$$P(\rho) = P_0(1-(\rho/\rho_a)^4),$$

we obtain

$$A(\rho) = A_0 - (P_0/i_a)\,(\rho/\rho_a)^2$$

for $0 \leqslant \rho \leqslant \rho_a$, where ρ_a is the normalized radius of the plasma boundary, and $i_a = i(\rho_a)$ is the corresponding rotational transform. The constant A_0 is determined in terms of the applied vertical field by (48):

$$A_0 = 2P_0/i_a + B_v/\epsilon^2 B_0. \tag{49}$$

In general, (34) determines a single magnetic axis position, given approximately (for $A_0 = O(1)$) by

$$\frac{\rho_x}{\rho_a} = \lambda\left\{\frac{A_0}{\rho_a i_a}\right\}^{\frac{1}{2}} - \lambda^3\left\{\frac{P_0}{i_a^2 \rho_a}\right\},$$

while the plasma boundary displacement $\delta\rho_a$, found from (35), is

$$\delta\rho_a = \lambda^3\left[\frac{A_0}{i_a} - \frac{P_0}{i_a^2} - \tfrac{5}{8}\rho_a^2\right],$$

both ρ_x and $\delta\rho_a$ being measured positive along $\theta = \pi$ (outwards).

Thus, surfaces close to the magnetic axis are displaced to a greater degree by a given change in the applied vertical field than are the surfaces near the plasma boundary. An interesting special case of this equilibrium has been studied previously by Yurchenko (1968) who used a Mercier expansion about the vacuum magnetic axis. The plasma boundary was assumed to be coincident with a vacuum field flux surface, which corresponds to setting $\delta\rho_a = -\frac{5}{8}\lambda^3\rho_a^2$. With the value of A_0 determined in this manner, Yurchenko's result for the axis shift is recovered from (34), and (49) shows that the vertical field is in fact $B_v = -\epsilon^2 B_0 P_0/i_a$. The appearance at the plasma edge of a stagnation point in the flux function places an upper limit on the range of pressures whose confinement this model can describe adequately. The limiting value can be estimated at $P_0 \leqslant i_a^2/2\epsilon$, that is $\beta = 2\mu_0 p/B_0^2 \leqslant i_a^2\,\epsilon$ (which is in any case inconsistent with the formal ordering).

In most situations of practical interest, the measured profiles of pressure and plasma current do not permit (27) to be solved analytically; however, its numerical solution for given boundary data is very simple. We illustrate the use of the above analysis in calculating specific equilibria by presenting some results obtained for typical equilibria in CLEO stellarator (Atkinson *et al.* 1976). In this device, consisting of a toroidal chamber of major radius 90 cm and minor radius 14 cm, hydrogen plasma with $T_e \simeq 200$ eV, and $T_i \simeq 100$ eV can be readily produced and sustained with an Ohmic heating current of several kilo-amperes, at an electron density in the range 10^{13}–10^{14} cm^{-3}. The main device characteristics used for calculations are listed in table 1, along with the relevant dimensionless parameters. The vacuum rotational transform at the plasma edge, i_a, is 0·4 for the stated winding current, and field-line following calculations (P. C. Johnson 1978, private communication) have shown that the separatrix lies outside the vacuum vessel, in agreement with a predicted separatrix radius of 16 cm for a straight $l = 3$ stellarator field (Morozov & Solovev 1966) with the same characteristics. A mean plasma pressure profile shown in figure 2 (lower curve) is determined from measured electron and ion temperatures and electron density in a discharge with plasma parameters as listed in table 2. The current density profile, determined from the temperature profile assuming Spitzer

Major radius, R_0	= 0·90 m
Liner minor radius	= 0·14 m
Radius of stellarator l-windings, a	= 0·175 m
Number of helical field periods, p	= 7
l-winding current	= 102 kA
Toroidal field at minor axis, B_0	= 1·84 tesla

Dimensionless parameters:

$\epsilon = a/R_0 = 0{\cdot}194$ $\quad \bar{p} = 2{\cdot}35$
$\lambda = 0{\cdot}58$ $\quad \alpha = 0{\cdot}887$

TABLE 1

Central electron temperature,	T_e	= 176 eV
ion temperature,	T_i	= 130 eV
electron density		= $4{\cdot}07 \times 10^{19}/\mathrm{m}^3$
Plasma current		= 6·5 kA
β (on axis)		= 0·15 %

TABLE 2

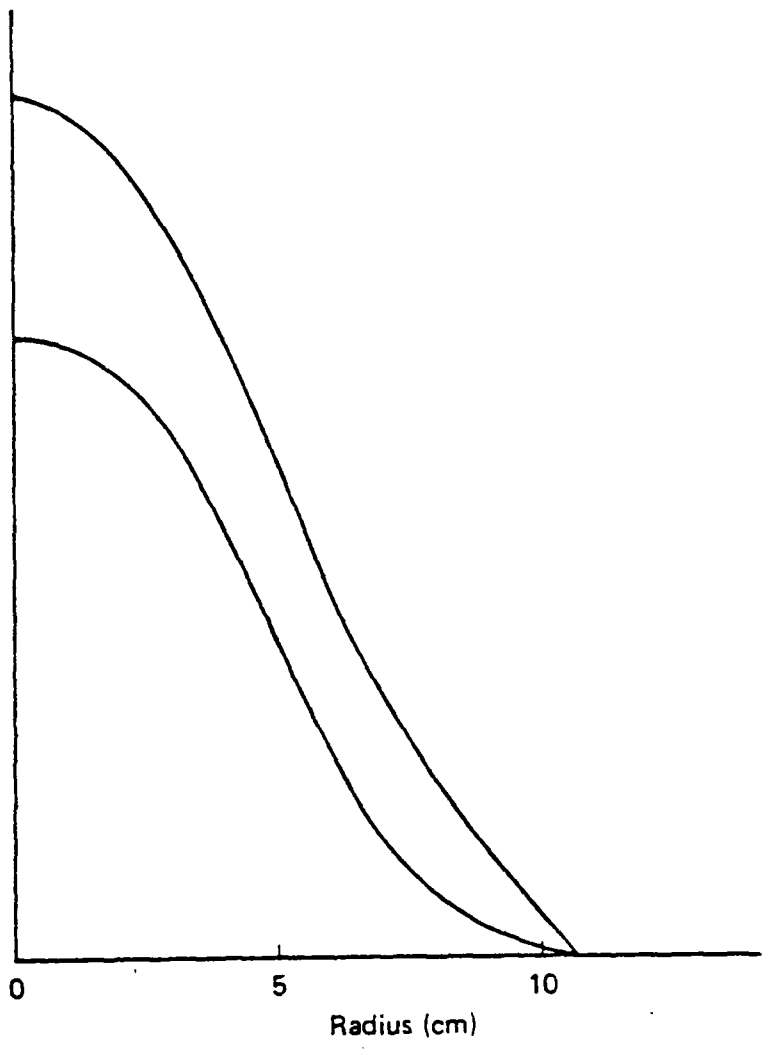

FIGURE 2. Normalized radial profiles of plasma pressure (lower curve) and current density.

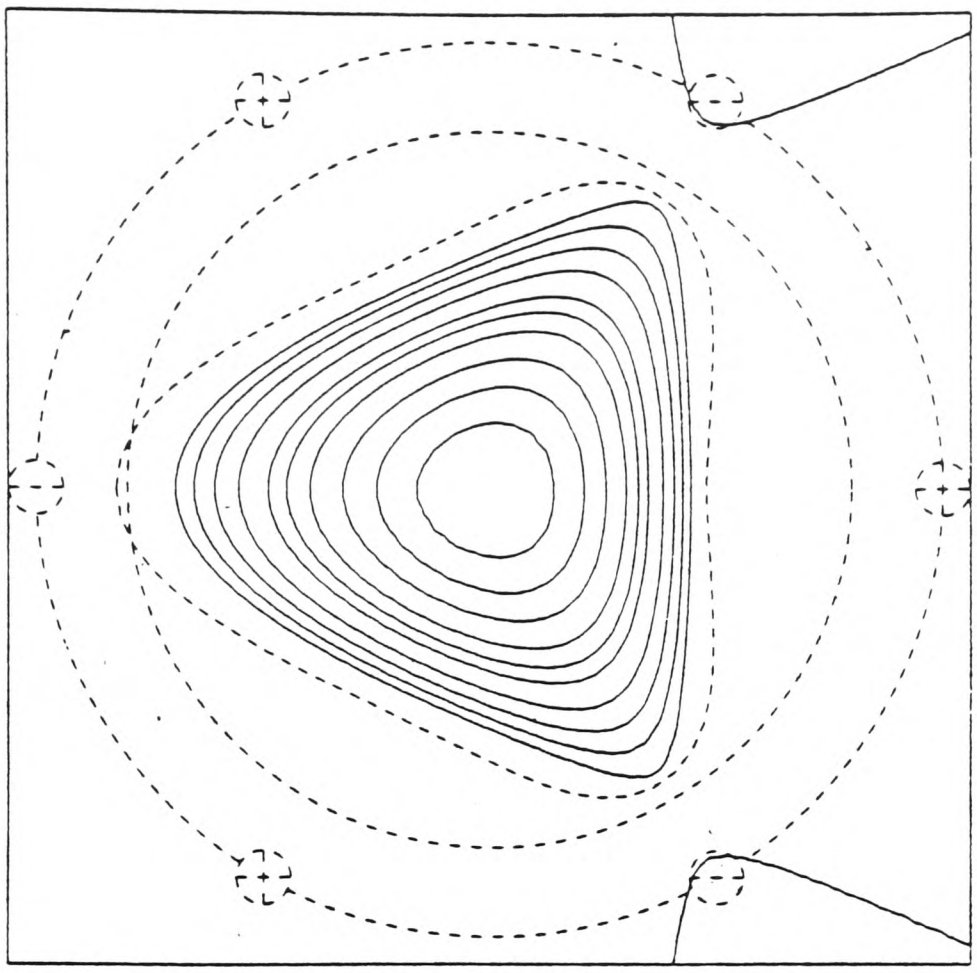

FIGURE 3. Flux surfaces of the vacuum magnetic field for the CLEO parameters given in table 1. The location of the stellarator windings is indicated (dashed) together with the direction of current flow (+ into the page), and the vacuum vessel position is marked by the inner circle (also dashed). A third-order flux surface (dashed line) is included for comparison. At the cross-section shown, $\bar{s} = \frac{1}{2}\pi$, the major axis lying to the left.

resistivity, is given by the upper curve in figure 2. The shift function $A(\rho)$ is determined at points within the plasma by a numerical shooting procedure using trial values of A_0 until the boundary condition (48) is satisfied for a given value of B_v. Then the flux function ψ may be calculated from (30) and the level contours plotted in any chosen minor cross-section. For simplicity we choose $\psi_0(\rho) = \frac{1}{2}b'(0)\rho^2 + \frac{1}{4}i_a\rho_a^{-2}\rho^4$. In practice, it is found that extending (30) by including terms at fourth order in λ does not significantly change the surfaces near the axis, so third-order accuracy for these is sufficient. However, the influence of toroidicity on the positions of the vacuum field separatrices is quite marked and in the present case it proves necessary to retain the fourth-order term so that λ yields a minimum separatrix radius greater than the liner radius (14 cm). In addition it proves convenient to re-express $\psi(\rho, \theta, \bar{s})$ in the form

$$\psi = \frac{b'(0)}{2}\psi_L + \frac{i_a\rho_a^{-2}}{4}\psi_L^2 + \lambda^3\rho\frac{\psi_0'(\rho)}{b^*(\rho)}A(\rho)\cos\theta + O(\lambda^4),$$

where ψ_L is given to third order by (30) with $\psi_0 = \rho^2$, and with $A(\rho)$ replaced by zero. In this way, the flux surface configuration shown in figure 3 was obtained for the vacuum field with table 1 parameters. The inner circle (dashed) indicates the position of the stainless-steel liner, and the location of the stellarator field

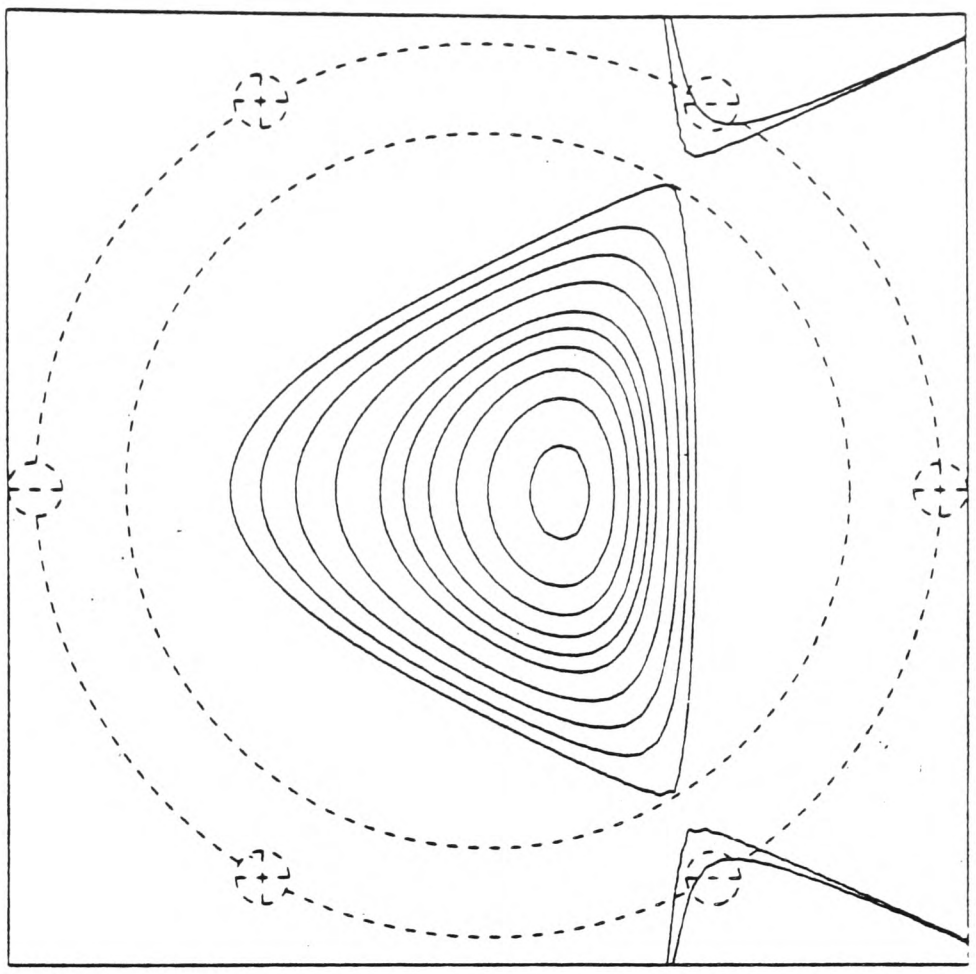

FIGURE 4. Equilibrium flux surfaces for the plasma parameters of table 2, with the profiles of figure 2 and the vacuum field as for figure 3, that is $B_v = 0$.

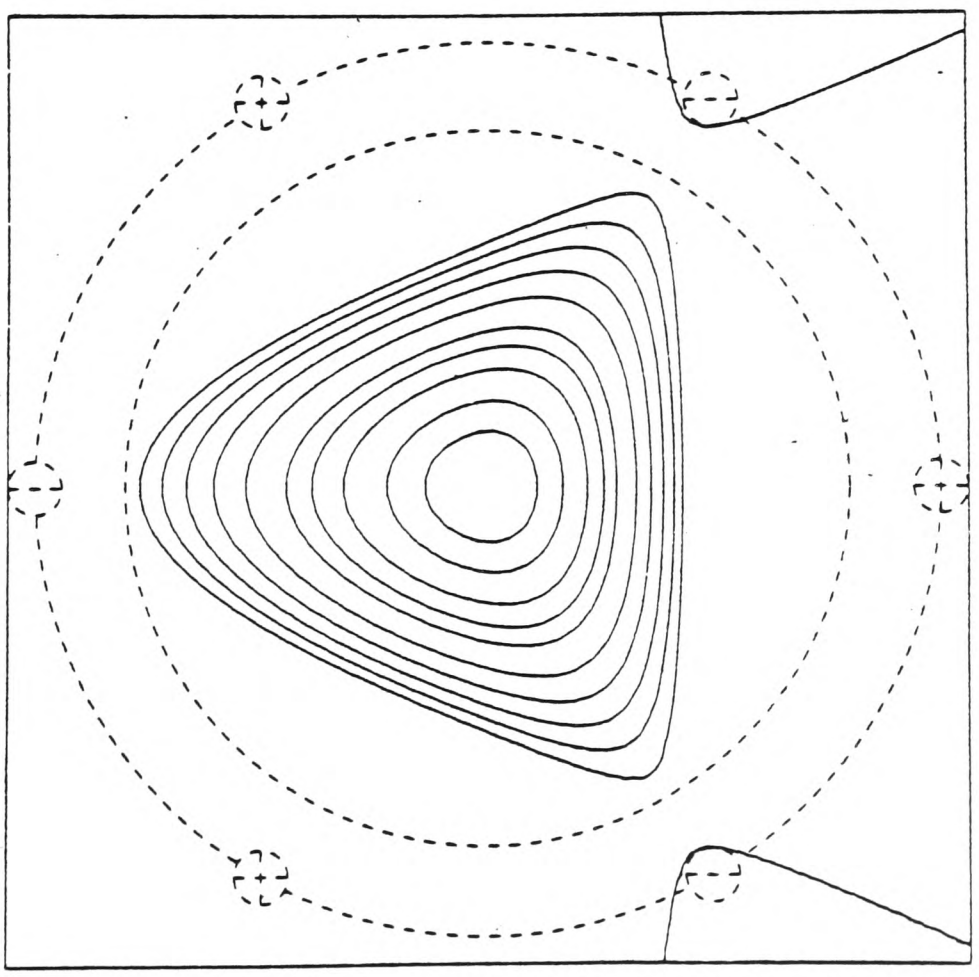

FIGURE 5. Flux surfaces as for figure 4, but with $B_v = 68{\cdot}4$ gauss.

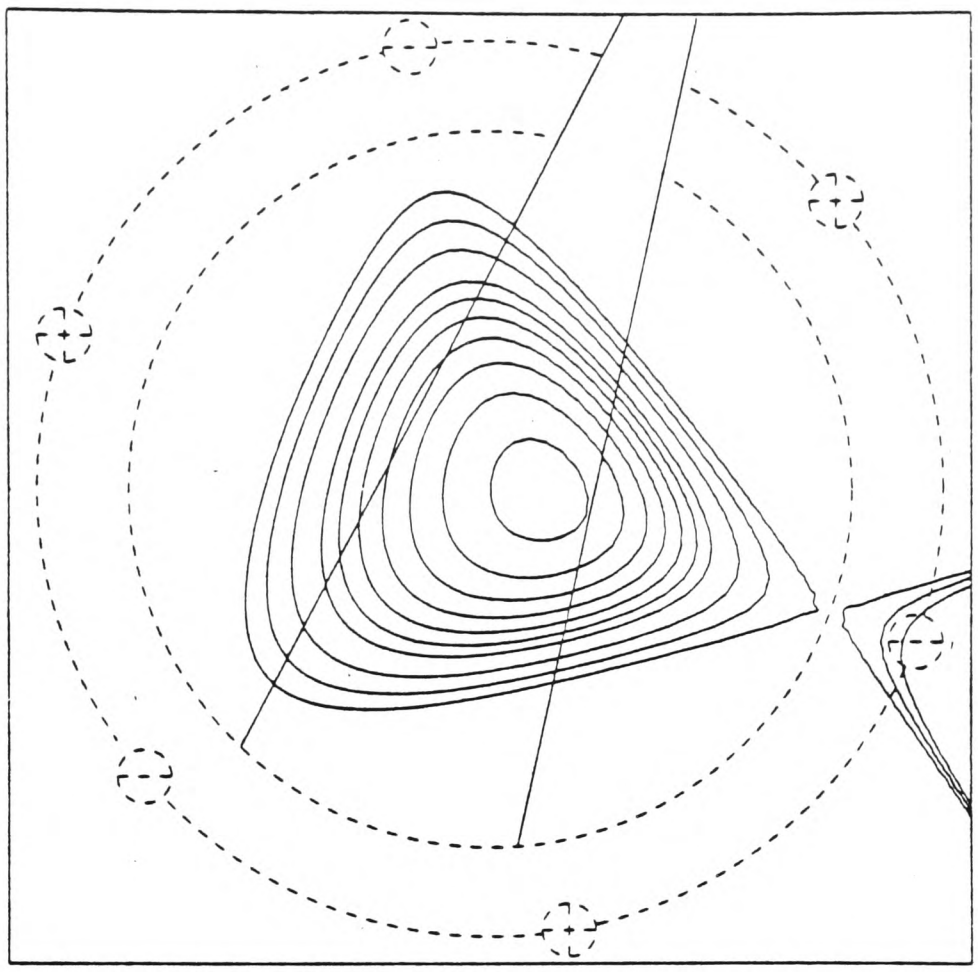

FIGURE 6. Plasma–detector configuration in CLEO. Soft X-ray emission along the two chords shown is measured with a pair of diodes. The equilibrium depicted has the parameters of figure 4, but with $B_v = 32$ gauss.

coils in this cross-section ($\bar{s} = \frac{1}{2}\pi$) is also shown. For comparison, the third-order 'boundary' flux surface, given by (35), is included (also dashed). Now using the measured profiles of figure 2, the equilibrium surfaces in figure 4 were obtained for the case where, as in the experiment, $B_v = 0$. The axis shift is found to be 2·5 cm and it is seen that there is considerable distortion of the flux surfaces near the magnetic axis. The application of a $+68$ gauss vertical field with the same profiles re-centres the magnetic axis, and, as shown in figure 5, considerably reduces the surface distortions. This property of an appropriately chosen vertical field has been noted previously by Bykov *et al.* (1977).

Direct experimental confirmation of the above value of B_v for re-centring is not possible, but satisfactory agreement has been found between the measured and calculated ratio of signals in two soft X-ray detectors, angled to receive emissions along chords intersecting the equatorial plane at approximately ± 4 cm on either side of the geometric axis. The detector characteristics are such that the signals are proportional to P_e^2 integrated along the lines of sight, where P_e denotes electron pressure. Figure 6 shows the plasma–detector configuration for the profiles of figure 2, with an applied field of 32 gauss, at which value the detector signals, as measured by $\int P^2\,dl$, become equal. Note that because the surfaces are asymmetrical this balance occurs when the plasma is still off-centred. In general, of course, the ratio of P_e to P will vary over the

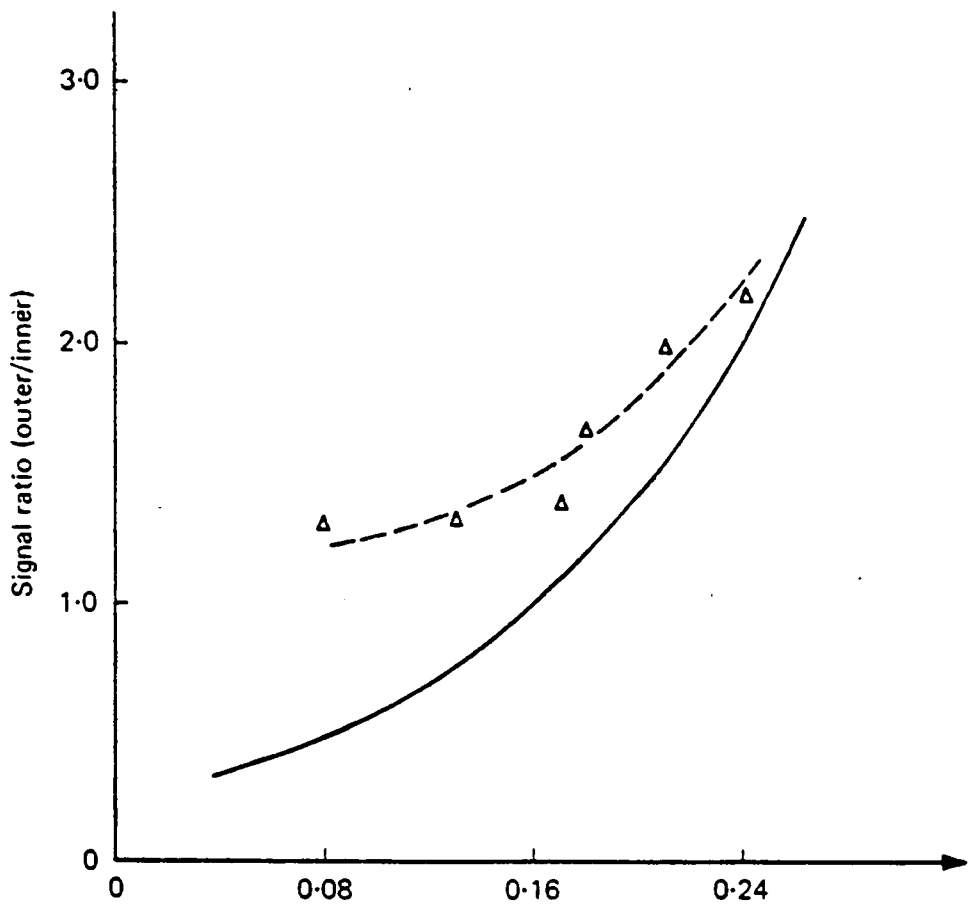

FIGURE 7. Variation of X-ray diode signal ratio *vs.* plasma β, at a fixed value of $B_v = 33$ gauss. At the higher values of β where species equilibration is better and the signals are stronger, the calculated (solid line) and measured (triangles) ratios are in quite good agreement.

cross-section but we shall assume for simplicity that ion–electron equilibration is sufficiently effective for such variation to be neglected. By changing the normalizing value of pressure at the geometric axis whilst retaining the same profiles and vertical field, we obtain the variation of signal ratio with β. This is shown in figure 7, for a fixed vertical field of 33 gauss, with corresponding data points taken from CLEO (shots 11757–11771). The plasma current was 8 kA, $B_\phi = 18{\cdot}6$ kG, and $I_L = 102$ kA. As the pressure is varied experimentally by raising or lowering the plasma density at nearly constant electron temperature, there is a systematic narrowing of the pressure profiles as β falls. This is not represented in our calculations and probably accounts for at least part of the divergence in the ratios at low β, where, in addition, species equilibration is poor and the errors in the measured signals are larger. Otherwise the agreement is generally good and may be taken as an indication of the extent to which our calculation successfully represents the stellarator flux surface structure, at least in the regions of higher pressure within the plasma.

Finally, we examine the effect of increasing the plasma pressure, retaining the same profiles and with remaining parameters as in tables 1 and 2. The value of β is set equal to 1 % on the axis and without a vertical field the equilibrium shown in figure 8 is obtained. Not only is the plasma column shifted outwards but the volume of confined plasma has been reduced owing to the destruction of surfaces. The application of a vertical field of 150 gauss has the effect shown in figure 9 of reducing the axis shift and the surface distortions as well as increasing the

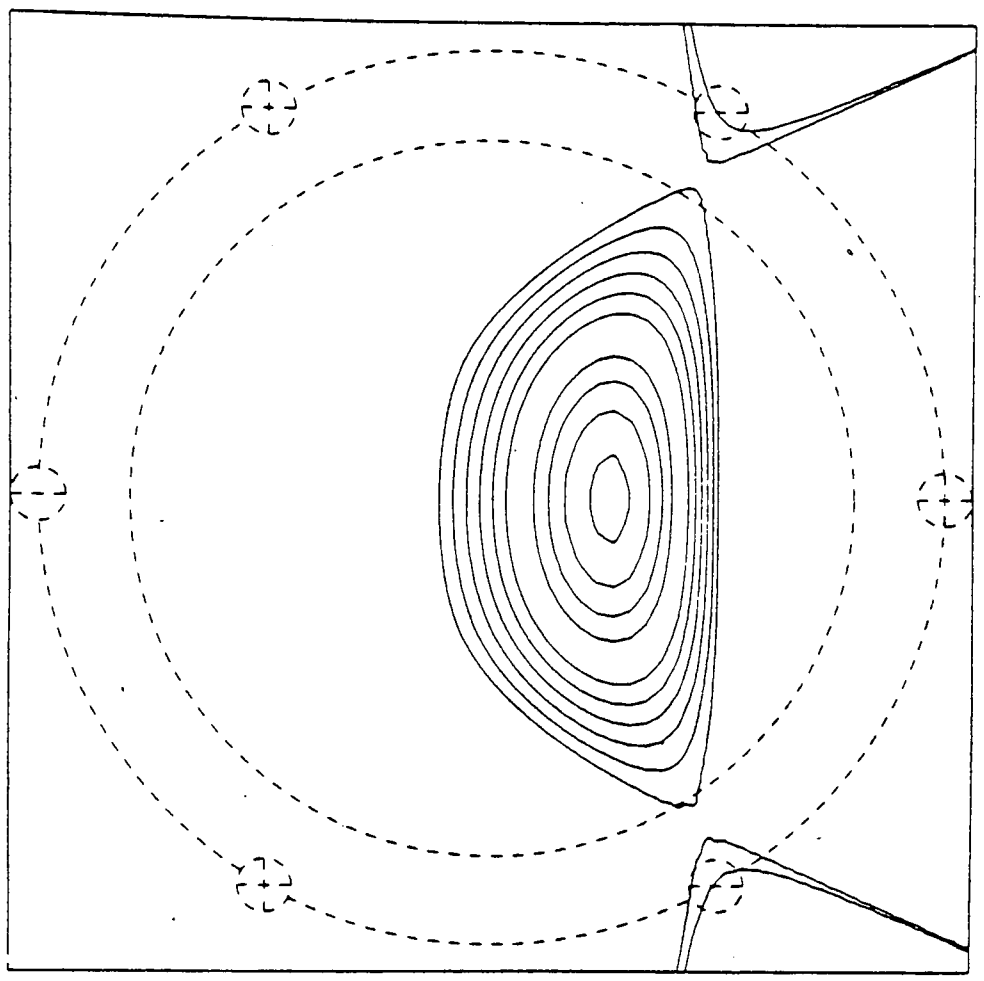

FIGURE 8. Flux surfaces as for figure 4 but with $\beta = 1\,\%$ on the axis.

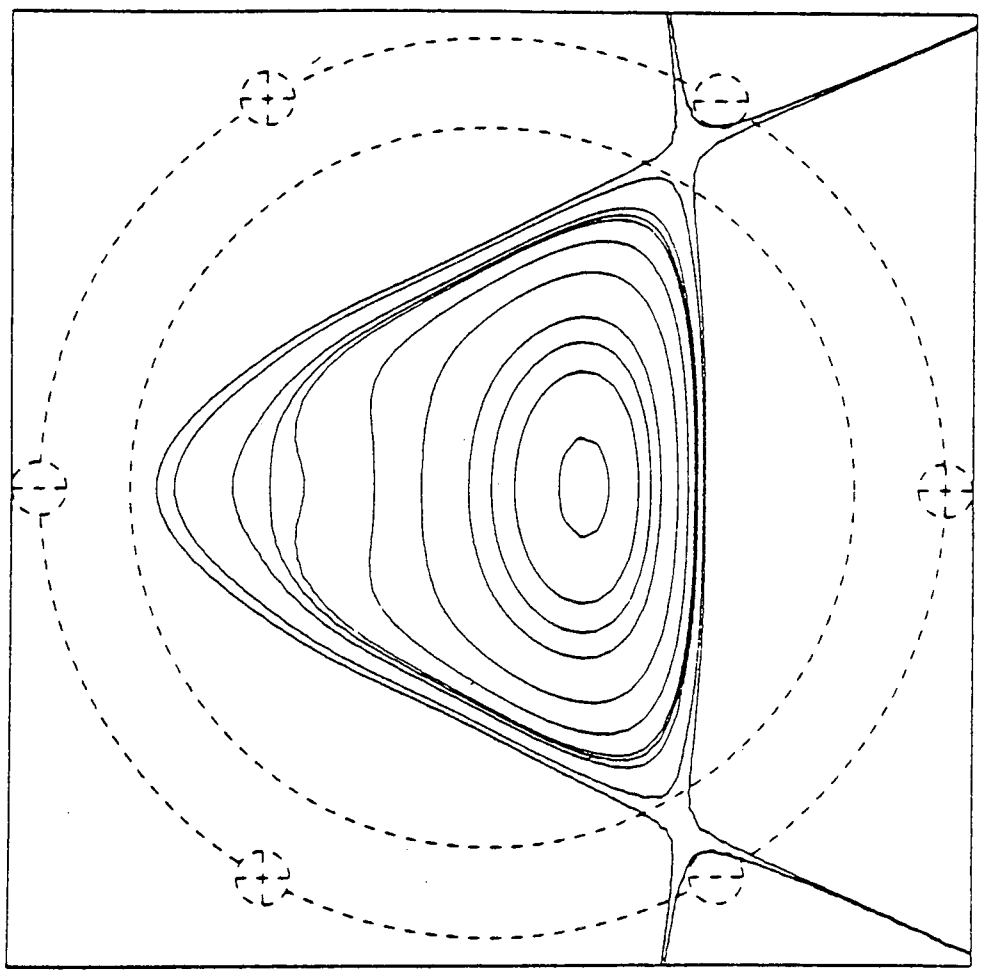

FIGURE 9. Flux surfaces for the equilibrium profiles of figure 8, but with $B_0 = 150$ gauss.

volume of confined plasma. Thus, while it is possible to obtain equilibria without a vertical field, at higher plasma pressures especially the application of such a field, suitably chosen in strength, results in a marked improvement in the equilibrium configuration.

7. Conclusions

By solving the equilibrium equations in an ordering based on the Dobrott–Frieman scheme for $l = 3$ toroidal stellarators, we have obtained the magnetic fields and flux surfaces for a current-carrying, low-beta plasma with arbitrary pressure and current density profiles. The flux surfaces are circular in lowest order with helical distortions and toroidal displacements appearing as higher-order corrections. The equation for the toroidal shift has been derived and the boundary value relation between this quantity and an applied vertical field was found.

Tokamak equilibria and a class of analytically soluble, current-free stellarator equilibria are recovered as special cases, and numerical results for CLEO stellarator are presented. The role of a vertical field in reducing distortions is shown, and results of calculation are shown to compare acceptably with measurements of plasma position. Finally, we draw attention to the increasing importance of a suitably chosen vertical field at high plasma pressure in stellarators like CLEO, notwithstanding their ability to sustain equilibrium without a vertical field.

The authors are particularly grateful to Dr P. C. Johnson and Dr P. Thomas for many discussions of this work, for giving us ready access to data for CLEO, and for their encouragement. One of us (P.J.F.) would also like to thank D. J. Lees and Dr E. Minardi for discussions on an early version of the present calculations. The remaining author wishes in addition to thank Dr C. J. H. Watson for encouragement, and Merton College, Oxford, for financial support.

Appendix A. Vacuum fields

The general solution of Laplace's equation for a potential field may be represented in terms of toroidal harmonics (Morse & Feshbach 1953) which are particularly well suited to problems where the boundary conditions are applied at toroidal surfaces. Solutions in this form are expressed in terms of orthogonal, toroidal co-ordinates $\{\eta, \tau, \xi\}$ defined about a ring of radius R_0, and related to the usual cylindrical polar co-ordinates (R, ϕ, z) measured about the axis of the ring, by

$$R = \frac{R_0 \sinh \eta}{\cosh \eta - \cos \tau}, \quad \phi = \xi \quad \text{and} \quad z = \frac{R_0 \sin \tau}{\cosh \eta - \cos \tau}.$$

Thus, the vacuum field of the stellarator can be represented by a potential V in the general form

$$V = B_0 R_0 \xi + (\cosh \eta - \cos \tau)^{\frac{1}{2}} \sum_{m,n=0}^{\infty} \{A_{m,n} P^{(m)}_{n-\frac{1}{2}}(\cosh \eta) + B_{m,n} Q^{(m)}_{n-\frac{1}{2}}(\cosh \eta)\} \exp[i(m\xi - n\tau)], \quad \text{(A 1)}$$

where $P^{(m)}_{n-\frac{1}{2}}$ and $Q^{(m)}_{n-\frac{1}{2}}$ are the associated Legendre functions of half-integral order.

For solutions which remain bounded at the origin, the coefficients $A_{m,n}$ must vanish, and as we are interested in representing a stellarator field which has exactly p periods round the torus, the solution form appropriate to the present discussion is

$$V = B_0 R_0 \xi + (\cosh\eta - \cos\tau)^{\frac{1}{2}} \sum_n B_{p,n} Q^{(p)}_{n-\frac{1}{2}}(\cosh\eta)\cos(n\tau - p\xi). \tag{A 2}$$

To recover the large aspect-ratio limit we revert to quasi-cylindrical co-ordinates (ρ, θ, ξ) and expand (A 2) in powers of ϵ. Using the 'optimal' ordering of Dobrott & Frieman (1971) for p, we obtain, for one harmonic,

$$\begin{aligned} V^p_n = B_{p,n}(\epsilon\rho)^n \Bigg\{ & \cos(n\theta + \bar{s}) + \frac{\bar{p}^2 \epsilon^{\frac{4}{3}} \rho^2}{4(n+1)} \cos(n\theta + \bar{s}) \\ & + \epsilon\rho \left(\frac{2n+1}{4}\right) \cos([n+1]\theta + \bar{s}) + \frac{\epsilon\rho}{4} \cos([n-1]\theta + \bar{s}) \\ & + \frac{\bar{p}^4 \epsilon^{\frac{8}{3}} \rho^4}{32(n+1)(n+2)} \cos(n\theta + \bar{s}) + \frac{\bar{p}^2 \epsilon^{\frac{8}{3}} \rho^3}{16(n+1)} \\ & \times \{(2n+3)\cos([n+1]\theta + \bar{s}) + 3\cos([n-1]\theta + \bar{s})\} \Bigg\} + O(\epsilon^{n+2}). \end{aligned} \tag{A 3}$$

If instead we had taken $p \propto \epsilon^{-1}$, as in the old stellarator ordering (Greene & Johnson 1961), then $p^n(\cosh\eta)^{-n} = O(1)$ since $e^{-\eta} = \frac{1}{2}\epsilon\rho + O(\epsilon^2)$ and the small aspect-ratio expansion would have produced an infinite series in powers of ρ all of equal order in ϵ, and giving rise to Bessel functions.

By choosing $B_{p,n} = 0$, $n = 0, 1$ and 2, and $\epsilon^3 B_{p,n} = A_n \epsilon^{\frac{3}{2}}(\alpha B_0 a/\bar{p})$, where $A_3 = 1$ and $A_n = O(1)$ for $n \geqslant 4$, we obtain a potential in which the $l = 3$ helical component is dominant, and which may be written as

$$V = \frac{B_0 a}{\bar{p}} \left\{ \frac{\bar{s}}{\epsilon^{\frac{1}{3}}} + \epsilon^{\frac{2}{3}} \alpha \rho^3 \cos(3\theta + \bar{s}) + \epsilon V^{(3)} + \epsilon^{\frac{4}{3}} V^{(4)} \ldots \right\}. \tag{A 4}$$

We fix the higher-order coefficients A_{n+3} by requiring that the associated terms represent only toroidal corrections to the lowest-order helical field. Thus, A_4 is determined by noting that $V^{(3)} = 0$ with the chosen form of coefficients $B_{p,n}$, so that

$$\frac{1}{\rho}\frac{\partial}{\partial\rho}\left(\rho \frac{\partial V^{(5)}}{\partial\rho}\right) + \frac{1}{\rho^2}\frac{\partial^2 V^{(5)}}{\partial\theta^2} + \left(\frac{\partial V^{(2)}}{\partial\rho}\cos\theta - \frac{\partial V^{(2)}}{\partial\theta}\sin\theta\right) = 0. \tag{A 5}$$

From the expression for $V^{(2)}$ in (A 4) it is clear that $V^{(5)}$ has no component proportional to $\cos(4\theta + \bar{s})$, apart from a possible homogeneous term in the solution of (A 5). Since $V^{(5)}$ is a correction term to $V^{(2)}$, however, all such homogeneous solutions are discarded and, to eliminate terms proportional to $\cos(4\theta + \bar{s})$ in

$V^{(5)}$, we choose $A_4 = -\frac{7}{4}$. Up to seventh-order in $\epsilon^{\frac{1}{3}}$, therefore, we can write V in the form

$$V = \frac{B_0 a}{\bar{p}}\left\{\frac{\bar{s}}{\epsilon^{\frac{1}{3}}} + \epsilon^{\frac{2}{3}}\alpha\rho^3\cos(3\theta+\bar{s}) + \epsilon^{\frac{4}{3}}\frac{\alpha\bar{p}^2}{16}\rho^5\cos(3\theta+\bar{s}) + \epsilon^{\frac{5}{3}}\frac{\alpha\rho^4}{4}\cos(2\theta+\bar{s}) + \epsilon^2\frac{\alpha\bar{p}^4}{640}\rho^7\cos(3\theta+\bar{s}) + \epsilon^{\frac{7}{3}}\frac{\alpha\bar{p}^2\rho^6}{64}\{3\cos(2\theta+\bar{s}) + \tfrac{17}{5}\cos(4\theta+\bar{s})\}\right\}, \quad \text{(A 6)}$$

which is the vacuum field given by Dobrott & Frieman (1971).

Toroidal co-ordinates are also useful in establishing the appropriate boundary condition at large distance from the sources of current, when the field solution is expressed in quasi-cylindrical co-ordinates. For the case of an axisymmetric poloidal field such as that discussed in § 5, it is convenient to make use of a poloidal flux function χ, in terms of which fields are given by

$$\mathbf{B} = B_0(\hat{\nabla}\chi\times\xi)/g^2.$$

For vacuum fields, χ must satisfy

$$\frac{\partial}{\partial\eta}\left(\frac{1}{R}\frac{\partial\chi}{\partial\eta}\right) + \frac{\partial}{\partial\tau}\left(\frac{1}{R}\frac{\partial\chi}{\partial\tau}\right) = 0. \quad \text{(A 7)}$$

The solutions of this equation can be expressed in the form (Shafranov 1960)

$$\chi = F(\eta,\tau)/(\cosh\eta - \cos\tau)^{\frac{1}{2}}, \quad \text{(A 8)}$$

where

$$F(\eta,\tau) = \sum_{n=0}^{\infty}\left\{A_n\frac{d}{d\eta}P_{n-\frac{1}{2}}(\cosh\eta) + B_n\frac{d}{d\eta}Q_{n-\frac{1}{2}}(\cosh\eta)\right\}\sinh\eta\, e^{in\tau},$$

and for a bounded solution at infinity ($\eta\to 0$) we have $B_n = 0$. Taking the large aspect-ratio limit in (A 8) and expanding in powers of ϵ we recover the appropriate form of solution for representing the axisymmetric fields in (46), by choosing

$$A_n = \epsilon^{2n+1}K_n\pi.2^{\frac{1}{2}}\{1+O(\epsilon)\}.$$

Thus, $$\chi = \epsilon K_0\left\{\left(2+\ln\frac{\rho\epsilon}{2}\right) - \epsilon\cos\theta\left[\tfrac{1}{2}\rho\left(1+\ln\frac{\rho\epsilon}{8}\right) + \frac{K_1}{\rho}\right]\right\} + O(\epsilon^3), \quad \text{(A 9)}$$

and from this the correct choice of coefficients subject to the boundary condition at infinity may be made in (46).

Appendix B. The equilibrium fields

We give here the full expressions for the fields up to sixth order which are derived in § 3,

$$b_\rho = \lambda^2\frac{3\alpha\rho^2}{\bar{p}}\cos(3\theta+\bar{s}) + \lambda^4 f^{(4)}(\rho)\cos(3\theta+\bar{s}) + \lambda^5\left\{\frac{\alpha\rho^3}{\bar{p}}\cos(2\theta+\bar{s}) + f^{(5)}(\rho)\sin(6\theta+2\bar{s})\right\} + \lambda^6\{A(\rho)\sin\theta + f_1^{(6)}\cos(3\theta+\bar{s}) + f_2^{(6)}(\rho)\cos(9\theta+3\bar{s})\}, \quad \text{(B 1a)}$$

$$b_\theta = -\lambda^2 \frac{3\alpha\rho^2}{\bar{p}} \sin(3\theta+\bar{s}) + \lambda^3 b(\rho) + \lambda^4 g^{(4)}(\rho)\sin(3\theta+\bar{s})$$
$$+\lambda^5\left\{-\frac{\alpha\rho^3}{2\bar{p}}\sin(2\theta+\bar{s}) + g^{(5)}(\rho)\cos(6\theta+2\bar{s})\right\}$$
$$+\lambda^6\{B(\rho)\cos\theta + g_1^{(6)}(\rho)\sin(3\theta+\bar{s}) + g_2^{(6)}(\rho)\sin(9\theta+3\bar{s})\}, \quad \text{(B 1}b\text{)}$$

$$b_\xi = 1+\lambda^3\{\rho\cos\theta - \alpha\rho^3\sin(3\theta+\bar{s})\}$$
$$+\lambda^5\left\{\frac{\bar{p}\rho}{3}g^{(4)}(\rho) + \frac{\alpha\rho^3\sigma(\rho)}{\bar{p}}\right\}\sin(3\theta+\bar{s})$$
$$+\lambda^6\left\{\left[2\bar{p}g^{(5)}(\rho) + \left(\frac{3\alpha\rho^2}{\bar{p}}\right)^2\frac{\sigma'(\rho)}{2\bar{p}}\right]\frac{\rho}{6}\cos(6\theta+2\bar{s}) - \frac{\alpha\rho^4}{2}\sin(4\theta+\bar{s})\right.$$
$$\left. -\frac{3\alpha\rho^4}{4}\sin(2\theta+\bar{s}) + \rho^2\cos^2\theta + b_\beta(\rho)\right\}. \quad \text{(B 1}c\text{)}$$

Recalling that $b(\rho)$ is the field of the third-order plasma current, we have

$$\frac{1}{\rho}\frac{d}{d\rho}(\rho b) = \sigma(\rho). \quad \text{(B 2)}$$

We have defined

$$\left.\begin{aligned} f^{(4)}(\rho) &= \tfrac{5}{16}\alpha\bar{p}\rho^4 + u(\rho), \\ g^{(4)}(\rho) &= -\tfrac{3}{16}\alpha\bar{p}\rho^4 - \frac{1}{3}\frac{d}{d\rho}(\rho u(\rho)), \end{aligned}\right\} \quad \text{(B 3)}$$

where

$$-\frac{1}{3\rho}\frac{d}{d\rho}\left(\rho\frac{d}{d\rho}(\rho u)\right) + \frac{3u}{\rho} = -\frac{3\alpha\rho^2\sigma'(\rho)}{\bar{p}^2}. \quad \text{(B 4)}$$

Similarly,

$$\left.\begin{aligned} f^{(5)}(\rho) &= V(\rho), \\ g^{(5)}(\rho) &= \frac{1}{6}\frac{d}{d\rho}(\rho V(\rho)), \end{aligned}\right\} \quad \text{(B 5)}$$

where

$$\frac{1}{6}\frac{d}{d\rho}\left(\rho\frac{d}{d\rho}(\rho V)\right) - 6V = -\left(\frac{3\alpha}{2\bar{p}^2}\right)^2\rho^6\frac{d}{d\rho}\left(\frac{\sigma'(\rho)}{\rho}\right). \quad \text{(B 6)}$$

$A(\rho)$ and $B(\rho)$ have been discussed already.

Next, the coefficients of the helical terms appearing in the sixth-order axial current, equation (20), are defined:

$$\sigma_1^{(6)} = +\frac{3\alpha}{2\bar{p}^2}\frac{1}{\rho^4}\frac{d}{d\rho}\left\{\left(\frac{3\alpha\rho^2}{2\bar{p}^2}\right)^2\rho^7\frac{d}{d\rho}\left(\frac{\sigma'(\rho)}{\rho}\right)\right\} - \alpha\rho^3\sigma(\rho) + \frac{1}{\bar{p}}\left\{\frac{9\alpha\rho b(\rho)}{\bar{p}} - f^{(4)}(\rho)\right\}\sigma'(\rho),$$

$$\sigma_2^{(6)} = +9\rho^2\left(\frac{\alpha\rho^2}{2\bar{p}^2}\right)^3\frac{d}{d\rho}\left(\frac{1}{\rho}\frac{d}{d\rho}\left(\frac{\sigma'(\rho)}{\rho}\right)\right).$$

Then $f_1^{(6)}$ and $g_1^{(6)}$ are given by

$$f_1^{(6)}(\rho) = \frac{7\alpha\bar{p}^3\rho^6}{640} + h(\rho),$$

$$g_1^{(6)}(\rho) = \frac{-3\alpha\bar{p}^3\rho^6}{640} + k(\rho),$$

where
$$\frac{1}{\rho}\frac{d}{d\rho}(\rho k(\rho))+\frac{3h(\rho)}{\rho}=\sigma_1^{(6)}(\rho),$$
$$\frac{1}{\rho}\frac{d}{d\rho}(\rho h(\rho))+\frac{3k(\rho)}{\rho}=-\bar{p}\rho\left\{\frac{\alpha\rho^2\sigma(\rho)}{\bar{p}}-\frac{\bar{p}}{9}\frac{d}{d\rho}(\rho u)\right\}.$$

Also,
$$f_2^{(6)}(\rho)=w(\rho),$$
$$g_2^{(6)}(\rho)=-\frac{1}{9}\frac{d}{d\rho}(\rho w(\rho)),$$

where
$$\frac{-1}{9\rho}\frac{d}{d\rho}\left(\rho\frac{d}{d\rho}(\rho w)\right)+\frac{9}{\rho}w=\sigma_2^{(6)}(\rho).$$

Finally, we recall that
$$\frac{db_\beta(\rho)}{d\rho}=-\left\{\frac{dP}{d\rho}+b(\rho)\,\sigma(\rho)\right\}-\frac{\sigma'(\rho)}{2\bar{p}}\left(\frac{3\alpha\rho^2}{\bar{p}}\right)^2.$$

In § 4, we introduced functions $\pi_1(\rho)$ and $\pi_2(\rho)$ in the expression for the flux function, (30). These are given by

$$\pi_1(\rho)=\left\{\frac{9\alpha\rho b(\rho)}{\bar{p}^3}-\frac{f^{(4)}(\rho)}{\bar{p}}\right\}\frac{d\psi_0}{d\rho}+\frac{3\alpha\rho^3}{2\bar{p}^2}\left\{6\left(\frac{3\alpha\rho^2}{2\bar{p}^2}\right)^2\frac{d}{d\rho}\left[\frac{1}{\rho}\frac{d\psi_0}{d\rho}\right]+\frac{d}{d\rho}\left[\left(\frac{3\alpha\rho^2}{2\bar{p}^2}\right)^2\rho\frac{d}{d\rho}\left[\frac{1}{\rho}\frac{d\psi_0}{d\rho}\right]\right]\right\}$$

and
$$\pi_2(\rho)=\frac{3\alpha\rho^2}{2\bar{p}^2}\left\{\frac{1}{3}\frac{d}{d\rho}\left[\left(\frac{3\alpha\rho^2}{2\bar{p}^2}\right)^2\rho\frac{d}{d\rho}\left[\frac{1}{\rho}\frac{d\psi_0}{d\rho}\right]\right]-2\left(\frac{3\alpha\rho^2}{2\bar{p}^2}\right)^2\frac{d}{d\rho}\left[\frac{1}{\rho}\frac{d\psi_0}{d\rho}\right]\right\}.$$

REFERENCES

Atkinson, D. W., Dellis, A. N., Gill, R. D., Lees, D. J., Millar, W., Powell, B. A., Shatford, P. A. & Webb, D. R. A. 1976 *Phys. Rev. Lett.* **37**, 1616.

Bykov, V. E., Kuznetsov, Yu. K., Pashnev, V. K. & Pinos, I. B. 1977 *Kharkov Physico-Technical Institute Report* KhFTI 77-5.

Dobrott, D. & Frieman, E. A. 1971 *Phys. Fluids*, **14**, 349.

Greene, J. M. & Johnson, J. L. 1961 *Phys. Fluids*, **4**, 875.

Greene, J. M., Johnson, J. L. & Weimer, K. E. 1971 *Phys. Fluids*, **14**, 671.

Kruskal, M. D. 1952 *U.S. Atomic Energy Commission Report* No. NYO-998(PM-S-5).

Lortz, D. & Nührenberg, J. 1976 *Z. Naturforschung*, **31a**, 1277.

Mercier, C. & Luc, H. 1974 *Lectures on Plasma Physics*, EUR 5127e, Commission of European Communities, Luxembourg.

Morozov, A. I. & Solovev, L. S. 1966 *Reviews of Plasma Physics* (ed. M. A. Leontovich), vol. 2. Consultants Bureau.

Morse, P. M. & Feshbach, H. 1953 *Methods of Theoretical Physics*, vol. II. McGraw-Hill.

Ohasa, K., Hamada, Y., Fujiwara, M. & Miyamoto, K. 1977 *J. Appl. Phys. Japan*, **16**, 617.

Shafranov, V. D. 1960 *Soviet Phys. JETP*, **37**, 775.

Shafranov, V. D. & Zakharov, L. E. 1972 *Nucl. Fusion*, **12**, 599.

Solovev, L. S. & Shafranov, V. D. 1970 *Reviews of Plasma Physics* (ed. M. A. Leontovich), vol. 5. Consultants Bureau.

Yurchenko, E. I. 1968 *Soviet Phys. Tech. Phys.* **12**, 1059.

Appendix Two

"Plasma Equilibrium and Stability in Toroidal Stellarators"

by

W.N.G. Hitchon

and

P.J. Fielding

Culham Preprint CLM-P627

(Accepted for Publication in Nuclear Fusion)

UKAEA

Preprint

PLASMA EQUILIBRIUM AND STABILITY IN TOROIDAL STELLARATORS

W. N. G. HITCHON
P. J. FIELDING

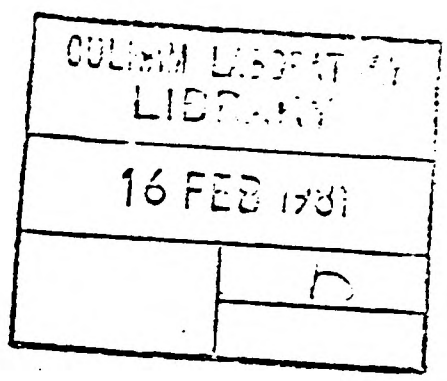

CULHAM LABORATORY
Abingdon Oxfordshire

1981

CLM-P627

PLASMA EQUILIBRIUM AND STABILITY IN TOROIDAL STELLARATORS

W.N.G. Hitchon† and P.J. Fielding

Culham Laboratory, Abingdon, Oxon, OX14 3DB, UK

(Euratom/UKAEA Fusion Association)

Abstract

The equations of MHD equilibrium are solved for a large class of low-β stellarators with arbitrarily prescribed pressure and current density profiles by means of a large aspect-ratio ordering scheme. The fields and flux surfaces are found to sufficiently high order that the surface shaping and the axis-shift are recovered; the relation between the latter and the applied vertical field is given. Using these equilibria, we evaluate the resistive interchange stability criterion [11]. We apply these results to discussion of several special cases, and note the potential advantages of an $\ell = 2$ configuration.

†Merton College and The Dept. of Engineering Science, Oxford, UK.

(Submitted for publication in Nuclear Fusion)

November 1980

1. INTRODUCTION

A great deal of effort is currently being devoted to the study of stellarator-like configurations, with a view to finding systems with steady-state reactor potential [1,2]. The prospects for true steady-state operation have been strengthened by recent experimental success in the production of current-free plasmas [3,4], and it seems possible that the well-known problems of access and structural design associated with conventional stellarator windings can be overcome by use of modular coil systems [5,6]. The potentially serious loss rates associated with ion ripple trapping may be greatly reduced by an ambipolar radial potential, and thus could account for the unexpectedly high beam trapping efficiency observed in WVIIA [3].

Recent theoretical work has included the development of 3D codes to study MHD equilibrium and stability [7,8], the results of which complement those obtained by analytic means. The latter remain valuable in that a relatively simple and general description can be obtained. In an earlier paper [9], we employed an expansion based on an ordering introduced by Dobrott and Frieman [10], in order to obtain the equilibrium configuration for a general class of low-β, $\ell = 3$ stellarators. Making use of the same ordering scheme, we obtain here an analytical description of the equilibrium of low-β stellarators with general winding number ℓ, and investigate their stability to resistive interchanges [11,12] in several special cases of interest.

We discuss briefly the features of an $\ell = 2$ configuration which, when constructed using modular coils, appears to be capable not only of matching the tokamak as the basis for a reactor, but also of offering significant advantages.

In order to solve the equilibrium equations, we use the quasi-cylindrical co-ordinates (r, θ, ξ) of Fig. 1, and expand in powers of the inverse aspect-ratio, ε.

The main (toroidal) field, $\vec{B}_o$, is in the ξ-direction; the stellarator field is introduced in leading order $\varepsilon^{2/3}$.

The number of field periods around the torus is $p = \bar{p}\varepsilon^{-2/3}$, where $\bar{p} \sim 0(1)$. These choices ensure that the vacuum rotational transform is of order unity, and that the toroidal and helical modulations of the field strength are of similar magnitude [10].

We make use of scaled variables $\rho = r/a$, (a being some convenient minor radius) and $\bar{s} = p\xi = \bar{p}\varepsilon^{-2/3}\xi$, and we define normalised magnetic field pressure and current density,

$$\vec{b} = \vec{B}/B_o \quad , \qquad \hat{P} = P/B_o^2 \quad , \quad \vec{J} = \vec{j}\, ga/B_o \quad ,$$

where $g = 1 - \varepsilon\rho\cos\theta$. Then with $\hat{\nabla} = ag\nabla$, the M.H.D. equilibrium equations become

$$\hat{\nabla}\hat{P} = \vec{J} \times \vec{b} \quad \text{(i)}; \qquad \vec{J} = \hat{\nabla} \times \vec{b} \quad \text{(ii)}; \quad \hat{\nabla} \cdot \vec{b} = 0 \quad \text{(iii)}. \qquad (1)$$

The various quantities are now expanded in powers of $\lambda = \varepsilon^{1/3}$;

$$\hat{P} = \lambda^6 P + \ldots ; \qquad \vec{J} = \lambda^3 \vec{J}^{(3)} + \ldots ; \quad \vec{b} = \hat{\xi} + \lambda^2 \vec{b}^{(2)} + \ldots$$

where P now denotes the leading order normalised pressure.

Thus $\beta \sim 0(\varepsilon^2)$, and the plasma current gives rise to rotational transform of order unity, as do the vacuum fields.

It proves instructive to write the plasma current in the form

$$\vec{J} = g\,h\,\vec{b} + \frac{\vec{b} \times \hat{\nabla}\hat{P}}{\vec{b}^2} \qquad (2)$$

so that

$$g\,\vec{b} \cdot \hat{\nabla} h = - (\vec{b} \times \hat{\nabla}\hat{P}) \cdot \hat{\nabla}\left(\frac{1}{\vec{b}^2}\right) \quad . \qquad (3)$$

We divide the force-free current h into parts, representing the

Pfirsch-Schlüter current by h_p, and denoting by h_c the remaining part which contains any mean toroidal current. Then

$$g\vec{b}\cdot\hat{\nabla}h_p = -(\vec{b}\times\hat{\nabla}P)\cdot\hat{\nabla}\left(\frac{1}{\vec{b}^2}\right) \tag{4}$$

and

$$g\vec{b}\cdot\hat{\nabla}h_c = 0 \quad . \tag{5}$$

With our ordering, this results in

$$h = \lambda^3 h_c^{(3)} + \lambda^4 h_c^{(4)} + \lambda^5 h_c^{(5)} + \lambda^6 h_c^{(6)} + \lambda^6 h_p^{(6)} + \ldots .$$

2. EQUILIBRIUM CALCULATION

The exact solution of Laplace's equation in toroidal coordinates may be expanded in our quasi-cylindrical coordinates, using the ordering $p = \bar{p}\varepsilon^{-2/3}$; the result, for one harmonic, is

$$V_n^p = B_{p,n}(\varepsilon\rho)^n \left\{\cos(n\theta+\bar{s}) + \frac{\bar{p}^2\varepsilon^{2/3}\rho^2}{4(n+1)}\cos(n\theta+\bar{s})\right.$$

$$+ \frac{\varepsilon\rho}{4}\left\{(2n+1)\cos([n+1]\theta+\bar{s}) + \cos([n-1]\theta+\bar{s})\right\}$$

$$+ \frac{\bar{p}^4\varepsilon^{4/3}\rho^4}{32(n+1)(n+2)}\cos(n\theta+\bar{s}) + \frac{\bar{p}^2\varepsilon^{5/3}\rho^3}{16(n+1)}\left\{(2n+3)\cos([n+1]\theta+\bar{s})\right.$$

$$\left.\left. + 3\cos([n-1]\theta+\bar{s})\right\}\right\} + O(\varepsilon^{n+2}) \quad . \tag{6}$$

In order to describe a stellarator with an $n = \ell$ winding which is slightly modulated, for instance in order to create a magnetic well or to 'centre' the separatrix with respect to the windings, we add in small amounts of $\ell = n \pm 1$,

$$V_{n+1}^p = B_{p,n}\left[\frac{\gamma}{4} - \frac{(2n+1)}{4}\right](\varepsilon\rho)^{n+1}\left\{\cos([n+1]\theta+\bar{s})\right.$$

$$\left. + \frac{\bar{p}^2\varepsilon^{2/3}\rho^2}{4(n+2)}\cos([n+1]\theta+\bar{s})\right\} \tag{7}$$

and

$$V^{p}_{n-1} = B_{p,n}\,\frac{\delta}{4}\,\varepsilon^{2}\,(\varepsilon\rho)^{n-1}\left\{\cos\left([n-1]\theta+\bar{s}\right) + \frac{\bar{p}^{2}\varepsilon^{2/3}\rho^{2}}{4n}\cos\left([n-1]\theta+\bar{s}\right)\right\} \quad . \tag{8}$$

We set $B_{p,n} = \varepsilon^{(2/3\,-n)}\,\alpha\,B_{o}a$, where α is determined by the currents flowing in the helical windings, and leave γ , δ as free parameters.

Suppose that the coils are wound on the surface $\rho = \rho_{c}$;

$$\left.\frac{d\phi}{d\theta}\right|_{coil} = \left.\frac{\varepsilon\rho_{c}j_{\phi}}{j_{\theta}}\right|_{\rho=\rho_{c}} = -\left.\frac{\varepsilon\rho_{c}b_{\theta}}{b_{\phi}}\right|_{\rho=\rho_{c}} \quad , \text{ where } b_{\theta,\phi}\ (j_{\theta,\phi})$$

correspond to the helical winding fields (currents) only.

We wish to describe a winding law $\frac{d\phi}{d\theta} \sim (1 + \varepsilon\Omega\cos\theta)$. From Eqs. (6), (7) and (8) with the above description of α ,

$$b_{\theta} \sim \sin\left(n\theta+\bar{s}\right) + \frac{\varepsilon\rho_{c}}{4n}\left\{\gamma(n+1)\sin\left([n+1]\theta+\bar{s}\right) + \frac{\delta}{\rho_{c}^{2}}(n-1)\sin\left([n-1]\theta+\bar{s}\right)\right\}$$

$$b_{\phi} \sim \sin\left(n\theta+\bar{s}\right) + \frac{\varepsilon\rho_{c}}{4}\left\{\gamma\sin\left([n+1]\theta+\bar{s}\right) + \frac{\delta}{\rho_{c}^{2}}\sin\left([n-1]\theta+\bar{s}\right)\right\}.$$

Hence, in general

$$\frac{d\phi}{d\theta} \sim \left(1 + \frac{\varepsilon\rho_{c}}{4n\sin\left(n\theta+\bar{s}\right)}\left\{\gamma\sin\left([n+1]\theta+\bar{s}\right) - \frac{\delta}{\rho_{c}^{2}}\sin\left([n-1]\theta+\bar{s}\right)\right\} + O(\varepsilon^{2})\right),$$

but if $\gamma = -\frac{\delta}{\rho_{c}^{2}}$, then $\frac{d\phi}{d\theta} \sim \left(1 + \frac{\varepsilon\gamma\rho_{c}}{2n}\cos\theta\right)$.

Thus a winding law of the desired form is represented by choosing $\gamma = \frac{2n\Omega}{\rho_{c}}$ and $\delta = -2n\rho_{c}\Omega$. Of course, a field with the same properties could also be generated by means of appropriately shaped modular coils.

The equilibrium fields are found by solving (1,i - iii) order by order in λ , up to 10th order, and details of the method are given in [9] for $\ell = 3$. We present here the results of this calculation, and comment briefly on the structure of the fields.

The full set of fields is:

$$b_\rho = \lambda^2 \frac{n\alpha\rho^{n-1}}{\bar{p}} \cos(n\theta+\bar{s}) + \lambda^4\left\{\bar{p}\alpha\rho^{n+1}\frac{(n+2)}{4(n+1)} + U(\rho)\right\}\cos(n\theta+\bar{s})$$

$$+ \lambda^5\left\{\frac{\alpha}{4\bar{p}}\left[\left(\rho^n(n+1)+\delta\rho^{n-2}(n-1)\right)\cos([n-1]\theta+\bar{s}) + \gamma\rho^n(n+1)\cos([n+1]\theta+\bar{s})\right]\right.$$

$$\left. + V(\rho)\sin 2(n\theta+\bar{s})\right\}$$

$$+ \lambda^6\left\{A(\rho)\sin\theta + \left(f(\rho) + \frac{\bar{p}^3\alpha(n+4)\rho^{n+3}}{32(n+1)(n+2)}\right)\cos(n\theta+\bar{s}) + W(\rho)\cos 3(n\theta+\bar{s})\right\}$$

$$b_\theta = -\lambda^2\frac{n\alpha\rho^{n-1}}{\bar{p}}\sin(n\theta+\bar{s}) + \lambda^3 b(\rho) - \lambda^4\left\{\bar{p}\alpha\rho^{n+1}\frac{n}{4(n+1)} + \frac{1}{n}\frac{d}{d\rho}(\rho U(\rho))\right\}\sin(n\theta+\bar{s})$$

$$- \lambda^5\left\{\frac{\alpha}{4\bar{p}}\left[\left(\rho^n+\delta\rho^{n-2}\right)(n-1)\sin([n-1]\theta+\bar{s}) + \gamma\rho^n(n+1)\sin([n+1]\theta+\bar{s})\right]\right.$$

$$\left. - \frac{1}{2n}\frac{d}{d\rho}(\rho V(\rho))\cos 2(n\theta+\bar{s})\right\}$$

$$+ \lambda^6\left\{B(\rho)\cos\theta + \left(g(\rho) - \frac{\bar{p}^3\alpha n\rho^{n+3}}{32(n+1)(n+2)}\right)\sin(n\theta+\bar{s}) - \frac{1}{3n}\frac{d}{d\rho}(\rho W(\rho))\sin 3(n\theta+\bar{s})\right\}$$

$$b_\xi = 1 + \lambda^3(\rho\cos\theta - \alpha\rho^n\sin(n\theta+\bar{s}))$$

$$- \lambda^5\left\{\frac{\alpha\bar{p}^2\rho^{n+2}}{4(n+1)} + \frac{\bar{p}\rho}{n^2}\frac{d}{d\rho}(\rho U(\rho)) - \frac{\alpha\rho^n\sigma(\rho)}{\bar{p}}\right\}\sin(n\theta+\bar{s})$$

$$+ \lambda^6\left\{\rho^2\cos^2\theta + \left[\frac{\bar{p}}{n}\frac{d}{d\rho}(\rho V(\rho)) + \left(\frac{n\alpha\rho^{n-1}}{\bar{p}}\right)^2\frac{\sigma'(\rho)}{2\bar{p}}\right]\frac{\rho}{2n}\cos 2(n\theta+\bar{s}) + b_\beta(\rho)\right.$$

$$\left. - \frac{\alpha}{4}\left((2+\gamma)\rho^{n+1}\sin([n+1]\theta+\bar{s}) + (3\rho^{n+1}+2\delta\rho^{n-1})\sin([n-1]\theta+\bar{s})\right)\right\} . \qquad (9)$$

The poloidal field component $\lambda^3 b(\rho)$ is produced by the mean toroidal current density $\sigma(\rho)$, the remaining functions of radius in Eq. (9) being defined in the appendix.

We solve $\vec{b}.\hat{\nabla}\psi = 0$, as discussed in [9], for the fields (9), and find the expression for ψ :

$$\psi = \psi_o(\rho) - \lambda \frac{n\alpha\rho^{n-1}}{\bar{p}^2} \sin(n\theta+\bar{s})\psi' - \lambda^2\left(\frac{n\alpha\rho^n}{2\bar{p}^2}\right)^2 \frac{1}{\rho}\frac{d}{d\rho}\left(\frac{\psi_o'}{\rho}\right) \cos 2(n\theta+\bar{s})$$

$$+ \lambda^3\left\{ \rho\frac{\psi_o'}{b^*} \cos\theta \left[A(\rho) + \alpha^2\rho^2(n-1)\frac{n}{4\bar{p}^3}\left(5n + (n+1)\gamma + \frac{(n-1)\delta}{\rho^2}\right)\right]\right.$$

$$\left. + \pi_1(\rho)\sin(n\theta+\bar{s}) + \pi_2(\rho)\sin 3(n\theta+\bar{s})\right\} + O(\lambda^4) \qquad (10)$$

where $\pi_1(\rho)$ and $\pi_2(\rho)$ are given in the appendix, and

$$b^* = b(\rho) - \frac{n^2(n-1)\alpha^2}{\bar{p}^3}\rho^{2n-3}.$$

Substituting $\sigma(\rho)$ for $\psi_o(\rho)$ we obtain an expression for h_c ; from (4) we find $h_p^{(6)} = 2\rho\frac{dP}{d\rho}\cos\theta / b^*$ and so the expressions for the fields, given in the appendix, may be understood by means of (1ii), (1iii) and (2).

3. EQUILIBRIUM QUANTITIES

The rotational transform is found, from the method of averaging [13], to be

$$i = \frac{b^*}{\rho} = \frac{b(\rho)}{\rho} + i_{vac}$$

$$i_{vac} = -\frac{n^2(n-1)\alpha^2}{\bar{p}^3}\rho^{2n-4}. \qquad (11)$$

Having defined $f = \int_0^\rho b^*(\rho)\, d\rho$, we locate the magnetic axis by rewriting (10) as

$$\psi = \psi_o \left(f + \lambda^3 \rho \cos\theta \left\{ A(\rho) + \alpha^2 \rho^{2(n-1)} \frac{n}{4\bar{p}^3} \left(5n + (n+1)\gamma + \frac{(n-1)\delta}{\rho^2} \right) \right\} \right) \tag{12}$$

where we have omitted helical terms, (valid for $n > 1$), and finding the point where $\nabla\psi = 0$.

To the required accuracy, its coordinates are (ρ_x, π) , where

$$b^*(\rho_x) = \lambda^3 \frac{d}{d\rho} (\rho A(\rho)) \Big|_{\rho=\rho_x} + \lambda^3 \frac{(2n-3)}{4n} \delta i_{vac} \quad . \tag{13}$$

The last term is only necessary for $\ell = 2$, where all the surfaces are shifted by this small amount; we neglect it henceforth.

If we also define $\Delta(\rho) = \frac{\rho A(\rho)}{b^*}$, then provided $\Delta(o) \sim 0(1)$, (13) becomes

$$b^*(\rho_x - \lambda^3 \Delta(\rho)) = 0 \quad . \tag{14}$$

The solution is then $\rho_x = \lambda^3 \Delta(o)$, to lowest order. In terms of $\Delta(\rho)$, Eq. (Ax) becomes

$$b^{*2}\Delta'' + b^*(2b^{*\prime} + \frac{b^*}{\rho})\,\Delta' + b^*\Delta \frac{d}{d\rho}\left(\frac{1}{\rho}\frac{d}{d\rho}(\rho b_o)\right)$$

$$= 2\rho P' - b^* b + \alpha^2 \rho^{2(n-1)} \frac{n}{4\bar{p}^3} \sigma' \left(5n + (n+1)\gamma + \frac{(n-1)\delta}{\rho^2} \right) \tag{15}$$

with

$$b_o = - \frac{n^2(n-1)\alpha^2}{\bar{p}^3} \rho^{2n-3} \quad ,$$

which is the toroidal shift equation [14], in the limit $\alpha = 0$, $\lambda^3\Delta(o)$ being the axis shift. A first integral of Eq. (15) can be obtained when $\ell = 2$, which reduces to the well-known result for

tokamaks [14] when $\alpha = 0$.

Use of $\Delta(\rho)$ is not always appropriate; for instance, if $\sigma = 0$ and $A_{(o)} \neq 0$, $\rho_x = \varepsilon^{1/(2n-3)} \left| \frac{A_o \bar{p}^3}{n^2(n-1)\alpha^2} \right|^{1/(2n-3)}$

(Note, however, that for $\ell = 2$, $\Delta(\rho)$ is always appropriate).

For "tokamak-like" configurations, where $\Delta(\rho)$ can be used, (for $\sigma \neq 0$, or for $\ell = 2$), we invert (10), to obtain

$$\rho(\psi,\theta,\bar{s}) = \rho_o(\psi) + \lambda \frac{n\alpha\rho_o^{n-1}}{\bar{p}^2} \sin(n\theta+\bar{s}) + \lambda^2 \left(\frac{n\alpha\rho_o^{n-1}}{\bar{p}^2}\right)^2 \frac{(2n-1)}{2\rho_o} \sin^2(n\theta+\bar{s})$$

$$+ \lambda^3 \Bigg[- \left[\Delta(\rho_o) + \frac{\alpha^2\rho_o^{2(n-1)}n}{b^*(\rho_o)4\bar{p}^3}\left(5n + (n+1)\gamma + \frac{(n-1)\delta}{\rho_o^2}\right)\right]\cos\theta$$

$$+ \left(\frac{U(\rho_o)}{\bar{p}} - \frac{n^2\alpha\rho_o^{n-2}}{\bar{p}^3} b(\rho_o)\right) \sin(n\theta+\bar{s}) + \cdots \Bigg] \qquad (16)$$

where we have omitted those vacuum terms from order λ^3 which are of order i_{vac} or smaller.

In [9] it is shown how the 'virtual casing principle' is used when applying the boundary condition at infinity. This determines the external vertical field, which is given by

$$B_v = \frac{\varepsilon^2 B_o}{2} \Bigg\{ A(\rho) + \frac{d}{d\rho}(\rho A(\rho)) + b(\rho)\left(\frac{3}{2} + \ell n\left(\frac{\varepsilon\rho}{8}\right)\right)$$

$$- \frac{\rho\sigma(\rho)}{b^*}\left[A(\rho) + \frac{\alpha^2\rho^{2(n-1)}n}{4\bar{p}^3}\left(5n+(n+1)\gamma + \frac{(n-1)\delta}{\rho^2}\right)\right]\Bigg\}_{\rho=\rho_b} \qquad (17)$$

(ρ_b is the lowest-order radius of a (closed) surface, outside the plasma). When $\alpha = 0$, this also reduces to the tokamak result, [14].

When $\sigma = 0$ Eq.(Ax) gives $- \frac{2\bar{p}^3\rho^{2(3-n)}}{n^2(n-1)\alpha^2} \frac{dP}{d\rho} = \frac{d}{d\rho}\left(\rho^3 \frac{dA}{d\rho}\right)$; using $P \equiv P(f)$, we choose $P = P_o\left(1 - (\rho/\rho_a)^{2(n-1)}\right)$, and find

$A(\rho) = A_o - \frac{P_o}{i_a}\frac{(n-1)}{2}\left(\frac{\rho}{\rho_a}\right)^2$, where ρ_a is the plasma boundary radius, and i_a is the rotational transform at ρ_a .

Finally, (17) becomes

$$B_v = \frac{\varepsilon^2 B_o}{2}\left\{A(\rho) + \frac{d}{d\rho}\,(\rho A(\rho))\right\}_{\rho=\rho_b} ,$$

so

$$\frac{B_v}{\varepsilon^2 B_o} = A_o - \frac{P_o(n-1)}{i_a} .$$

Specific equilibrium surfaces were computed in [9] for the parameters of CLEO stellarator ($\ell = 3$) using Eq. (10). It was found that although equilibrium could be maintained by the helical fields alone, it is desirable to apply a suitably chosen vertical field in order to reduce the distortion and destruction of flux surfaces induced by the plasma pressure.

Since the rotational transform is constant across the minor cross-section in $\ell = 2$ stellarators, we would expect that the flux surfaces are less sensitive to the effects of finite pressure than is the case for $\ell = 3$ where the transform in the centre is small. For the case of $\ell = 2$, we have calculated equilibria with $\beta \sim 1 - 2\%$ for the parameters of WVII [3]. Typical results for current-free plasmas are depicted in Figs. 2 and 3, where we see that despite the absence of a vertical field the loss of confined plasma volume remains small with increase of pressure. It is interesting to note that in these calculations we observe a spiralling of the magnetic axis about the lowest-order position given by the planar shift $\lambda^3\Delta(0)$. By including the higher order corrections in determining ρ_x , we find

$$\rho_x \simeq \lambda^3\Delta(0)\left(1 - \frac{4\alpha\lambda}{\bar{p}^2}\sin\bar{s}\right) .$$

Since $\lambda \simeq \frac{1}{2}$, the spiral amplitude is about 50% of the lowest-order shift in agreement with the numerical results.

4. STABILITY

In order to determine whether a plasma equilibrium is stable or not, it is necessary to begin by studying the possible ideal M.H.D. instabilities; if the system proves stable to these, it is possible to proceed to investigate the influence of non-ideal effects, and particularly of resistivity, to see if they allow instability.

In a stellarator without a net longitudinal current, the expected ideal M.H.D. instabilities are localised pressure-driven modes. The Mercier criterion [15], written in terms of surface-averaged quantities, determines the stability of modes which are localised radially but not azimuthally, i.e. interchange-like. Ballooning modes [16], however, are able to localise azimuthally in regions of 'unfavourable curvature', when the plasma pressure is sufficiently high. Since the equilibria under discussion have low $\beta \sim \varepsilon^2$, the pressure-driven modes can exhibit ballooning character only in regions of locally enhanced pressure gradient [16]. In the absence of such steep gradients therefore, the ideal pressure-driven modes are interchanges and so their stability in the limit of large mode number is determined by the Mercier criterion.

Given stability to modes capable of growing on the ideal time-scale, it is then appropriate to test for stability to non-ideal modes.

Criteria for stability against resistive interchanges are given in [11], [12] and [17] although that in [17] results from the other two only when the poloidal "β" is small. In [12] it is shown that the resistive criterion derived is always more stringent than the Mercier criterion, and so it will be adequate for our purposes to evaluate the

resistive criterion. Further, in the large aspect-ratio, large toroidal field case, the results given in [11] and [12] can be shown to be equivalent, and for our purposes the more convenient is that given in [11]:

$$W^{(o)} - A_2 > 0 \tag{18}$$

for stability against resistive interchanges.

$$W^{(o)} = \frac{1}{\phi'^2}\,(P'V'' + I'\chi'' - J'\phi'') - \frac{1}{\phi'^2}\,(\phi'\chi'' - \chi'\phi'')\,\langle\omega\rangle$$

$$- \left(\frac{2\pi P'}{\phi'}\right)^2 \left\langle \frac{\sqrt{g}}{\vec{B}^2} \right\rangle \quad ,$$

$$A_2 = \left(\frac{2\pi}{\phi'}\right)^2 \quad \left\langle \tilde{\omega}^2 \sqrt{g}\, \frac{\vec{B}^2}{g^{II}} \right\rangle$$

$\phi(\chi)$ and $I(J)$ are the longitudinal (transverse) magnetic and current fluxes. $\omega = \frac{\vec{J}.\vec{B}}{\vec{B}^2}$. $\langle x \rangle$ is the average of x over a flux-surface, and $\tilde{x} = x - \langle x \rangle$. The g^{ik} are the metric coefficients of the flux-coordinate system employed, in which current and field lines are straight: $x^1 \equiv a$, the radial coordinate, and $' \equiv \frac{d}{da}$.

In [17], (replacing averages over closed field-lines by surface averages), we have an expression for V** :

$$V^{**} = V'' + \frac{I'\chi'' - J'\phi''}{P'} - \frac{(\phi'\chi'' - \chi'\phi'')}{P'} \quad \frac{\langle \omega \vec{B}^2 \rangle}{\langle \vec{B}^2 \rangle}$$

$$- P' \left\langle (\vec{B}^2)^{-1} \right\rangle$$

where $'$ denotes the derivative taken with respect to some flux surface coordinate. For convenience we shall take this to be the toroidal flux ϕ.

When the main toroidal field is large, $\frac{\langle \omega \vec{B}^2 \rangle}{\langle \vec{B}^2 \rangle} \simeq \langle \omega \rangle$, and allowing for the fact that $\sqrt{g} \approx aR(1 + O(a/R))$ in [11], we see that

$W^{(o)} = \frac{dP}{da} \cdot V^{**} = P' 2\pi a B_\xi V^{**}$. Thus $W^{(o)} - A_2 > 0$ is equivalent to a modified form of the V^{**} criterion:

$$V^{**} - \frac{1}{P' 2\pi a B_\xi} \quad A_2 < 0 . \tag{19}$$

We may write this last expression in terms of our dimensionless variables by introducing the following dimensionless equivalents of the quantities above:

If $[x] = \int_o^{2\pi} d\theta \int_o^{2\pi} d\bar{s} \int_o^{\rho(\psi, \theta, \bar{s})} x\rho(1 - \varepsilon\rho \cos\theta) d\rho$, then $V = [1]$, $U = [\vec{b}^2]$, $L = [(\vec{b}^2)^{-1}]$ and $\hat{\phi} = \frac{1}{2\pi}[b_\xi / (1 - \varepsilon\rho \cos\theta)]$, $' \equiv \frac{d}{d\hat{\phi}}$.

Henceforth we work in terms of these quantities (and drop the $\hat{}$ on $\hat{\phi}$).

If we put

$$V^{**} = V'' - \frac{V'}{U'} U'' - P'V' \left(\frac{V'}{U'} + \frac{L'}{V'} \right),$$

then taking the leading order forms of $\sqrt{g}$, g^{11}, in A_2 we find the criterion

$$V^{**} - 4\pi \hat{P}' q^2 < 0 , \tag{20}$$

with $q = \rho / b^*$.

With the present ordering, V', U' and L' are all $\sim 2\pi + O(\varepsilon^{4/3})$; so $V^{**} = V'' - U'' - 4\pi\hat{P}'$ to the required accuracy, which proves to be a convenient form, as $V-U = 2[1 - b] - [(b-1)^2]$, where $b = |\vec{b}|$.

The first part of this expression contains the destabilising magnetic hill term associated with the geodesic curvature of the stellarator field and the second contains stabilising terms arising from favourable average curvature. However the ordering is non-optimal with respect to the stability criterion, so that whereas the

magnetic hill is $0(\varepsilon^{4/3})$, the curvature terms are $0(\varepsilon^2)$.

Higher order terms in general represent only corrections to those already described, although in the interesting special case of a current-free $\ell = 2$ stellarator we shall see that pressure-dependent effects cancel exactly in $0(\varepsilon^2)$ so that finite pressure terms are recovered only at $0(\varepsilon^{8/3})$. In this case we shall assume that $\beta_p = 8\pi P/(\varepsilon B_o i)^2$ is sufficiently small for the contribution of this term to be neglected.

For "tokamak-like" configurations, (16) can be rewritten in terms of coordinates (ρ', θ', ξ) centred on the magnetic axis by replacing $\Delta(\rho_o)$ by $\Delta'(\rho_o) = \Delta(\rho_o) - \Delta(o)$, and writing ρ' for ρ and θ' for θ . We shall work in terms of these coordinates throughout the rest of this section, although dropping the primes on ρ', θ' and Δ' .

Let us consider the terms in V-U ; the second, $[(b-1)^2]$, is easily evaluated, and to lowest order is

$$\left[\varepsilon^2 \left(\rho \cos\theta - \alpha\rho^n \sin\left(n\theta+\bar{s}\right)\right)^2\right]^{\sim} + 0\left(\varepsilon^{7/3}\right)$$

$$= \pi^2\varepsilon^2 \left(\frac{\rho_o^4}{2} + \frac{\alpha^2 \rho_o^{2(n+1)}}{(n+1)}\right) + 0(\varepsilon^{7/3})$$

$[(1-b)]$ is less useful than $[(1-b)]'$, which is also simpler to evaluate, being given by

$$[(1-b)]' = \int_0^{2\pi} d\theta \int_0^{2\pi} d\bar{s}\, \frac{1}{2} \frac{d\rho^2}{d\phi} (1-\varepsilon\rho\cos\theta)(1-b) ,$$

where $\rho = \rho(\psi, \theta, \bar{s})$.

To evaluate this latter we need b and $\frac{d\rho^2}{d\phi}$;

$$b = \left(b_\xi^2 + b_\rho^2 + b_\theta^2\right)^{1/2} = b_\xi + \frac{1}{2}\left(b_\rho^2 + b_\theta^2\right) + 0\left(\varepsilon^{7/3}\right)$$

and so

$$- \left(1-\varepsilon\rho\cos\theta\right)\left(1-\bar{b}\right) = \frac{1}{2}\left(b_\rho^{\,2} + b_\theta^{\,2}\right)$$

$$+ \varepsilon\left(\rho\cos\theta - \alpha\rho^n \sin\left(n\theta+\bar{s}\right)\right) + \varepsilon^{5/3}\, b_\xi^{(5)} \sin\left(n\theta+\bar{s}\right)$$

$$+ \varepsilon^2 \left\{ b_\beta + - - - - \right\}$$

omitting periodic terms, which, on averaging, will vanish to this order.

$$b_\rho^{\,2} + b_\theta^{\,2} = \varepsilon^{4/3}\, \frac{n^2\alpha^2\rho_o^{\,2(n-1)}}{\bar{p}^2}\left[1 + \varepsilon^{1/3}\, \frac{2n\alpha\rho_o^{\,2(n-2)}}{\bar{p}^2} \sin\left(n\theta+\bar{s}\right) + O\left(\varepsilon^{2/3}\alpha^2\right)\right]$$

We find ϕ, from its definition, to be

$$\phi = \pi\left(\rho_o^{\,2} + \varepsilon^{2/3}\, \frac{n^3\alpha^2}{\bar{p}^4}\, \rho_o^{\,2(n-1)}\right) + O\left(\varepsilon^{4/3}\right)$$

and, consequently,

$$\frac{d\rho^2}{d\phi} = \frac{1}{\pi}\left(1 + \varepsilon^{1/3}\, n^2\, \frac{\alpha}{\bar{p}^2}\, \rho_o^{\,n-2} \sin\left(n\theta+\bar{s}\right) - \varepsilon^{2/3}\, n^3\, \frac{(n-1)}{\bar{p}^4}\, \alpha^2\rho_o^{\,2(n-2)} \cos 2\left(n\theta+\bar{s}\right)\right.$$

$$\left. - \frac{\varepsilon\cos\theta}{\rho_o}\, \frac{\partial}{\partial\rho_o}\left[\frac{\rho_o^{\,2}}{b^*(\rho_o)}\left(A(\rho_o) + \frac{n\alpha^2\rho_o^{\,2(n-1)}}{4\bar{p}^3}\left[5n + (n+1)\gamma + \frac{(n-1)\delta}{\rho_o^{\,2}}\right]\right)\right]\right)$$

$$+ O\left(\varepsilon\alpha^2\right) .$$

Finally, integrating the product in the expression for $[1-b]'$, we obtain our criterion in the form

$$\frac{d}{d\phi} D - \varepsilon^2 4\pi\, \frac{dP}{d\phi}\, q^2 < 0 \quad , \tag{21}$$

where

$$D = \varepsilon^{4/3} 2\pi \frac{n^2\alpha^2}{\bar{p}^2} \rho_o^{2(n-1)}$$

$$+ \varepsilon^2 2\pi \left(-\frac{\rho_o^2}{2} + 2 \int_o^{\rho_o} b(\rho)\sigma(\rho)d\rho - b^2(\rho_o) \right.$$

$$\left. + \frac{1}{\rho_o} \frac{d}{d\rho_o} \left[\rho_o^2 \Delta(\rho_o) + \frac{\alpha^2 \rho_o^{2(n+1)}}{b^*(\rho_o) 4\bar{p}^3} \left(5n + (n+1)\gamma + \frac{(n-1)\delta}{\rho_o^2} \right) \right] \right)$$

$$+ \quad - - -$$

In obtaining this result we neglect the contribution in $0(\varepsilon^2)$ of terms proportional to i_{vac}, some of which represent corrections to the leading order magnetic hill, since they are expected to be small.

Thus,

$$\frac{dD}{d\phi} - 4\pi\varepsilon^2 q^2 \frac{dP}{d\phi} = \varepsilon^{4/3} 2n^2 (n-1) \frac{\alpha^2}{\bar{p}^2} \rho_o^{2(n-2)}$$

$$+ \varepsilon^2 \left(-1 + 2\left(\frac{b(\rho_o)}{\rho_o} \right) + \left[\Delta'' + \frac{3\Delta'}{\rho_o} - \frac{2\rho_o P'}{b^{*2}} \right] + \frac{1}{\rho_o} \frac{d}{d\rho_o} \frac{1}{\rho_o} \frac{d}{d\rho_o} \Omega(\rho_o) \right) \quad (22)$$

where

$$\Omega(\rho_o) = \frac{n\alpha^2 \rho_o^{2n}}{4\bar{p}^2} q \left[5n + (n+1)\gamma + \frac{(n-1)\delta}{\rho_o^2} \right] ,$$

and

$$q = \frac{\rho_o}{b^*(\rho_o)}$$

$\left(\Delta'' + \frac{3\Delta'}{\rho_o} - \frac{2\rho_o P'}{b^{*2}} \right)$ can be found from Eq. (15); using $\frac{q'}{q} = \left(\frac{1}{\rho} - \frac{b^{*\prime}}{b^*} \right)$

we have

$$\Delta'' + \frac{3\Delta'}{\rho_o} - \frac{2\rho_o P'}{b^{*2}} = -\frac{b}{b^*} + \frac{\sigma'}{\rho_o^2 b^*}\,\Omega(\rho_o) + 2\Delta'\,\frac{q'}{q} - \frac{\Delta}{b^*}\,\frac{d}{d\rho_o}\,\frac{1}{\rho_o}\,\frac{d}{d\rho_o}\,(\rho_o b_o)$$

and for $\ell = 2$ we are able to integrate this to give

$$\Delta' = \frac{1}{\rho_o b^{*2}} \int_o^{\rho_o} \left[2\rho P' - b^* b + \frac{\sigma'}{\rho^2}\, b^* \Omega(\rho) \right] \rho d\rho \quad ,$$

as the term in Δ vanishes.

From Eq. (22) we see that for the general $\ell = 2$ stellarator, negative shear ($q'/q > 0$) is stabilising, as has been shown for tokamaks [11]; however in the absence of an axial current, the shear vanishes for $\ell = 2$, and as noted previously, the pressure dependent terms cancel in $0(\varepsilon^2)$ of the stability criterion (21), which then yields

$$\frac{8\alpha^2}{\bar{p}^2}\,\varepsilon^{4/3} - (11 + 3\gamma)\,\varepsilon^2 = \varepsilon^2 \left(2p\,|i_{vac}| - (11 + 3\gamma) \right) < 0 \,. \qquad (23)$$

The first term arises from the destabilising "magnetic hill" generated by the stellarator field, while the remaining stabilising term results from the effects of toroidal curvature. Since the flux-surface ellipticity $\eta = \frac{4\alpha\lambda}{\bar{p}^2}$, this result coincides in the limit of low β_p with the ideal M.H.D. criterion (67) given in ref. [18] which was obtained by means of an expansion in radius. The pressure dependent term in $0(\varepsilon^{8/3})$, omitted from (23) is found in ref. [18] to be destabilising and is given by $\varepsilon^2 P'(\rho)\,\frac{i_{vac}\beta_p}{2\pi p}$. Thus, provided $\beta_p \leq 1$ this term is indeed negligible in (23). It is interesting to note that the already substantial margin of stability obtained with a pure $\ell = 2$ winding ($\gamma = 0$) can be enlarged significantly by an appropriately phased poloidal modulation ($\gamma > 0$) of the ℓ-winding pitch, as discussed in section 2.

In the case of current-free stellarators with $\ell \geq 3$ the axis

shift can be large and this prevents us from using the above analysis which assumes $\rho_x \sim 0(\varepsilon)$. However, in the special case where $A_o = 0$, corresponding to a particular choice of vertical field, this assumption remains valid and then for $\ell = 3$ stellarators (without coil modulation) we find the criterion

$$2pi_{vac}(\rho) - 6 - \frac{2}{\rho}\frac{P'(\rho)}{i^2_{vac}(\rho)} < 0 \qquad (24)$$

showing that finite pressure is destabilising, especially near the axis. In the limit of vanishing pressure the criterion reduces to $V^{**} < 0$, which has been discussed previously in [10], although we find the stabilising term to be somewhat larger. A comparison of (23) and (24) thus suggests that $\ell = 2$ stellarators without plasma current are more stable to resistive interchanges than their $\ell = 3$ counterparts, but this neglects the well-deepening to be expected with a larger axis shift [19] and to examine this in general it would be necessary to evaluate criterion (20) for equilibria with $A_o \neq 0$. A numerical approach to this question should be possible, but lies outside the scope of the present investigation.

5. DISCUSSION

Although numerous variants of the stellarator concept have been proposed, the engineering problems of designing, constructing and maintaining a device of reactor size impose strict constraints which virtually exclude the more complex systems. As is the case with tokamak reactor designs, cost and output power considerations lead to low aspect ratio, and the many problems associated with conventional ℓ-windings have led to several proposals for the use of coils with a modular construction [5,6]. The solution proposed by Wobig and

Rehker [5] to this problem is particularly attractive in that a single set of coils, which could be individually demountable for maintenance, would provide both the toroidal and helical equilibrium fields, and leave adequate access for neutral injection or R.F. heating, and so on.

The choice of ℓ-number in the stellarator field is effectively limited to $\ell = 2$ or $\ell = 3$ by the difficulty of achieving satisfactory rotational transform in a low aspect ratio device by means of coils which necessarily must be separated from the vacuum vessel by a substantial thickness of blanket material. Since high rotational transform in the centre of the plasma as well as at the edge is desirable to ensure good confinement of energetic ions, $\ell = 2$ would appear to be preferable, and as the equilibrium calculations in section 3 have shown, the $\ell = 2$ flux surfaces are not sensitive to finite plasma pressure, obviating the need for a vertical field system, which would be desirable for an $\ell = 3$ stellarator [9], and essential in a tokamak. Although the detrimental effect of the stellarator "magnetic hill" on interchange stability increases with rotational transform, and tends therefore to be stronger in the centre of an $\ell = 2$ stellarator than in the centre of an $\ell = 3$ device, we have seen that there is nonetheless a substantial margin of stability due to toroidal effects. From the criterion (23) for $\ell = 2$ current-free stellarators we see that if $i_{vac} \sim 0.5$ which is likely to be the situation encountered in practice, then provided the number of winding periods p is not too large, say $p \lesssim 8$, then a sufficient well can be formed and stability against resistive interchanges is possible over a useful range of poloidal beta values. In addition, it has been shown that a modular $\ell = 2$ system exhibits substantial negative shear [5], even in the absence of a plasma

current, which may be beneficial for interchange stability.

6. CONCLUSION

We have studied a general class of low-beta toroidal stellarator equilibria in which plasma pressure and current density profiles may be prescribed arbitrarily as functions of the mean flux surface radius. Between the general stellarator equilibrium and the low-beta tokamak which forms a special case, there is a strong similarity made evident by our calculation. By evaluating the resistive interchange criterion it is seen that notwithstanding the destabilising effect of the magnetic hill a substantial margin of stability is available in $\ell = 2$ stellarators, which if constructed using a modular coil design would appear to be an attractive alternative to the tokamak, especially in view of the possibility of steady-state operation.

Acknowledgement

We should like to acknowledge several useful discussions with R.J. Hastie.

REFERENCES

[1] SHAFRANOV V.D. e.g. 9th. European Conference on Controlled Fusion and Plasma Physics, Oxford 1979, Invited Paper p. 503.

[2] LORTZ D. and NUHRENBERG J., Z. Naturforschung (1976) 31a, 1277.

[3] WVII A-team, Neutral Injection Team, Proc. 8th. Int. Conf. on Plasma Physics and Controlled Nuclear Fusion Research, Brussels, 1980, papers H2-1 and H2-2.

[4] CLEO team, Ibid, papers H1-1 and H1-2.

[5] REHKER S. and WOBIG H., IPP Garching, Report No 2/215 (1973).

[6] HAMBERGER S.M., SHARP L.E. and PETERSON L.F., 9th. European Conf. on Controlled Fusion and Plasma Physics, Oxford 1979, Contributed Paper BP20.

[7] CHODURA R. and SCHLUTER A., IPP Garching, Report No. 1/180 (1980).

[8] BAUER F., BETANCOURT O. and GARABEDIAN P., J. Computational Physics 35 (1980), 341.

[9] FIELDING P.J. and HITCHON W.N.G., Culham Preprint CLM-P605 (1980).

[10] DOBROTT D. and FRIEMAN E.A., Phys. Fluids 14, (1971) 349.

[11] MIKHAILOVSKII A.B., Nucl. Fusion 15 (1975) 95.

[12] GLASSER A.H., GREENE J.M. and JOHNSON J.L., Phys. Fluids 18, (1975) 875.

[13] MOROZOV A.I. and SOLOV'EV L.S., "Reviews of Plasma Physics" 1966, (ed. Leontovich M.A.), vol. 2, Consultants Bureau, New York.

[14] GREENE J.M., JOHNSON J.L. and WEIMER K.E. Phys. Fluids 14, (1971) 671.

[15] GREENE J.M. and JOHNSON J.L., Phys. Fluids 5 (1962) 510.

[16] CONNOR J.W., HASTIE R.J. and TAYLOR J.B., Proc. Roy. Soc. A 365 (1979) 1.

[17] JOHNSON J.L. and GREENE J.M., Plasma Physics 9, (1967) 611.

[18] SHAFRANOV V.D., Nucl. Fusion 8, (1968) 329.

[19] TAYLOR J.B., Phys. Fluids 8 (1965) 1203.

APPENDIX

In stating the expressions for the fields, (7), we have employed the following definitions:

$h_c^{(3)} \equiv h_c^{(3)}(\rho) = \sigma(\rho)$ is the toroidal current, and the associated poloidal field is $b(\rho)$, given by

$$\frac{1}{\rho}\frac{d}{d\rho}(\rho b) = \sigma(\rho) \tag{Ai}$$

$$-\frac{1}{n\rho}\frac{d}{d\rho}\left(\rho\frac{d}{d\rho}(\rho U)\right) + \frac{nU}{\rho} = -\frac{n\alpha\rho^{n-1}}{\bar{p}^2}\sigma' \tag{Aii}$$

$$\frac{1}{2n}\frac{d}{d\rho}\left(\rho\frac{d}{d\rho}(\rho V)\right) - 2nV = -\left(\frac{n\alpha\rho^n}{2\bar{p}^2}\right)^2\frac{d}{d\rho}\left(\frac{\sigma'}{\rho}\right) \tag{Aiii}$$

$$\frac{db_\beta}{d\rho} = -\left(\frac{dP}{d\rho} + b(\rho)\sigma(\rho) + \left\{\left(\frac{n\alpha\rho^{n-1}}{\bar{p}^2}\right)^2\frac{\bar{p}\sigma'}{2}\right\}\right) . \tag{Aiv}$$

If we write

$$\sigma_1(\rho) = \left\{-\frac{\alpha\rho^{n+1}}{4}\frac{(n+2)}{(n+1)} + \frac{n\alpha\rho^{n-2}}{\bar{p}^3}b(\rho) - \frac{U(\rho)}{\bar{p}}\right\}\sigma' - \alpha\rho^n\sigma$$

$$+\left(\frac{n\alpha\rho^{n-1}}{2\bar{p}^2}\right)^3\left[4n\frac{d}{d\rho}\left(\frac{\sigma'}{\rho}\right) + \rho^2\frac{d}{d\rho}\left(\frac{1}{\rho}\frac{d}{d\rho}\left(\frac{\sigma'}{\rho}\right)\right)\right] \tag{Av}$$

and

$$\sigma_2(\rho) = \frac{1}{3}\left(\frac{n\alpha\rho^n}{2\bar{p}^2}\right)^3\frac{1}{\rho}\frac{d}{d\rho}\left(\frac{1}{\rho}\frac{d}{d\rho}\left(\frac{\sigma'}{\rho}\right)\right) \tag{Avi}$$

then

$$\frac{1}{\rho}\frac{d}{d\rho}(\rho g) + \frac{nf}{\rho} = \sigma_1(\rho) \tag{Avii}$$

and

$$\frac{1}{\rho}\frac{d}{d\rho}(\rho f) + \frac{ng}{\rho} = -\left\{\alpha\rho^n\sigma(\rho) - \frac{\bar{p}^2}{n^2}\rho\frac{d}{d\rho}(\rho U)\right\} \tag{Aviii}$$

$$- \frac{1}{3n\rho} \frac{d}{d\rho} \left(\rho \frac{d}{d\rho} (\rho W) \right) + \frac{3n}{\rho} W = \sigma_2 (\rho) \quad . \tag{Aix}$$

Finally,

$$- b^*(\rho A'' + 3A') + \rho A\sigma' + 2\rho P' - b^*b$$

$$+ \frac{n\alpha^2 \rho^{2n-1}}{4\bar{p}^3} \sigma' \left[5n + (n+1)\gamma + \frac{(n-1)\delta}{\rho^2} \right] = 0 \tag{Ax}$$

and

$$\frac{1}{\rho} \frac{d}{d\rho} (\rho A) - \frac{B(\rho)}{\rho} = - b(\rho) \quad . \tag{Axi}$$

The surface function ψ involves two functions as yet unspecified:

$$\pi_1 (\rho) = \left\{ - \frac{\alpha \rho^{n+1}}{4} \frac{(n+2)}{(n+1)} + \frac{n\alpha\rho^{n-2}}{\bar{p}^3} b(\rho) - \frac{u(\rho)}{\bar{p}} \right\} \psi_o'$$

$$+ \left(\frac{n\alpha\rho^{n-1}}{2\bar{p}^2} \right)^3 \left[4n \frac{d}{d\rho} \left(\frac{\psi_o'}{\rho} \right) + \rho^2 \frac{d}{d\rho} \left(\frac{1}{\rho} \frac{d}{d\rho} \left(\frac{\psi_o'}{\rho} \right) \right) \right] \Bigg\} \tag{Axii}$$

and

$$\pi_2 (\rho) = \frac{1}{3} \left(\frac{n\alpha\rho^n}{2\bar{p}^2} \right)^3 \frac{1}{\rho} \frac{d}{d\rho} \left(\frac{1}{\rho} \frac{d}{d\rho} \left(\frac{\psi_o'}{\rho} \right) \right)$$

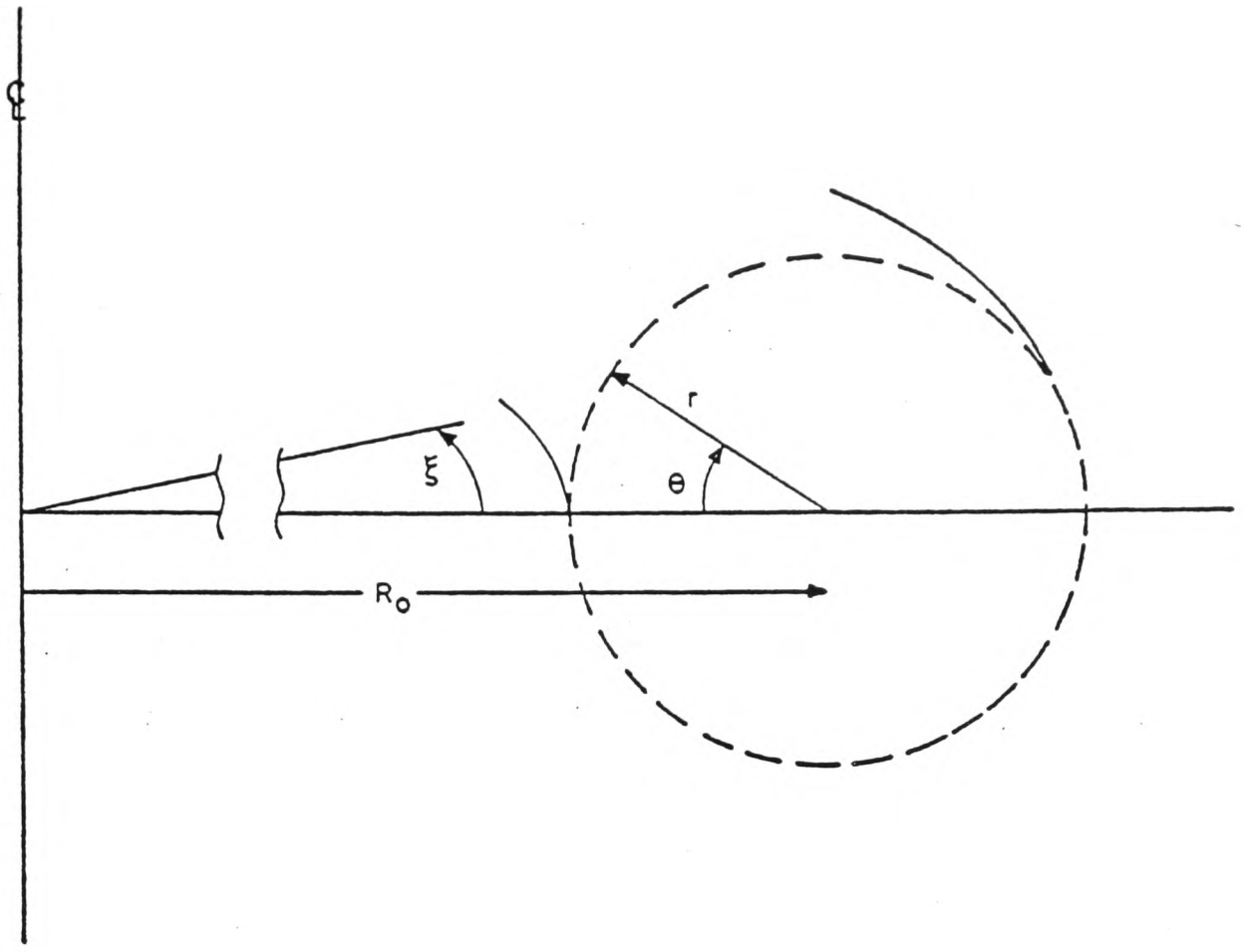

Fig.1 Coordinate geometry.

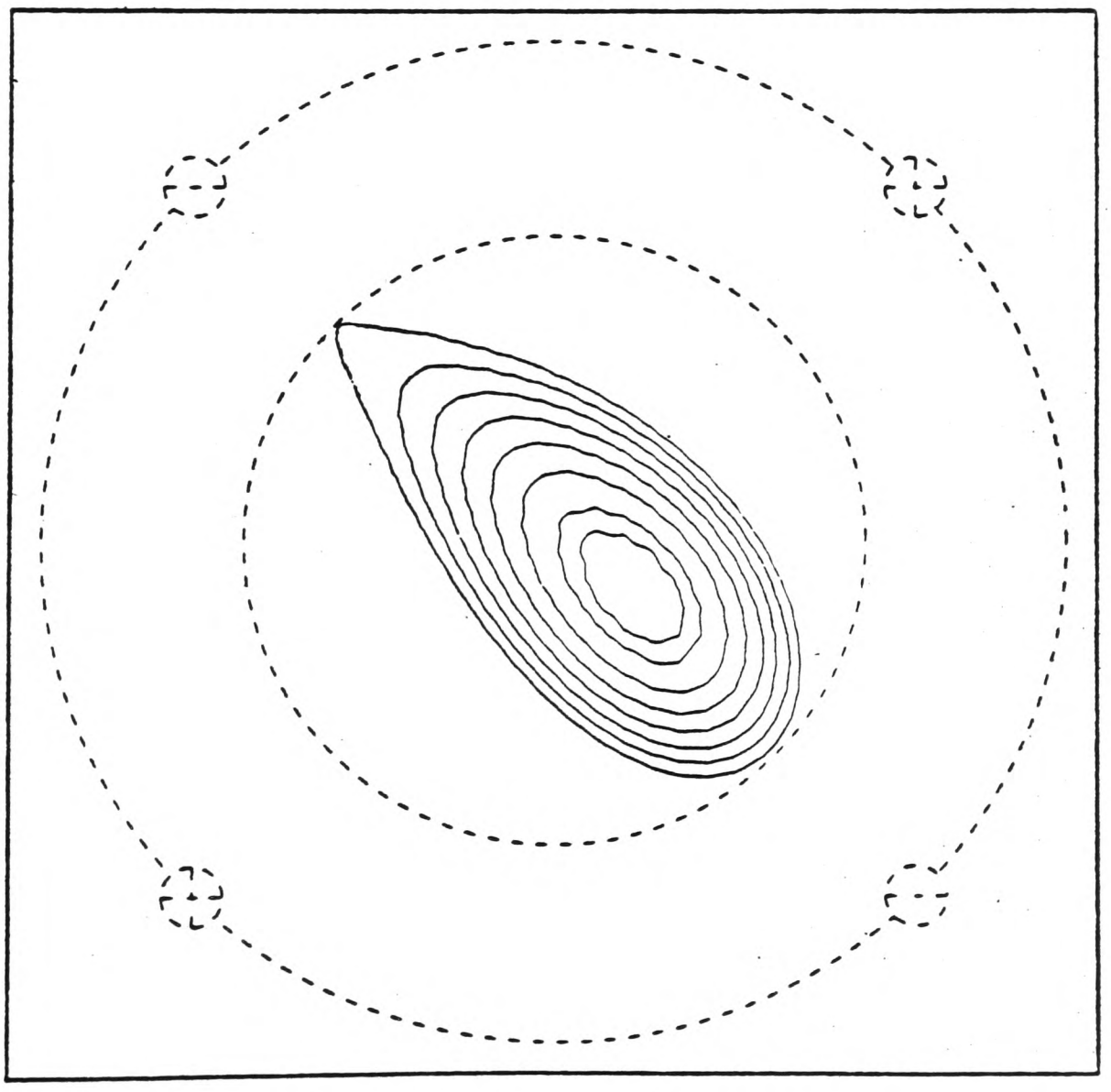

Fig.2 WVII flux surfaces for i = 0·5, $\beta \sim 1\%$, $B_v = 0$. The torus axis is to the left of the figure, the location of the stellarator windings in this cross-section and their polarity (+ into the paper) being indicated on the outer circle (dashed). The limiter radius is given by the inner dashed circle.

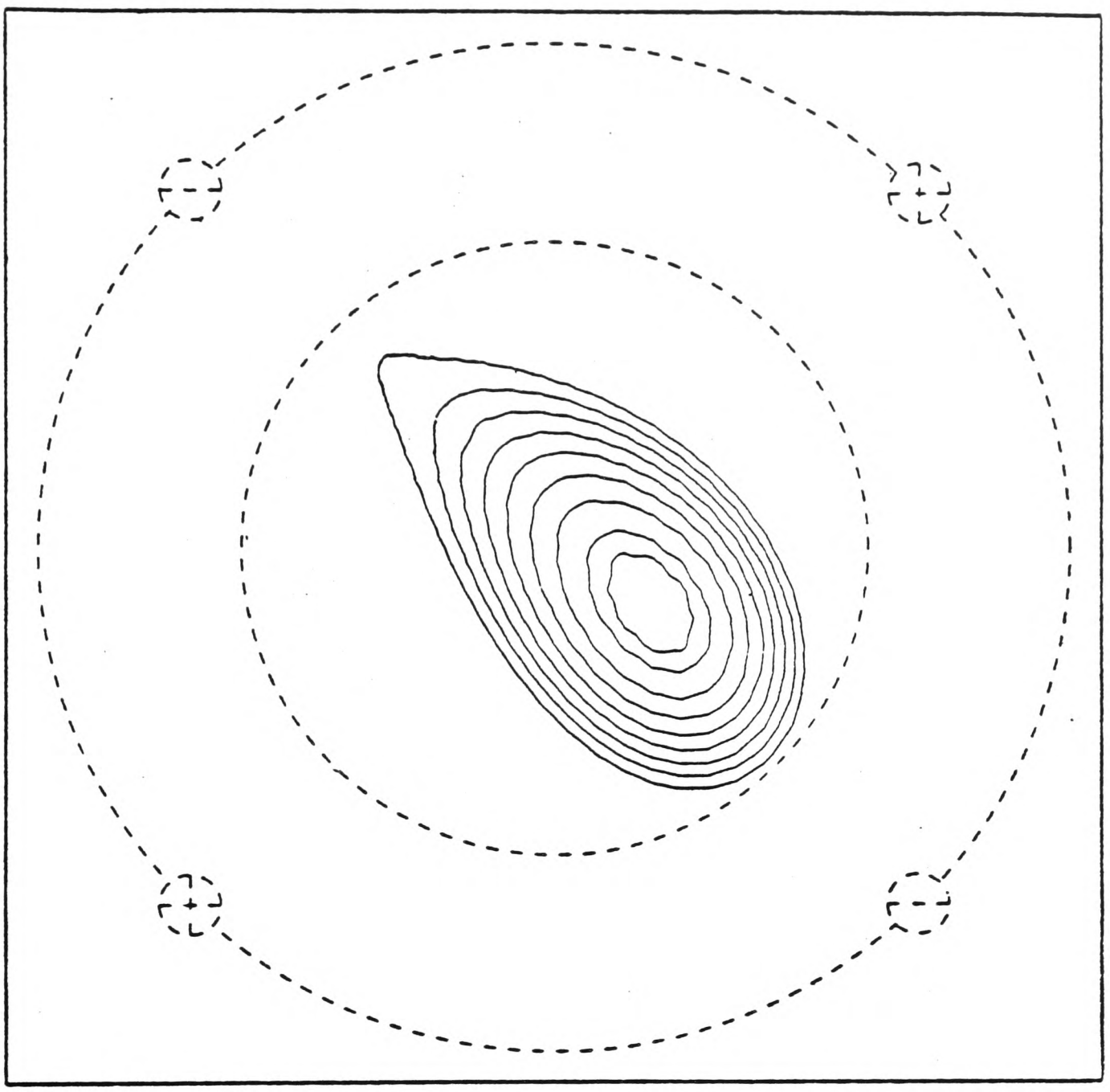

Fig.3 WVII flux surfaces for i = 0·5, $\beta \sim 2\%$, $B_v = 0$. Although β is twice as large as in the case of Fig.2, the flux surface displacements are only slightly greater.

Appendix Three

90MW of RF power are envisaged on Starfire in order to maintain the steady state current, although this is also roughly equal to the heating required for startup, assuming Alcator scaling. This constitutes a minimum power requirement which could prove troublesome if the confinement were better than Alcator. For the sake of consistency we shall consider here the possibility that Alcator scaling is also appropriate to the Stellarator reactor, although there is experimental evidence that energy confinement in Stellarators is better than in similar sized Tokamaks.

Taking $\tau_E = 5 \times 10^{-21} na^2$, the required input power scales as

$$P = \frac{60nTa\ Rm}{10^{-20}\ na^2} = 6 \times 10^{21}\ RmT$$

(A factor of 1/2 has been included to allow for alpha-particle heating as ignition is approached.) If T is expressed in keV then the power required is simply RmT. Thus devices with large major radius will be penalised economically by the cost of heating, if these assumptions are correct. For instance, the heating required in our proposed device, which has a relatively modest major radius, would be 130MW. The figure quoted for Starfire is obtained from the Starfire report [6].

For the sake of comparison with Starfire we now give a set of costs for a Stellarator with the same wall loading and thermal output power (the electrical output powers will differ, because of the recirculated power to the lower hybrid drive). On the basis of the costs given in chapter seven, we have estimated the costs of the major components to be (in $M, and at 1976 prices):

Item	Starfire	Stellarator
TF coils	90	102
PF coils	40	-
Wall+Blanket	69	123
Heating	90	130
Buildings	13	19
Conv. Plant	300	300
Miscellaneous	150	150
Total	752	824
Cost/kW (£)	742	706

The thermal power output is in each case 3.5GW. Assuming a conversion efficiency of 1/3, we find the electrical power from the generators - but in the case of Starfire we subtract 152.7MW from it before calculating the cost per kilowatt, to allow for the recirculated power.